THE SYNTHESIS AND REACTIONS OF FUNCTIONALISED TRANSITION METAL SUBSTITUTED PARAFFINS

by

MARTIN OPIYO ONANI

Submitted in fulfilment of the academic
requirements for the degree of
Doctor of Philosophy in the
School of Pure and Applied Chemistry,
University of Natal
Durban

July 2002

DEDICATION

This work is dedicated to my loving late mother Esther Atieno, Grandma Hellena Wayodi.

dad Hezron Onani, my wife Achieng, son Otieno and daughter Adhiambo.

ABSTRACT

The compounds $[Cp(CO)_3W\{(CH_2)_nX\}]$ (X = Br, I; n = 3 – 6) were prepared in high yield by the reaction of $Na[Cp(CO)_3W]$ with $Br(CH_2)_nBr$. The bromoalkyl compounds were subsequently reacted with NaI to give the corresponding iodoalkyl complexes. The crystal structures of $[Cp(CO)_3W\{(CH_2)_5I\}]$ and $[Cp(CO)_3W\{(CH_2)_3Br\}]$ are reported for the first time. The former compound forms orthorhombic crystals in the space group $P2_1nb$ and the latter forms triclinic crystals in the space group $P\bar{1}$. Both have W–C bond lengths of 2.35 Å. The C–I bond length is 2.12 Å; the C–Br bond length is 1.94 Å. In a similar manner to the above, the compounds $[Cp(CO)_2(PPh_iMe_{3-i})Mo\{(CH_2)_nBr\}]$ (Cp = η^5-C_5H_5, n = 3, 4; i = 0 – 3) and $[Cp^*(CO)_3Mo\{(CH_2)_nBr\}]$ (Cp^* = η^5-$C_5(CH_3)_5$, n = 3, 4) were prepared in medium to high yield by the reaction of the corresponding anion $[Cp(CO)_2(PPh_iMe_{3-i})Mo]^-$ or $[Cp^*(CO)_3Mo]^-$ with $Br(CH_2)_nBr$. The bromoalkyl compounds were subsequently reacted with NaI to give the corresponding iodoalkyl compounds $[Cp(CO)_2(PPh_iMe_{3-i})Mo\{(CH_2)_nI\}]$ (n = 3, 4; i = 0 – 3) and $[Cp^*(CO)_3Mo\{(CH_2)_nI\}]$ (n = 3, 4) respectively. The iodoalkyl compounds were also prepared by the reaction of the corresponding anion and α,ω-diiodoalkane in much lower yields. These compounds have been fully characterised and their properties are discussed. The crystal and molecular structure of $[Cp(CO)_2(PPh_3)Mo\{(CH_2)_3I\}]$ is also reported, again for the first time. The compound forms crystals in the monoclinic space group $P2_1/n$; with a Mo–C bond length of 2.40 Å and a C–I bond length of 2.13 Å

These halogenoalkyl compounds were used as precursors to the new heterobimetallic complexes $[Cp(CO)_3W(CH_2)_nMo(CO)_3Cp]$ n = 3 – 6; $[Cp(CO)_3W(CH_2)_nMo(CO)_3Cp^*]$ n = 3,4; $[Cp(CO)_3W(CH_2)_nMo(CO)_2(PPh_iMe_{3-i})Cp]$ n = 3,4; i = 0 – 3 and $[Cp(CO)_2Fe(CH_2)_nMo(CO)_2(PPh_iMe_{3-i})Cp]$ n = 3,4; i = 0 – 3. The heterobimetallic complexes were prepared by the direct displacement of the iodide of a metallo-iodoalkyl complex with the appropriate anion. The complexes have been fully characterised by IR, ^1H NMR, ^{13}C NMR, COSY, HETCOR or HSQC and elemental analyses. X-ray diffraction studies are for the first time reported for the complexes

$[Cp(CO)_3W(CH_2)_3Mo(CO)_2(PPh_3)Cp]$ and $[Cp(CO)_2(PPh_3)Mo(CH_2)_3Fe(CO)_2Cp]$. Both compounds form monoclinic crystals in the space group P 21/c. The former, with a W–C bond length of 2.32 Å and Mo–C bond length of 2.35 Å and the latter with a Mo–C bond length of 2.37 Å and Fe–C bond length of 2.08 Å.

The reactions of some of the above halogenoalkyl compounds with some simple inorganic molecules were investigated. The reactions of $[Cp(CO)_3W\{(CH_2)_4Br\}]$ and $[Cp(CO)_2(PPhMe_2)Mo\{(CH_2)_3Br\}]$ with silver nitrate in acetonitrile formed orange products, $[Cp(CO)_3W\{(CH_2)_4ONO_2\}]$ and $[Cp(CO)_2(PPhMe_2)Mo\{(CH_2)_3ONO_2\}]$ respectively. The compounds $[Cp(CO)_3W\{(CH_2)_5CN\}]$, $[Cp(CO)_3W\{(CH_2)_4CN\}]$, $[Cp(CO)_2(PPhMe_2)Mo\{(CH_2)_3CN\}]$, $[Cp(CO)_3W\{(CH_2)_4N_3\}]$, $[Cp(CO)_3W\{(CH_2)_5N_3\}]$, $[Cp(CO)_2(PPhMe_2)Mo\{(CH_2)_3N_3\}]$ were also obtained from various reactions using the reagents; AgCN, KCN, NaCN and NaN_3. Similar reactions with molybdenum analogs gave cyclic carbene compounds.

Reaction studies were also done on some of the above heterobimetallic compounds with tertiary phosphines; carbon monoxide gas and trityl salt, and thermolyses were also investigated. The reactions of PPh_3 with $[Cp(CO)_3W\{(CH_2)_3\}ML_y]$ $\{ML_y = Mo(CO)_3Cp$, $Mo(CO)_3Cp^*$ and $Mo(CO)_2(PMe_3)Cp\}$ were found to be totally metalloselective, with the phosphines always attacking the expected metal site predicted by the reactions of the corresponding monometallic or homodinuclear alkyl species. A similar reaction involving CO with $[Cp(CO)_3W(CH_2)_3Mo(CO)_3Cp]$ and $[Cp(CO)_2Fe(CH_2)_3Mo(CO)_2(PMe_3)Cp]$ was also metalloselective. The reaction of $[Cp(CO)_2Fe(CH_2)_4Mo(CO)_3)Cp^*]$ with trityl salt gave the expected complex $[Cp(CO)_2Fe(C_4H_7)Mo(CO)_3)Cp^*]PF_6$. It is believed that the structure of the trityl salt complex has the iron atom π-bonded whilst the molybdenum is σ-bonded to the butyl chain. The compounds $[Cp(CO)_3W(CH_2)_3Mo(CO)_3Cp^*]$ and $[Cp(CO)_2Fe(CH_2)_3Ru(CO)_2Cp]$ both gave cyclopropane on thermolysis, indicating a β – elimination and reductive processes taking place. The crystal structure of $[Cp(CO)_3W\{(CH_2)_3COOH\}]$, which was obtained in one of the reaction studies, where the compound $[Cp(CO)_3W(CH_2)_3Mo(CO)_2(PMe_3)Cp]$ was reacted with excess PPh_3 in acetonitrile, is reported.

PREFACE

The experimental work described in this thesis was carried out in the School of Pure and Applied Chemistry, University of Natal, Durban, from March 1998 to January 2002, under the supervision of Dr. Holger Bernhard Friedrich.

These studies represent original work by the author and have not otherwise been submitted in any form for any degree or diploma to any tertiary institution. Where use has been made of the work of others it is duly acknowledged in the text.

CONTENTS

Page No.

LIST OF FIGURES

LIST OF REACTION SCHEMES AND MOLECULAR FORMULAE

LIST OF TABLES

ACKNOWLEDGEMENTS

I am deeply indebted to many people and organizations for their support for the duration of this work.

I have to thank my supervisor, Dr. H. B. Friedrich, for providing a very conducive atmosphere for research, his invaluable advice and encouragement, and meticulous comments on the whole thesis.

I am grateful to the technical staff of the School of Pure and Applied Chemistry in particular Alton Blose, Anita Naidoo, Emanuel Damoyi and Zarina Sayed Ally for general assistance in the lab, Dilip Jagjivan for training me to operate the NMR spectrometer, Bret Parel for distilling the solvents, Gregory Moodley and Harvey Sishi for the purchase of chemicals, Jodi Couling for workshop related matters, Kishore Singh for computer related work, Logan Murugas for running around to buy dry ice for me and Mr. James Ryan (PMB) for mounting the crystals used in the X-ray diffraction studies.

I have to thank Prof. B.S. Martincigh for her motherly support and interest in my work that has been a deep source of inspiration. Many academic staff members at the University of Natal have contributed to the success of this research: Dr. Glenn Maguire for useful discussions in the lab, Dr. Orde Munro for solving the crystal structures, Prof. Michael Laing for valuable discussions on the molecular structures and Dr. Alan Howie of Aberdeen University (UK) for the refinement of the crystal structures.

I wish to thank Dr. Peter Gorst-Allman of LECO Company for organising the acquisition of the mass spectral data.

I owe much to my colleague Vikash Gokul, who welcomed me to South Africa and made my stay and work pleasurable. Special thanks also go to Elena Friedrich, Nirad Singh and his wife Jyotshna, Wayne Tammadge and family, my Kenyan brothers: Ali Mohammed, Peter

Cheplogoi, Wallyambila Waudo, the Simon Oloo family, Mr. Joseph Aloyo, Prof. Sarima Chacha, and Prof. Festus Kaberia.

To my colleagues and friends in the School, especially Avashnee Sewllal and Kirsten Barnes, Nishlan Govender, Jonathan Chetty, Abdulsamad Mahomed, and Rivash Panday for their invaluable friendship and support.

I wish to acknowledge with gratitude, the generous financial support from several bodies: the Deutscher Akademischer Austauschdienst (DAAD), the Kenyan Government through my employer Jomo Kenyatta University of Agriculture and Technology, the National Research Foundation (NRF) and the University of Natal.

Finally, I wish to heartily thank my wife Lydia Achieng and our children, for their support, sacrifice and great understanding during my whole study period. The encouragement from my father Hezron Onani has meant much to me. To end it all, very special thanks is due to my friends Dr. Joseph Okil and the late Steve Opiyo, for persuading me to change my career from a librarian to lecturer.

PUBLICATIONS AND CONFERENCE PRESENTATIONS

Parts of this thesis have been published and presented at conferences as detailed below:

PAPERS:

1. "Preparation and Properties of the Halogenoalkyl Compounds $[(\eta^5\text{-}C_5H_5)(CO)_2(PPh_iMe_{3-i})Mo\{(CH_2)_nX\}]$ (n = 3, 4; i = 0–3, X = Br, I) and $[\{\eta^5\text{-}C_5(CH_3)_5\}(CO)_3Mo\{(CH_2)_nX\}]$ (n = 3, 4; X = Br, I) and the crystal structures of $[(\eta^5\text{-}C_5H_5)(CO)_3W\{(CH_2)_5I\}]$, $[(\eta^5\text{-}C_5H_5)(CO)_3W\{(CH_2)_3Br\}]$ and $[(\eta^5\text{-}C_5H_5)(CO)_2(PPh_3)Mo\{(CH_2)_3I\}]$",
   Holger B. Friedrich, Martin O. Onani and Orde Q. Munro, Journal of Organometallic Chemistry, **633**, 2001, 39-50.

2. "Transition metal substituted paraffins: synthesis and properties of some μ-saturated heterobimetallic Complexes containing Mo and W or Fe and the crystal structures of $[(\eta^5\text{-}C_5H_5)(CO)_3W(CH_2)_3Mo(CO)_2(PPh_3)(\eta^5\text{-}C_5H_5)]$ and $[(\eta^5\text{-}C_5H_5)(CO)_2(PPh_3)Mo(CH_2)_3Fe(CO)_2(\eta^5\text{-}C_5H_5)]$",
   Holger B. Friedrich, Martin O. Onani and Orde Q. Munro, Journal of Organometallic Chemistry, submitted.

CONFERENCE CONTRIBUTIONS:

1. Poster titled "The Chemistry of Some New ω–Halogenoalkyl Complexes", M.O. Onani and H. B. Friedrich, presented at the 35th Convention of the South African Chemical Institute, Potchefstroom, RSA, September 2000.

2. Poster titled "A study of some μ-saturated hydrocarbon heterobimetallic complexes", M.O. Onani and H.B. Friedrich, presented at the 34th International Conference of Co-ordination Chemistry, Edinburgh, Scotland, July 2000.

3. Talk titled "The Transition Metal Substituted Parrafins: μ-saturated Heterobimetallic Complexes" presented by Martin Onani at the South African Chemical Institute Post-Graduate Symposium, University of Natal, Durban, RSA, September 2001.

4. Short talk and poster titled "Transition Metal Substituted Paraffins: Some μ – Saturated Heterobimetallic Complexes", M.O. Onani, H. B. Friedrich and O.Q. Munro, presented at Combined CATSA and SACI (Inorganic Chemistry Division) Conference on Inorganic Chemistry and Catalysis, Bakgatla, RSA, November 2001.

5. Poster titled "Reaction Studies on Some Heteronuclear Organometallic Compounds", M.O. Onani and H.B. Friedrich, presented at Combined CATSA and SACI (Inorganic Chemistry Division) Conference on Inorganic Chemistry and Catalysis, Bakgatla, RSA, November 2001.

6. Talk titled "The Chemistry of Some New ω-Halogenoalkyl Complexes", M.O. Onani, H.B. Friedrich and O.Q. Munro presented at the 36th Convention of the South African Chemical Institute, Port Elizabeth, RSA, July 2002.

AWARDS:

The author of this thesis was awarded the Sasol Post-graduate Medal of the South African Chemical Institute in 2002. This medal is awarded to "young innovative chemists who show innovation, independence and enterprising feats".

ABBREVIATIONS

Cp	=	η^5-C_5H_5
Cp*	=	η^5-$C_5(CH_3)_5$
COSY	=	correlated spectroscopy
d	=	doublet
dec	=	decomposed
DH	=	monoanion of dimethylglyoxime
ether	=	diethyl ether
esi	=	electrospray ionisation
h	=	hours
Hg	=	mercury
HETCOR	=	heteronuclear correlation
HMPA	=	hexamethylphosphoramide
HSQC	=	heteronuclear single-quantum coherence
IR	=	Infrared (vs = very strong, s = strong, m = medium, w = weak, sh = shoulder, b = broad, sm = small, wb = weak broad, vsb = very strong broad)
L, L_x, L_y	=	ligand(s)
L_yM	=	transition metal and its associated ligands, $n \geq 1$, X = halogen
m	=	multiplet
M	=	transition metal
Me	=	methyl group
$MePh_2P$	=	methyldiphenylphosphine
Me_2PhP	=	dimethylphenylphosphine
Me_3P	=	trimethylphosphine
m.p.	=	melting point
ms	=	mass spectrometry
m/z	=	mass to charge ratio

NMR	=	nuclear magnetic resonance (m = multiplet, qn = quintet, q = quartet, t = triplet, d = doublet, s = singlet)
N-N	=	Me_2-bipy
Nu	=	Nucleophile
PBu_3	=	tributylphosphine
Ph	=	phenyl group
PPh_3	=	triphenylphosphine
ppm	=	parts per million
PR_3	=	tertiary phosphine
p	=	product
py	=	pyridine
pyen	=	bis(2-pyridyl)ethylenediamine
pzH	=	pyrazole
qn	=	quintet
R	=	alkyl group
RT	=	room temperature
s	=	singlet
sm	=	starting material
t	=	triplet
THF	=	tetrahydrofuran
t-Bu	=	tertiary butyl group
TMS	=	tetramethysilane

NOTE: COMPOUND AND FIGURE NUMBERS ARE VALID WITHIN EACH INDIVIDUAL CHAPTER ONLY.

CHAPTER 1

INTRODUCTION

This thesis focuses on the synthesis of ω-halogenoalkyl transition metal compounds, their reactions and application in the synthesis of heterodinuclear complexes. This Chapter therefore reviews the current literature relevant to these aspects before providing a detailed outline of this work.

1.1 General Introduction to Organometallic Compounds

The history of organometallic chemistry contains a large number of main-group examples. In 1760, Louis Claude Cadet de Gassicourt isolated "Cadet's fuming liquid" while working on cobalt-based invisible ink. It was mainly a mixture of $(Me_2As)_2$ and $(Me_2As)_2O$. Main group organometallic compounds have been known since then and Victor Grignard won a Nobel Prize in 1912 for developing the Grignard reagents. Organometallic complexes contain, by definition, at least one direct metal to carbon bond. Generally speaking, the reactivity and physical properties of these compounds are very different from classical coordination complexes. They can either be produced synthetically or exist in nature as bioinorganic compounds. An example of the latter is Vitamin B_{12}. Although other compounds such as gold cyanide or calcium carbonate are, strictly speaking, organometallic compounds, they are regarded as inorganic compounds. These types of compounds were widely used for material synthesis, but their chemistry will not be considered, as this thesis concentrates on organometallic compounds containing transition metals.

A pioneering chemist, Sir Edward Frankland, who was responsible for the discovery of the idea of valency, also invented the science of organometallic chemistry (1849). The oldest transition metal (*d*-block) organometallic compound is $PtCl_2(C_2H_4).KCl.H_2O$ (**1**), and was prepared by W.C. Zeise, a Danish Chemist, in 1827. In the1890's Ludwig Mond and co-workers synthesised the first metal carbonyl, tetracarbonylnickel (**2**).

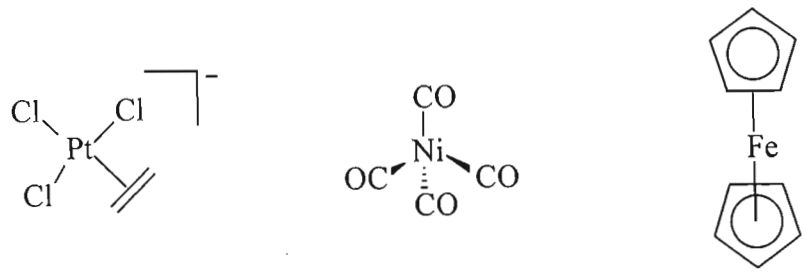

1 **2** **3**

Figure 1.1: Structures of Zeise Salt (1), Nickel tetracarbonyl (2) and Ferrocene (3)

The discovery and characterisation of the structure of ferrocene, $Fe(C_5H_5)_2$ (**3**) followed much later in 1951, and led to an explosion of interest in the chemistry of the *d*-block metal carbon bonded compounds. All these discoveries brought about development and the now flourishing study of organometallic chemistry. However, the structures of these complexes were difficult to deduce using the chemical methods available at the time. The advent of characterisation instruments such as the NMR spectrometer and single crystal *X*-ray diffractometers in the 1950's made it possible to solve the structures of complexes (**1 – 3**) in solution and the solid state respectively. Consequently, there resulted a rapid growth in the study of organometallic compounds by research groups around the world, and a Nobel Prize was awarded in 1973 to Ernst Fisher and Geoffrey Wilkinson for their contribution to the field. The historical perspective and the early discoveries in organometallic chemistry are well documented [1].

Organometallic compounds play a role of ever-growing importance in organic synthesis. Many organometallic processes are now unsurpassed in elegance and efficiency, and have proliferated into many related areas of research, making the field an interdisciplinary one. Also, with the ever increasing attention to environmental concerns, organometallic compounds are being viewed as 'green chemicals' of the day. They are proving to be excellent catalytic agents for many chemical processes, and thus have passed the barrier from research to industrial applications. The last three decades has seen a steadily growing trend in the complexity of organometallic transformations, which interestingly can make multistep processes proceed in a single operation [2].

Transition metal alkyls and their derivatives are well known organometallic compounds [3], and have been proposed as intermediates in a variety of important catalytic processes.

For this reason transition metal alkyls have been used as model compounds for homogenous catalysis [4,5].

1.2 Halogenoalkyl Complexes

Halogenoalkyl compounds are functionalised transition metal alkyl compounds, which have been associated with some novel chemistry. Functionalised organometallic compounds have been shown to be important intermediates in organic synthesis [6]. Specifically, the halogenoalkyl transition metal compounds of the type $[L_yM\{(CH_2)_nX\}]$ (M = transition metal, X = Cl, Br, I or F, $n \geq 1$) have been implicated in many catalytic processes [7-9]. To emphasize their importance, these compounds have recently been grouped in a separate class of alkyl compounds, though not much is known about them [10]. These compounds have been found to be potential and versatile precursors for a wide range of useful compounds. They are useful precursors to cationic carbene complexes $[L_yM{=}CH_2]^+$ [11], cyclic carbenes [12 -14], hydroxymethyl complexes $[L_yMCH_2OH]$ [15], methylene-bridged complexes $[L_yMCH_2\ M'L_x]$ (M' = M, M'≠ M) [10,16 -18], dendrimers [19] as well as many other classes of functionalised alkyl compounds [20,21], olefin metathesis [22,23] and alkyne metathesis [24]. We will now review the available literature on the functionalised transition metal paraffins, with particular reference to ω-halogenoalkyl compounds and their derivatives.

The synthesis and chemistry of a number of halogenoalkyl complexes can easily be found in the literature [3f,12,16,25-28]. Friedrich [3c] and Moss [3c,29] have presented comprehensive reviews on this class of compounds where many of the known halogenoalkyl transition metal complexes are well covered. These compounds have been proposed as models for the Fischer-Tropsch process [3f,30] and other significant catalytic processes [31]. Transition metal organometallic compounds are widely known as important synthons in organic synthesis [32]. Halogenoalkyl (or haloalkyl) complexes as organometallic compounds are important utility intermediates in organic synthesis [33]. Also, the halogenoalkyl compounds of the main group metals have been extensively studied and shown to be important reagents in synthetic chemistry [34]. The last decade has seen relatively few articles published in this field, and we hope to include most of them for the purpose of our work that is to follow. We will restrict this work to the less known ω-halogenoalkyl compounds, and consider monohalogenomethyl and polyhalogenoalkyl

compounds outside our scope. Specifically, we intend to review the compounds containing some or all of the known transition metal stabilizing ligands: carbonyls, cyclopentadienyls and substituted phosphines. Metal carbonyls are readily available and widely used as starting materials for the preparation of many organometallic compounds; carbonyls are unsaturated electron rich ligands that rarely undergo attack once coordinated to a transition metal. Joe Chatt promoted the use of tertiary phosphines as flexible ligands in transition metal chemistry [35]. He demonstrated the advantage of using triethylphosphine ligands in the preparation of air-stable and crystalline samples of platinum metal complexes. The first report of a tertiary phosphine complex of a transition metal has been attributed to Hofmann in 1857 [36]. The application of proton, and then phosphorus, NMR spectroscopy led coordination chemists of the time, particularly Benard Shaw and his co-workers, to venture extensively into the use of phosphine ligands [37]. These phosphine ligands have very simple but informative proton NMR spectra, especially in the light of the virtual coupling phenomenon of *trans* phosphines. We hope to exploit these valuable properties and use them to study the chemistry of the heterodinuclear complexes we intend to synthesize.

We now present a general review of the ω-halogenoalkyl transition metal compounds of the type $[L_yM\{(CH_2)_nX\}]$ with particular reference to their reported synthetic methods, reactions and uses.

1.2.1 ω-Halogenoalkyl Complexes

The earlier preparations of alkyl and aryl compounds of iron, containing π-cyclopentadienyl and carbonyl or nitrosyl ligands involved the reaction of the alkali metal salts of carbonyl hydride derivatives, with various alkyl or aryl halides [38]. For example, $Na[Cp(CO)_iM]$ (M = Fe, Cr, Mo, W, i = 2 or 3) reacted with RI as shown in Equation 1 to give nearly quantitative yields of the product $[Cp(CO)_iMR]$ for i = 2, M = Fe and for i = 3, M = Cr, Mo and W; R = CH_nCH_3, n = 0 - 2).

$$Na[Cp(CO)_2M] + RI \xrightarrow{THF} [Cp(CO)_2MR] + NaI \quad (1)$$

Though these types of products were not ω-halogenoalkyl compounds, the method used for their preparations is of importance, because the procedure later became applicable to the

preparation of compounds with σ-bonds between a transition metal and a carbon as well as other elements, by use of suitable halides [35].

King and Bisnette reported that the reaction of $Na[Cp(CO)_3M]$ (M = Cr, Mo, W) with 1,n-dibromoalkane gave $[Cp(CO)_3M\{(CH_2)_nBr\}]$ (n = 3, 4, M = Mo or W) [39]. The displacement of only a single bromine from the α,ω-dibromoalkanes gave relatively stable tungsten derivatives compared to their molybdenum analogs. These compounds had physical properties reflecting those of the above $[Cp(CO)_iMR]$ compounds.

The $Na[(CO)_5Mn]$ anion was reported to react with $ClC(O)(CH_2)_nCl$ (n = 3, 4) to give $[(CO)_5Mn\{C(O)(CH_2)_nCl\}]$ (n = 3, 4), which was then decarbonylated to yield the desired ω-halogenoalkyl compounds $[(CO)_5Mn\{(CH_2)_nCl\}]$ [40]. The compounds $[(CO)_5Mn\{(CH_2)_nCl\}]$ readily reacted with neutral compounds such as phosphines, L, to give products containing carbonyl inserted groups, $[(CO)_4LMn\{C(O)(CH_2)_nCl\}]$. These products could in turn be decarbonylated to give the desired manganese complexes $[(CO)_4LMn\{(CH_2)_nCl\}]$ (n = 3, 4). It has recently been shown that the decarbonylation process is a general route to the manganese complexes above [41].

In 1971, Cotton and Lukehart reported that the reaction of $[Cp(CO)_3Mo\{(CH_2)_3Br\}]$ (**4**) with PPh_3 in acetonitrile yielded the cyclic carbene complex $[Cp(CO)_2(PPh_3)Mo\{\overline{CO(CH_2)_2CH_2}\}]Br$ (**5**) (Scheme 1.1).

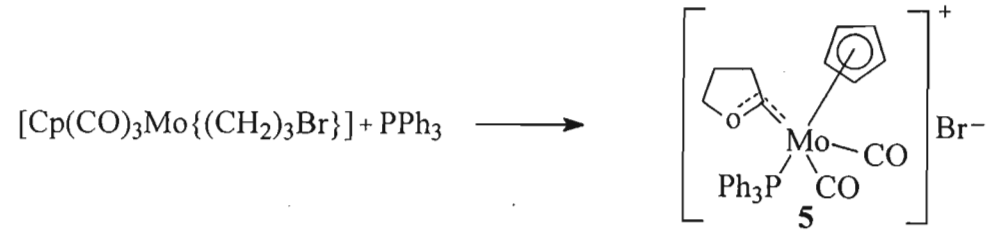

Scheme 1.1: The formation of $[Cp(CO)_2(PPh_3)Mo\{\overline{CO(CH_2)_2CH_2}\}]Br$ (**5**)

A mechanism for the formation of compound **5** has been proposed. It presumably proceeds by an initial attack of PPh_3 on the molybdenum metal, resulting in alkyl migration onto the carbonyl group forming an intermediate acyl derivative

$[Cp(CO)_2(PPh_3)Mo\{C(O)(CH_2)_3Br\}]$ **6**. This intermediate species spontaneously undergoes internal nucleophilic attack on the acyl oxygen atom on the γ-carbon atom to displace the bromide ion and finally form the cyclic carbene cation (**5**) as shown in Scheme 1.2 [42]. A more detailed discussion on alkyl migration will be seen in Chapter 4.

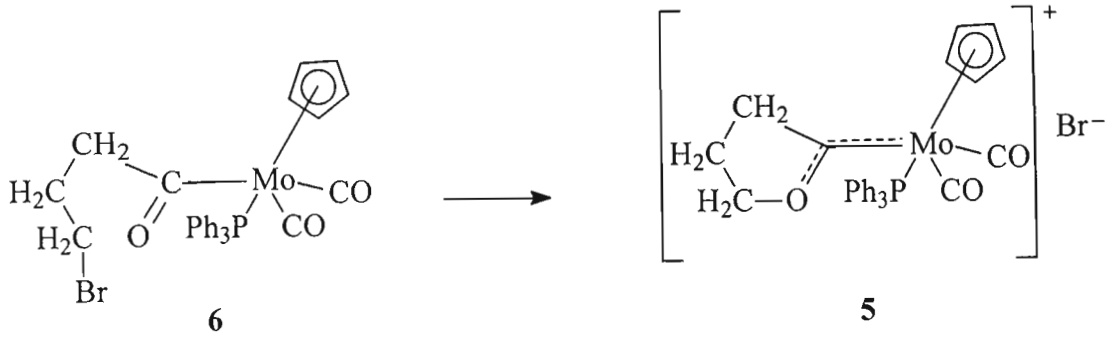

Scheme 1.2: The mechanism for the spontaneous formation of **5**

A similar mechanism to Scheme 1.2 has been shown to generate the cyclic carbene species $Cp(CO)_2Mo(I)\{\overline{CO(CH_2)_2CH_2}\}]$ (**7**). The $Na[Cp(CO)_3Mo]$ anion reacts with diiodopropane in tetrahydrofuran to give $[Cp(CO)_3Mo\{(CH_2)_3I\}]$ **8**, which reacts further under reflux to form **7** [43].

Compound **4** was found to readily react with LiI, but not LiBr, to give compound **7**. The nucleophile, I^-, is reported to initiate the attack on **4** or **8**, and generates an intermediate species $[Cp(CO)_2Mo(I)\{C(O)(CH_2)_3X\}]^-$ (X = Br, I), that undergoes a fast spontaneous cyclisation to form **7**. The compound $[Cp(CO)_3Mo\{(CH_2)_4I\}]$ **9**, interestingly, reacts with LiI to form only $[Cp(CO)_3MoI]$ and not a cyclic carbene complex as would be expected [40]. Other nucleophiles such as CN^- and SPh^- also react with compound **4** to give the cyclic carbene complex $[Cp(CO)_2Mo(Z)\{\overline{CO(CH_2)_2CH_2}\}]$ (Z = CN, SPh). The cyclisation process was found not to involve the cyclopentadienyl ring nor a proton substituted ring.

The tungsten carbene analog of compound **7**, $[Cp(CO)_2W(X)\{\overline{CO(CH_2)_2CH_2}\}]$ (X = I, CN), was similarly formed from the reaction of $[Cp(CO)_3W\{(CH_2)_3Br\}]$ **9** with iodide and cyanide ions, though at a slower rate compared to that of **7** [44]. The mechanism for the formation of this tungsten carbene complex was reported to follow the reaction path shown in Scheme 1.3. Again as seen in Schemes 1.1 and 1.2 during the reaction, the nucleophile

I^- or CN^-, coordinates onto the central tungsten metal, followed by migration of the alkyl group from tungsten onto an adjacent carbonyl group [41].

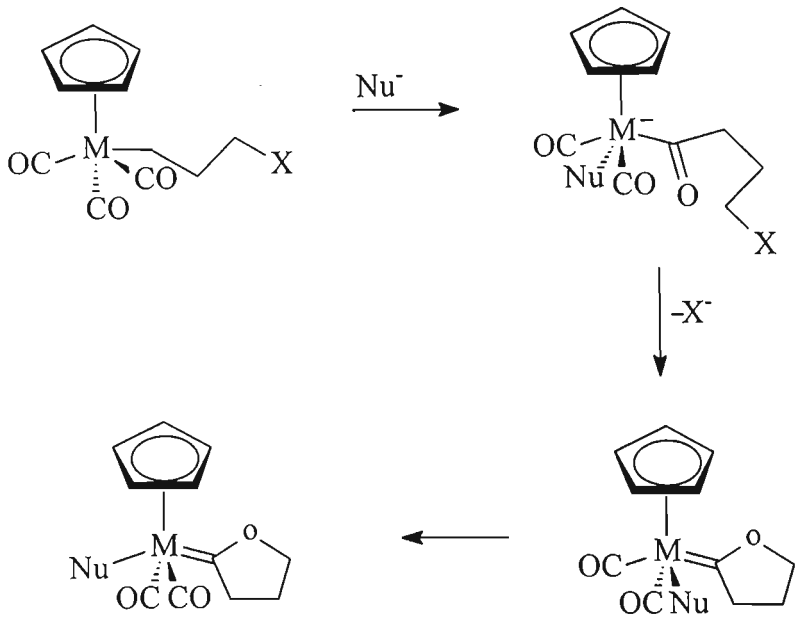

Nu = Nucleophile

Scheme 1.3: General mechanism for the formation of the carbene compounds
e.g. $[Cp(CO)_2W(X)\{CO(CH_2)_2CH_2\}]$ [42]

The formation of these oxacycloalkylidene complexes was found to be dependent on the alkyl chain involved and on the halide of the halogenoalkyl group. Consequently, $[Cp(CO)_3Mo\{(CH_2)Cl\}]$ **10**, would react with the neutral nucleophile PPh_3 in acetonitrile to give the halogenoacyl compound *trans*-$[Cp(CO)_2(PPh_3)Mo\{C(O)(CH_2)Cl\}]$while $[Cp(CO)_3Mo\{(CH_2)_4I\}]$ **9** gave $[Cp(CO)_2(PPh_3)Mo\{C(O)(CH_2)_4I\}]$**11**. Similar complexes containing acyl groups were obtained when the compounds $[Cp(CO)_3Mo\{(CH_2)_nBr\}]$ (n = 4, 5) reacted with PPh_3 as shown in Equation 2 below [41].

$$[Cp(CO)_3Mo\{(CH_2)_nBr\}] + PPh_3 \longrightarrow [Cp(CO)_2(PPh_3)Mo\{C(O)(CH_2)_nBr\}] \qquad (2)$$

Cotton and Lukehart further investigated the formation of these acyl compounds by using kinetic methods. Their findings were that these reactions proceed due to two competitive pathways that result after the initial nucleophillic attack on the central metal. Either a fast intramolecular cyclisation occurs to form the *cis* isomer or intramolecular geometrical isomerism to form the *trans*-halogenoalkyl compound occurs. Therefore, compound **10**

forms a halogenoacyl complex because of the high electronegativity of Cl, that renders it a poorer leaving group than Br. This property results in a decrease in the rate of cyclisation relative to isomerisation [41].

Winter and co-workers prepared the dimer [{$Cp(CO)_2LMo\}_2$] (L = PPh_3, $P(OMe)_3$) by literature methods [45], and reduced it with Na/Hg amalgam to give the anions $Na[Cp(CO)_2LMo]$, which they then reacted with $Br(CH_2)_3Br$ to give the bromoalkyl complexes [$Cp(CO)_2LMo\{(CH_2)_3Br\}$] **12**. On reaction with iodide ion, the compound **12** did not form carbene complexes as expected [12]. In contrast, the complexes with propyl chains like [$Cp(CO)_3M\{(CH_2)_3I\}$] (M = Mo, W) were previously believed to always react with excess iodide ions to form the corresponding cyclic carbene complexes [$Cp(CO)_2M(I)\{\overline{CO(CH_2)_2CH_2}\}$] [13].

Similarly, transition metal anions have also been reported to be able to induce cyclisation reactions giving carbenes, for example, during the reaction of $Na[Cp(CO)_3Mo]$ with diiodopropane to form compound **4**, the anion $Na[Cp(CO)_3Mo]$ reacts further with **4** forming an intermediate anionic acyl complex that finally undergoes elimination, removing Br^-, yielding a cyclic carbene. The mechanism proceeds in a similar manner to that shown in Scheme 1.3. Also, the corresponding tungsten derivatives can undergo cyclic carbene formations in the same manner.

The complexes containing a Cp* as a ligand are known to be more nucleophillic relative to those of Cp. This is because of the inductive effects of the methyl substituents that pile their electron density onto the ring and in turn onto the central metal. Hence, the formation of complexes of the type [$Cp^*(CO)_3M\{(CH_2)_3Br\}$] (M = Mo (**13**), W (**14**) is easier than those of the Cp analogs [14]. Compound **13** reacts with LiI giving *cis*- and *trans*- carbenes [$Cp^*(CO)_2Mo(I)\{\overline{CO(CH_2)_2CH_2}\}$], and with CN^- to give only a *trans* compound [$Cp^*(CO)_2Mo(CN)\{\overline{CO(CH_2)_2CH_2}\}$]. Also, Winter and co-workers showed that compound **13** reacts with either Br^- or SCN^- to form the respective carbene complexes, whereas the Cp analog does not [14]. Similarly, compound **14** reacts with I^- to form the expected cyclic carbene complex.

The anions $Na[Cp(CO)_2Fe]$ and $Na[Cp^*(CO)_2Fe]$ react with an excess of α,ω-$X(CH_2)_nX$ in tetrahydrofuran to form [$Cp(CO)_2Fe\{(CH_2)_nX\}$] **15** (n = 3 – 10, X = Br; n = 3, X = Cl)

according to Equation 3, and $[Cp^*(CO)_2Fe\{(CH_2)_nX\}]$ **16** (X = Br, n = 3 – 5) as shown in Equation 4, respectively [3f,46].

$$Na[Cp(CO)_2Fe] + X(CH_2)_nX \xrightarrow{-20\ °C,\ THF} [Cp(CO)_2Fe\{(CH_2)_nX\}] + NaX \quad (3)$$

$$Na[Cp^*(CO)_2Fe] + X(CH_2)_nX \xrightarrow{-50\ °C,\ THF} [Cp^*(CO)_2Fe\{(CH_2)_nX\}] + NaX \quad (4)$$

Casey and Smith later showed that such complexes as $[Cp(CO)_2Fe\{(CH_2)_3X\}]$ (X = Br, Cl) and $[Cp(CO)_2Fe\{(CH_2)_2CH(CH_3)Br\}]$, when reacted with $AgBF_4$, are good cyclopropane precursors in organic synthesis [47]. Similar derivatives with longer chains, like where n = 4 – 5, were found to be slow and rather inefficient in this type of complex reactions. The participation of the central metal iron in the release of the cyclopropane and the corresponding cycloalkanes from the reaction of γ-halogenoalkyl iron complexes was reported to be very essential, as it facilitates the cleavage of the γ-carbon-halogen bond [44].

Also, the compound $[Cp(CO)_2Fe\{(CH_2)_3Br\}]$ was reported to react with PPh_3 in acetonitrile to form a cyclic carbene compound and an acyl compound as represented in Equation 5 below [3f].

$$[Cp(CO)_2Fe\{(CH_2)_3Br\}] + PPh_3 \xrightarrow{reflux,\ CH_3CN} [Cp(CO)(PPh_3)Fe\{\overline{CO(CH_2)_2CH_2}\}]Br$$

$$\downarrow \text{reflux, } PPh_3$$

$$[Cp(CO)(PPh_3)FeC(O)(CH_2)_3PPh_3]Br \quad (5)$$

The synthesis of the iodo- analogs of **15** and **16** was realised by Friedrich *et al.*, by reacting the bromo- derivatives of the complexes with NaI in acetone (Equation 6) [43]. The iodoalkyl compounds generated were then shown to be good precursors to various heterobimetallic alkanediyl complexes as will be seen later.

$$[(\eta^5\text{-}C_5R_5)(CO)_2Fe\{(CH_2)_nBr\}] + NaI \xrightarrow{acetone} [(\eta^5\text{-}C_5R_5)(CO)_2Fe\{(CH_2)_nI\}] + NaBr \quad (6)$$

R = H, n = 3 – 10; R = CH_3, n = 3 – 5

In addition to the above complexes (**15,16**), Friedrich *et al.* have also reported the synthesis and properties of the complexes $[Cp(CO)_2Ru\{(CH_2)_nX\}]$ (n = 3, X = Cl, Br, I; n = 4 – 5, X = Br, I) [25]. These types of complexes are known to be useful precursors to the preparation of ruthenium-containing heterobimetallic compounds, again this will be seen shortly [48].

Harrison and Stobart reacted $[(\mu\text{-pz})(CO)_2Ir]_2$ with $I(CH_2)_3I$ to form a stable μ-iodoalkyl complex $[(\mu\text{-pz})_2(CO)_4Ir_2(I)\{(CH_2)_3I\}]$ [49].

Scott and Puddephatt synthesized the adducts **18a-d** shown in Scheme 1.4, by reacting $[Me_2(bipym)Pt]$ (bipym = 2,2'-bipyrimidine) with excess $I(CH_2)_nI$ [50].

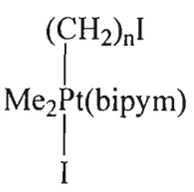

18

Compound	n
a	3
b	4
c	5
d	6

Scheme 1.4: Molecular formulae of compounds **18**.

The adducts were found to easily react with $[Me_4(\mu\text{-}SMe_2)_2Pt_2]$ to give compounds $[Me_4(\mu\text{-bipym})Pt_2(I)\{(CH_2)_nI\}]$ **19a-d** and not the expected compounds $[Me_4(\mu\text{-bipym})Pt_2(I)_2\{(\mu\text{-}CH_2)_n\}]$ **20** (Scheme 1.5).

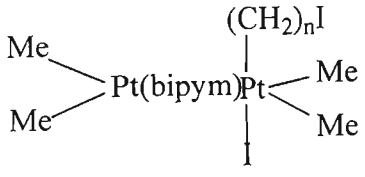

19

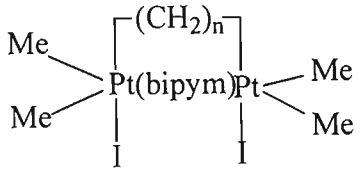

20

Compound	n
a	3
b	4
c	5
d	6

Scheme 1.5: Molecular formulae of compounds **19** and **20**

The Pt(II) centre is reported to experience a ring strain and/or steric hindrance in the transition state, that prevents it from participating in the intramolecular oxidative addition which is taking place [46].

Also, the adducts **18**, undergo intermolecular oxidative addition with [Me_2(bipym)Pt] to give compounds **21** as represented in Scheme 1.6.

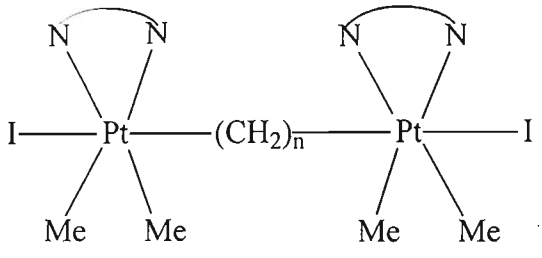

Compound	n
a	3
b	4
c	5
d	6

Scheme 1.6: Molecular formulae of compounds **21**

The oxidative addition of diiodoalkane to [(μ-pyen)Me_4Pt_2] **22** gave the iodoalkyl compounds [(μ-pyen)$Me_4Pt_2(I_2)\{(CH_2)_nI\}_2$] (n = 3 – 6) **23**. The reaction pathway when **22** was reacted with $I(CH_2)_5I$ proceeded via the formation of the intermediate [(μ-pyen)$Me_4Pt_2(I_2)I\{(CH_2)_5I\}$] **24**. Unfavourable conformational effects were cited to be the reasons for the failure of the intermediate **24** to undergo an intramolecular oxidative addition forming the expected μ-polymethylene compound [51].

The halogenoalkyl compounds of the type [(Co)$\{(CH_2)_nX)\}$] (Co) = Vitamin B_{12} (n = 3, X = Br, Cl; n = 4, X = Br), were reportedly prepared from the reaction of vitamin B_{12} with

the respective dihaloalkanes [3c]. When n = 4, the compound $[(Co)\{(CH_2)_4X)\}]$ was obtained as a minor product, and the μ-polymethylene homobimetallic compound $[(Co)(CH_2)_4(Co)]$, was obtained as the major product.

The monoanion of dimethylglyoxime halogenoalkyl complexes of the type $[Co(DH)_2py\{(CH_2)_nX)\}]$ have been reported [3c]. Their preparations follow Equation 7 below. Also, these compounds can serve as important utilities in organic synthesis.

$$[Co(DH)_2pyCl] + X(CH_2)_nX \xrightarrow{MeOH,\ NaBH_4} [Co(DH)_2py\{(CH_2)_nX)\}] \quad (7)$$

X = Br, n = 3 – 7; X = I, n = 3

The halogenoalkyl complexes of the type $[Rh(TPP)\{(CH_2)_nX\}]$ **25** {(X = Br,Cl, n = 3 – 5); X = I, n = 3 – 6); TPP = dianion of tetraphenylporphyrin} have been reported [52]. Their electrochemical behaviour was investigated. The nature of the species $(-CH_2)_nX$ present in the complex was found to dictate the observed overall electrochemical behaviour.

Collman and co-workers synthesized a macrocyclic halogenopropyl rhodium (I) complex as shown in Equation 8 below [53].

$$2[Rh\{E\}]^{+l} + X(CH_2)_nX \longrightarrow [Rh\{E\}(X)\{(CH_2)_nX\}] \quad (8)$$

$\{E\} = \{C_2(DO)(DOBF_2)_{pn}\}$

= {difluoro(N,N'-bis(3-pentanon-2-ylidene)-1,3-diaminopropane dioximato)borate}

X = Br, Cl, I, (n = 2, 3)

This group also discussed from their reactivity investigations, that the ratio of the mononuclear to binuclear products they obtained was always solvent dependent. Also, the solubility of the macrocyclic $[Rh\{E\}]^{+l}$ complexes themselves led to variations in the product ratios in different solvents [53].

In 1993, Zhou and Gladysz reported that the reaction of $Na[(CO)_5Re]$ with $I(CH_2)_4I$ in THF yielded $[(CO)_5Re\{(CH_2)_4I\}]$ [54]. This was done with a view to synthesizing μ-halogen bimetallic halogenoalkyl complexes having the iodide ion further away from the rhenium atom. Complexes having this type of structure were discovered to possess an enhanced stability [53].

Yin and Moss reported the preparation and properties of ω-halogenoalkyl compounds $[Cp(CO)_3W\{(CH_2)_nX\}]$ (n = 3 – 7, X = Br,I) and $[Cp^*(CO)_3W\{(CH_2)_nX\}]$ (n = 3, 4, X = Br,I). These compounds were synthesized by the reaction of $Na[Cp(CO)_3W]$ or $Na[Cp^*(CO)_3W]$ with appropriate dibromoalkanes, or diiodoalkanes. The compounds were shown to be again, good precursors to the preparation of binuclear complexes (see compound **34**) [55].

Most recently, we have reported on the synthesis and properties of halogenoalkyl compounds $[Cp(CO)_2(PPh_iMe_{3-i})Mo\{(CH_2)_nBr\}]$ (n = 3, 4; i = 0 – 3) and $[Cp^*(CO)_3Mo\{(CH_2)_nBr]$ (n = 3, 4) [56, and this thesis]. The new complexes were prepared as generally represented in Equation 9.

$$Na[CpMo(CO)_2L] + Br(CH_2)_nBr \longrightarrow [Cp(CO)_2LMo\{(CH_2)_nBr\}] + NaBr \qquad (9)$$

n = 3 – 4; L = PPh_3, PPh_2Me, $PPhMe_2$, PMe_3

The iodoalkyl derivatives of these compounds were prepared by reacting the corresponding bromoalkyl compounds with NaI, in a similar manner as detailed in Equation 6 above.

Contrary to the general expectations, we reacted $Na[Cp(CO)_3W]$ with excess $Br(CH_2)_nBr$ (n = 3 – 6) under reflux in THF to give the compounds $[Cp(CO)_3W\{(CH_2)_nBr\}]$ in high yield, confirming that the anion $[Cp(CO)_3W]^-$ is a significantly weaker nucleophile than the cyclopentadienyldicarbonyl anions of iron and ruthenium [57]. The reaction follows Equation 9 above and the corresponding iodoalkyl derivatives were again generated in similar manner to Equation 6 [56, and this thesis].

Friedrich and Moss, in the first ever review to appear on halogenoalkyl complexes of transition metals, reported no molecular structure for halogenoalkyl compounds of the type $[L_yM\{(CH_2)_nX\}]$, where n > 1 [3c]. A decade later, we still find no such type of structures reported, except those of $[Cp(CO)_2(PPh_3)Mo\{(CH_2)_3I\}]$, $[CpCO)_3W\{(CH_2)_3Br\}]$ and $[CpCO)_3W\{(CH_2)_5I\}]$ recently reported by us [56, and this thesis].

In general, these compounds were very useful as precursors of new heterodinuclear alkanediyl complexes, as will be seen later. We now review some of the binuclear alkanediyl complexes reported in the literature, with a major focus on ω-methylene bridged heterodinuclear species.

1.2.2 Heterodinuclear Transition Metal Alkanediyl Compounds

Heterodinuclear transition metal alkanediyl compounds are compounds which contain two different transition metal centers joined together by a hydrocarbon chain. These metal centers could be either directly bonded to one another and to the alkyl group as in Figure 1.2 **A** or through an alkyl bridge only (Figure 1.2 **B**).

Figure 1.2: Bonding in heterodinuclear alkanediyl complexes

The complexes of Figure 1.2 **A** are called dimetallocycloalkanes while those of Figure 1.2 **B** are simply termed polymethylene bridged compounds [58]. These complexes are of general interest as they may be used as possible study models for surface intermediates in various metal-catalysed industrial reactions such as the Fischer Tropsch process, Ziegler-Natta polymerizations [31a] or platinum-catalysed hydrocarbon rearrangements [31b].

Most of the early work in the area of alkanediyl compounds, which is well covered in a review by Moss and Scott [54], involved homobimetallic complexes, and these were either monomethylene or ethylene bridged. The earliest synthesized heterodinuclear compounds had ethylene bridges. They were prepared by nucleophillic addition of the metal anion to a cation of an ethylene complex as shown in Equation 10 [59].

$$[Cp(CO)_3Mo(C_2H_4)]^+ + Na[Cp(CO)_3W] \longrightarrow [Cp(CO)_3Mo(CH_2)_2W(CO)_3Cp] \qquad (10)$$

Similar compounds to the above that have been reported include $[Cp(CO)_3M(CH_2)_2Re(CO)_5]$ (M = Mo (**26**), W (**27**) [55]. Compound **26** was reportedly

stable below -15 °C while **27** up to +20 °C. This property was attributed to the difference in bond strength between Mo–C and W-C, which is greater for the latter. The Re–C bond is known to be much stronger than both of the above [60]. The compound $[(CO)_5Re(CH_2)_2Mn(CO)_5]$ was prepared in a similar manner to the above and reported [61].

In 1967, King and Bisnette reported on an attempt to synthesize polymethylene bridged compounds of the type $[L_xM(CH_2)_nM'L_y]$ ($M \neq M'$, L_xM and $M'L_y$ are transition metals and the associated ligands) containing two different transition metal atoms [36]. They reacted $[Cp(CO)_3Mo\{(CH_2)_nBr\}]$ **4** (n = 3 – 4) with $Na[Cp(CO)_2Fe]$ and $Na[(CO)_5Mn]$ in THF. Only the homobinuclear compounds, methylene bridged $[\{Cp(CO)_2Fe\}_2\{\mu\text{-}(CH_2)_n\}]$ (n = 3 – 4) and the metal-metal bridged $[(CO)_5MnMn(CO)_4\{CO(CH_2)_2CH_2\}]$ **28** which was later shown to be a cyclic carbene, were obtained [37]. Also, Winter and co-workers later showed that **4** reacts with $Na[Cp(CO)_3W]$ to give $[Cp(CO)_2(Br)MoC(O)(CH_2)_2CH_2W(CO)_3Cp]$ [13]. However, the reaction of compound **4** with a more reactive species, namely $Na[(CO)_5Mn]$, gave exclusively the dimanganese species **28** and $Na[Cp(CO)_2Fe]$ gave $[\{Cp(CO)_2Fe\}_2\{\mu\text{-}(CH_2)_3\}]$. In both reactions, the $Cp(CO)_3Mo$- moiety was eliminated. On the other hand, the anion $Na[Cp(CO)_3W]$ displaces the bromide ion from $[Cp(CO)_3W\{(CH_2)_nBr\}]$, instead of reacting with the compound at the tungsten centre as might be expected and forms the dimetallapropane compound $[\{Cp(CO)_3W\}_2\{\mu\text{-}(CH_2)_3\}]$ **29** in moderate yield [13]. In a similar manner, the anion $Na[Cp(CO)_3W]$ reacts with diidobutane in THF to give **29** via the monohalogenoalkyl intermediate $[Cp(CO)_3W\{(CH_2)_4I\}]$. Also, the molybdenum analog of **29** $[\{Cp(CO)_3Mo\}_2\{\mu\text{-}(CH_2)_3\}]$ is prepared in similar manner, involving the monohalogenoalkyl intermediate $[Cp(CO)_3Mo\{(CH_2)_4I\}]$ [13]. In contrast to the latter reaction, the analogous Cp* compound $[Cp^*(CO)_3Mo\{(CH_2)_3Br\}]$ reacts with $Na[Cp(CO)_2Fe]$ to give $[Cp^*(CO)_3Mo(CH_2)_3Fe(CO)_2Cp]$ [14]. Again, as explained above, this is because the Cp* contain the methyl substituents constantly piling their electrons into the ring creating a stronger nucleophillic complex than the Cp analog.

Moss reacted $[Cp(CO)_2Fe\{(CH_2)_3Br\}]$ with $Na[Cp(CO)_3Mo]$ and achieved the expected product $[Cp(CO)_2Fe(CH_2)_3Mo(CO)_3Cp]$, though in low yield [3f]. This reaction proceeded when the reaction condition was changed from room temperature to reflux; the reaction is shown in Equation 11.

$$[Cp(CO)_2Fe\{(CH_2)_3Br\}] + Na[Cp(CO)_3Mo] \xrightarrow{\Delta} [Cp(CO)_2Fe(CH_2)_3Mo(CO)_3Cp] + NaBr \quad (11)$$

Friedrich *et al.* have reported the synthesis of many heterobimetallic alkanediyl complexes of the type $[(\eta^5\text{-}C_5R_5)(CO)_2Fe(CH_2)_nML_y]$ **30** (R = H, ML_y = $[Cp(CO)_2Ru]$, $[Cp(CO)_3Mo]$, $[Cp(CO)_3W]$, $[(CO)_5Re]$, n = 3 – 6; R = CH_3, ML_y = $[Cp(CO)_2Ru]$, n = 3 – 5; ML_y = $[(CO)_5Re]$, n = 4 [17,45]. These syntheses were generally achieved as shown in Equation 12.

$$[Cp(CO)_2Fe\{(CH_2)_nX\}] + Na[ML_y] \longrightarrow [Cp(CO)_2Fe(CH_2)_nMLy] + NaX \quad (12)$$

These were prepared by a different method to that shown in Equation 11, in that the bromoalkyl compounds were first converted into iodoalkyl compounds, before being used in further reactions to prepare the heterodinuclear compounds. The reagents for the preparation of these bimetallic complexes were added together at -78 °C, and then the solution was allowed to warm to room temperature, giving medium to high yields of products. This route to the preparation of binuclear complexes has since proved to be the most viable.

The preparative methods for hydrocarbon bridged complexes has been comprehensively surveyed and outlined by Beck *et al.* [3b]. A few of the relevant techniques will be discussed below:

1.2.2.1 General Addition Reactions

These are achieved by the addition of suitable organometallic nucleophiles to π-coordinated hydrocarbons in cationic complexes. The anions used contain a relatively high degree of nucleophilicity [62], resulting in the formation of a compound with a M-C σ-bond that is stable [63], an example is shown in Scheme 1.7.

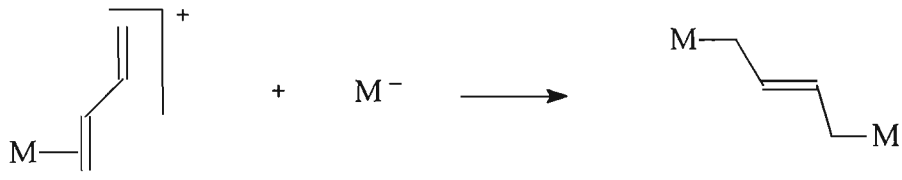

Scheme 1.7: A general addition reaction of organometallic nucleophile M^- to π-bound hydrocarbon in a cationic complex

Some heterodinuclear complexes synthesized in a similar manner have been described above (see compounds **26**, **27**).

1.2.2.2 Reactions of Metal Complexes Containing an Anionic Hydrocarbon Ligand with Halo-Complexes

Several compounds containing σ,π-bridged complexes can be synthesized by the reaction of a lithiated species with halometal complexes. A fascinating compound such as the trimetallic compound **31**, shown in Scheme 1.8 below, may be obtained by this method. Lithiation of the dimetallic complex $[Cp(CO)_2Fe\text{-}(\eta^1\text{:}\eta^5\text{-}C_5H_4Mn(CO)_3]$ with BuLi, followed by a subsequent reaction with $[Cp(CO)_2FeI]$ forms compound **31** [64].

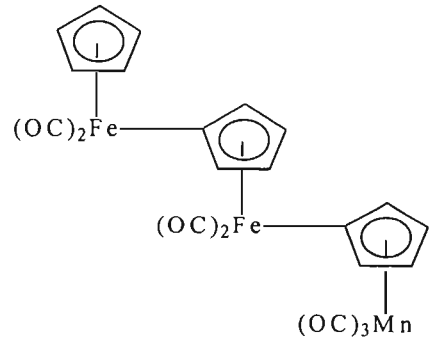

Scheme 1.8: The structure of the trimetallic compound **31**

1.2.2.3 Substitution of Halogen or Triflate Substituents in Hydrocarbons by Nucleophillic Complexes

Many homodinuclear μ-polymethylene complexes have been prepared by this method. King, Lindner, Moss, and Puddephatt in their effort to prepare compounds that could act as

models for hydrocarbons bound to the surface of metal catalysts, made use of this technique [65]. The compounds were synthesized by the reaction of α,ω-dihaloalkanes with carbonyl metallate nucleophiles as represented in Equation 13.

$$X(CH_2)_nX + 2[L_xM]^- \longrightarrow [L_xM(CH_2)ML_x] \quad (13)$$

X = Br, ML_x = $Cp(CO)_2Fe$ (n = 3 – 6) [66]; X = Br, I, ML_x = Co(DH)(pyridine) (n = 3 – 7) [67]; X = I, OSO_2CF_3, ML_x = $Cp(CO)_3Mo$, $Cp(CO)_3W$, (n = 4 – 5, 10) [13,68]; X = OSO_2CF_3, ML_x = $(CO)_5Mn$, (n = 2 – 6, 10) [62c,64-69]; X = OSO_2CF_3, ML_x = $(CO)_5Re$, (n = 2 – 5, 10) [64,65a,70]; X = OSO_2CF_3, ML_x = $Cp(NO)(PPh_3)Re$, (n = 3 – 5, 8) [71].

The heterobimetallic compounds of type **30**, above, were prepared by the reaction of ω-iodoalkyl complexes with carbonylmetalate anions. In this reaction, the carbonylmetalate anion displaces the iodine of the iodoalkyl complex, forming the heterobimetallic complexes as shown in Equation 12 above [17,45]. This method was also successfully used in the preparation of the cobaloxime compounds containing ω-hydrocarbon bridges; $[py(DH)Co(CH_2)_nCo]$ n = 4 – 8 [63a].

Other synthetic pathways which are covered in the review by Beck *et al.* include; Reactions of dianionic hydrocarbons with metal complexes, Insertion reactions, preparation of complexes with C_n bridges and the organometallic polymers with hydrocarbon bridges [3b].

Most recently, Wheatley and Kalck reviewed the structure and reactivity of the early to late heterobimetallic complexes [72]. They summarized the methods used for the synthesis of these compounds as involving metathesis of a halide ligand with an organometallic anion. The most common reaction of choice is the replacement of the halide ligand on a group 4 metal by an anionic complex such as $Na[Cp(CO)_2M]^-$ (M = Fe, Ru) [73] or $[(OC)_4M]^-$ (M = Co, Rh) [69b,69c,74]. The heterobimetallic compounds of lanthanide group [75] and group 6 metals have also been reported to be formed in a similar manner [76].

The formation via an oxidative addition reaction, of the μ-Polymethylene heterobimetallic complexes of the type $[L_xM(CH_2)_nPtI(N\text{-}N)Me_2]$ **32** (L_xM = $Cp(CO)_3W$ (n = 3 – 5), $Cp^*(CO)_3W$ (n = 3 – 4), $Cp(CO)_2Fe$ (n = 4), $Cp^*(CO)_2Fe$ (n = 4), $Cp(CO)_2Ru$ (n = 4),

$(OC)_5Re$ (n = 4), have been reported [18]. In general, the reactions proceed according to Equation 14 to give complexes **32** in high yields.

$$[L_xM\{(CH_2)_nI\}] + [(N\text{-}N)Me_2Pt] \longrightarrow [L_xM(CH_2)PtI(N\text{-}N)Me_2] \qquad (14)$$

In this thesis we will report on new heterobimetallic complexes $[Cp(CO)_3W(CH_2)_nMo(CO)_3Cp]$ n =3 – 6; $[Cp(CO)_3W(CH_2)_nMo(CO)_3Cp^*]$ n = 3,4;$[Cp(CO)_3W(CH_2)_nMo(CO)_2(PPh_iMe_{3-i})Cp]$ n = 3,4 i = 0 – 3 and $[Cp(CO)_2 Fe(CH_2)_nMo(CO)_2(PPh_iMe_{3-i})(Cp]$ n = 3,4 i = 0 – 3. We will also report on the synthesis of $[Cp(CO)_2 Fe(CH_2)_nMo(CO)_3Cp^*]$ n = 3,4 [77]. All the complexes were synthesized by the direct displacement of the iodine of a iodoalkyl compound.

1.3 Some Reactions Studies on the Transition Metal Functionalized Paraffins

Reaction studies on the halogenoalkyl compounds were shown above together with their synthesis. We will, therefore, mainly discuss the reactions of binuclear complexes with some simple inorganic molecules, as documented in the literature. For example, the methylene bridged complex $[ClMe_2(bipy)PtCH_2Au(PPh_3)]$ (bipy = 2,2'-bipyridine) reacted with electrophiles HCl, Cl_2 and $HgCl_2$ by selective cleavage of the Au–C bond, resulting in $[Cl(PPh_3)Au]$ and $[(bipy)ClMe_2Pt(CH_2Y)]$, Y = H, Cl or HgCl [78].

King and Bisnette reacted triphenylcarbeniumhexafluorophosphate with the compounds $[\{Cp(CO)_2Fe\}_2(\mu\text{-}CH_2)_3]$ **33**, and obtained the orange cationic complex $[\{Cp(CO)_2Fe\}_2(\mu\text{-}C_3H_5)][PF_6]$ **34** [36]. The behaviour of this compound **34** in solution was later investigated by Moss *et al.* and shown to be fluxional [79]. This dynamism was established by a ^1H NMR spectroscopy study. Further, a crystal structure analysis of **34** showed that it exists as a transition metal stabilized carbonium ion with the positive charge located on the central carbon atom of the three carbon chain [30]. The iron atoms were shown to be weakly linked to the β-CH group of the allylic system as shown in Scheme 1.9.

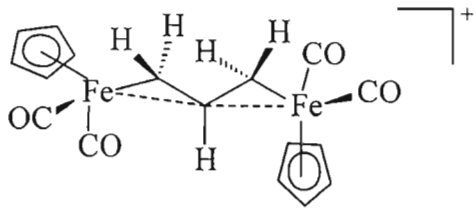

Scheme 1.9: Schematic diagram for the allylic system of compound 34

Amongst the major interests of inorganic and organometallic chemists, is the use of sterically crowding ligands to manipulate reactivity and effect stabilization of otherwise unknown and unstable compounds [80]. If only Sachse, and later Mohr, had never questioned Baeyer's assumption that all cyclic structures were planar, we may not be talking about 'bulk crowding' as a rationalization for the distortion of planarity today [81]. Coville and White have profoundly detailed the quantification of steric sizes [80]. Two general methods for the determination of steric size are presented, either chemical properties (Taft-Dubois steric parameter) or physical properties (cone angle, solid angle and ligand repulsive angle). The latter approach has been adopted by the inorganic chemists and the former, by the organic chemists [80]. Much earlier, in 1977, Tolman had specifically comprehensively reviewed the effect of phosphorus and its derivatives in organometallic chemistry based on their steric factors [82]. The phosphorus atom is capable of forming multiple bonds and contains a lone pair that makes it act as a soft acid [83a]. The ability of the phosphorus as a ligand to compete for coordination positions could not be explained in terms of electronic factors alone. This led to the advent of ligand cone angles. The ligands such as $P(OCH_2)Me$ (114°), PMe_3 (118°), $P(OPh)_3$ (128°), PPh_3 (145°), PCy_3 (170°) and $P(t\text{-}Bu)_3$ (182°) were reported to show a decreasing binding ability in that order. These ligands had their angles (in parenthesis) that they subtend from the central metal measured and later became known as Tolman cone angles [82] (See Figure 1.3).

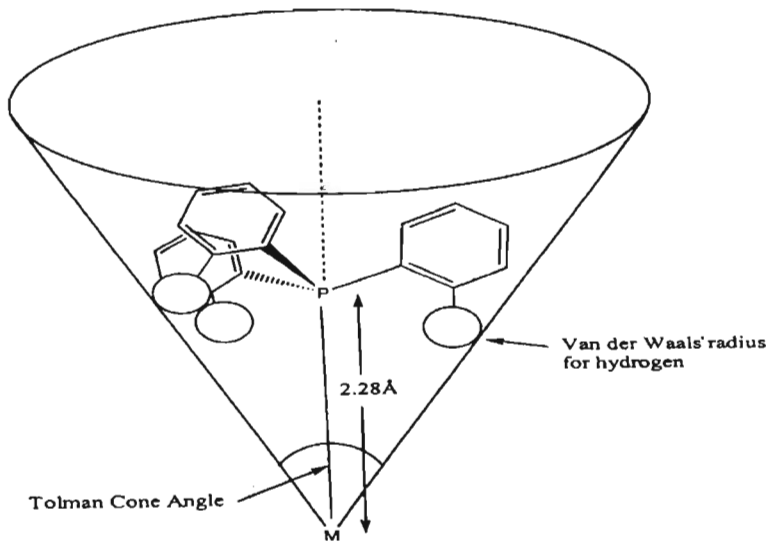

Figure 1.3: Illustration of the definition of the Tolman cone angle for a typical aryl phosphine ligands [83b]

Reger and Culbertson studied the thermolysis of $[Cp(CO)(PPh_3)Fe\{(CH_2CH_2CH_2CH_3)\}]$ **35**, and found that its decomposition in xylene at 61 °C takes place via a loss of the PPh_3 ligand reversible β-hydride elimination, and dissociation of butenes [84]. In contrast to this mononuclear compound, the thermolysis of the diiron complex **33** at 125 – 196 °C in toluene gave 1:5.3 – 10.6 ratio of propene:cyclopropane. The C–C bond formation leading to the cyclopropane distinguishes this bimetallic system from the decomposition of the related mononuclear alkyl compounds [62b]. The same group observed that photolysis of **33** gives a much higher ratio of propene:cyclopropane. This was postulated to occur through the same diiron cyclopentane intermediate as proposed for the previous reaction except that in this case the intermediate undergoes a further photolysis reaction with the loss of a second CO group. A coordinatively unsaturated intermediate therefore results, which then undergoes a β-hydride elimination forming propene. When the β-hydride elimination was blocked by using a methyl group, only a single product, cyclopropane, was obtained [85].

More comprehensive reaction studies on heterodinuclear alkanediyl complexes were reported by Friedrich and Moss [86]. The heterobimetallic complex $[Cp(CO)_2Fe(CH_2)_3Mo(CO)_3Cp]$ **36**, reacted with the neutral molecules L (PPh_3 or $PPhMe_2$) in acetonitrile to give monoacyl species $[Cp(CO)_2Fe(CH_2)_3C(O)Mo(CO)_2LCp]$ **37** as shown in Equation 14.

$$[Cp(CO)_2Fe(CH_2)_3Mo(CO)_3Cp] + L \longrightarrow [Cp(CO)_2Fe(CH_2)_3C(O)Mo(CO)_2LCp] \quad (14)$$

The reaction was observed to be metalloselective, with the phosphines attacking only the molybdenum site. However, varying the length of the μ-methylene chain was reported not to affect the product obtained. Complex **36** was reacted with CO gas in acetonitrile, again the attack took place on the molybdenum site forming $[Cp(CO)_2Fe(CH_2)_3C(O)Mo(CO)_3Cp]$ **38**. The observations were compared to their mononuclear alkyl derivatives, where molybdenum alkyl complexes were found to undergo CO insertion/alkyl migration reactions more readily than the iron analogues [87]. The compound $[Cp(CO)_2Fe(CH_2)_3Ru(CO)_2Cp]$ was reacted with PPh_3 in tetrahydrofuran under reflux, to give the compound $[Cp(CO)_2FeC(O)(CH_2)_3Ru(CO)_2Cp]$ **39** as the product [86]. Thus, the nucleophile PPh_3 attacked compound **39** on the iron site. This was a

confirmation of an observation seen in earlier reactions, *i.e.* iron carbonyl alkyl compounds had been reported to undergo insertion reactions with tertiary phosphines [87b, 87c], while the corresponding ruthenium complexes are known to do so reluctantly [88]. Comparing the reactivity of PPh_3 with $[Cp(CO)_2Fe(CH_2)_3Ru(CO)_2Cp]$and $[\{Cp(CO)_2Fe\}_2\{\mu\text{-}(CH_2)_3\}]$ in refluxing tetrahydrofuran, Friedrich and Moss reported that the former reaction was complete first. They then proposed that the observations suggested that the iron compound was slightly activated towards the phosphine's attack by the Ru atom present in the same molecule [86].

The generally predictable metalloselectively observed above was fascinating, because it differed with what was known to take place on heterobimetallic compounds with direct metal-metal bonds, where the site of nucleophillic attack was not always predictable [89].

The reactions of various heterobimetallic complexes with trityl salt were also reported, the behaviour of the products was shown to follow a similar pattern much similar to that of compound **34** in Scheme 1.9. A proposed structures of the compounds are summarized in Scheme 1.20 below [86].

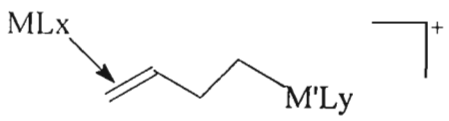

ML_x	$M'L_y$
$Cp(CO)_2Fe$	$Cp(CO)_3Mo$
$Cp(CO)_2Fe$	$Cp(CO)_2Ru$
$Cp(CO)_2Ru$	$Cp(CO)_2Fe$
$Cp(CO)_2Fe$	$Cp(CO)_3W$
$Cp(CO)_2Fe$	$Cp(CO)_2Fe$

Scheme 1.20: Proposed structures of the heterobimetallic cationic complexes

These complexes were believed to have structures as depicted in Scheme 1.20, in which one iron atom is π-bonded and the other σ-bonded to the alkyl chain.

The compound $[Cp(CO)_2Fe(CH_2)_5Ru(CO)_2Cp]$ was reacted with I_2 in dichloromethane at 0 °C, and the cleavage products $[Cp(CO)_2FeI]$, $[Cp(CO)_2RuI]$ and trace of $I(CH_2)_5I$ were obtained.

1.4 Crystal Structures of Binuclear Compounds of type $[L_xM(CH_2)_nML_y]$, n >1

A number of X-ray crystal studies have been carried out on the homobinuclear compounds, and some of the results are summarized in Table 1.1 below. Some of the structures show novel features. As yet, no molecular structure has been reported for a heterobimetallic compound of the type $[L_xM(CH_2)_nM'Ly]$, n >1 ($M \neq M'$).

Table 1.1: M–C and C–C bond lengths of some homobimetallic structures

Compound	M–C bond length (Å)	C–C bond length (Å)	Ref.
$[(Cp(CO)_3Mo)_2(\mu\text{-}(CH_2)_4)]$	2.356 (4)	1.53	*13*
$[(Cp(CO)_2Fe)_2(\mu\text{-}(CH_2)_3)]$	2.08 (3)	1.54	*30*
$[(Cp(CO)_2Fe)_2(\mu\text{-}(CH_2)_4)]$	2.08 (12)	1.55	*30*
$[(CO)_5Re)_2(\mu\text{-}(CH_2)_2)]$	1.52 (17)	1.52	*90a*
$[(Cp(CO)_2Ru)_2(\mu\text{-}(CH_2)_5)]$	2.17 (9)	1.54	*90b*

1.5 Outline of the Project

Organometallic materials containing saturated or unsaturated hydrocarbon bridges are emerging as interesting new materials for use in advanced technologies. Model catalytic compounds, molecular wires, liquid crystal and nonlinear optical materials have all been touted as potential uses of these materials. Lately, the extensive use of organometallic complexes in organic synthesis has become apparent and therefore the need exists for the efficient synthesis of numerous exotic organometallic complexes [91].

Transition metals are known good catalysts for industrially important catalytic reactions such as Fischer-Tropsch, which is operated as a whole division of its own in South Africa (SASOL and Mossgas), Malaysia (Shell) and in Russia. Metal alkyl species on the transition metal catalyst surface are reported to be key intermediates in the Fischer-Tropsch technology, and since it is difficult to study the homo- and heterogeneous catalyst surfaces, model compounds can be used which contain alkyl groups [29]. From a study of these model compounds one can achieve a better understanding of the mechanisms of important catalytic reactions with the hope of developing more selective and efficient catalysts.

King and Bisnette, back in 1967, thought of funtionalised metal alkyl compounds as synthetically valueless, this has of late been shown to be untrue, because these compounds provide an opportunity to carry out chemistry at the functional group as well as at the metal end of the molecule. Despite the ω-halogenoalkyl compounds being promising intermediates for carrying out chemistry at the ω-carbon atom remote from the metal center, relatively few compounds of the type $[L_yM\{(CH_2)_nX\}](n > 3)$ were known until recently, as has been discussed above [29]. Molybdenum halogenoalkyl compounds are far much less known than their tungsten analogs in the literature. Very few phosphine substituted compounds $[Cp(CO)_2LMo(CH_2)_nX]$ (L = tertiary phosphine or phosphite) have been reported. Only compounds where L = $(OPh)_3P$) and X = Br, Cl and I where n = 1 are known [92]. The only previously reported long-chain halogenoalkyl compounds of molybdenum are $[Cp(CO)_3Mo\{(CH_2)_nX\}]$ (n = 3, X = Cl, Br, I; n = 4, X = Br, I), $Cp^*(CO)_3Mo\{(CH_2)_3Br\}]$ and $[Cp(CO)_2(PPh_3)Mo\{(CH_2)_3Br\}]$ [13,14,39,47], this shows how little has been done in this area and thus justifies any further investigations on similar compounds to them. With the availability of ω-halogenoalkyl complexes, especially the

iodoalkyl type, there exists an opportunity to synthesize heterodinuclear alkanediyl complexes as has been achieved by the different research groups cited in the literature.

Heterodinuclear complexes present a yet more stimulating study opportunity for the metal alkyl complexes by having two active sites. The imagination that both of these sites, though different, would be available as catalyst surfaces for industrial reaction studies, should help justify their preparation. Thus one metal may influence the chemistry of the other at the other end of a paraffin chain. Many heterobimetallic catalysts have been reported to be superior in activity, selectivity and efficiency to catalysts derived from either of the respective monometallic components. Consequently we proposed to prepare heterodinuclear compounds which may be useful as models for catalytic intermediates, as catalysts precursors or as catalysts themselves. Since different metals also have different potentials, heterodinuclear compounds with suitably semi- or conjugated ligands may also find application as molecular switches or one-dimensional conductors.

Moss and Scott reported that the reactions of the polymethylene bridged complexes with tertiary phosphines showed the reaction rate being dependent on the length of the chain [93]. Friedrich and Moss later reported that this type of reaction was after all independent of the length of the alkyl chain [86]. We wished to investigate these conflicting reports.

Synthesis and reactivity studies in organometallic chemistry have traditionally been carried out in organic solutions. Equivalent studies, however, can also be carried out in the solid state, and this type of work has been very recently reviewed by Coville and Cheng [91]. All the syntheses and reactivity studies in this thesis will be carried out in solution as tradition demands. Previous work has shown that iodoalkyl compounds of iron (II) can be reacted with a variety of transition metal anions to form heterodinuclear compounds in high yields as shown in Equation 15 below [17].

$$[Cp(CO)_2Fe\{(CH_2)_nI\}] + NaML_y \longrightarrow [Cp(CO)_2Fe(CH_2)_nML_y] + NaI \qquad (15)$$

$ML_y = Cp(CO)_3W$, $Cp(CO)_3Mo$, $(CO)_5Re$, $Cp(CO)_2Ru$, n = 3 – 6

We will exploit this technique, which has been proven to be the most viable, and apply it to other metal and ligand systems, with the aim of preparing a wider variety of compounds with different properties. Thus the compounds $[Cp(CO)_3W(CH_2)_nBr]$ (n = 3 – 6) will be

prepared, of which the compounds where n = 5 and 6 will be new. The previous route to the compounds where n = 3 and 4 gave the compounds in low yield and we will work towards improving these reported low yields. The preparation of the new compounds will follow Equation 16 below. This work will be extensively discussed in Chapter 2.

$$Na[Cp(CO)_3W] + Br(CH_2)_nBr \longrightarrow [Cp(CO)_3W\{(CH_2)_nBr\}] + NaBr \quad n = 3 - 6 \qquad (16)$$

The bromoalkyl compounds will subsequently be converted to the iodo-derivatives since iodide ion has been shown to be a superior leaving group to bromide (Equation 17).

$$[Cp(CO)_3W\{(CH_2)_nBr\}] + NaI \longrightarrow [Cp(CO)_3W\{(CH_2)_nI\}] \quad n = 3 - 6 \qquad (17)$$

These iodo compounds will be used as precursors to tungsten containing heterodinuclear compounds (Equation 18), and further reactions to give compounds with different transition metals, ligand patterns and chain lengths are planned and will be discussed in Chapter 4.

$$[Cp(CO)_3W\{(CH_2)_3I\}] + Na[Cp(CO)_3Mo] \longrightarrow [Cp(CO)_3W(CH_2)_3Mo(CO)_3Cp] \qquad (18)$$

Previous work has shown that the reactions of the Fe/M (metal center different from iron) compounds in Equation 15 above undergo metalloselective reactions in most cases. No conclusive proof of intermetallic communication was obtained; however, similar experiments to determine if the W/M (metal center different from tungsten) compounds react metalloselectively or whether there is communication between the metals are planned. For example, a reaction which particularly interests us, would be the reaction of the W/M and or Fe/M (Cp*) compounds with Ph_3CPF_6 (trityl salt) as depicted in Equation 19.

$$[Cp(CO)_3W(CH_2)_nMo(CO)p] + Ph_3CPF6 \longrightarrow [Cp(CO)_3W(CH_2)_{n-2}(CHCH_2)Mo(CO)p]PF_6 \qquad (19)$$

Whilst we would expect a hydride to be abstracted from a β-C to a metal, it is not clear which side would be attacked. The resulting product would have a more conjugated carbon chain, perhaps enhancing the possibility of intermetallic communication. By using

heterobimetallic compounds bridged by bidentate and tridentate phosphine ligands as catalysts, Rida and Smith showed that two or more metal centers can cooperate during the homogenous catalysis of the hydroformylation of alkenes [94]. This investigation and its findings are both reported in Chapter 4.

I found this piece of information by Akio Yamamoto very touching: "Handling very air-sensitive compounds requires great patience because of many precautions that have to be taken. A split of a second of carelessness may instantly destroy an important sample that has been synthesized with painstaking effort. It is, however, through these failures, disconcerting as they may be that an organometallic chemist is trained to perfection. If we think of the difficulties and risk that Frankland and his co-workers encountered in handling inflammable alkylzinc compounds over a century ago, one can only wonder at how they worked. How did they cope with the dangerous compounds that spontaneously catch fire on contact with air and react with water explosively using such rudimentary apparatus? Frankland describes in his report how he distilled dimethylzinc in an apparatus filled with dry hydrogen (!) in Bunsen's laboratory. When he tried the action of water on the residue, a greenish-blue flame several feet high shot out of the tube and diffused an abominable odour throughout the laboratory. We also wonder how Zeise reached the correct formulation of his platinum-ethylene complex when none of the modern experimental techniques, such as X-ray crystallography, gas chromatography, IR, NMR and mass spectroscopy, was available" [95]. We are indeed very ready to venture into this field and share the experiences of the challenging work that organometallic chemistry poses.

1.6 References

[1] (a) J.S. Thayer, *Adv. Organomet. Chem.*, **13** (1975) 1.

(b) G. Wilkinson, *J. Organomet. Chem.*, **100** (1975) 273.

[2] A. de Meijere, *Chem. Rev.*, **100** (2000) 1.

[3] (a) N. Wheatley, P. Kalck, *Chem. Rev.*, **99** (1999) 3419.

(b) W. Beck, B. Niemer, M. Wieser, *Angew. Chem. Int. Ed. Engl.*, **32** (1993) 923.

(c) H.B. Friedrich, J.R. Moss, *Adv. Organomet. Chem.*, **33** (1991) 235.

(d) J.P. Colman, L.S. Hegedus, J.R. Norton, R.G. Finke, "Principles and Applications of Organotransition Metal Chemistry", University Science Books, Sausalito, California 1987.

(e) C.P. Casey, J.D. Audett, *Chem. Rev.*, **86** (1986) 339.

(f) J.R. Moss, *J. Organomet. Chem.*, **231** (1982) 229.

(g) R.R. Schrock, G.W. Parshall, *Chem. Rev.*, **76** (1976) 243.

(h) D.P. Davidson, M.F. Lappart, R. Pearce, *Chem. Rev.*, **76** (1976) 219.

(i) G.W. Parshall, J.J. Mrowca, *Adv. Organomet. Chem.*, 7 (1968) 157.

(j) M.R. Churchill, "Perspectives in Structural Chemistry", Vol. 3, Wiley, New Yolk, (1970) p91.

(k) P.S. Braterman, R.J. Cross, *Chem. Soc. Rev.*, **2** (1973) 271.

(l) R. J. van Haaren, J.N.H. Reek, H. Oevering, B.B. Coussens, G.P.F. van Strijdonck, P.C.J. Kramer, P.W.N.M. van Leeuwen, *J. Chem. Educ.*, **79** (2002) 588.

[4] H.-F. Klein, *Angew. Chem., Int. Ed. Engl.*, **19** (1980) 362 and references therein.

[5] R.D. Adams, *Polyhedron*, 7 (1988) 2251.

[6] P. Knochel, T-S. Chou, C. Jubert, D. Rajagopal, *J. Org. Chem.*, **58** (1993) 588.

[7] G. Henrici-Olivé, S. Olivé, *Angew. Chem., Int. Ed. Engl.*, **15** (1976) 136.

[8] C.P. Casey, M.A. Andrews, D.R. McAllister, J.E. Rinz, *J. Amer. Chem. Soc.*, **102** (1980) 1927.

[9] J.C. Calabrese, D.C. Roe, D.L. Thorn, T.H. Tulip, *Organometallics*, **3** (1984) 1223.

[10] F.A. Cotton, G. Wilkinson, "Advanced Inorganic Chemistry" 6th Ed., Wiley, New Yolk, (1988) p1167.

[11] D.L. Thorn, *Organometallics*, **1** (1982) 879.

[12] N.A. Bailey, P.L. Chell, C.P. Manuel, A. Mukhopadhyay, D. Rodgers, H.E. Tabron, M.J. Winter, *J. Chem. Soc., Dalton Trans.*, (1983) 2397.

[13] H. Adams, N.A. Bailey, M.J. Winter, *J. Chem. Soc., Dalton Trans.*, (1984) 273.

[14] N.A. Bailey, D.A. Dunn, C.N. Foxcroft, G.R. Harris, M.J. Winter, S. Woodward, *J. Chem. Soc., Dalton Trans.*, (1988) 1449.

[15] V. Guerchais, C Lapinte, *J. Chem. Soc., Chem. Commun.*, (1986) 663 and references therein.

[16] Y.C. Lin, J.C. Calabrese, S.S Wreford, *J. Amer. Chem. Soc.*, **105** (1983) 1679.

[17] H.B. Friedrich, J.R. Moss B. K. Williamson; *J Organomet. Chem.*, **394** (1990) 313.

[18] X. Yin, J.R. Moss, *J. Organomet. Chem.*, **557** (1998) 259.

[19] (a) Y. –H. Liao, J.R. Moss, *J. Chem. Soc., Chem. Commun.*, (1993) 1774.
(b) Y. –H. Liao, J.R. Moss *Organometallics*, **14** (1995) 2130.
(c) Y. –H. Liao, J.R. Moss *Organometallics*, **15** (1996) 4307.
(d) S. Lebreton, S. Monaghan, M Bradley, *Aldrichimica Acta*, **34** (2001) 75.

[20] J.R. Moss, M.L. Niven, P.M. Stretch, *Inorg. Chim. Acta*, **119** (1986) 177.

[21] H.B. Friedrich, Ph.D. Thesis, University of Cape Town, South Africa, 1990.

[22] K.J. Ivin, "Olefin Metathesis", Academic, New Yolk, 1983.

[23] J.P. Morgan, C. Morrill, R.H. Grubbs, *Organic Letters*, **4** (2002) 67.

[24] A.Furstner, C. Mathes, C.W. Lehmann, *Chem. Eur. J.*, **7** (2001) 5299.

[25] H.B. Friedrich, K.P. Finch, M.A. Gafoor, J.R. Moss, *Inorg. Chim. Acta*, **206** (1993) 225.

[26] J.R. Moss, S. Pelling, *J. Organomet. Chem.*, **236** (1982) 221.

[27] S. Pelling, C. Botha, J.R. Moss, *J. Chem. Soc., Dalton Trans*, (1983) 1495.

[28] H.B. Friedrich, J.R. Moss, *J. Organomet. Chem.*, **453** (1993) 85.

[29] J.R. Moss, *Trends Organomet. Chem.*, **1** (1994) 211.

[30] L. Pope, P. Somerville, M.J. Laing, K.J. Hindson, J.R. Moss, *J. Organomet. Chem.*, **112** (1976) 309.

[31] (a) H. Sinn, W. Kaminsky, *Adv. Organomet. Chem.*, **18** (1980) 99.
(b) G.A. Somorjai, S.M. Davies, *Platinum Met. Rev.*, **27** (1983) 54.
(c) F. Garnier, P. Krausz, J.E. Dubois, *J. Organomet. Chem.*, **170** (1979) 195.
(d) P.Petrici, G. Vitulli, *Tetrahedron Lett.*, **21** (1979) 1897.

[32] K.M. Nicholas, *Tetrahedron*, **56** (2000) 9.

[33] T. Satoh, K. Yamakawa, *Synlett.*, **6** (1992) 455.

[34] (a) J. Barluenga, P.J. Campers, J.C. Garcia-Martin, M.A. Roy, G. Asensio, *Synthesis*, **893** (1979), and references therein.
(b) D. Syferth, H. Shih, *J. Org. Chem.*, **39** (1974) 2329.

(c) D. Seyferth, S.B Andrews, *J. Organomet. Chem.*, **30** (1971) 151 and references therein.

[35] G.J. Leigh, J. Chatt, *Coord. Chem. Rev.*, **108** (1991) 1.

[36] A. W. Hofmann, *Liebigs, Ann. Chim.*, **103** (1857) 357.

[37] B.L. Shaw, J.M. Jenkins, *J. Chem. Soc.(A)*, (1966) 770.

[38] T.S. Piper, G. Wilkinson, *J. Inorg. Nucl. Chem.*, **3** (1956) 104.

[39] R.B. King, M. Bisnette, *J. Organomet. Chem.*, **7** (1967) 311.

[40] (a) C.P. Casey, *J. Chem. Soc., Chem. Commun.*, (1970) 1220.
(b) C.P. Casey, R.L. Anderson, *J. Amer. Chem. Soc.*, **93** (1971) 3554.

[41] A. P. Masters, T.S. Sorensen, *Can. J. Chem.*, **68** (1990) 502.

[42] F.A. Cotton, C.M. Lukehart, *J. Amer. Chem., Soc.*, **93** (1971) 2672.

[43] N.A Bailey, P.L. Chell, A. Mukhpadhyay, H.E Tarbborn, M.J. Winter, *J.Chem. Soc., Chem. Commun.*, (1982) 215.

[44] F.A. Cotton, C.M. Lukehart, *J. Amer. Chem., Soc.*, **95** (1973) 3552.

[45] R.J. Klinger, W. Butler, M.D. Curtis, *J. Amer. Chem. Soc.*, **97** (1975) 3535.

[46] H.B. Friedrich, P.A. Makhesha, J.R. Moss, B.K. Williamson, *J. Organomet. Chem.*, **384** (1990) 325.

[47] C.P. Casey, L.J. Smith, *Organometallics*, **7** (1988) 2419.

[48] S. J. Archer, K. P. Finch, H. B. Friedrich, J. R. Moss, *Inorg. Chim. Acta*, **182** (1991) 145-152

[49] D.G. Harrison, S.R. Stobart, *J. Chem. Soc., Chem. Commun.*, (1986) 285.

[50] J.D. Scott, R.J. Puddephatt, *Organometallics*, **5** (1986) 1538.

[51] J.D. Scott, M. Crespo, C.M. Anderson, R.J. Puddephatt, *Organometallics*, **6** (1987) 1772.

[52] J.E Anderson, Y.H. Liu, K.M. Kadish, *Prog. Inorg. Chem.*, **18** (1973) 172.

[53] J.P. Collman, J.I. Brauman, A.M Madonik, *Organometallics*, **5** (1986) 218.

[54] Y. Zhou, J.A. Gladysz, *Organometallics*, **12** (1993) 1073.

[55] X. Yin, J.R. Moss, *J. Organomet. Chem.*, **574** (1999) 252.

[56] H.B. Friedrich, M.O. Onani, O.Q. Munro, *J. Organomet. Chem.*, **633** (2001) 39.

[57] R.B. King, *Acc. Chem. Res.*, **3** (1970) 417.

[58] J.R. Moss, L.G. Scott, *Coord. Chem. Rev.*, **60** (1984) 171.

[59] (a) W. Beck, B. Olgemöller, *J. Organomet. Chem.*, **127** (1977) C45.
(b) W. Beck, B. Olgemöller, *Chem. Ber.*, **114** (1981) 867.

[60] H.C. Lewis Jr., B.N. Storhoff, *J. Organomet. Chem.*, **43** (1972) 1.

[61] A. Rosan, M. Rosenblum, J. Tancrede, *J. Amer. Chem. Soc.*, **95** (1973) 3062.

[62] (a) R.E. Dessy, R.L. Pohl, R.B. King, *J. Amer. Chem. Soc.*, **88** (1966) 5121.
(b) M.S. Corraine, C.K. Lai, Y. Zhen, M.R. Churchill, L.A. Buttrey, J.W. Ziller, J.D. Atwood, *Organometallics*, **11** (1992) 35.

[63] J.A. Al-Takhin, H.A. Connor, J. Skinner, *J. Organomet. Chem.*, **259** (1983) 313.

[64] T. Orlova, V.N. Setkina, P.V. Petrovskii, A.I. Yanovskii, A.S. Batsanov, Y.T. Struchkov, *Organomet. Chem.*, USSR **1** (1988) 725.

[65] (a) W.A. Hermann, *Angew. Chem. Int. Ed.*, **94** (1982) 118; **21** (1982) 117.
(b) C. Masters, *Adv. Organomet. Chem.*, **17** (1979) 61.

[66] (a) R.B. King, *Inorg. Chem.*, **2** (1963) 531.
(b) R. B. King, D.M. Braitsch, *J. Organomet. Chem.*, **54** (1973) 9.
(c) M. Cooke, N.J. Forrow, S.A.R. Knox, *J. Organomet. Chem.*, **222** (1981) C21.
(d) M. Cooke, N.J. Forrow, S.A.R. Knox, *J. Chem. Soc., Dalton Trans.*, (1983) 2435.

[67] (a) M.R. Domingo, A. Irving, Y-H. Liao, J.R. Moss, A. Nash, *J. Organomet. Chem.*, **443** (1993) 233.
(b) K.P. Finch, J.R. Moss, *J. Organomet. Chem.*, **346** (1988) 253.

[68] E. Lindner, M. Pabel, R. Fawzi, H.A. Mayer, K. Wurst, *J. Organomet. Chem.*, **435** (1992) 109.

[69] (a) E. Lindner, M. Pabel, K. Eichele, *J. Organomet. Chem.*, **386** (1990) 187.
(b) E. Lindner, M. Pabel, K. Eichele, *J. Organomet. Chem.*, **414** (1991) C19.

[70] S.F. Mapolie, J.R. Moss, *J. Chem. Soc., Daltons Trans.*, (1990) 299.

[71] C. Roger, T. –S. Peng, J.A. Gladysz, *J. Organomet. Chem.*, **439** (1992) 163.

[72] N. Wheatley, P. Kalck, *Chem. Rev.*, **99** (1999) 3419.

[73] (a) B. Findeis, M. Schubart, C. Platzek, L.H. Gade, I. Scowen, M. McPartlin, *J. Chem. Soc., Chem. Commun.*, (1996) 219.
(b) S. Friedrich, L.H. Gade, I.J. Scowen, M. McPartlin, *Angew. Chem. Int. Ed. Engl.*, **35** (1996) 1338.
(c) S. Friedrich, H. Memmer, L.H. Gade, II.W.S. Li, I.J. Scowen, M. McPartlin, C.E. Housecroft, *Inorg. Chem.*, **35** (1996) 2433.
(d) D. Selent, M. Ram,, C. Janiak, *J. Organomet. Chem.*, **501** (1995) 235.

(e) J.Sundermeyer, D. Runge, J.S. Field, *Angew. Chem. Int. Ed. Engl.*, **33** (1994) 678.

(f) J. Sundermeyer, D. Runge, *Angew. Chem. Int. Ed. Engl.*, **33** (1994) 1255.

[74] (a) D. Selent, R. Beckhaus, J. Pickardt, *Organometallics*, **12** (1993) 2857.

(b) D. Selent, R. Beckhaus, T. Bartik, *J. Organomet. Chem.*, **405** (1991) C15.

(c) T. Bartik, B. Happ, A. Sarkau, K.–H. Thiele, G. Palyi, *Organometallics*, **8** (1989) 558.

[75] I.P. Beletskaya, A.Z. Voskoboynikov, E.B. Chuklanova, N.I. Kirrilova, A.K. Shestakova, A.I. Parshina, A.I. Gusev, G.K-I. Magomedov, *J. Amer. Chem. Soc.*, **115** (1993) 3156.

[76] (a) F.E. Hong, I-R. Lue, S-C. Lo, Y-C Yang, C-C. Lin, *Polyhedron*, **15** (1996) 2793.

(b) F.E. Hong, I-R. Lue, S-C. Lo, C-C. Lin, *Polyhedron*, **14** (1995) 1419.

[77] H.B. Friedrich, M.O. Onani, O.Q. Munro, *unpublished results*.

[78] G.J. Arsenault, M. Crespo, R.J. Puddephatt, *Organometallics*, **6** (1987) 2255.

[79] G.E. Jackson, J.R. Moss, L.G. Scott, *S. Afr. J. Chem.*, **36** (1983) 69.

[80] D. White, N.J. Coville, *Adv. Organomet. Chem.*, **36** (1994) 95.

[81] (a) H. Sachse, *Chem. Ber.*, **23** (1890) 1363.

(b) E. Mohr, *J. Prakt. Chem.*, **98** (1918) 315.

(c) A. Baeyer, *Chem. Ber.*, **18** (1885) 2269.

[82] C.A. Tolman, *Chem. Rev.*, **77** (1977) 315.

[83] (a) G.J. Leigh, N. Winterton, "Modern Coodination Chemistry; The Legacy of Joseph Chatt", RSC, London, (2002) p307.

(b) G.J. Leigh, N. Winterton, "Modern Coodination Chemistry; The Legacy of Joseph Chatt", RSC, London, (2002) p73.

[84] D.L. Reger, E.C. Culbertson, *J. Amer. Chem. Soc.*, **98** (1976) 2789.

[85] S.C. Kao, C.H. Thiel, R. Pettit, *Organometallics*, **2** (1983) 914.

[86] H.B. Friedrich, J.R. Moss, *J. Chem. Soc., Dalton Trans.*, (1993) 2863.

[87] (a) I.S. Butler, F. Basolo, R.G. Pearson, *Inorg. Chem.*, **6** (1967) 2074.

(b) M. Green, D.J. Westlake, *J. Chem. Soc. A*, (1971) 367.

(c) A. Wojcicki, *Adv. Organomet. Chem.*, **11** (1973) 87.

[88] (a) M.L. Green, L.C. Mitchard, M.G. Swanwick, *J. Chem. Soc. A*, (1971) 794.

(b) J.A.S. Howell, A.J. Rowan, *J. Chem. Soc., Chem. Chemun.*, (1979) 484.

(c) J.A.S. Howell, A.J. Rowan, *J. Chem. Soc., Dalton Trans.*, (1980) 1845.

[89] P. Johnson, G.J. Hutchings, N.J. Covillle, *J. Amer. Chem. Soc.*, **111** (1989) 1902.

[90] (a) K. Raab, U. Nagel, W. Beck, *Z. Naturforsch.*, **38b** (1983) 1466.
(b) K.P. Finch, J.R. Moss, M.L. Niven, *Inorg. Chim. Acta*, **166** (1989) 181.

[91] N.J. Coville, L. Cheng, *J. Organomet. Chem.*, **571** (1998) 149 and references therein.

[92] D.H. Gibson, S.K. Mandal, K. Owen, W.E. Sattich, J.O. Franco, *Organometallics*, **8** (1989) 1114.

[93] J.R. Moss, L.G. Scott, *J. Organomet. Chem.*, **363** (1989) 351.

[94] G.J. Leigh, N. Winterton, "Modern Coodination Chemistry; The Legacy of Joseph Chatt", RSC, London, (2002) p154.

[95] Akio Yamamoto, "Organotransition metal chemistry: Fundamental concepts and applications", Wiley, New Yolk, (1986) p162.

CHAPTER 2

HALOGENOALKYL COMPOUNDS OF TUNGSTEN

2.1 Introduction

The synthesis of halogenoalkyl complexes is interesting because they are the basic precursors for polymethylene bridged complexes. King had first synthesized the hydrocarbon bridged metal centres from the reaction of a number of 1,n dibromoalkanes with transition metal anions [1]. Bailey et al. have reported the synthesis of a number of the halogenoalkyl complexes containing molybdenum [2,3]. Moss and Friedrich have reported the syntheses of a number of analogous complexes containing Fe, Ru and W [4-6]. Puddepphatt et al. had also reported on the same kind of complexes, but of Pt and Pd [7]. The ability to isolate monometallated intermediates has been reported to be very important as they can be used to synthesize heterobimetallic compounds with saturated hydrocarbon bridges [8]. Moss also noted that the choice of the dihaloalkanes used in the reactions is very important as the desired product is only obtained with dibromoalkanes and not dichloroalkanes [9]. These are some significant factors that cannot be avoided, as our ultimate goal was to synthesize some new heterobimetallic complexes, starting from halogenoalkyl compounds.

Whilst halogenomethyl complexes of some transition metals are fairly well known, longer-chain halogenoalkyl compounds have been comparatively little studied [4]. Indeed, until very recently, only those of platinum [7], ruthenium [5] and iron [6] had been studied in any detail. Various derivatives of transition metal carbonyl anions have gained significance as intermediates in the preparation of interesting organometallic compounds. Importantly, compounds of the type $[L_yM\{(CH_2)_nX\}]$ (L_yM = transition metal and its associated ligands, $n \geq 1$, X = halogen) are known precursors of cyclic carbene complexes as well as homo- and heterodinuclear compounds, which have been proposed as models for intermediates in several important catalytic processes. The application of several of these compounds in organic synthesis has also been described [4].

Generally, the study of group VI metal hexacarbonyls is made easy by a unique property, that they undergo extensive ligand substitution reactions. The organometallic compounds

prepared from alkali metal derivatives of metal carbonyls include compounds in which a transition metal of a metal carbonyl moiety is σ-bonded to another atom such as a carbon atom in an alkyl, acyl, aryl, or perfluoroalkyl group. In this chapter application of the anions derived from substituted tungsten carbonyls in the synthesis of halogenoalkyl derivatives and the chemistry of these derivatives thus synthesized will be discussed. King had attempted to synthesize the tungsten halogenoalkyl compounds $[Cp(CO)_3W\{(CH_2)_nBr\}]$ (n = 3 - 4), and obtained very low yields (13 – 23%) [8]. Very recently, independent to this work, the majority of the halogenoalkyl compounds of tungsten presented in this chapter were published [10]. Our method of synthesis and purification differed, however, and the work reported in this chapter had been completed prior to this publication.

2.2 Preparation and Properties of the Halogenoalkyl Compounds $[Cp(CO)_3W\{(CH_2)_nX\}]$ (n = 3 - 6, X = Br, I)

The most useful method for obtaining anionic substituted metal carbonyl derivatives for preparative purposes is by the reduction of various substituted metal carbonyls with an alkali metal or amalgam, generally in the presence of a basic solvent such as liquid ammonia or various ethers. The anions, $[Cp(CO)_3W]^-$, may essentially be prepared by the following two steps:

(i) Heating the tungsten hexacarbonyl with an alkali metal cyclopentadienide in an ethereal solvent:

$$W(CO)_6 + M(C_5H_5) \longrightarrow M[Cp(CO)_3W] + 3CO \qquad M = Na \text{ or } Li \qquad (1)$$

Suitable reaction systems include lithium cyclopentadienide with tungsten hexacarbonyl in dimethylformamide at 110 °C [11], and sodium cyclopentadienide with tungsten hexacarbonyl in boiling tetrahydrofuran [12] or 1,2-dimethoxyethane [1,13].

(ii) Reduction of the dimeric compound, $[\{Cp(CO)_3W\}_2]$, with sodium [14] or sodium amalgam [15] in a tetrahydrofuran solution.

The tungsten dimer, $[\{Cp(CO)_3W\}_2]$, was prepared by using the reported literature method [13]. The general synthesis follows the Equations 2 and 3 below.

$$W(CO)_6 + Na(C_5H_5) \longrightarrow Na[Cp(CO)_3W] + 3CO \quad (2)$$

$$Na[Cp(CO)_3W] + 2Fe(III) \longrightarrow [\{Cp(CO)_3W\}_2] + 2Fe(II) + 2Na \quad (3)$$

The unreacted tungsten hexacarbonyl was sublimed off the dimer under reduced pressure by using a cold finger sublimation apparatus which was set up in an oil bath at 70 °C. The purified dimer could then be stored under nitrogen in the dark. The dimer could be reduced by ~1% Na/Hg (Equation 4) to yield the tungsten anion.

$$[\{Cp(CO)_3W\}_2] + Na/Hg \longrightarrow 2Na[Cp(CO)_3W] \quad (4)$$

This tungsten anion was then used in the preparation of the bromoalkyl compounds according to the reaction pathway shown in Scheme 2.1.

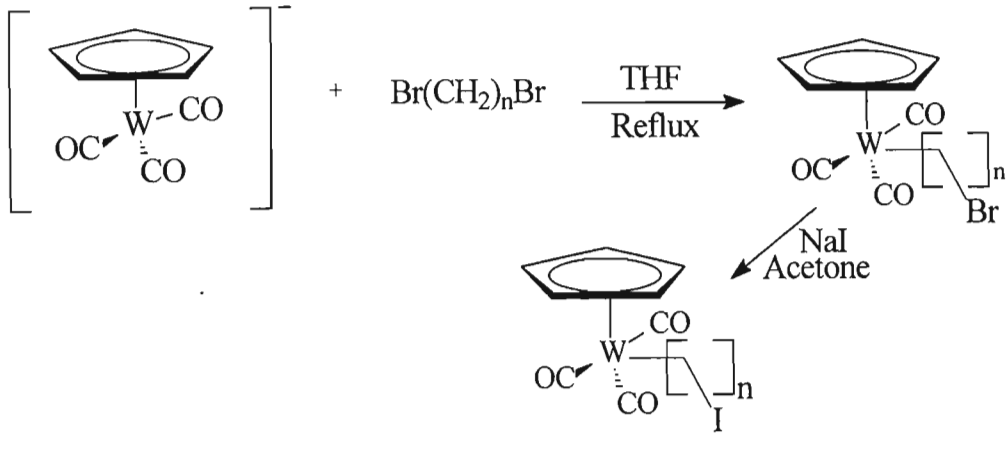

Scheme 2.1: The synthetic pathway for the compounds, $[Cp(CO)_3W\{(CH_2)_nX\}]$, n = 3 – 6

Although the bromoalkyl compounds of iron and ruthenium, $[Cp(CO)_2M\{(CH_2)_nX\}]$ (M = Fe, Ru; X = Br, I), have to be prepared at low temperature to prevent the formation of the binuclear compounds, $[Cp(CO)_2M(CH_2)_nM(CO)_2Cp]$, these conditions give very low yields for the analogous tungsten and molybdenum compounds, regardless of reaction times. It has also been reported that different types of products are obtained in the reactions of $Na[Cp(CO)_2Fe]$ [1], $Na[Cp(CO)_3Mo]$, $Na[Cp(CO)_3W]$ [1,16] and $Na[Mn(CO)_5]$ [17] with 1,3-dibromopropane due to the nucleophilicity of the metal carbonyl anions involved, and the ease with which the initially formed 3-bromo-n-propyl

complex undergoes carbonyl insertion or nucleophilic attack at $-CH_2Br$ [18]. Thus acyl and cyclic carbene compounds can also form. King studied the reactivity rate of the metal anions, towards the organic halides and from his report the tungsten anion is a relatively weaker nucleophile than Fe and Ru (Table 2.1) [19].

Table 2.1: Relative nucleophilicities of some metal carbonyl anions

Anion	Relative nucleophilicity[a]
$C_5H_5(CO)_2Fe^-$	70,000,000
$C_5H_5(CO)_2Ru^-$	7,500,000
$C_5H_5(CO)Ni^-$	5,500,000
$(CO)_5Re^-$	25,000
$C_5H_5(CO)_3W^-$	~500
$(CO)_5Mn^-$	77
$C_5H_5(CO)_3Mo^-$	67
$C_5H_5(CO)_3Cr^-$	4
$(CO)_4Co^-$	1

[a] These relative nucleophilicities were measured electrochemically in 1,2-dimethoxymethane solution in the presence of tetrabutylammonium perchlorate. The nucleophilicity of $(CO)_4Co^-$ was arbitrarily taken as 1.

The tungsten anion, $Na[Cp(CO)_3W]$ was eacted with an excess of $Br(CH_2)_nBr$ (n = 3 – 6) in refluxing, producing the compounds $[Cp(CO)_3W\{(CH_2)_nBr\}]$ in high yields according to Equation 5 below.

$$Na[Cp(CO)_3W] + Br(CH_2)_nBr \longrightarrow [Cp(CO)_3W\{CH_2)_nBr\}] + NaBr \quad n = 3 - 6 \qquad (5)$$

Clearly the halogenoalkyl compounds of tungsten are less thermally labile than expected. The binuclear compounds, $[Cp(CO)_3W(CH_2)_nW(CO)_3Cp]$, are not formed, nor is a cyclic carbene compound formed when n = 3. This further confirms that the anion $[Cp(CO)_3W]^-$ is actually a significantly weaker nucleophile than the cyclopentadienyldicarbonyl anions of iron and ruthenium. This is not a general method, however, the molybdenum bromoalkyl compounds do form cyclic carbene compounds where n = 3 as will be seen in Chapter 3.

The compounds, $[Cp(CO)_3W\{(CH_2)_nBr\}]$ n = 3 – 6, were obtained in analytically pure form by a newly developed recrystallisation procedure, from a dilute dichloromethane/hexane solution at –78 °C. Generally, the yields obtained from this method were well in excess of 80%, some 20% higher than the recently reported data [10]. Chromatography of these compounds, which is essential for the iron analogues [4], is not needed and leads to product loss due to decomposition. The compounds are fairly stable in air in the solid state and are stable in solution under nitrogen, but decompose very rapidly in organic solvents in air. Remarkably, they dissolve in water in air to give stable yellow solutions. The unchanged halogenoalkyl compound can then be recovered. The decomposition product in hexane appears to be the dimer, $[\{Cp(CO)_3W\}_2]$, whilst the decomposition products in chloroform appear to include elemental tungsten as was judged mainly by the blue colour of the sediment formed. The bromoalkyl compounds were converted into the iodoalkyl compounds using the Finkelstein reaction [20]. Thus they were stirred overnight with sodium iodide in acetone according to Equation 6 below.

$$[Cp(CO)_3W\{(CH_2)_nBr\}] + NaI \longrightarrow [Cp(CO)_3W\{(CH_2)_nI\}] + NaBr \quad n = 3 - 6 \qquad (6)$$

All the bromo- and the iodo- halogenoalkyl compounds were obtained as yellow solids, and their characterisation data are given in Tables 2.2 – 2.4 below. Elemental analysis results of a number of the compounds are reported in the experimental section (Section **5.2.3** and **5.2.4**). From Table 2.2, it can be seen that the melting points of the bromo compounds where n is an odd number are significantly higher than the melting points of those compounds where n is an even number. This even/odd effect has been observed previously [21] and is believed to be due to crystal packing factors (Figure 2.11 **3b** and 2.13 **1a**) [9,22,23]. No such effect is observed for the iodo compounds. All the compounds show two intense carbonyl bands in their infrared absorption spectra. There is no significant difference in the positions of the carbonyl stretching frequencies between the bromo and the corresponding iodo compounds, and only a very slight shift towards lower wave numbers as the carbon chain lengthens from n = 3 to n = 6 is observed. The infrared data thus follows the same pattern reported for the analogous iron compounds [6]. Also, our infrared, melting point and ^1H NMR data for the compounds **1a** and **2a** correspond to those reported by King and Bisnette [8].

Table 2.2: Data for the compounds, $[Cp(CO)_3W\{(CH_2)_nX\}]$, n = 3 - 6; X = Br, I

Compound		Yield (%)	m.p. (°C)	IR (ν(CO), cm^{-1}) [a]
$[Cp(CO)_3W\{(CH_2)_3Br\}]$	**1a**	89	120–121	2019s, 1930vs
$[Cp(CO)_3W\{(CH_2)_3I\}]$	**1b**	84	63-65	2019s, 1930vs
$[Cp(CO)_3W\{(CH_2)_4Br\}]$	**2a**	85	66–67	2017s, 1928vs
$[Cp(CO)_3W\{(CH_2)_4I\}]$	**2b**	92	108–109 (dec)	2017s, 1927vs
$[Cp(CO)_3W\{(CH_2)_5Br\}]$	**3a**	83	118-122	2016s, 1927vs
$[Cp(CO)_3W\{(CH_2)_5I\}]$	**3b**	73	135 (dec)	2017s, 1928vs
$[Cp(CO)_3W\{(CH_2)_6Br\}]$	**4a**	81	51-55	2016s, 1927vs
$[Cp(CO)_3W\{(CH_2)_6I\}]$	**4b**	76	64-66	2016s, 1926vs

[a] Measured in hexane.

The ^1H NMR data for all the compounds are summarized in Table 2.3. Figure 2.1 shows a sample of a ^1H NMR spectrum and Figure 2.2 the COSY of $[Cp(CO)_3W\{(CH_2)_6Br\}]$. Since two classes of compounds were prepared (bromo- and iodo-), we also present a ^1H NMR spectrum (Figure 2.3) and the COSY (Figure 2.4) of one of new iodo compounds prepared, $[Cp(CO)_3W\{(CH_2)_5I\}]$. Peak assignments for the data presented in Table 2.3 were made with the aid of COSY experiments. The CH_2X peaks were all observed as triplets with coupling constants between 6.8 and 7.2 Hz. This is within the accepted range of between 6 – 8 Hz for this type of proton. Either quintets or multiplets were observed for the coupling of the rest of the protons.

In general, the CH_2Br and CH_2CH_2Br peaks show no further shift downfield with increasing chain length after n = 3, suggesting that the inductive or steric effect of the tungsten group is no longer felt by the terminal protons at chain lengths exceeding three carbons. The upfield shift of *ca.* 0.2 ppm, for the CH_2X peaks as X is changed from Br to I is as expected from the difference in their electronegativities. The Cp peaks are observed within the expected range, between 5.35 ppm and 5.39 ppm, only a *ca.* 0.03 ppm difference from similar data reported [6]. There is a difference of 0.2 ppm between the Cp moieties of compounds **1a** and **1b**, again we see here the electronegative effect of the halogen attached at the end of the alkyl chain as explained above. On moving from n = 3 to n = 6, the chemical shifts of β-CH_2, γ-CH_2, δ-CH_2 gradually show a decline in the influence of the attached halogen at the end of the alkyl chain.

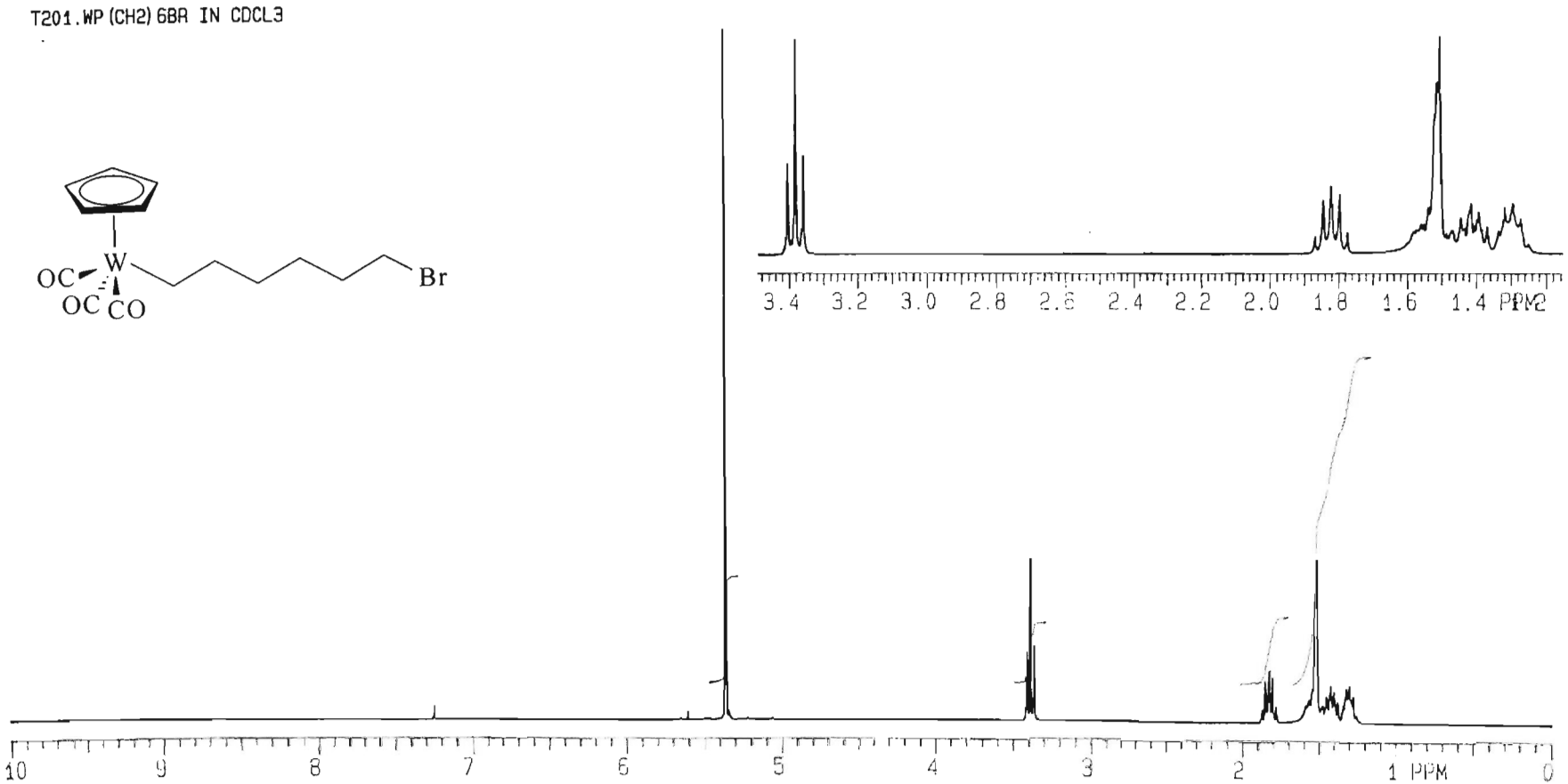

Figure 2.1: ^{1}H NMR spectrum of $[Cp(CO)_3W\{(CH_2)_6Br\}]$.

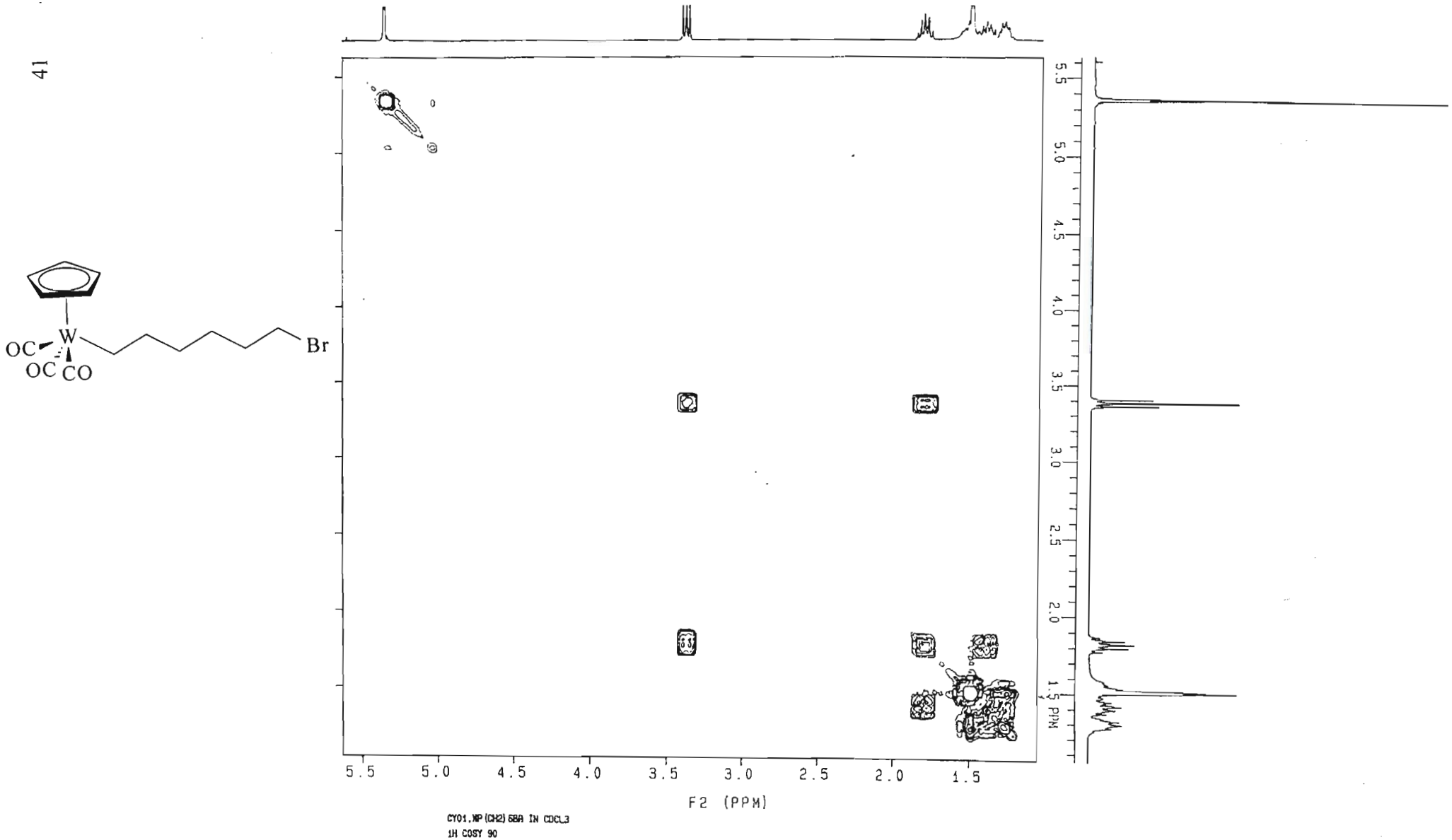

Figure 2.2: COSY of $[Cp(CO)_3W\{(CH_2)_6Br\}]$.

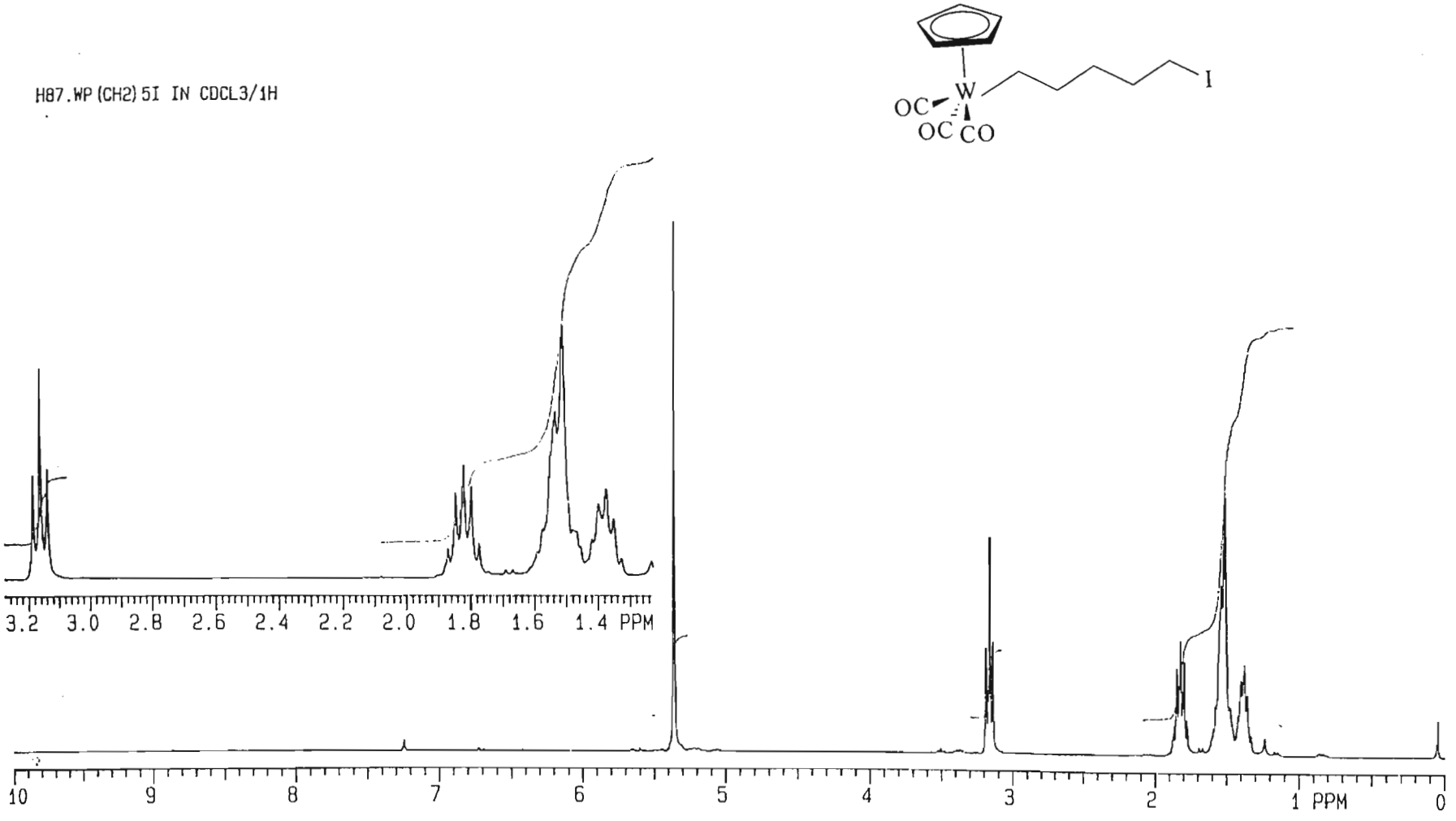

Figure 2.3: ^{1}H NMR spectrum of $[Cp(CO)_3W\{(CH_2)_5I\}]$

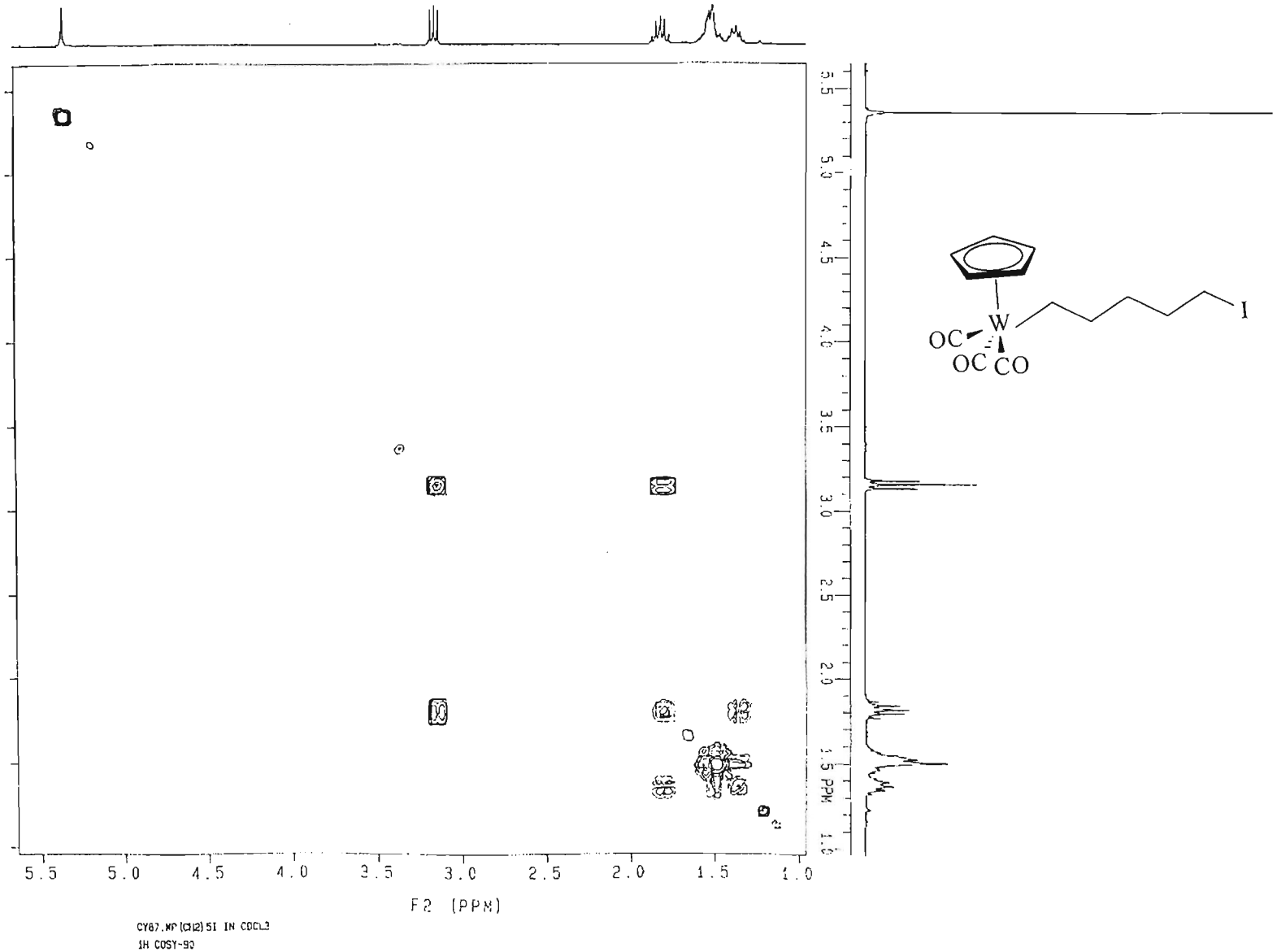

Figure 2.4: COSY of $[Cp(CO)_3W\{(CH_2)_5I\}]$

Table 2.3: ^{1}H NMR Data for $[Cp(CO)_3W\{(CH_2)_n\}X]$, n = 3 – 6 [a]

n	X	Cpd	Cp	α-CH_2	CH_2X	CH_2CH_2X	β-CH_2	γ-CH_2	δ-CH_2
3	Br	**1a**	5.38, 5H, s	1.44m	3.30t, 2H, 7.2[b]	2.06qn, 2H, 7.6			
	I	**1b**	5.36, 5H, s	1.46m	3.11t, 2H, 7.2	2.01m			
4	Br	**2a**	5.38, 5H, s	1.48m	3.43t, 2H, 7.2	1.85m	1.70m		
	I	**2b**	5.39, 5H, s	1.47m	3.20t, 2H, 7.2	1.82qn, 2H, 6.8	1.64m		
5	Br	**3a**	5.35, 5H, s	1.41m	3.38t, 2H, 6.8	1.86m	1.49m	1.52m	
	I	**3b**	5.35, 5H, s	1.38m	3.15t, 2H, 7.2	1.82m	1.51m	1.53m	
6	Br	**4a**	5.35, 5H, s	1.41m	3.40t, 2H, 6.8	1.86m	1.49m	1.49m	1.52n
	I	**4b**	5.35, 5H, s	1.29m	3.16t, 2H, 7.2	1.79m	1.41m	1.38m	1.35r

[a] Measured in $CDCl_3$; peaks are externally referenced to TMS (δ = 0.00 ppm), α-CH_2 refers to the CH_2-group α- to tungsten etc. [b]Coupling constants, $^{3}J(HH)$ are given in Hz.

Assignments of the ^{13}C NMR spectra (Table 2.4) were made using HETCOR and HSQC experiments. Neither the halogen nor the chain length appears to affect the positions of the Cp or carbonyl peaks of the compounds. The Cp peaks were mostly observed between 91.43 ppm and 92.58 ppm, whilst the CO peaks appeared at between 217.42 ppm and 218.71 ppm.

Table 2.4: ^{13}C NMR Data for $[Cp(CO)_3W\{(CH_2)_nX\}]$, n = 3 – 6 [a]

n	X		CO	Cp	α-CH_2	CH_2X	CH_2CH_2X	β-CH_2	γ-CH_2	δ-CH_2
3	Br	**1a**	218.42[b]	92.58	-13.62	38.79	41.14			
	I	**1b**	218.49	92.57	-10.86	12.79	42.07			
4	Br	**2a**	217.51	91.48	-12.43	35.04	38.34	33.54		
	I	**2b**	218.58	92.56	-11.53	8.16	40.08	38.54		
5	Br	**3a**	217.71	91.47	-10.84	35.23	32.33	34.36	35.94	
	I	**3b**	217.59	91.47	-10.91	7.47	33.00	35.65	36.64	
6	Br	**4a**	217.56	91.43	-10.51	34.10	34.94	36.56	33.64	27.23
	I	**4b**	220.44	94.32	-7.59	10.25	32.85	39.47	37.61	36.44

[a] Measured in $CDCl_3$; [b]All peaks observed as singlets; peaks are externally referenced to TMS (δ = 0.00 ppm), α-CH_2 refers to the CH_2-group α to tungsten etc.

The halogen affects the chemical shift of the carbon α to tungsten where n = 3 or 4 possibly due to some induced electronic interaction, after that little or no effect is observed. The chemical peaks due to the α carbons are highly shielded for the compounds with

smaller values of n, this was also observed for the iron analogues [6]. This is contrary to what one would expect from the consideration of the inductive effects of the halogens and may imply a weak interaction between the halogen and tungsten, as has been proposed previously [6,24]. Also clear in the ^{13}C NMR spectra is the large chemical shift difference, *ca.* 26-27 ppm, between the carbons α to Br and I, reflecting the known different electron withdrawing abilities of the halogens. The chain length and the halogen do not appear to affect the positions of the Cp peaks or those of the CO peaks. Also, the chemical shifts of α-CH_2 for n = 5 or 6 appear reversed because of a general shift in the peak of the external reference used, there is no effect on the halogen at the remote end of these longer chains by the central metal [6]. The ^{13}C NMR spectrum of $[Cp(CO)_3W\{(CH_2)_6Br\}]$ is shown in Figure 2.5, and the HETCOR and HSQC in Figures 2.6 and 2.7 respectively. A sample spectrum of a ^{13}C NMR, Figure 2.8 and HETCOR, Figure 2.9 of $[Cp(CO)_3W\{(CH_2)_5I\}]$ are also presented. Crystal structures of the compounds $[Cp(CO)_3W\{(CH_2)_5I\}]$ and $[Cp(CO)_3W\{(CH_2)_3Br\}]$ were obtained and a few reactions of the halogenoalkyl compounds were investigated and will now be discussed.

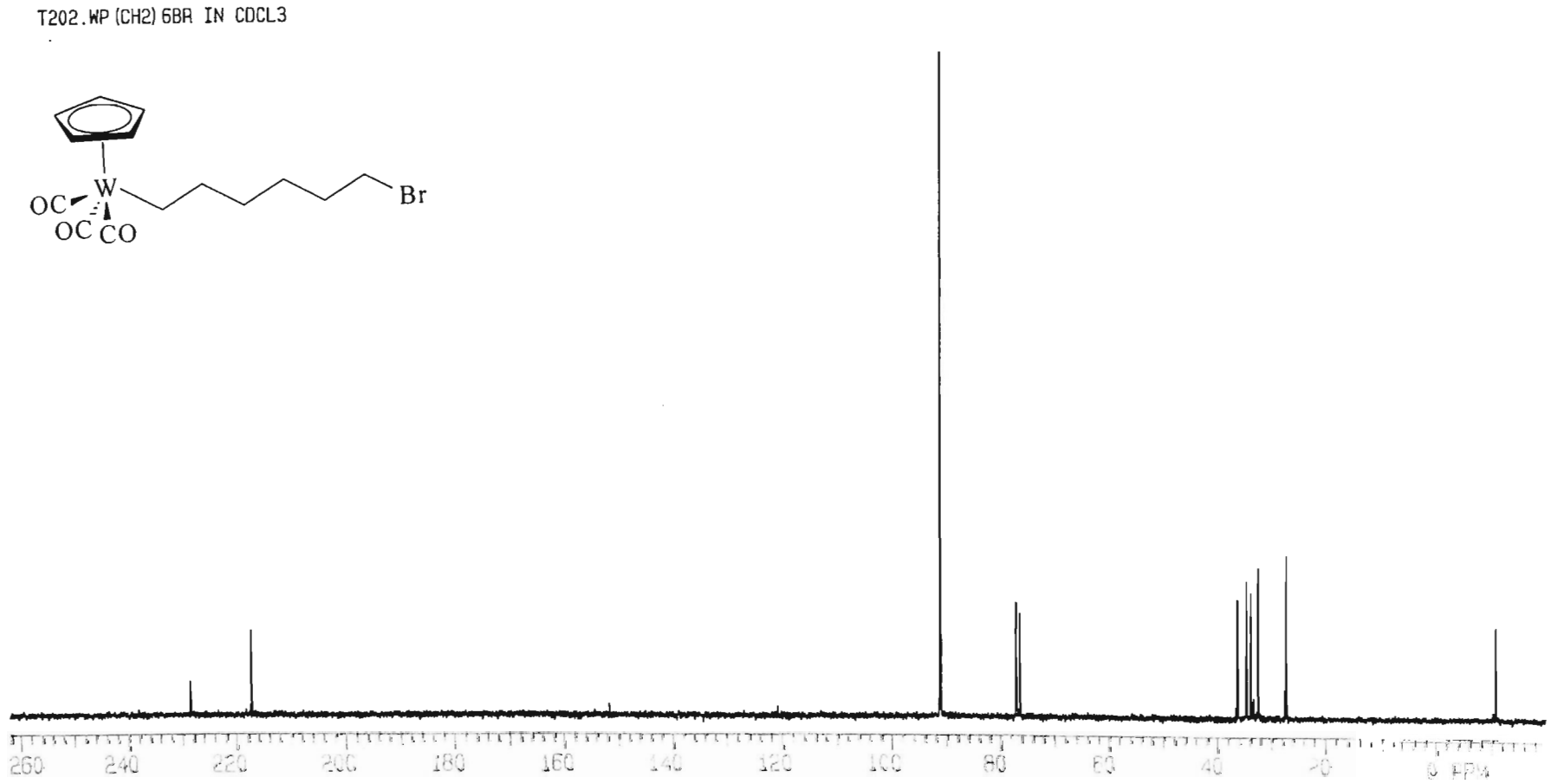

Figure 2.5: ^{13}C NMR spectrum of $[Cp(CO)_3W\{(CH_2)_6Br\}]$

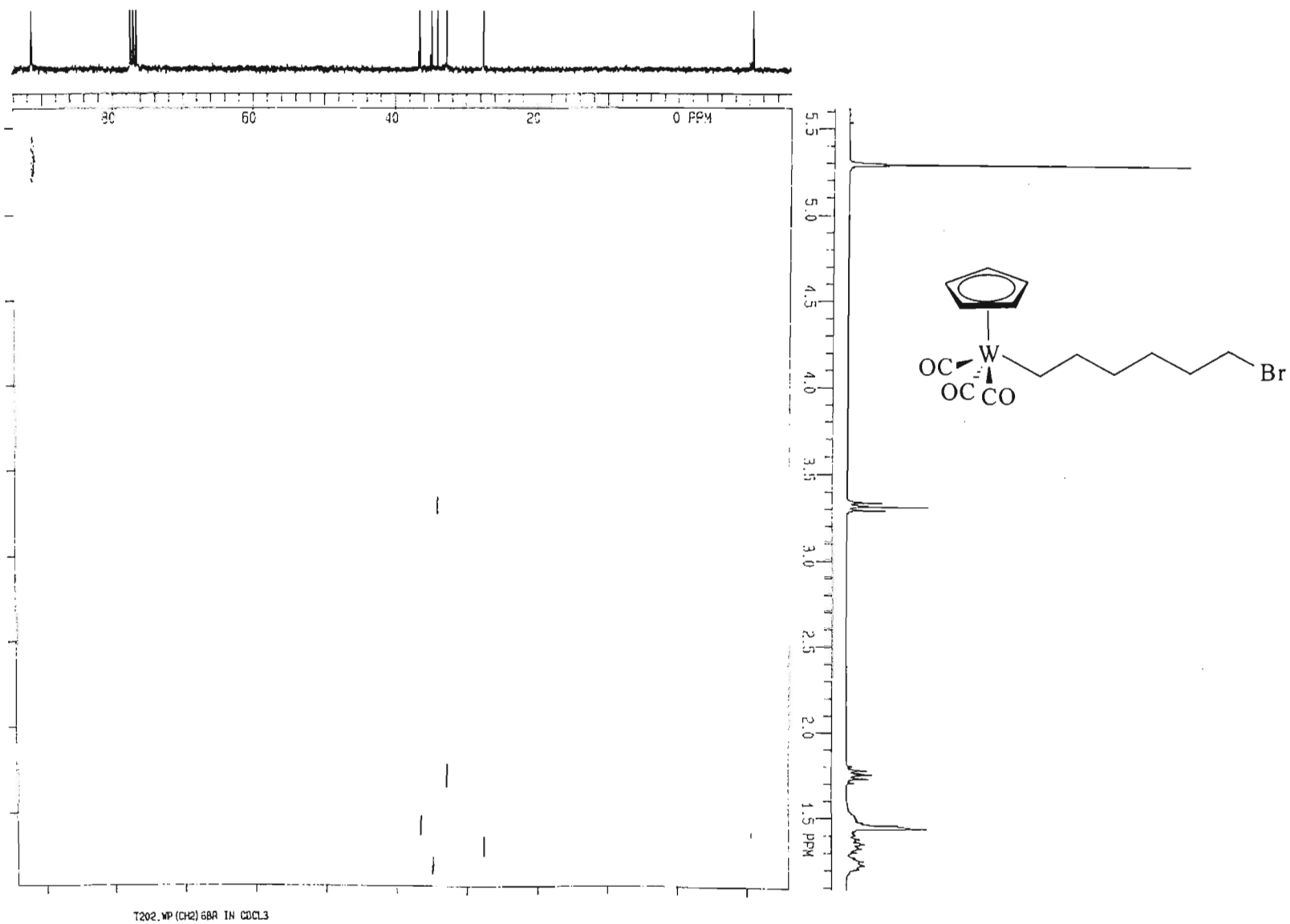

Figure 2.6: HETCOR of $[Cp(CO)_3W\{(CH_2)_6Br\}]$

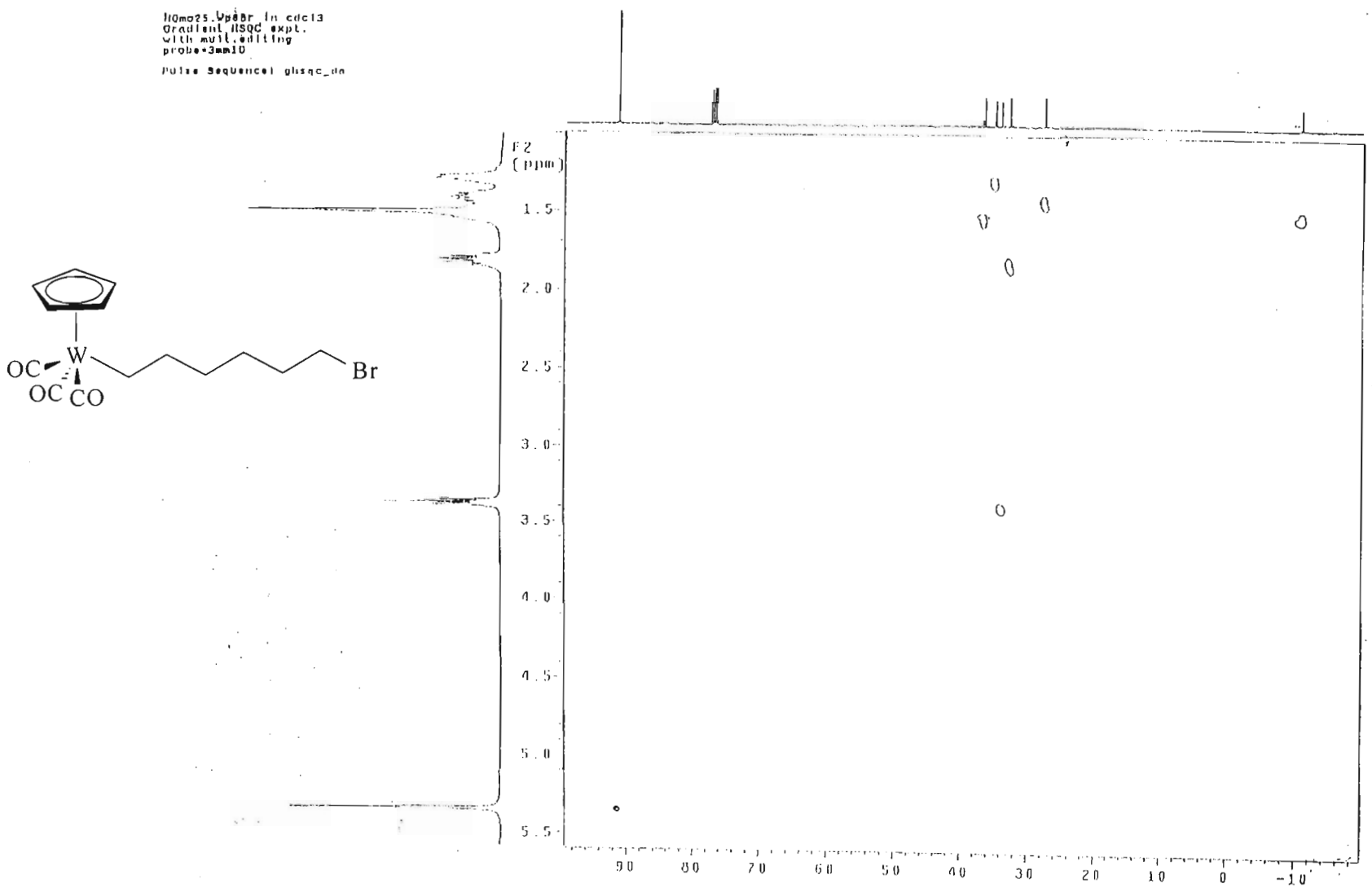

Figure 2.7: HSQC of $[Cp(CO)_3W\{(CH_2)_6Br\}]$.

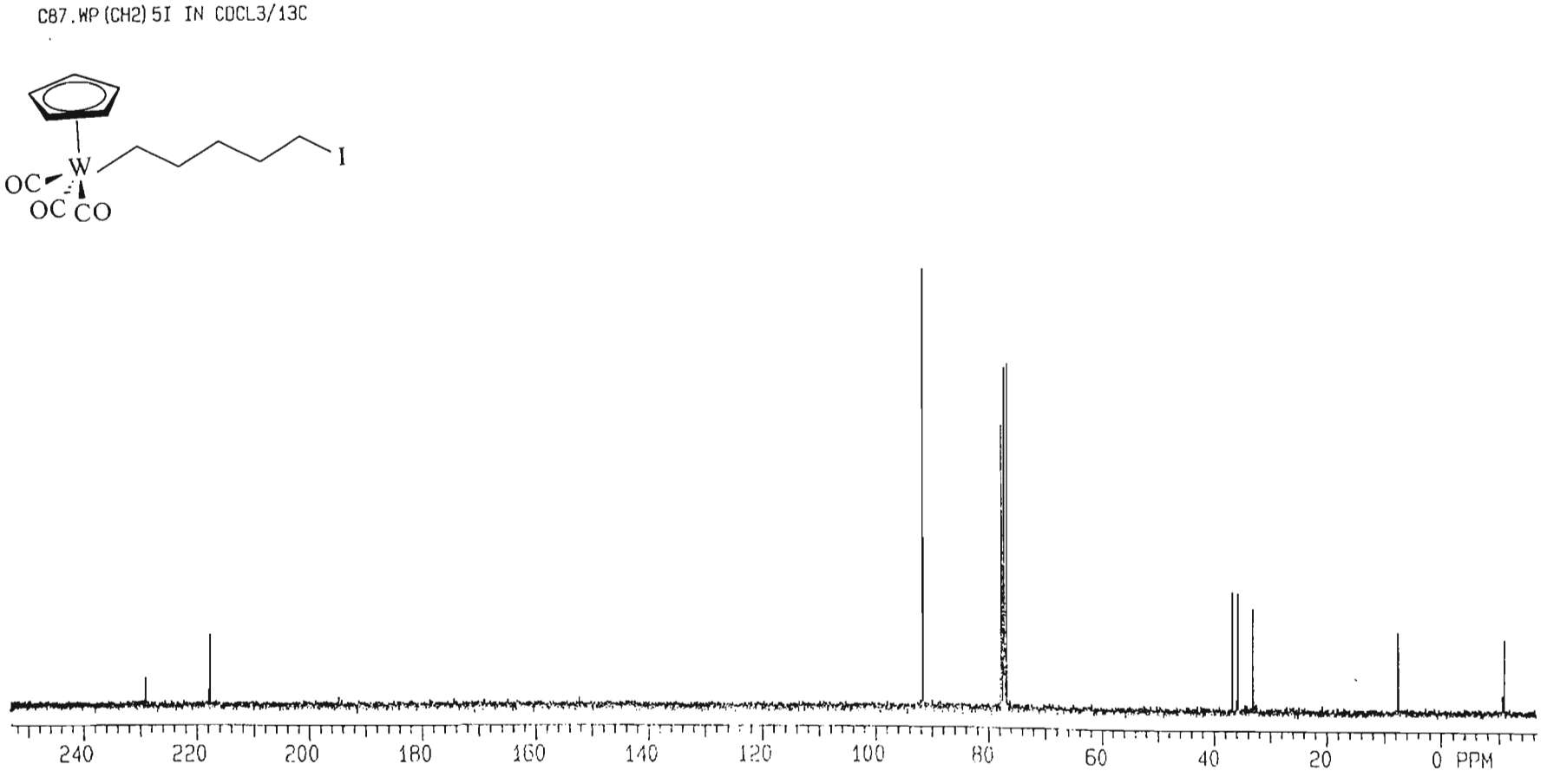

Figure 2.8: ^{13}C NMR spectrum of $[Cp(CO)_3W\{(CH_2)_5I\}]$

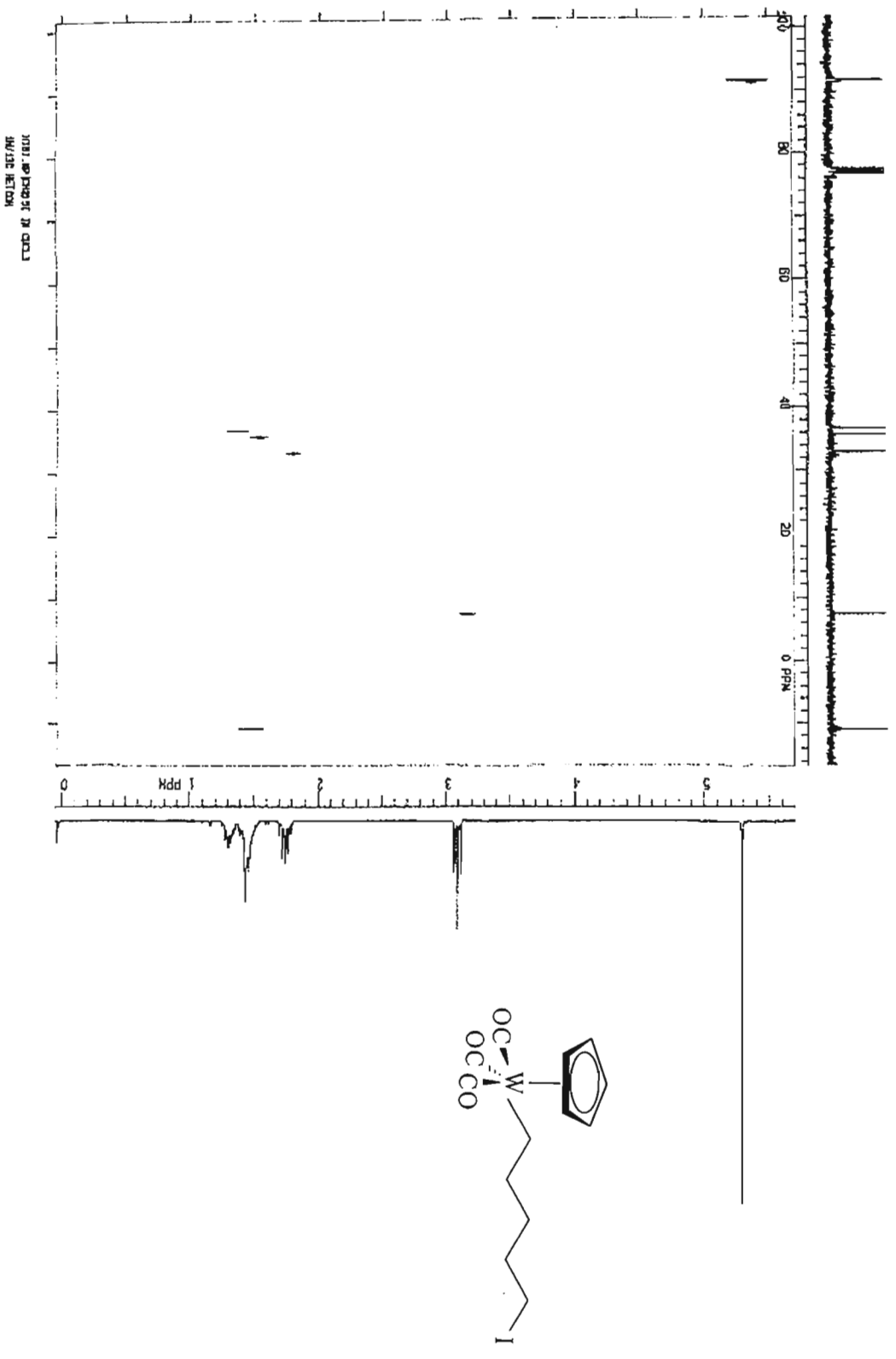

Figure 2.9: HETCOR of $[Cp(CO)_3W\{(CH_2)_5I\}]$

2.3 Crystal Structures of the Compounds $[Cp(CO)_3W\{(CH_2)_5I\}]$ and $[Cp(CO)_3W\{(CH_2)_3Br\}]$

Crystals of the compounds **1a** and **3b** were obtained from slow cystallisation over several days in a dichloromethane/hexane mixture at –10 °C [25]. We present here the first ever reported crystal structures of halogenoalkyl group VIb compounds. Furthermore, the crystal structure of $[Cp(CO)_3W\{(CH_2)_5I\}]$, **3b,** is the longest chain crystal structure ever reported for any halogenoalkyl compound. The compound, $[Cp(CO)_3W\{(CH_2)_5I\}]$, forms orthorhombic crystals in the space group $P2_1nb$. The structure of the molecule and packing in the crystal are shown in Figures 2.10 **3b** and 2.11 **1a** respectively. Selected bond lengths and angles for this compound are given in Tables 2.5 and 2.6; listings of atomic coordinates, anisotropic temperature factors, H atom coordinates and complete crystallographic details are given in Appendix 1 and in the attached compact disc. The supplementary material related to the crystal has been deposited with the Cambridge Crystallographic Data Centre [26]. In the crystal, the compound shows the classical "bump in hollow" packing (Figure 2.10 **3b**), as is also observed in the packing of paraffins [27]. The following (< 4 Å) intermolecular contacts more quantitatively reflect the close packing that is visually evident in the Figure 2.11 **3b**: I···O(1), 3.95(2) Å; O(1)···C(8), 3.38(4) Å; O(3)···C(8), 3.64(4) Å; C(p2)···C(6), 3.89(4) Å; C(p3)···C(6), 3.95(1) Å; C(p3)···C(8), 3.91(2) Å; C(p4)···C(6), 3.86(4) Å; C(p4)···C(7), 3.98(5) Å; and C(p5)···C(6), 3.76(2) Å. As is usual, the alkyl chain lies in an energetically favoured extended staggered conformation [28]. While this is true of the ligand conformation, it is noteworthy that the C(2)–W–C(4)–C(5) dihedral angle is nearly eclipsed (9.7°) rather than staggered (180°). This apparently reflects the conformational dictates of facilitating favourable packing of the alkyl chains ("bump in hollow") and the fact that the long W–C bonds that make up the dihedral angle permit a less strained eclipsed configuration than in a simple C–C–C–C dihedral angle. The W–C (4) bond in the alkyl chain was found to be 2.35 Å. To our knowledge, no simple alkyl compounds of the $Cp(CO)_3W$ moiety have been reported, but this bond length is in the general range of reported W–C bonds (2.18–2.36 Å) [29-31], though most of these compounds have different ligands bonded to the metal. The bond length is very similar to that in $[\eta^5\text{-}C_5H_4CH_2\text{-n-}CH_2)(CO)_3W]$ (2.36 Å), the most similar structure [31].

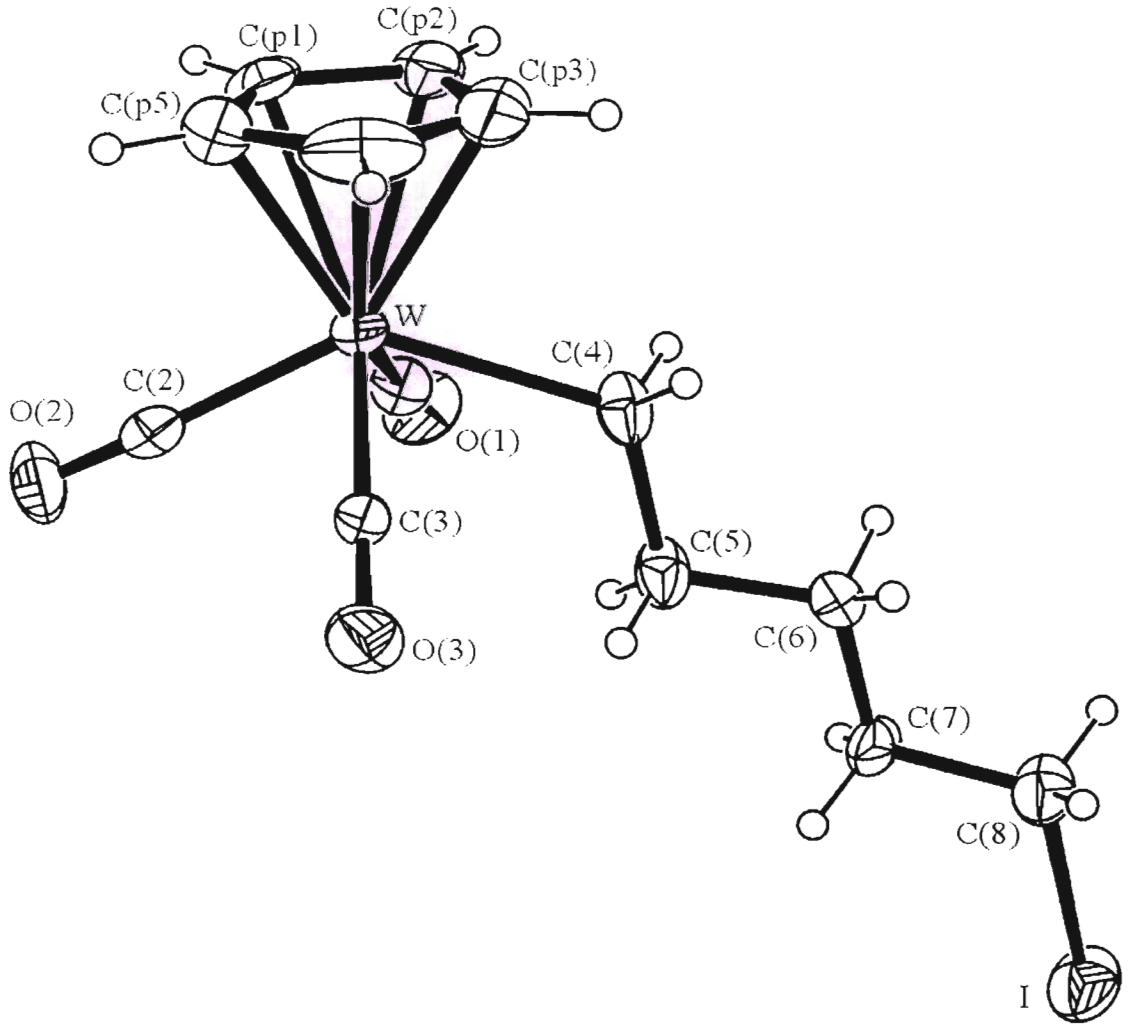

Figure 2.10: ORTEP diagram of the X-ray structure of $[Cp(CO)_3W\{(CH_2)_5I\}]$ **3b**; selected atom labels are shown. Thermal ellipsoids are contoured at the 35% probability level; H atoms have an arbitrary radius of 0.1 Å.

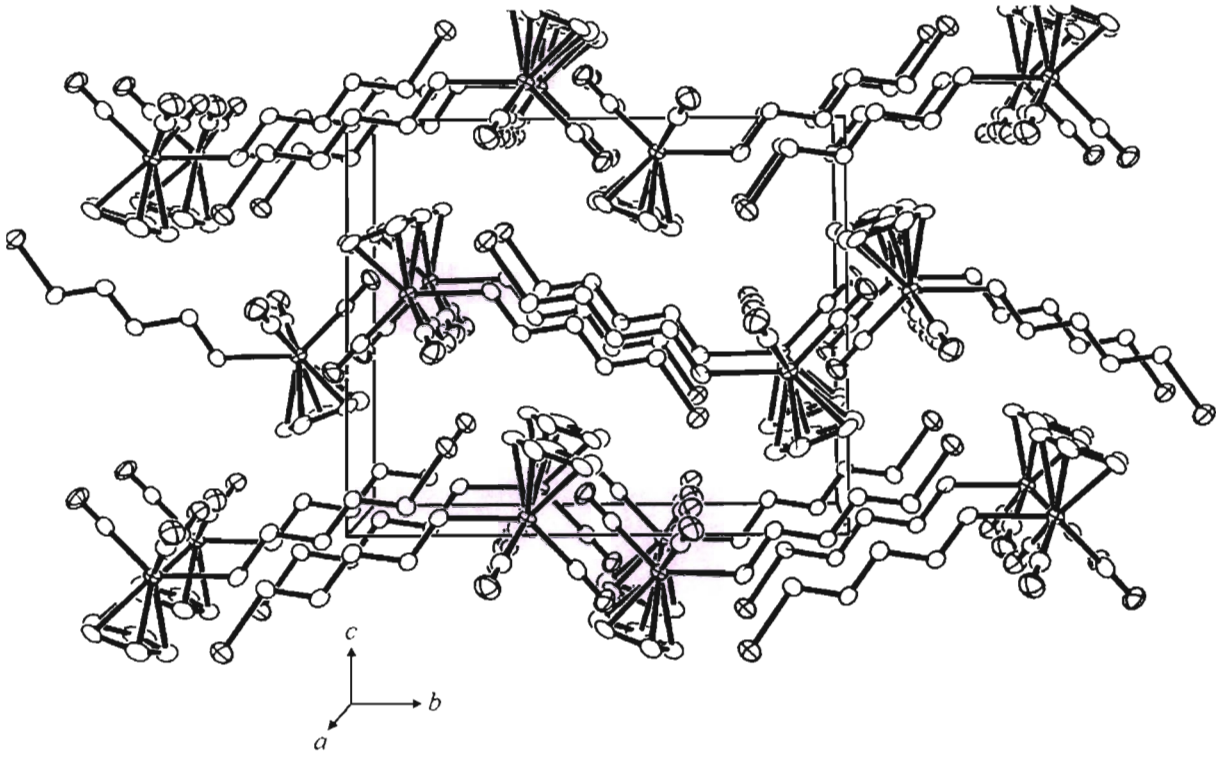

Figure 2.11: ORTEP diagram showing the unit cell packing of $[Cp(CO)_3W\{(CH_2)_5I\}]$ **3b** viewed down the crystallographic *a*-axis. Thermal ellipsoids are contoured at the 35% probability level; H atoms have been omitted for clarity.

Table 2.5: Bond distances for $[Cp(CO)_3W\{(CH_2)_5I\}]$ [a]

Bond	Distance (Å)	Bond	Distance (Å)
W–C(3)	1.88(3)	W–C(2)	1.994(10)
W–C(1)	2.08(3)	W–C(p1)	2.347(12)
W–C(p2)	2.373(19)	W–C(p5)	2.307(14)
W–C(4)	2.348(10)	W–C(p3)	2.349(8)
W–C(p4)	2.308(19)	I–C(8) [b]	2.121(10)
O(2)–C(2)	1.140(12)	O(1)–C(1)	1.12(4)
O(3)–C(3)	1.14(3)	C(p1)–C(p2)	1.391(7)
C(p1)–C(p5)	1.391(7)	C(p2)–C(p3)	1.391(7)
C(p3)–C(p4)	1.391(7)	C(p4)–C(p5)	1.391(7)
C(4)–C(5)	1.532(16)	C(5)–C(6)	1.505(11)
C(6)–C(7)	1.507(12)	C(7)–C(8)	1.491(16)

[a] The esd's of the least significant digits are given in parentheses. [b] Symmetry transformation used to generate equivalent atoms: $x, y - 1/2, -z + 5/2$.

Table 2.6: Bond angles for $[Cp(CO)_3W\{(CH_2)_5I\}]$ [a]

Bond angle	(°)	Bond angle	(°)
C(3)–W–C(2)	74.6(11)	C(3)–W–C(1)	106.7(3)
C(2)–W–C(1)	82.3(11)	C(3)–W–C(p1)	147.7(9)
C(2)–W–C(p1)	95.6(6)	C(1)–W–C(p1)	102.2(9)
C(3)–W–C(p2)	150.9(10)	C(2)–W–C(p2)	128.4(8)
C(1)–W–C(p2)	95.2(10)	C(p1)–W–C(p2)	34.3(3)
C(3)–W–C(p5)	113.2(9)	C(2)–W–C(p5)	88.6(5)
C(1)–W–C(p5)	134.9(10)	C(p1)–W–C(p5)	34.76(17)
C(p2)–W–C(p5)	57.5(3)	C(3)–W–C(4)	77.2(12)
C(2)–W–C(4)	133.2(3)	C(1)–W–C(4)	71.0(12)
C(p1)–W–C(4)	126.8(7)	C(p2)–W–C(4)	92.6(7)
C(p5)–W–C(4)	137.2(5)	C(3)–W–C(p3)	116.6(11)
C(2)–W–C(p3)	146.4(4)	C(1)–W–C(p3)	120.0(11)
C(p1)–W–C(p3)	57.3(3)	C(p2)–W–C(p3)	34.3(2)
C(p5)–W–C(p3)	57.8(3)	C(4)–W–C(p3)	80.1(3)
C(3)–W–C(p4)	98.3(10)	C(2)–W–C(p4)	115.9(9)
C(1)–W–C(p4)	152.5(11)	C(p1)–W–C(p4)	57.8(3)
C(p2)–W–C(p4)	57.5(3)	C(p5)–W–C(p4)	35.1(3)
C(4)–W–C(p4)	104.5(7)	C(p3)–W–C(p4)	34.74(19)
C(p2)–C(p1)–C(p5)	108.0	C(p2)–C(p1)–W	73.9(5)
C(p5)–C(p1)–W	71.0(9)	C(p1)–C(p2)–C(p3)	108.0
C(p1)–C(p2)–W	71.9(4)	C(p3)–C(p2)–W	71.9(6)
C(p2)–C(p3)–C(p4)	108.0	C(p2)–C(p3)–W	73.8(8)
C(p4)–C(p3)–W	71.0(8)	C(p5)–C(p4)–C(p3)	108.0
C(p5)–C(p4)–W	72.4(4)	C(p3)–C(p4)–W	74.2(7)
C(p4)–C(p5)–C(p1)	108.0	C(p4)–C(p5)–W	72.5(5)
C(p1)–C(p5)–W	74.2(9)	O(1)–C(1)–W	177(3)
O(2)–C(2)–W	170(4)	O(3)–C(3)–W	179(2)
C(5)–C(4)–W	121.0(8)	C(6)–C(5)–C(4)	112.7(10)
C(5)–C(6)–C(7)	113.9(7)	C(8)–C(7)–C(6)	114.3(9)
C(7)–C(8)–I [b]	113.0(9)		

[a] The esd's of the least significant digits are given in parentheses. [b] Symmetry transformation used to generate equivalent atoms: $x, y + 1/2, -z + 5/2$. (9.7°) rather than staggered (180°). This apparently reflects the conformational dictates of facilitating favourable packing of the alkyl

The structure of $[Cp(CO)_3W\{(CH_2)_3Br\}]$ is similar to that of the iodo compound above; bond lengths and angles for this compound are given in Tables 2.7 and 2.8 respectively. Complete listings of all crystallographic data for this compound are given in Appendix 1, the attached compact disc and the supplementary material [32]. There are two independent molecules per asymmetric unit; the structure of the molecule and packing in the crystal are shown in Figures 2.11 **3b** and 2.13 **1a**. The W–C bond length of 2.35 Å is identical to the same bond in the iodo compound above and the C–Br bond of 1.95 Å is within the range found for "paraffinic" alkyl bromide compounds [33]. Whilst the structure clearly shows that there is no bending of the bromine towards the tungsten in the solid state (as possibly indicated in solution), the C(4)–C(5) bond length at 1.48 Å is 0.5 Å shorter than the equivalent bond in the longer chained iodoalkyl compound, which may account for the unusual spectral characteristics of the α-carbons in halogenopropyl compounds. Interestingly, the unit cell packing of $[Cp(CO)_3W\{(CH_2)_3Br\}]$ **1a**, shown in Figure 2.13, reveals that the conformation of the alkyl ligand is probably a compromise between (1) minimizing an unfavourable C(5)···C(8) intramolecular contact between the alkyl and Cp ligands and (2) the reality that "bump in hollow" packing similar to that of Figure 2.11 **3b** only becomes more favourable as the alkyl chain gets longer. The 3-carbon alkyl chain appears to be too short to favour the "bump in hollow" packing observed for $[Cp(CO)_3W\{(CH_2)_5I\}]$. The alkyl ligand thus exhibits a C(2)–W(1)–C(4)–C(5) dihedral angle that is closer to 90° than 180° in both independent molecules of the asymmetric unit (119.1° and 118.0° for molecules A and B, respectively).

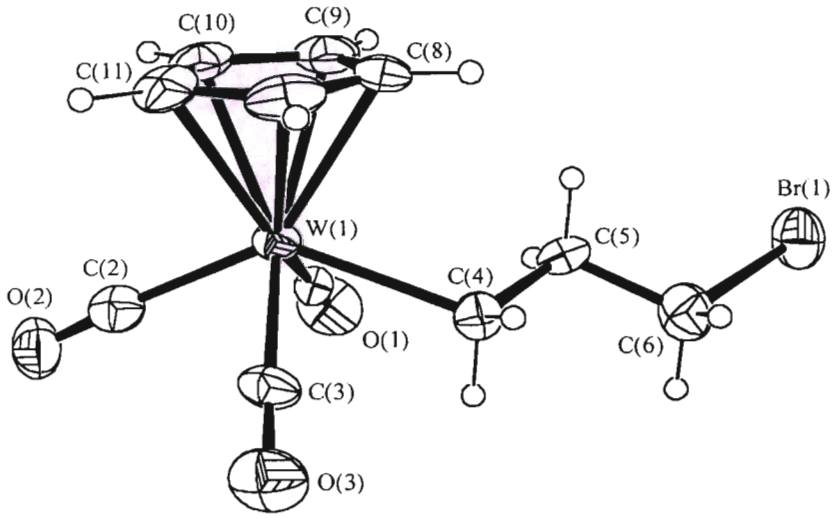

Molecule A

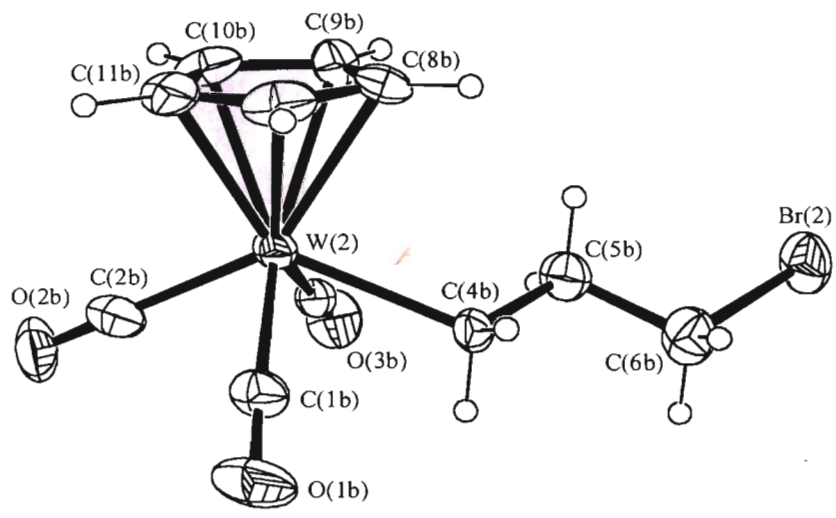

Molecule B

Figure 2.12: ORTEP diagrams showing the crystallographically independent molecules (A and B) of the X-ray structure of $[Cp(CO)_3W\{(CH_2)_3Br\}]$ **1a**; selected atom labels are indicated. Thermal ellipsoids are contoured at the 35% probability level; H atoms have an arbitrary radius of 0.1 Å.

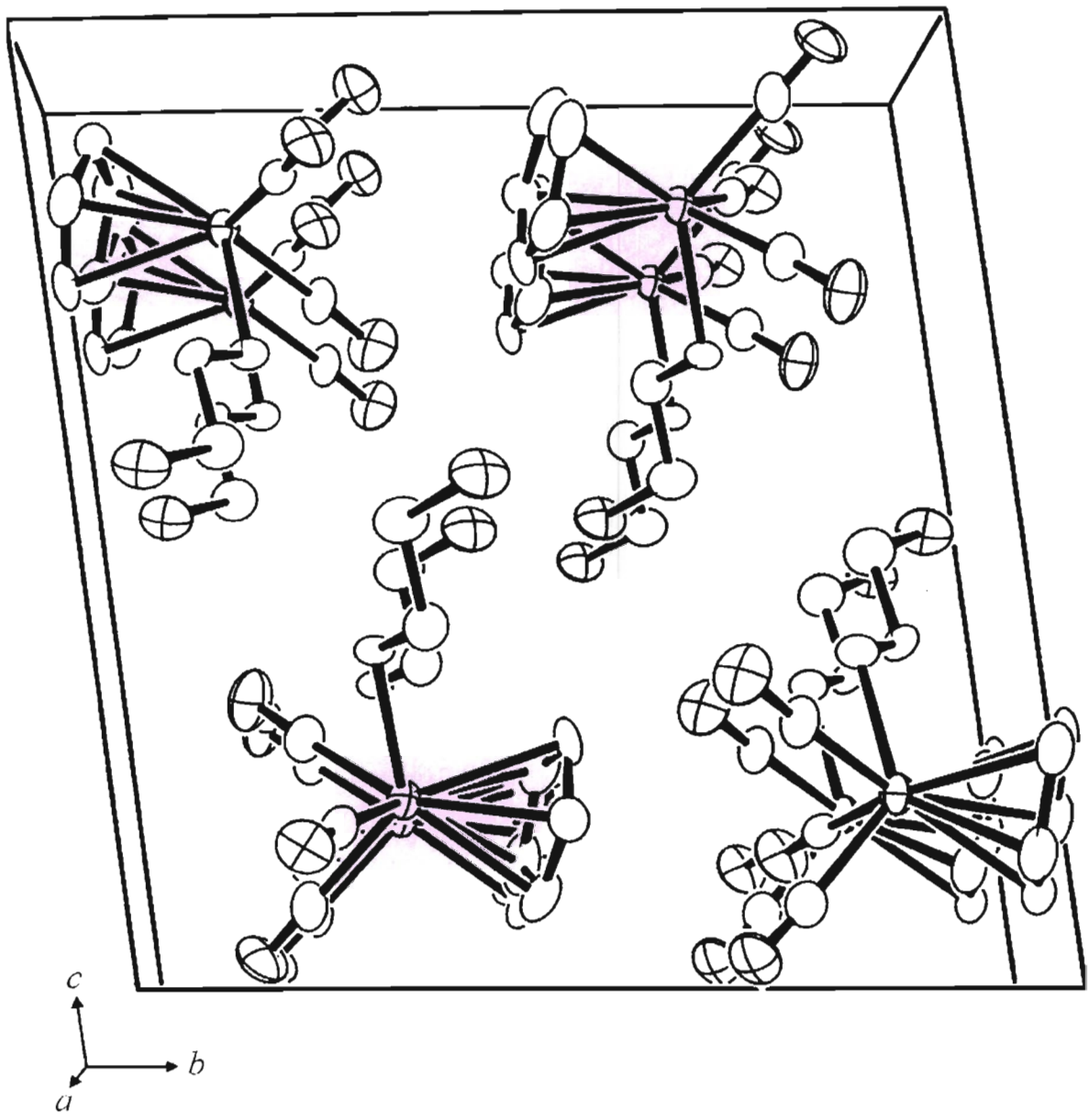

Figure 2.13: ORTEP diagram showing the unit cell packing of $[Cp(CO)_3W\{(CH_2)_3Br\}]$ **1a** viewed down the crystallographic *a*-axis. Thermal ellipsoids are contoured at the 35% probability level; H atoms have been omitted for clarity.

Table 2.7: Bond distances for $[Cp(CO)_3W\{(CH_2)_3Br\}]$ [a, b]

Bond	Distance (Å)	Bond	Distance (Å)
W(1)–C(3)	1.949(17)	W(1)–C(1)	1.983(17)
W(1)–C(9)	2.304(17)	W(1)–C(11)	2.326(15)
W(1)–C(4)	2.347(15)	W(1)–C(7)	2.356(16)
W(1)–C(8)	2.362(16)	Br(1)–C(6)	1.946(17)
O(1)–C(1)	1.149(18)	O(2)–C(2)	1.06(2)
O(3)–C(3)	1.17(2)	C(4)–C(5)	1.48(2)
C(5)–C(6)	1.51(2)	C(7)–C(8)	1.39(3)
C(7)–C(11)	1.44(3)	C(8)–C(9)	1.37(3)
C(9)–C(10)	1.39(3)	C(10)–C(11)	1.39(3)
W(2)–C(1b)	1.964(17)	W(2)–C(3b)	2.013(18)
W(2)–C(2b)	2.03(2)	W(2)–C(11b)	2.285(16)
W(2)–C(10b)	2.308(17)	W(2)–C(9b)	2.324(17)
W(2)–C(4b)	2.336(14)	W(2)–C(8b)	2.361(16)
W(2)–C(7b)	2.364(18)	Br(2)–C(6b)	1.941(17)
O(1b)–C(1b)	1.15(2)	O(2b)–C(2b)	1.04(2)
O(3b)–C(3b)	1.118(19)	C(4b)–C(5b)	1.51(2)
C(5b)–C(6b)	1.53(2)	C(7b)–C(8b)	1.40(3)
C(7b)–C(11b)	1.40(3)	C(8b)–C(9b)	1.37(3)
C(9b)–C(10b)	1.40(3)	C(10b)–C(11b)	1.36(3)

[a] The esd's of the least significant digits are given in parentheses. [b] Atoms belonging to the second independent molecule in the asymmetric unit (molecule B) are W(2), Br(2), and all those listed with alphanumeric labels containing the letter b.

Table 2.8: Bond angles for $[Cp(CO)_3W\{(CH_2)_3Br\}]$ [a, b]

Bond angle	(°)	Bond angle	(°)
C(3)–W(1)–C(1)	106.7(7)	C(3)–W(1)–C(2)	78.9(7)
C(1)–W(1)–C(2)	78.2(6)	C(3)–W(1)–C(10)	144.7(7)
C(1)–W(1)–C(10)	104.1(7)	C(2)–W(1)–C(10)	90.9(7)
C(3)–W(1)–C(9)	152.8(8)	C(1)–W(1)–C(9)	94.9(6)
C(2)–W(1)–C(9)	122.6(8)	C(10)–W(1)–C(9)	35.1(7)
C(3)–W(1)–C(11)	110.5(7)	C(1)–W(1)–C(11)	137.7(7)
C(2)–W(1)–C(11)	89.5(7)	C(10)–W(1)–C(11)	35.0(7)
C(9)–W(1)–C(11)	58.3(7)	C(3)–W(1)–C(4)	72.4(6)
C(1)–W(1)–C(4)	74.6(6)	C(2)–W(1)–C(4)	132.2(6)
C(10)–W(1)–C(4)	133.4(7)	C(9)–W(1)–C(4)	98.4(7)
C(11)–W(1)–C(4)	136.1(7)	C(3)–W(1)–C(7)	98.4(7)
C(1)–W(1)–C(7)	151.3(7)	C(2)–W(1)–C(7)	121.1(7)
C(10)–W(1)–C(7)	58.3(7)	C(9)–W(1)–C(7)	57.3(7)
C(11)–W(1)–C(7)	35.8(7)	C(4)–W(1)–C(7)	100.6(7)
C(3)–W(1)–C(8)	118.8(8)	C(1)–W(1)–C(8)	118.1(7)
C(2)–W(1)–C(8)	146.5(7)	C(10)–W(1)–C(8)	57.8(7)
C(9)–W(1)–C(8)	34.1(7)	C(11)–W(1)–C(8)	58.4(7)
C(4)–W(1)–C(8)	81.3(6)	C(7)–W(1)–C(8)	34.3(7)
O(1)–C(1)–W(1)	176.6(14)	O(2)–C(2)–W(1)	176.4(18)
O(3)–C(3)–W(1)	177.3(17)	C(5)–C(4)–W(1)	116.2(10)
C(4)–C(5)–C(6)	109.0(13)	C(5)–C(6)–Br(1)	113.1(13)
C(8)–C(7)–C(11)	107.6(17)	C(8)–C(7)–W(1)	73.1(9)
C(11)–C(7)–W(1)	70.9(9)	C(9)–C(8)–C(7)	108.1(18)
C(9)–C(8)–W(1)	70.6(10)	C(7)–C(8)–W(1)	72.6(10)
C(8)–C(9)–C(10)	109.4(18)	C(8)–C(9)–W(1)	75.3(10)
C(10)–C(9)–W(1)	72.0(10)	C(9)–C(10)–C(11)	108.6(18)
C(9)–C(10)–W(1)	72.9(10)	C(11)–C(10)–W(1)	73.9(10)
C(10)–C(11)–C(7)	106.2(17)	C(10)–C(11)–W(1)	71.1(9)
C(7)–C(11)–W(1)	73.2(10)		
C(1b)–W(2)–C(2b)	77.6(7)		

[a] The esd's of the least significant digits are given in parentheses. [b] Atoms belonging to the second independent molecule in the asymmetric unit (molecule B) are W(2), Br(2), and all those listed with alphanumeric labels containing the letter b.

2.4 Reactions of Some of the Halogenoalkyl Compounds of Tungsten

The bromoalkyl compound where n = 3 has been shown to react with potassium cyanide and lithium iodide in refluxing methanol or tetrahydrofuran respectively to form the cyclic carbene compounds $[XCp(CO)_2W\{CO(CH_2)_2CH_2\}]$ X = I, CN [3] at room temperature, whilst we have shown that $[Cp(CO)_3W\{(CH_2)_nBr\}]$ will react with sodium iodide in acetone to form $[Cp(CO)_3W\{(CH_2)_nI\}]$ thus demonstrating the significant effect of temperature and solvent on the reactions of these halogenoalkyl compounds - both in terms of yield and in which product is formed. In view of the above observations, the reactions described below were carried out at room temperature, because the formation of the cyclic carbenes was not in our objectives at the onset of our work.

Compound **2a** was reacted with silver nitrate in acetonitrile forming an orange product, $[Cp(CO)_3W\{(CH_2)_4ONO_2\}]$ (see Equation 7).

$$[Cp(CO)_3W\{CH_2)_4Br\}] + AgNO_3 \longrightarrow [Cp(CO)_3W\{(CH_2)_4ONO_2\}] + AgBr \qquad (7)$$

The IR spectrum showed the expected typical ν(N=O) stretches at 1628 cm^{-1} (sym) and 1263 cm^{-1} (asym). The ^1H NMR spectrum (Figure 2.14) showed a significant downfield shift of *ca.* 1 ppm due to CH_2ONO_2 protons. The carbon attached to these protons was confirmed by the ^{13}C NMR spectrum to be highly deshielded, at 72.88 ppm, compared to 8.16 ppm for the starting material (Figure 2.15). Thus, the nitrate ion, besides being characteristically a stronger nucleophile than bromide, appeared to be very electronegative as well, possibly due to the presence of the three oxygen atoms, which help to draw away the electrons from the C-ONO_2 carbon, making it highly deshielded.

The reaction of silver cyanide with $[Cp(CO)_3W\{(CH_2)_3I\}]$ in acetonitrile gave the compound, $[Cp(CO)_3W\{(CH_2)_3CN\}]$ (Equation 8), as judged by the spectroscopic results obtained.

$$[Cp(CO)_3W\{(CH_2)_3I\}] + AgCN \longrightarrow [Cp(CO)_3W\{(CH_2)_3CN\}] + AgI \qquad (8)$$

There was a small sharp peak at 2244 cm^{-1}, characteristic of ν(CN) in the infrared spectrum.

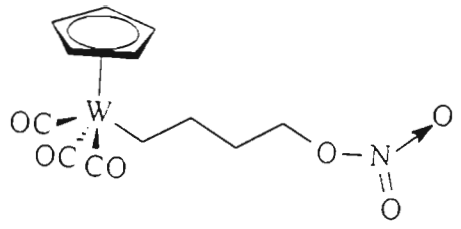

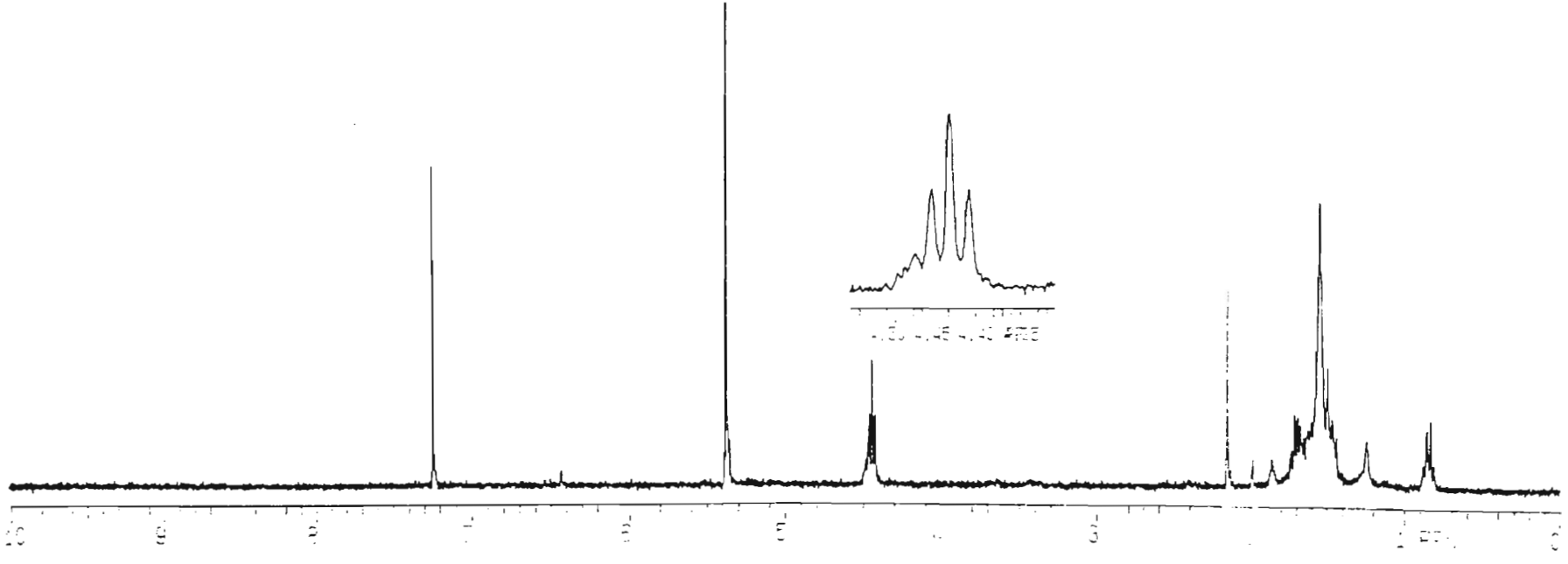

Figure 2:14: ^{1}H NMR spectrum of $[Cp(CO)_3W\{(CH_2)_4ONO_2\}]$

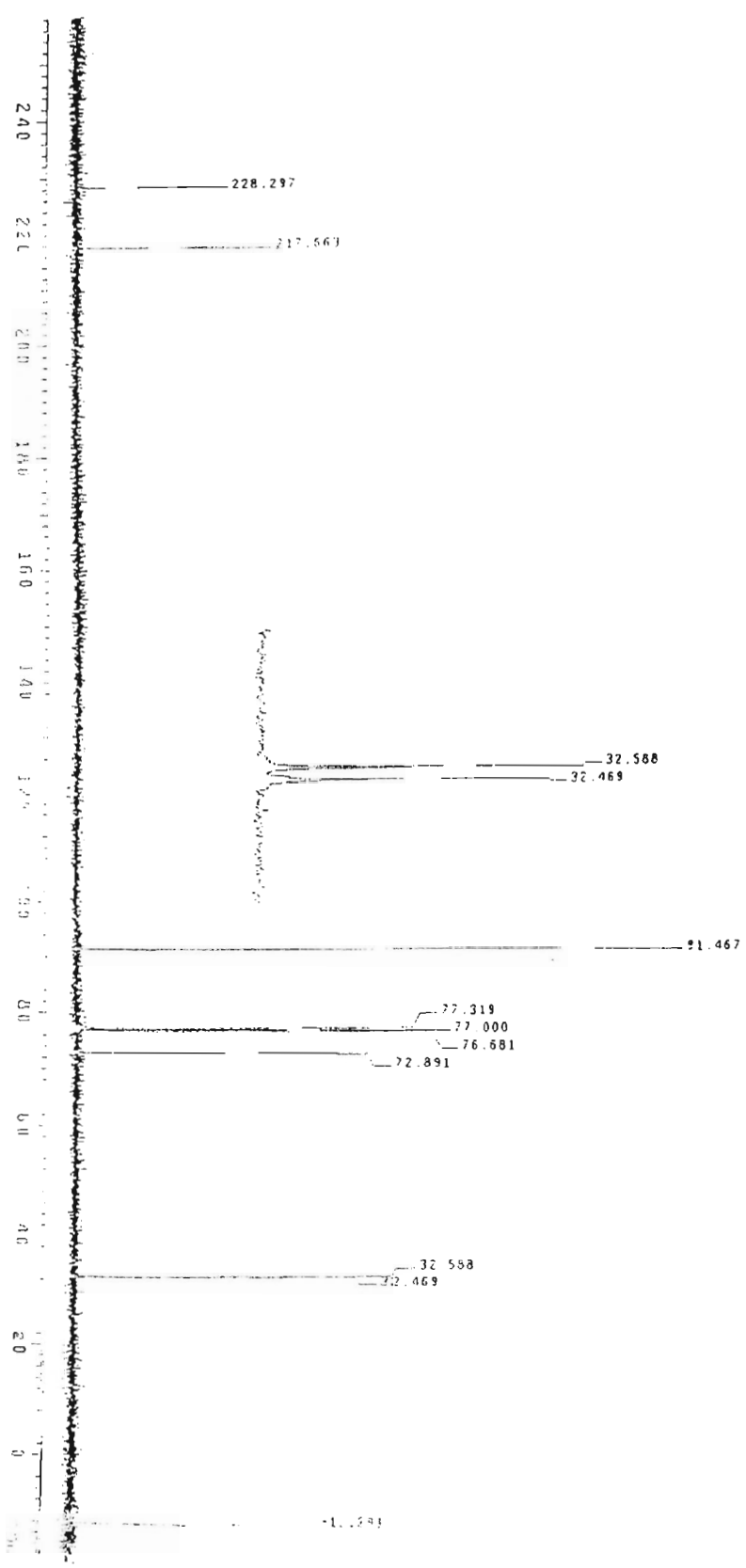

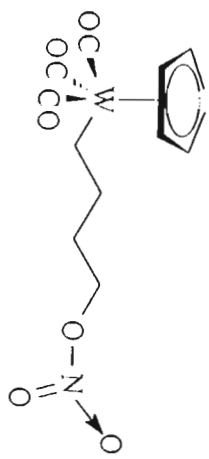

Figure 2.15: ^{13}C NMR spectrum of $[\eta$-p(CO)$_3$W{(CH$_2$)$_4$ONO$_2$}]

The ^{1}H NMR spectrum had the peaks around 2.3 ppm (CH_2CN) and 1.7 pm (CH_2CH_2CN) in the upfield region. The reaction proceeded slowly, as found by monitored ^{1}H NMR spectroscopy over several days for the disappearance of the CH_2I peak, and did not reach completion. The ^{13}C NMR spectrum showed a peak at 119 ppm, which is attributable to the cyano group. Consequently, the cyanide ion successfully displaced the iodide ion.

Previous attempts to displace the bromine or iodine of the compounds, $[Cp(CO)_3W\{(CH_2)_4Br\}]$, **2a**, $[Cp(CO)_3W\{(CH_2)_3I\}]$, **1b** and $[Cp(CO)_3W\{(CH_2)_5I\}]$, **3b** with sodium cyanide and potassium cyanide in acetonitrile failed. This shows that the formation of silver iodide through the reaction of silver cyanide, creates a stronger driving force that aids the forward reaction than either of the other two cyano compounds, this is presumably due to the strong affinity of Ag for I^-. A change of reaction medium was also found to have a significant effect on the reaction. We succeeded in reacting sodium cyanide with **3b** when we used an equi-volume mixture of nitrogen saturated double distilled de-ionised water and tetrahydrofuran over a period of 4 days. A yellow compound showing all the expected characteristics was obtained. The medium for reactions is known to have great influence on the manner in which a reaction proceeds.

The reactions of the compounds, $[Cp(CO)_3W\{(CH_2)_4Br\}]$, **2a** and $[Cp(CO)_3W\{(CH_2)_5I\}]$, **3b** with sodium azide, gave $[Cp(CO)_3W\{(CH_2)_4N_3\}]$ and $[Cp(CO)_3W\{(CH_2)_5N_3\}]$ respectively (Equation 9).

$$[Cp(CO)_3W\{(CH_2)_5I\}] + NaN_3 \longrightarrow [Cp(CO)_3W\{(CH_2)_5N_3\}] + NaI \qquad (9)$$

In both of these reactions, there was a change in the $\nu(CO)$ region in the infrared spectrum after only 5 minutes from the start of the reaction. A medium, broad band was observed at 1639 cm^{-1}, giving an indication that there was an alkyl migration reaction. However, no acyl bond was seen in the final product. As expected, a small peak was observed at 2155 cm^{-1} that could be attributed to the stretching vibrations of $-N{=}N^{+}{=}N^{-}$. No siginificant difference was observed between the starting material and the product obtained, from the ^{1}H and ^{13}C NMR spectra. This type of reaction is expected to proceed to completion because the azides have been shown to displace the halogens from the alkylhalide compounds [34]. The kinetic investigation showed that the reactivity rate of the 1-

bromobutane and with an azide ion (Equation 10), is forty fold in HMPA on comparison to acetonitrile [34].

$$CH_3CH_2CH_2CH_2Br + N_3^- \longrightarrow CH_3CH_2CH_2CH_2N_3 + Br^- \quad (10)$$

Both the acetonitrile and HMPA have been suggested to be the ideal solvents for this type of reaction, because they do not have a positively polarized hydrogen atom (either O-H nor N-H) for hydrogen bonding to the anions [35]. The two solvents would then stabilize the cations through the interaction with their negatively polarized oxygen. Though, HMPA would be most appropriate because of its low dielectric constant of 30 compared to that of the acetonitrile which is 37.5, it has a higher boiling point and thus makes the product difficult to isolate. The dielectric constant plays a major role in determining the relative free energy necessary for a reaction to proceed to the transition state. The higher the dielectric constant of a solvent the lower the free energy, consequently the higher the rate of a reaction [33].

Flakes of disodium sulfide ($Na_2S.2H_2O$) clearly reacted with the compound **2a** as deduced from changes in the carbonyl stretching frequencies of the infrared spectrum, but the ^1H and ^{13}C NMR spectra were very ''messy'' and did not yield any useful information. A repeat of this reaction in methanol instead of acetonitrile gave similar results to the above. Probably a mixture of products was obtained, which could not be separated. As a result, the compound could not be fully characterised, and no further reaction attempts were made with sodium sulphide, so the product reported in Scheme 2.2 below is merely speculative. Some characterisation data of the products obtained from the above reactions are listed in Table 2.9 below while the reactions are summarized in Scheme 2.2.

Table 2.9: IR, Yields and ^{1}H NMR NMR Data from Reaction Studies of Some of the Tungsten Halogenoalkyl Compounds

Cpd	IR ν(CO)[a] cm^{-1}	Yield (%)	Cp	α-CH_2	CH_2Nu	CH_2CH_2Nu	β-CH_2	γ-CH_2
$[Cp(CO)_3W\{(CH_2)_3CN\}]$	2012sb, 1914sb	95	5.38s, 5H[b]	1.44m	2.3t, 2H, 7.2	1.70m		
$[Cp(CO)_3W\{(CH_2)_4CN\}]$	2011sb, 1912sb	92	5.38s, 5H	1.46m	3.42t, 2H, 7.2	1.84m	1.64m	
$[Cp(CO)_3W\{(CH_2)_3ONO_2\}]$	2011ss, 1912sb	97	5.36s, 5H	1.49m	4.43t, 2H, 6.6	1.71m		
$[Cp(CO)_3W\{(CH_2)_4N_3\}]$	2011ss, 1912sb	98	5.38s, 5H	1.45m	3.42t, 2H, 6.7	1.85m	1.67m	
$[Cp(CO)_3W\{(CH_2)_5N_3\}]$	2010ss, 1910sb	95	5.35s, 5H	1.51m	3.16 t, 2H, 6.7	1.82m	1.37m	1.47m

^{13}C NMR Data from Reaction Studies of Some of the Tungsten Halogenoalkyl Compounds

Cpd	CO	CN	Cp	α-CH_2	CH_2Nu	CH_2CH_2Nu	β-CH_2	γ-CH_2
$[Cp(CO)_3W\{(CH_2)_3CN\}]$	228s, 217s[b]	119.3s	91.5s	-11.9s	11.7s	40.9s		
$[Cp(CO)_3W\{(CH_2)_4CN\}]$	228s, 217s	119.1s	91.0s	-12.4	33.5s	35.0s	38.3s	
$[Cp(CO)_3W\{(CH_2)_3ONO_2\}]$	217s		91.5s	-12.3s	72.9s	32.6s		
$[Cp(CO)_3W\{(CH_2)_4N_3\}]$	228s, 217s		91.0s	-12.4	33.6s	35.1s	38.4s	
$[Cp(CO)_3W\{(CH_2)_5N_3\}]$	228s, 217s		91.5s	-12.4	33.6s	35.1	38.5s[c]	38.5s[c]

[a] Measured in CH_2Cl_2; [b] measured in $CDCl_3$ relative to TMS (δ = 0.00 ppm), J values are given in Hz; α-CH_2 refers to the CH_2-group α- to tungsten *etc.* [c] Peaks overlap.

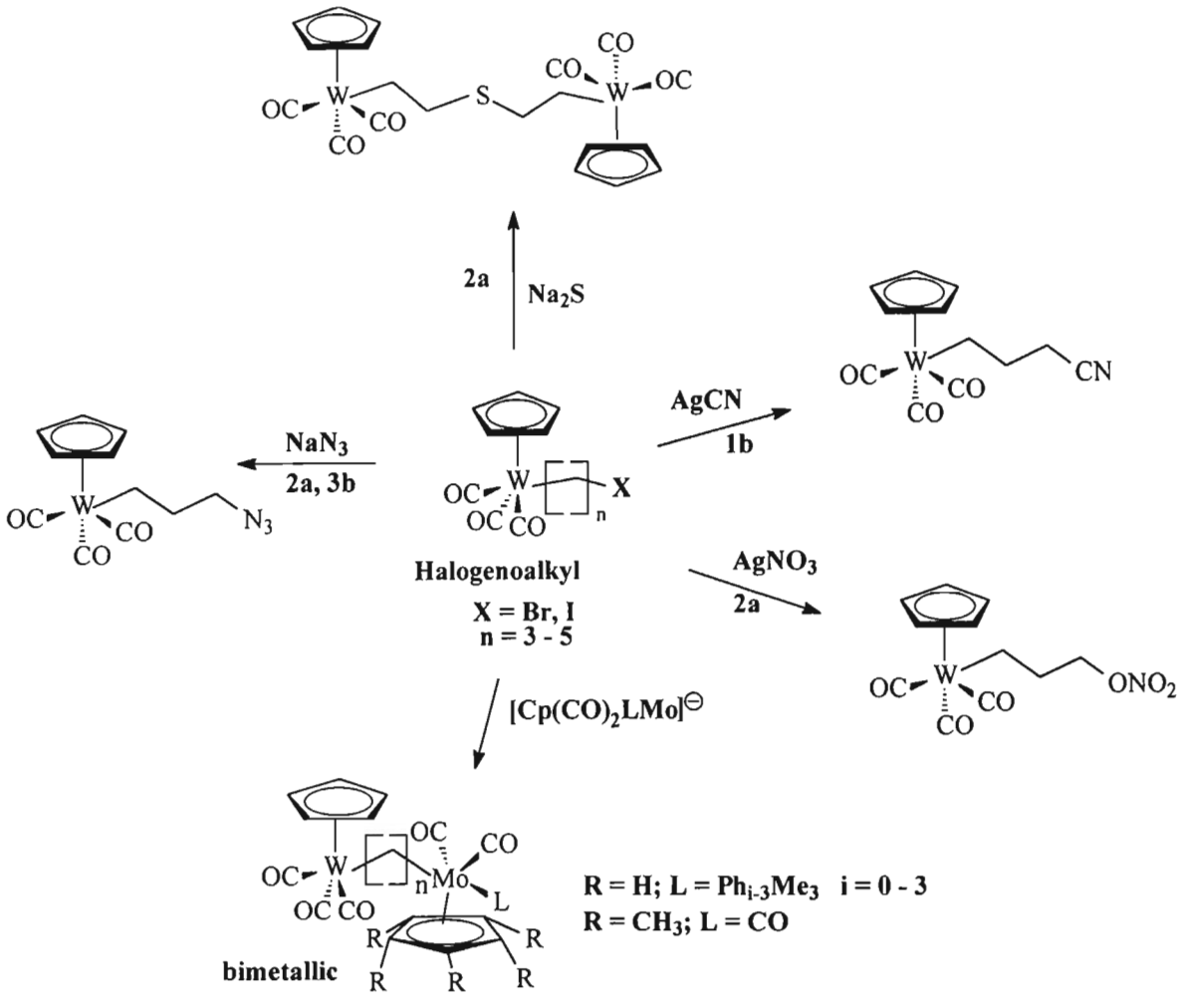

Scheme 2.2: Summary of some of the reactions of the tungsten halogenoalkyl compounds.

2.5 Conclusions

The compounds $[Cp(CO)_3W\{(CH_2)_nX\}]$ n = 3 - 6; X = Br, I) were prepared by a new high yielding synthetic route, by refluxing the corresponding anion $[Cp(CO)_3W]^-$ with $Br(CH_2)_nBr$, n = 3 – 6. The bromoalkyl compounds were subsequently reacted with NaI to give the corresponding iodoalkyl compounds $[Cp(CO)_3W\{(CH_2)_nI\}]$ (n = 3 – 6). New compounds were synthesized and those previously known were obtained in higher yield and further characterised.

Alongside the confirmation of some of the reported results in the literature, we have detailed an alternative approach to the recrystallisation procedure of using dilute dichloromethane/hexane mixture at −78 °C to give analytically pure products for these compounds.

Reaction studies were also successfully carried out on some of the new compounds. Through this, we have shown that the tungsten halogenoalkyl compounds react further at the halogen end and not on the metal site as would be expected. This property was exploited for the synthesis of heterodinuclear compounds containing tungsten as one of the metal.

The crystal and molecular structures of $[Cp(CO)_3W\{(CH_2)_3Br\}]$ and $[Cp(CO)_3W\{(CH_2)_5I\}]$ are reported for the first time. The two crystal structures display a geometry that may be described as 'three legged piano stool'. Whilst the structure of the former clearly shows that there is no bending of the bromine towards the tungsten in the solid state (as possibly indicated in solution), the C(4)–C(5) bond length at 1.48 Å is 0.5 Å shorter than the equivalent bond in the longer chained iodoalkyl compound, which may account for the unusual spectral characteristics of the α-carbons in halogenopropyl compounds.

It is worth noting, that the results presented here were independently obtained and without prior knowledge of recently reported similar work [10]. As a matter of fact, they pre-empted a paper of this work, which was about to be sent for publication. Nevertheless, we used different methods to obtain the halogenoalkyl compounds and some of our data differs from the previous report. Our yields were in excess of 90%, which are some 20%

higher than those reported [10]. The following data from Tables 2.2 – 2.4 for our compounds differ significantly (Literature data in parenthesis); $[Cp(CO)_3W\{(CH_2)_4Br\}]$ **2a**: m.p. = 66–67 °C (58 –66); $[Cp(CO)_3W\{(CH_2)_4I\}]$ **2b**: m.p. = 109–110 °C (67 – 69); $[Cp(CO)_3W\{(CH_2)_6Br\}]$ **4a**: m.p. = 51–55 °C (61 – 63); $[Cp(CO)_3W\{(CH_2)_6I\}]$ **4b**: m.p. = 64–66 °C (57 – 58).

We observed the chemical shifts for the CO in the ^{13}C NMR data to be between 217 - 220 ppm while those reported in the literature were all observed at 217 ppm. Our Cp peaks were observed between 91 - 94 ppm while the literature values were all reported at 91 ppm and the α-CH_2 peaks were observed at –7 - –13 ppm, while the literature values were reported at –10 - –14 ppm.

These halogenoalkyl compounds are known to be precursors to heterodinuclear compounds, a property that is further explored in Chapter 4.

2.6 References

[1] R.B. King, *Inorg. Chem.*, **2** (1963) 531.

[2] N.A. Bailey, D.A. Dunn, C.N. Foxcroft, G.R. Harris, M.J. Winter, S. Woodward, *J. Chem. Soc., Dalton Trans.*, (1988) 1449.

[3] N.A. Bailey, P.L. Chell, C.P. Manuel, A. Mukhopadhyay, D. Rodgers, H.E. Tabron, M.J. Winter, *J. Chem. Soc., Dalton Trans.*, (1983) 2397.

[4] H.B. Friedrich, J.R. Moss, *Adv. Organomet. Chem.*, **33** (1991) 235.

[5] H.B. Friedrich, K.P. Finch, M.A. Gafoor, J.R. Moss, *Inorg. Chim. Acta*, **206** (1993) 225.

[6] H.B. Friedrich, P.A. Makhesha, J.R. Moss, B.K. Williamson, *J. Organomet. Chem.*, **384** (1990) 325.

[7] P.K. Monaghan, R.J. Puddephatt, *J. Chem. Soc., Dalton Trans.*, (1988) 595.

[8] R.B. King, M.B. Bisnette, *J. Organomet. Chem.*, **7** (1967) 311.

[9] L. Pope, P. Somerville, M.J. Laing, K.J. Hindson, J.R. Moss, *J. Organomet. Chem.*, **112** (1976) 309.

[10] X. Yin, J.R. Moss, *J. Organomet. Chem.*, **574** (1999) 252.

[11] E.O Fischer, W Hafner, H.O. Stahl, *Z. Anorg. Allgem. Chem.*, **282** (1955) 47.

[12] M.A. El-Hinnawi, A.K. El-Qaseer,, *J. Organomet. Chem.*, **281** (1985) 119.

[13] R. Birdwhistell, P. Hackett and A. R. Manning, *J. Organomet. Chem.*, **157** (1978) 239.

[14] E.W. Abel, A. Singh, G. Wilkinson, *J. Chem. Soc.*, (1960) 1321.

[15] R.G. Hayter, *Inorg. Chem.*, **2** (1963) 1031.

[16] H. Adams, N.A. Bailey, M.J. Winter, *J. Chem. Soc., Dalton Trans.*, (1984) 273.

[17] C.P. Casey, R.L.Anderson, *J. Amer. Chem. Soc.*, **93** (1971) 3554.

[18] J.R. Moss, *J. Organomet. Chem.*, **231** (1982) 229.

[19] R.B. King, *Acc. Chem. Res.*, **3** (1970) 417.

[20] J. March, "Advanced Organic Chemistry: Reactions, Mechanisms and Structure", 4th edn., Wiley-Interscience, New Yolk, 1992, p 430.

[21] J.R. Moss and L.G. Scott, *J. Organomet. Chem.*, **282** (1985) 255.

[22] R. Boese, H.-C. Weiss, D. Bläser, *Angew. Chem. Int. Ed. Engl.*, **38** (1999) 988.

[23] A.P. Malanoski, P.A. Monson, *J. Chem. Phys.*, **110** (1999) 664.

[24] C.P. Casey, L.J. Smith, *Organometallics*, **7** (1988) 2419.

[25] P.G. Jones, *Chemistry in Britain*, **17** (1981) 222.

[26] Cambridge Crystallographic Data Centre, CCDC No. 158285 for, **3b**, $[Cp(CO)_3W\{(CH_2)_5I\}]$.

[27] A.I. Kitaigorodskii, "Organic Chemical Crystallography", Consultants Bureau, New York, 1961, p 65.

[28] R.O. Hill, C.F. Marais, J.R. Moss, K.J. Naidoo, *J. Organomet. Chem.*, **587** (1999) 28.

[29] D.J. Darensbourg, R. Kudaroski, *J. Amer. Chem. Soc.*, **106** (1984) 3672.

[30] D.J. Debad, P. Legzdins, S.J. Rettig, J.E. Veltheer, *Organometallics*, **12** (1993) 2714.

[31] F. Amor, P. Royo, T.P. Spaniol, J. Okuda, *J. Organomet. Chem.*, **604** (2000) 126.

[32] Cambridge Crystallographic Data Centre, CCDC No. 158287 for **1a**, $[Cp(CO)_3W\{(CH_2)_3Br\}]$.

[33] A.I. Kitaigorodskii, "Organic Chemical Crystallography", Consultants Bureau, New York, 1961, p3.

[34] J. McMurry, "Organic Chemistry", 3rd edn., Brooks, California, 1992, p373.

[35] R.O.C. Norman, J.M. Coxon, "Principles of Organic Synthesis", 3rd edn., Blackie Academic and Professional, London, 1993.

CHAPTER 3

HALOGENOALKYL COMPOUNDS OF MOLYBDENUM

3.1 Introduction

Since King synthesized the hydrocarbon bridged metal complexes by the reaction of a number of 1,n dibromoalkanes with transition metal anions [1], several complexes of this type have been synthesized, as shown in Chapter 2. Bailey *et al.* have also reported on the synthesis of a number of halogenoalkyl complexes containing molybdenum [2,3]. Interestingly, although the halogenomethyl compounds $[(\eta^5\text{-}C_5R_5)(CO)_3Mo\{CH_2X\}]$ (R = H, CH_3; X = Cl, Br, I) are now known [4,5], very few phosphine substituted compounds $[Cp(CO)_2LMo\{CH_2X\}]$ (L = tertiary phosphine or phosphite) have been reported. Only compounds where L = $P(OPh)_3$ and X = Cl, Br and I are known [6]. The only previously reported long-chain halogenoalkyl compounds of molybdenum but not fully characterised are $[Cp(CO)_3Mo\{(CH_2)_nX\}]$ (n = 3, X = Cl, Br, I; n = 4, X = Br, I), $[Cp^*(CO)_3Mo\{(CH_2)_3Br\}]$ and $[Cp(CO)_2(PPh_3)Mo\{(CH_2)_3Br\}$[2,3, 7-9]. We now report on the syntheses and properties of the newly synthesized compounds.

3.2 Synthesis and Properties of Some New Molybdenum Halogenoalkyl Compounds

The molybdenum dimers, $[\{Cp(CO)_2LMo\}_2]$, where L is triphenylphosphine, methyldiphenylphosphine, dimethylphenylphosphine and trimethylphosphine, were prepared following the method used by Nataro [10]. The hexacarbonylbis(pentahapto-cyclopentadienyl)dimolybdenum was prepared by an improved method to the literature [11], similar to that used for the tungsten dimer, $[\{Cp(CO)_3W\}_2]$, as shown in the previous chapter. Molybdenum hexacarbonyl was refluxed in acetonitrile as shown in Equation 1, and the product then reacted with cyclopentadiene, Equation 12.

$$Mo(CO)_6 + 3CH_3CN \xrightarrow{\Delta} [(CO)_3(CH_3CN)_3Mo] + 3CO \quad (1)$$

$$[(CO)_3(CH_3CN)_3Mo] + C_5H_6 \xrightarrow{\Delta} [\{Cp(CO)_3Mo\}_2] + H_2 + 6CH_3CN \quad (2)$$

The prepared dimeric compound is stripped of two carbonyls, to form a dark unstable triple bonded Mo≡Mo species by heating in diglyme as shown in Equation 3,

$$[\{Cp(CO)_3Mo\}_2] \xrightarrow{\text{diglyme, } \Delta} [\{Cp(CO)_2Mo\}_2] + 2CO \quad (3)$$

Two equivalents of either triphenylphosphine, methyldiphenylphosphine, dimethylphenyl phosphine or trimethylphosphine were added to form the respective dimers, $[\{Cp(CO)_2(PPh_iMe_{3-i})Mo\}_2]$, i = 0 – 3 as represented in Equation 4.

$$[\{Cp(CO)_2Mo\}_2] + 2PPh_iMe_{3-i} \longrightarrow [\{Cp(CO)_2(PPh_iMe_{3-i})Mo\}_2] \quad i = 0 - 3 \quad (4)$$

This manner of dimer preparations had been reported earlier by Klinger and co-workers when they added the soft nucleophiles, phosphites ($P(OMe)_3$) and phosphines (PPh_3) to $[\{Cp(CO)_2Mo\}_2]$, to give addition products in which the metal to metal π-bonds are displaced (Equation 5).

$$[\{Cp(CO)_2Mo\}_2] + 2L \longrightarrow [\{Cp(CO)_2LMo\}_2] \qquad L = PPh_3, P(OMe)_3 \quad (5)$$

Similar compounds to those in Equations 4 and 5 were prepared by CO displacement from $[\{Cp(CO)_3Mo\}_2]$ using flash photolysis [12].

Pentamethylcyclopentadienyltricarbonylmolybdenum dimer was prepared according to an improved literature method [13].

The synthesized dimers were then reduced to their anions, which were used for the preparation of the bromoalkyl compounds as shown in Equation 6 below.

$$[\{Cp(CO)_2(PPh_iMe_{3-i})Mo\}_2] + Na/Hg \longrightarrow 2Na[Cp(CO)_2(PPh_iMe_{3-i})Mo] \quad i = 0 - 3 \quad (6)$$

As reported in the previous chapter, the bromoalkyl compounds of iron and ruthenium, $[Cp(CO)_2M\{(CH_2)_nX\}]$ (M = Fe, Ru), have to be prepared at low temperature to prevent the formation of the binuclear compounds, $[Cp(CO)_2M(CH_2)_nM(CO)_2Cp]$, and these conditions give very low yields for the analogous tungsten and molybdenum compounds,

regardless of reaction times. We have used this basic knowledge with modifications to prepare some of the first phosphine substituted halogenoalkyl compounds synthesized in the manner described below [14].

It has also been shown that $[CpL(CO)_2Mo]^-$ L = PPh_3 , $P(OMe)_3$ reacts smoothly with $Br(CH_2)_3Br$ with the loss of a single bromide ion giving $[CpL(CO)_2Mo\{(CH_2)_3Br\}]$ as the only isolated products [3]. Using the prepared phosphine substituted molybdenum dimers, the compounds $[Cp(CO)_2(PPh_iMe_{3-i})Mo\{(CH_2)_nBr\}]$ (n = 3, 4; i = 0 – 3) were synthesized by the method shown in Equation 7, i.e. by reacting the corresponding anion with a dibromoalkane at room temperature.

$$Na[CpMo(CO)_2L] + Br(CH_2)_nBr \rightarrow [Cp(CO)_2LMo\{(CH_2)_nBr\}] + NaBr \quad (7)$$

n = 3 – 4; L = PPh_3, PPh_2Me, $PPhMe_2$, PMe_3

The bromoalkyl compounds were then reacted with sodium iodide in acetone at room temperature (Finkelstein reaction) to give the corresponding iodo compounds, $[Cp(CO)_2LMo\{(CH_2)_nI\}]$, in high yield as shown in Equation 8.

$$[Cp(CO)_2LMo\{(CH_2)_nBr\}] + NaI \longrightarrow [Cp(CO)_2LMo\{(CH_2)_nI\}] + NaBr \quad (8)$$

n = 3, 4; L = PPh_3, PPh_2Me, $PPhMe_2$, PMe_3

The compounds $[Cp^*(CO)_3Mo\{(CH_2)_nBr\}]$ (n = 3, 4) were synthesized as shown in Equation 9 below.

$$Na[Cp^*(CO)_3Mo] + Br(CH_2)_nBr \longrightarrow [Cp^*(CO)_3Mo\{(CH_2)_nBr\}] + NaBr \quad (9)$$

Again, the bromoalkyl compounds from Equation 9 were reacted with sodium iodide in acetone overnight to yield the corresponding iodoalkyl compounds according to Equation 10.

$$[Cp^*(CO)_3Mo\{(CH_2)_nBr\}] + NaI \rightarrow [Cp^*(CO)_3Mo\{(CH_2)_nI\}] + NaBr \quad (10)$$

The bromoalkyl compound, $[Cp(CO)_2(PPh_3)Mo\{(CH_2)_nBr\}]$ where n = 3 has been shown to react with potassium cyanide or lithium iodide in refluxing methanol or tetrahydrofuran respectively, to form the cyclic carbene compounds $[XCp(CO)(PPh_3)Mo\{\overline{CO(CH_2)_2CH_2}\}]$.

reactions of these halogenoalkyl compounds — both in terms of yield and in which product is formed. The molybdenum bromoalkyl compounds where n = 3, do however, form cyclic carbene compounds on reaction with sodium iodide in acetone over longer reaction times (>24 h).

Some of the molybdenum iodoalkyl compounds were also obtained by the reaction of the respective anion with the diiodoalkane, $I(CH_2)_nI$, which, after chromatography under nitrogen, gave analytically pure compounds. Yields, however, are low and the method is not viable.

All compounds were obtained as yellow solids or oils. Characterisation data for the compounds are reported in Tables 3.1 –3.3. The elemental analysis data of the newly synthesized compounds can be found in the Experimental section **5.3.2** and **5.3.3**. From Table 3.1, it can be seen that the melting points of the compounds decrease steadily as methyl groups sequentially replace phenyl groups in the coordinated tertiary phosphine. The melting points thus decrease with decreasing cone angle and increasing pK_a of the phosphine. This is not surprising because of the expected increase in the backbonding abilities. The melting points for the compounds where n = 3 are higher than those for where n = 4. This is as observed for halogenoalkyl iron compounds, as well as for linear unsubstituted paraffins, and can be ascribed to crystal packing factors [10,15,16]. Little difference is seen in the melting points between the iodo and bromo compounds with the same chain length and phosphine substituents.

In the infrared spectra, the carbonyl bands move to slightly lower wave numbers as the halogen changes from Br to I, presumably reflecting the weaker electron withdrawing character of the iodine. As one would expect, the carbonyl bands shift to lower wave numbers with increasing pK_a of the phosphines, with this effect being more prominent for the compounds where n = 4. This is presumably so because the electronegative halogen is further from the metal centres in these latter compounds and hence competes less for electrons. Since the phosphines are *cis* and not *trans* to the carbonyl groups, as will be shown later, their effects are relatively small.

The ^1H NMR data for these compounds are shown in Table 3.2 and sample spectra can be seen in Figures 3.1 (**6a**) 3.2 (**10b**) and a COSY of **6a** is shown in Fig 3.3 and **10b** in 3.4.

Assignments of the peaks were made in comparison to similar data available in the literature and COSY experiments. The MoCH_2 peaks generally show a slight shift upfield with increasing chain length from n = 3 to n = 4, reflecting the weakening of the inductive effect of the halogen with increasing chain length. A shift upfield of the MoCH_2 peak is also generally observed as the pK_a values of the phosphines increase and the cone angles decrease, as would be expected.

This effect is more pronounced in the compounds where n = 4, because the electronegative halogen is further away. The *ca.* 0.2 ppm upfield shift of the CH_2X peaks as X is changed from Br to I is as expected from the difference in their electronegativities.

For the compounds where n = 3, the CH_2X peaks also shift slightly upfield with increasing pK_a of the phosphines. This is not observed for the compounds where n = 4, presumably because the phosphine is too far away. For the iodo compounds, the CH_2CH_2I peaks are at higher field for the compounds where n = 3 and both sets of peaks move to slightly lower field positions with increasing pK_a of the phosphines. Neither effect is observed for the bromo compounds.

Table 3.1: Data for $[Cp(CO)_2(PPh_iMe_{3-i})Mo\{(CH_2)_nX\}]$, i = 0 – 3 and $[Cp^*(CO)_3Mo\{(CH_2)_nX\}]$, n = 3, 4; X = Br, I.

Compound	no	Yield (%)	m.p. (°C)	IR (ν(CO), cm^{-1}) [a]
$[Cp(CO)_2(PPh_3)Mo\{(CH_2)_3Br\}]$	**1a**	57	120–121	1945s, 1868vs
$[Cp(CO)_2(PPh_3)Mo\{(CH_2)_3I\}]$	**1b**	96	>124 (dec)	1943s, 1868vs
$[Cp(CO)_2(PPh_3)Mo\{(CH_2)_4Br\}]$	**2a**	87	103–105	1941s, 1865vs
$[Cp(CO)_2(PPh_3)Mo\{(CH_2)_4\}I]$	**2b**	92	96–110	1940s, 1865vs
$[Cp(CO)_2(PPh_2Me)Mo\{(CH_2)_3Br\}]$	**3a**	51	98–101	1938s, 1860vs
$[Cp(CO)_2(PPh_2Me)Mo\{(CH_2)_3I\}]$	**3b**	30	97–99	1938s, 1860vs
$[Cp(CO)_2(PPh_2Me)Mo\{(CH_2)_4Br\}]$	**4a**	40	Oil	1935s, 1857vs
$[Cp(CO)_2(PPh_2Me)Mo\{(CH_2)_4I\}]$	**4b**	46	Oil	1935s, 1856vs
$[Cp(CO)_2(PphMe_2)Mo\{(CH_2)_3Br\}]$	**5a**	54	72–76	1934s, 1856vs
$[Cp(CO)_2(PphMe_2)Mo\{(CH_2)_3I\}]$	**5b**	28	74–76	1934s, 1856vs
$[Cp(CO)_2(PphMe_2)Mo\{(CH_2)_4Br\}]$	**6a**	42	Oil	1933s, 1856vs
$[Cp(CO)_2(PphMe_2)Mo\{(CH_2)_4I\}]$	**6b**	21	Oil	1931s, 1853vs
$[Cp(CO)_2(PMe_3)Mo\{(CH_2)_3Br\}]$	**7a**	64	35–39	1935s, 1857vs
$[Cp(CO)_2(PMe_3)Mo\{(CH_2)_3I\}]$	**7b**	29	38–40	1935s, 1857vs
$[Cp(CO)_2(PMe_3)Mo\{(CH_2)_4Br\}]$	**8a**	96	Oil	1933s, 1855vs
$[Cp(CO)_2(PMe_3)Mo\{(CH_2)_4I\}]$	**8b**	23	Oil	1931s, 1854vs
$[Cp^*(CO)_3Mo\{(CH_2)_3Br\}]$	**9a**	38	84–85	2008s, 1924vs
$[Cp^*(CO)_3Mo\{(CH_2)_3I\}]$	**9b**	78	80–82	2007s, 1922vs
$[Cp^*(CO)_3Mo\{(CH_2)_4Br\}]$	**10a**	18	32–34	2006s, 1919vs
$[Cp^*(CO)_3Mo\{(CH_2)_4I\}]$	**10b**	74	34–38	2007s, 1919vs

[a] Measured in hexane.

Table 3.2: ^{1}H NMR Data for $[Cp(CO)_2(PPh_iMe_{3-i})Mo\{(CH_2)_nX\}]$[a], i = 0 – 3 and $[Cp^*(CO)_3Mo\{(CH_2)_nX\}]$, n = 3, 4; X = Br, I.

Cpd	Cp*	Cp	α-CH_2	CH_2X	CH_2CH_2X	β-CH_2	P–Ph	P–CH_3
1a		4.73s, 5H	1.44t, 2H, 7.0[b]	3.37t, 2H, 7.5	2.00qn, 2H,7.7		7.37s, 15H	
1b		4.70s, 5H	1.48m	3.15 t, 2H, 7.5	2.18m		7.40s, 15H	
2a		4.72s, 5H	1.49m	3.40 t, 2H, 7.0	2.10m	1.93m	7.39s, 15H	
2b		4.72s, 5H	1.49m	3.24 t, 2H, 6.8	2.08m	1.90m	7.39s, 15H	
3a		4.71s, 5H	1.38m	3.35 t, 2H, 7.5	2.11m		7.48m, 10H	2.11s, 3H,8.1
3b		4.71s, 5H	1.36t, 2H, 8.2	3.14 t, 2H, 7.4	2.10m		7.40m, 10H	2.11s, 3H,8.0
4a		4.71s, 5H	1.46m	3.46 t, 2H, 7.0	1.89m	1.99m	7.49m, 10H	2.11s, 3H,8.2
4b		4.72s, 5H	1.46m	3.25 t, 2H, 7.2	1.93m	1.99m	7.39m, 10H	2.11s, 3H,8.2
5a		4.70s, 5H	1.33m	3.34 t, 2H, 7.4	1.81m		7.41m, 5H	2.15d, 6H,8.7
5b		4.71s, 5H	1.33m	3.12 t, 2H, 7.6	1.84m		7.42m, 5H	1.83d, 6H,8.7
6a		4.71s, 5H	1.36m	3.46 t, 2H, 7.1	1.90m	2.01m	7.39m, 5H	1.80d, 6H,8.6
6b		4.71s, 5H	1.32m	3.24 t, 2H, 7.0	1.92m	2.05m	7.39m, 5H	1.82d, 6H,8.6
7a		4.89s, 5H	1.22m	3.32 t, 2H, 7.4	2.10m			1.52, 9H,10.6
7b		4.88s, 5H	1.33m	3.10 t, 2H, 7.6	2.12m			1.52, 9H,10.9
8a		4.88s, 5H	1.32m	3.44 t, 2H, 6.9	1.70m	1.88m		1.52, 9H,8.9
8b		4.89s, 5H	1.32m	3.22 t, 2H, 7.2	1.75m	1.86m		1.52, 9H,8.9
9a	1.85s, 15H		0.81m	3.37 t, 2H, 7.2	2.04m			
9b	1.85s, 15H		0.83m	3.14 t, 2H, 7.4	2.04m			
10a	1.84s, 15H		2.37m	3.40 t, 2H, 6.8	2.01m	1.77m		
10b	1.84s, 15H		2.37m	3.17 t, 2H, 6.7	2.01m	1.76m		

[a] Measured in $CDCl_3$; peaks are externally referenced to TMS (δ = 0.00 ppm);Cpd = Compound; [b]coupling constants, J values are given in Hz; α-CH_2 refers to the CH_2-group; α- to molybdenum etc.

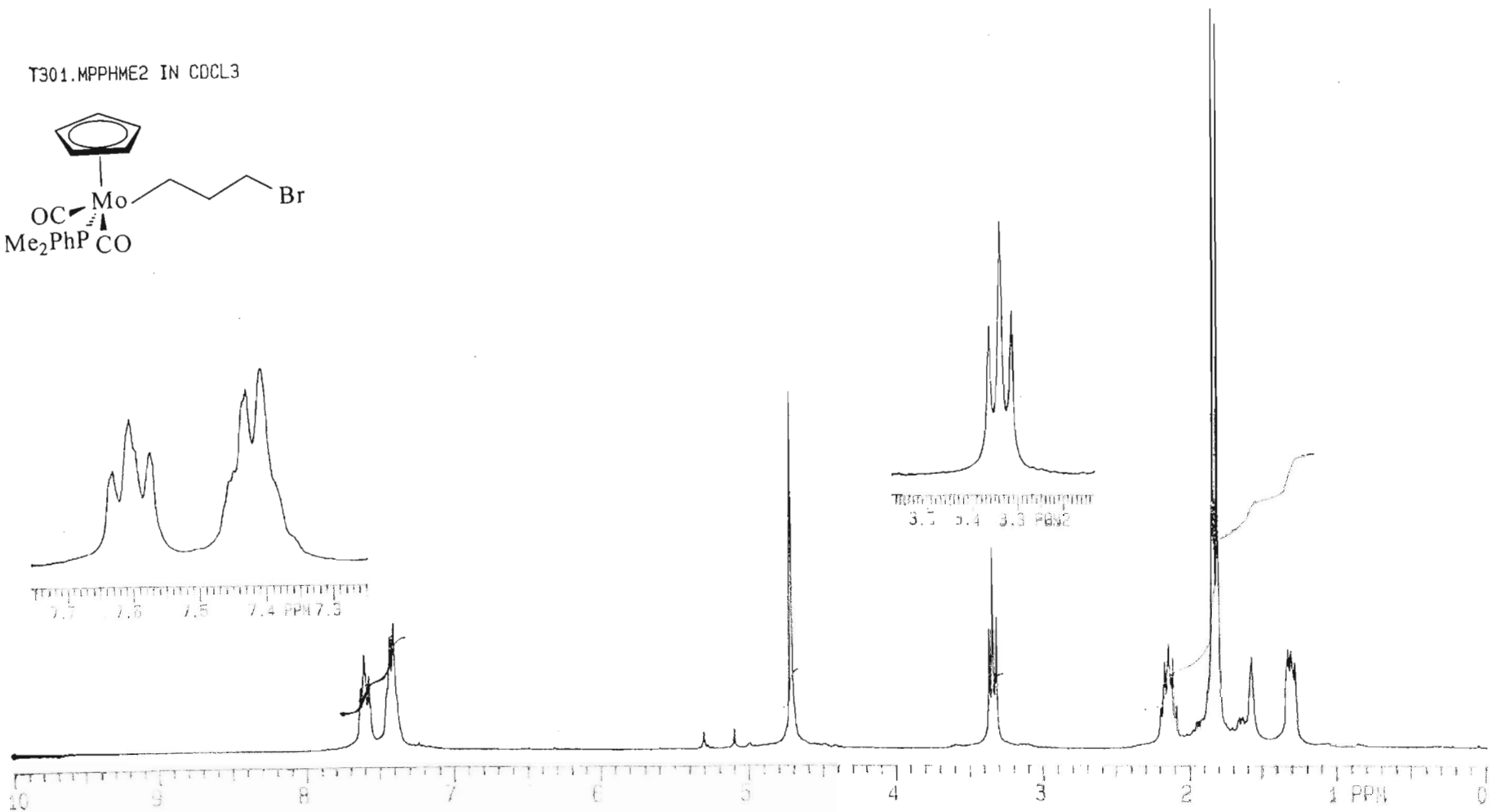

Figure 3.1: ^{1}H NMR spectrum of $[Cp(CO)_2(PPhMe_2)Mo\{(CH_2)_3Br\}]$

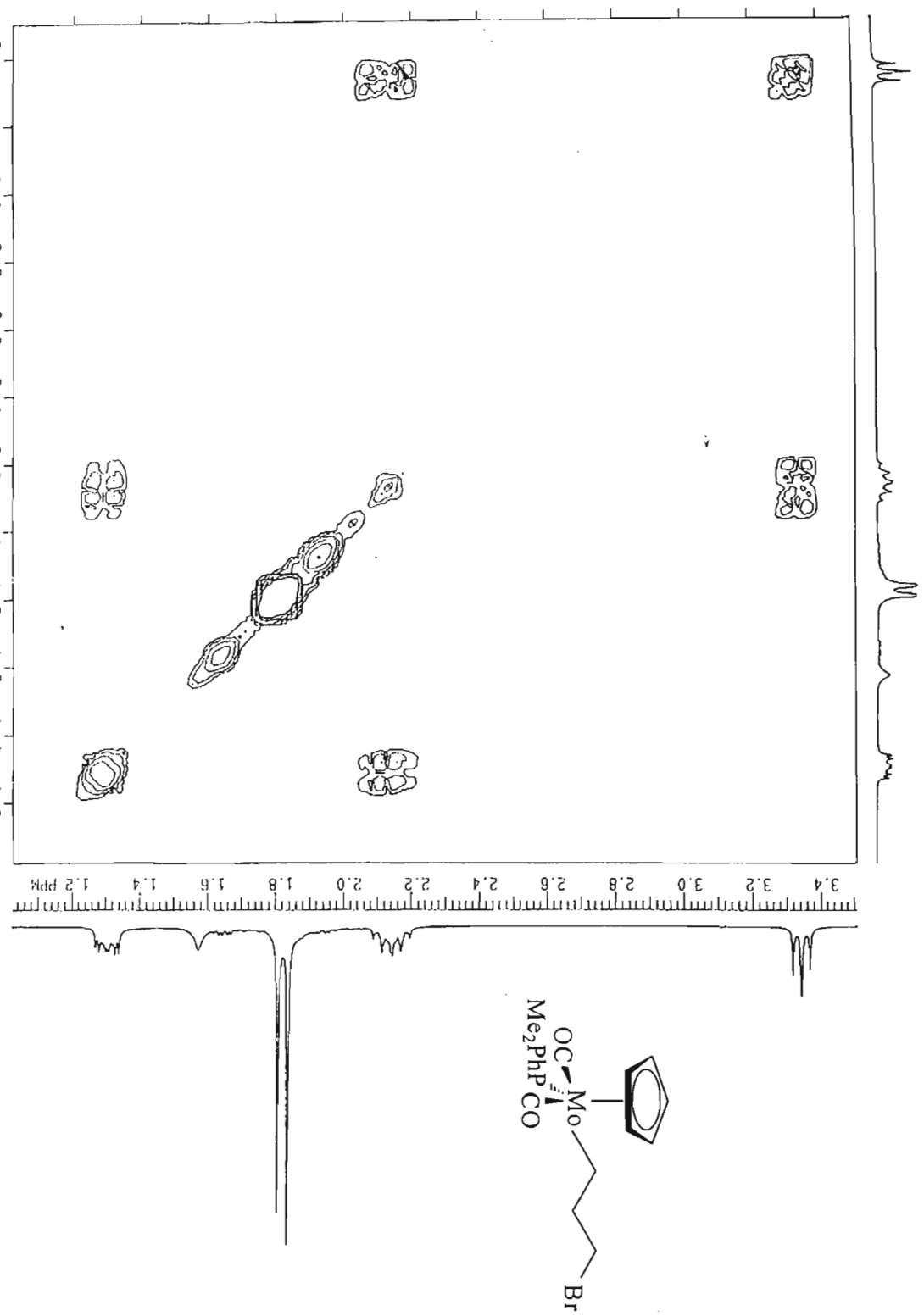

Figure 3.2: COSY of [$(\eta$-$C_5H_5)(CO)_2(PPhMe_2)Mo\{(CH_2)_3Br\}$]

hmo24.Mp*(CH2)4I in cdcl3
probe=5mmASW

Pulse Sequence: s2pul

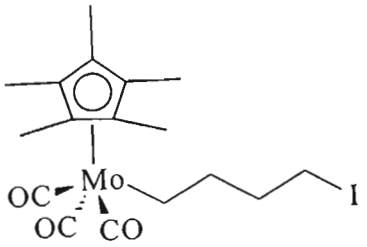

INDEX	FREQUENCY	PPM	HEIGHT
1	2895.586	7.240	12.0
2	1276.356	3.191	20.5
3	1269.580	3.174	41.5
4	1262.804	3.157	21.1
5	957.345	2.394	18.9
6	950.020	2.375	38.1
7	942.694	2.357	21.4
8	832.634	2.082	21.7
9	830.619	2.077	5.4
10	802.234	2.006	200.0
11	754.987	1.888	9.0
12	748.211	1.871	11.8
13	746.929	1.868	12.3
14	744.548	1.862	6.8
15	739.787	1.850	13.2
16	733.011	1.833	6.2
17	709.204	1.773	5.4
18	701.879	1.755	13.2
19	697.301	1.744	6.9
20	694.737	1.737	13.9
21	687.229	1.718	8.2
22	491.647	1.229	11.9
23	18.074	0.045	11.3

Figure 3.3: ^{1}H NMR spectrum of $[Cp^*(CO)_3Mo\{(CH_2)_4I\}]$

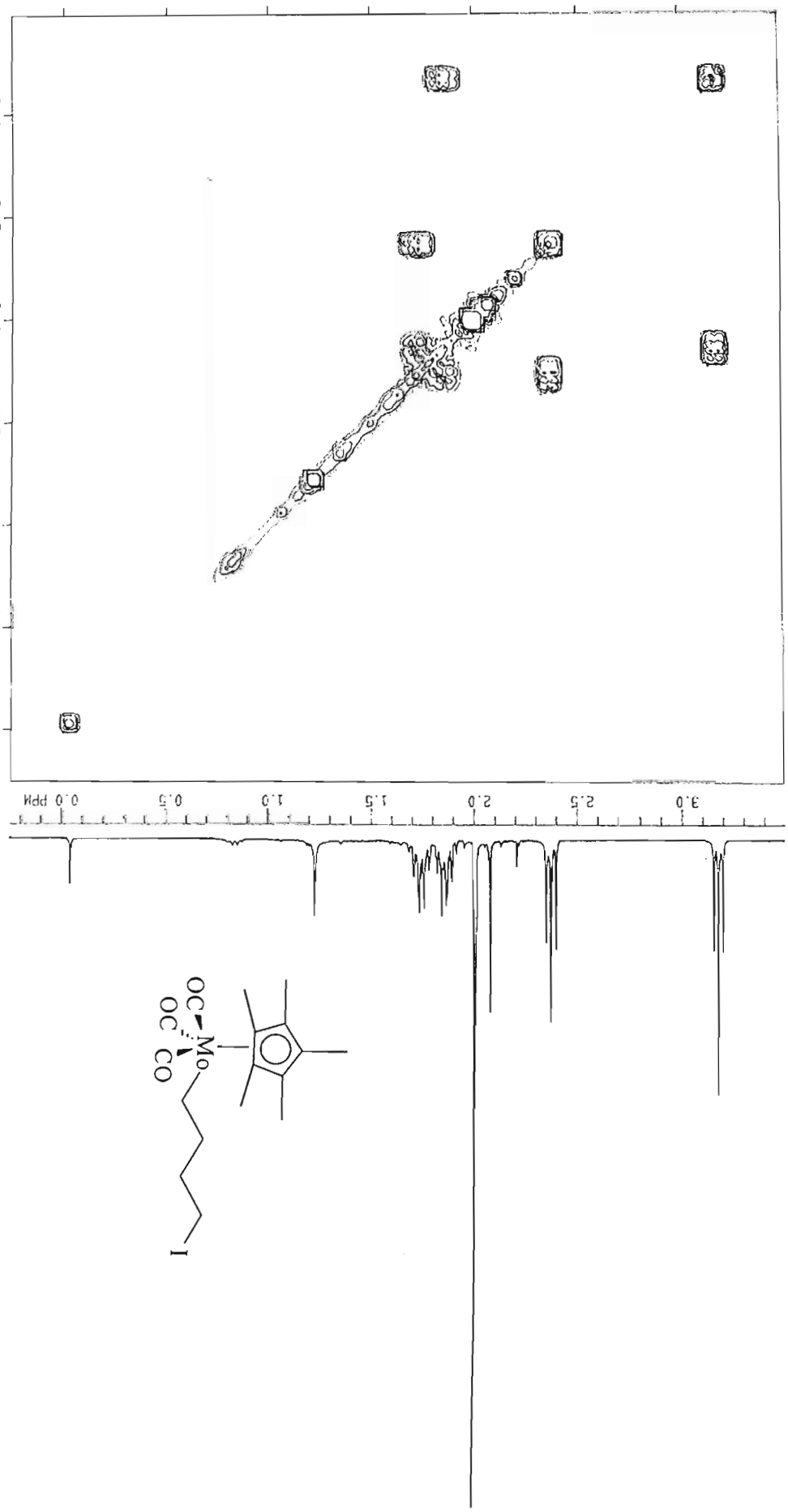

Figure 3.4: COSY of $[Cp^*(CO)_2Mo\{(CH_2)_4I\}]$

Assignments of the ^{13}C NMR spectra (Table 3.3) were carried out with the help of HSQC or HETCOR experiments, together with the comparison with similar data from the literature. Representative spectra of the ^{13}C NMR and HETCOR spectra for compounds **6a** and **10b** are presented in Figures 3.5 – 3.8.

The observation of only a single carbonyl peak (as a doublet) for all the compounds, strongly suggests that the phosphine is *trans* to the alkyl chain, while the two carbonyl groups occupy equivalent *cis* positions to the phosphine ligand. This is confirmed by the crystal structure $[Cp(CO)_2(PPh_3)Mo\{(CH_2)_3I\}]$ **1b**, obtained as can be seen in Figure 3.9. Varying the phosphine does not appear to significantly affect the chemical shift of the CO group. Neither the halogen nor the chain length appears to greatly affect the positions of the Cp or carbonyl peaks. There is, however, a trend to lower δ values for the Cp peaks as the cone angle of the phosphine decreases and the pK_a increases in going from triphenylphosphine to trimethylphosphine. This is because the increased electron density increases the shielding of the Cp carbons. The halogen affects the chemical shift of the carbon α to molybdenum. As observed from Chapter 2 and the iron and tungsten analogues [6,7], the peaks due to the α-carbons are shifted upfield for compounds with smaller values of n. This is contrary to what one would expect from consideration of the inductive effects of the halogens and may imply a weak interaction between the halogen and iron, as has been proposed previously [6,16]. The Mo*C*H_2 peaks are at significantly higher field for the iodo compounds than the bromo compounds where n = 3, and the opposite effect is observed where n = 4. The inverse to the above is observed for the Cp*Mo*C*H_2 peaks. The α-CH_2 chemical shift for compound **10b** appears to be unsually high, we cannot explain this but suspect that the chain may bend backwards towards the metal and hence we are trying to grow a crystal of this compound for X-ray analysis of the structure. The Mo*C*H_2 peaks also shift to lower field positions with increasing pK_a of the phosphines where X = Br and n = 3, whilst the opposite is observed where X = Br, I and n = 4. The *C*H_2I peaks for the compounds where n = 3 are at a very much higher field than those are where n = 4.

The data above indicate that there are significant differences between the compounds where n = 3 and 4. Specifically, it seems that the functionalised ends of the alkyl chain can exert an influence up to a chain length of three carbons, after which negligible or no effect

Table 3.3: ^{13}C NMR Data for $[Cp(CO)_2(PPh_iMe_{3-i})Mo\{(CH_2)_nX\}]$[a], i = 0 – 3 and $[Cp^*(CO)_3Mo\{(CH_2)_nX\}]$, n = 3, 4; X = Br, I.

Cpd	CO	Cp*(C)	Cp*(CH_3)	Cp	α-CH_2	CH_2X	CH_2CH_2X	β-CH_2	P–Ph	P–CH_3
1a	237.94d, 23.3[b]			92.72s	0.15s	37.67s	39.54s		128.17d, 9.8	
1b	218.49s			92.70d, 27.3	2.24s	35.85s	40.68s		128.17d, 9.7	
2a	218.51s			92.65s	2.23s	34.34s	30.95s	38.77s	128.17d, 9.7	
2b	218.43s			92.65s	1.90s	36.79s	33.19s	39.46s	128.10d, 9.7	
3a	236.93d, 22.7			92.38s	0.53d, 10.4	39.94s	37.63s		128.31d, 9.6	21.55d, 34.4
3b	236.93d, 22.6			92.36s	2.42s	11.93s	41.05s		128.24d, 9.6	21.54d, 34.5
4a	236.91d, 22.7			92.58s	1.73d, 10.1	34.90s	34.41s	38.99s	128.54d, 9.6	21.13d, 34.7
4b	236.95d, 22.7			92.34s	1.32s	29.69s	37.11s	39.50s	128.29d, 9.6	21.58d, 34.1
5a	236.98d, 22.7			91.83s	1.03s	37.69s	40.17s		128.54d, 9.6	20.91d, 34.4
5b	236.94, 22.6			92.98s	1.89s	12.09s	35.82s		128.27d, 9.5	20.43d, 34.3
6a	236.94d, 22.7			91.75s	1.07d, 10.1	34.16s	34.83s	38.82s	128.47d, 9.5	20.96d, 32.4
6b	236.95d, 22.7			91.76s	1.00s	33.79s	29.67s	39.17s	128.29d, 9.6	20.37d, 31.8
7a	235.07d, 31.8			91.02s	0.15s	37.74	40.39			21.71d, 29.7
7b	236.04d, 34.2			92.21d, 25.1	0.99s	18.45s	34.50s			21.60d, 32.9
8a	237.27d, 34.1			90.96s	0.80s	35.01s	34.20s	38.88s		21.76d, 29.9
8b	237.46d, 34.4			90.95s	1.09s	39.64s	33.81s	39.91s		21.78d, 32.8
9a	231.26s	104.15s	10.31s		1.00s	37.81s	38.86s			
9b	231.26s	104.31s	10.33s		0.97s	11.48s	39.79s			
10a	[c]	104.04s	10.31s		0.33s	36.35s	30.87s	32.91s		
10b	[c]	121.51s	10.54s		5.60s	25.84s	32.54s	32.59s		

[a] Measured in $CDCl_3$; [b]peaks are externally referenced to TMS (δ = 0.00 ppm), J values are given in Hz. α-CH_2 refers to the CH_2-group α- to molybdenum etc. [c] Not observed

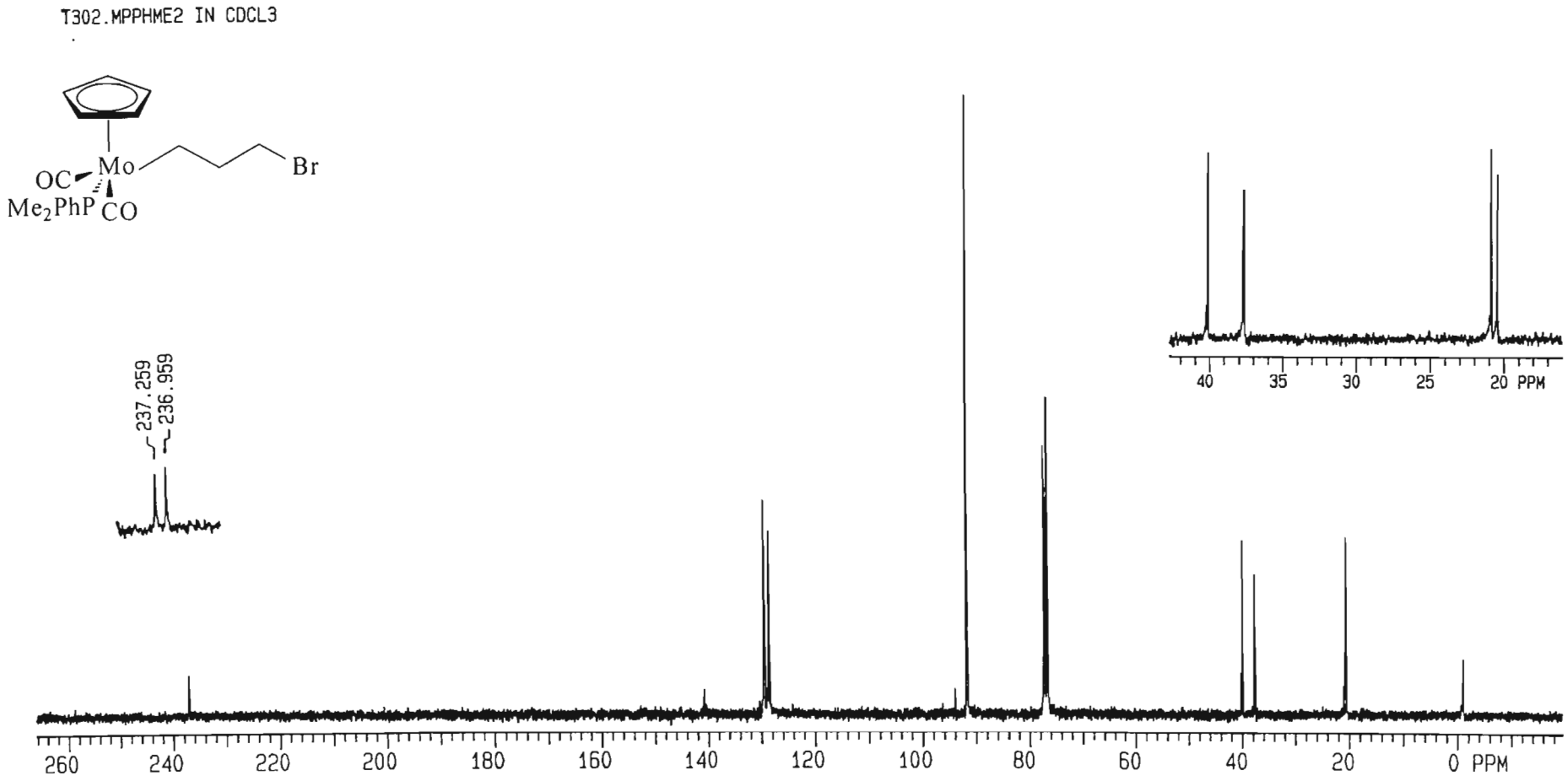

Figure 3.5: ^{13}C NMR spectrum of $[Cp(CO)_2(PPhMe_2)Mo\{(CH_2)_3Br\}]$

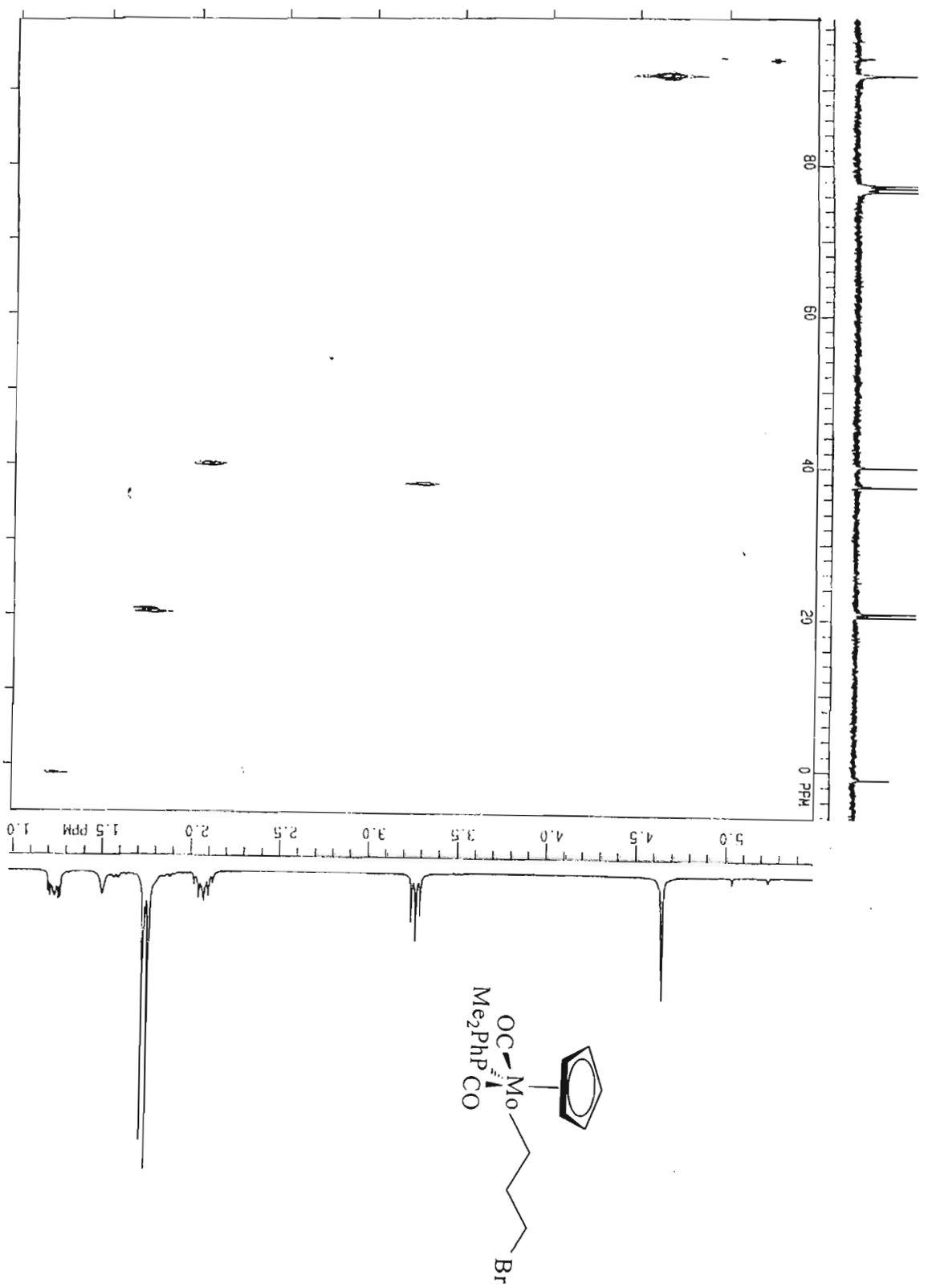

Figure 3.6: HETCOR of [$C_5H_5(CO)_2(PPhMe_2)Mo\{(CH_2)_3Br\}$]

Pulse Sequence: s2pul

2	12242.745	121.739	15.4
3	7796.498	77.526	90.6
4	7764.362	77.207	98.9
5	7732.226	76.887	100.0
6	3304.931	32.863	37.4
7	3292.571	32.741	41.4
8	3005.823	29.889	8.6
9	2583.940	25.694	35.1
10	1080.160	10.741	45.7
11	586.590	5.833	33.3

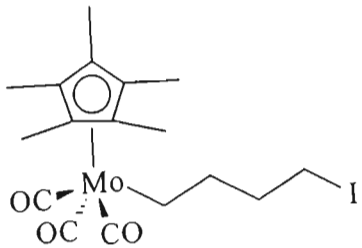

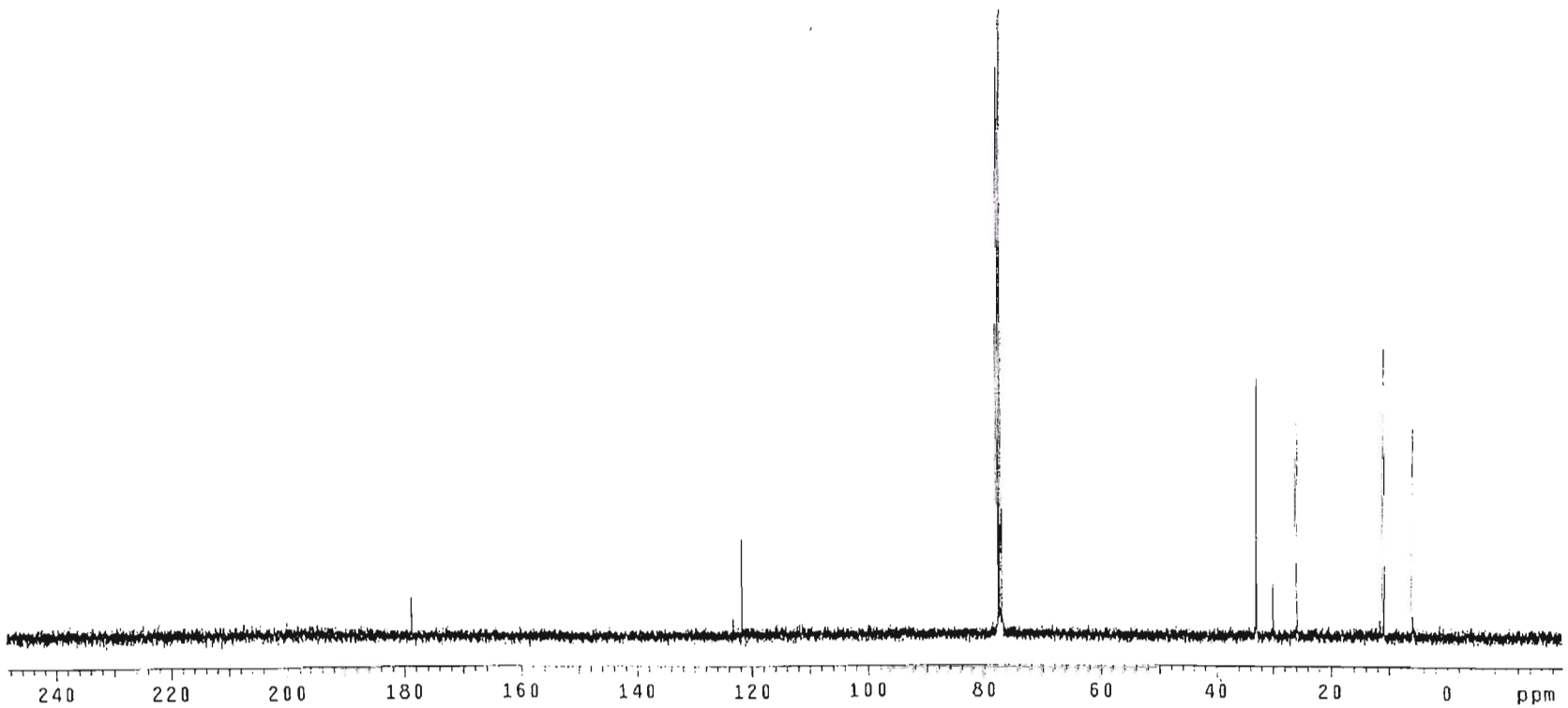

Figure 3.7: ^{13}C NMR spectrum of $[Cp^*(CO)_3Mo\{(CH_2)_4I\}]$

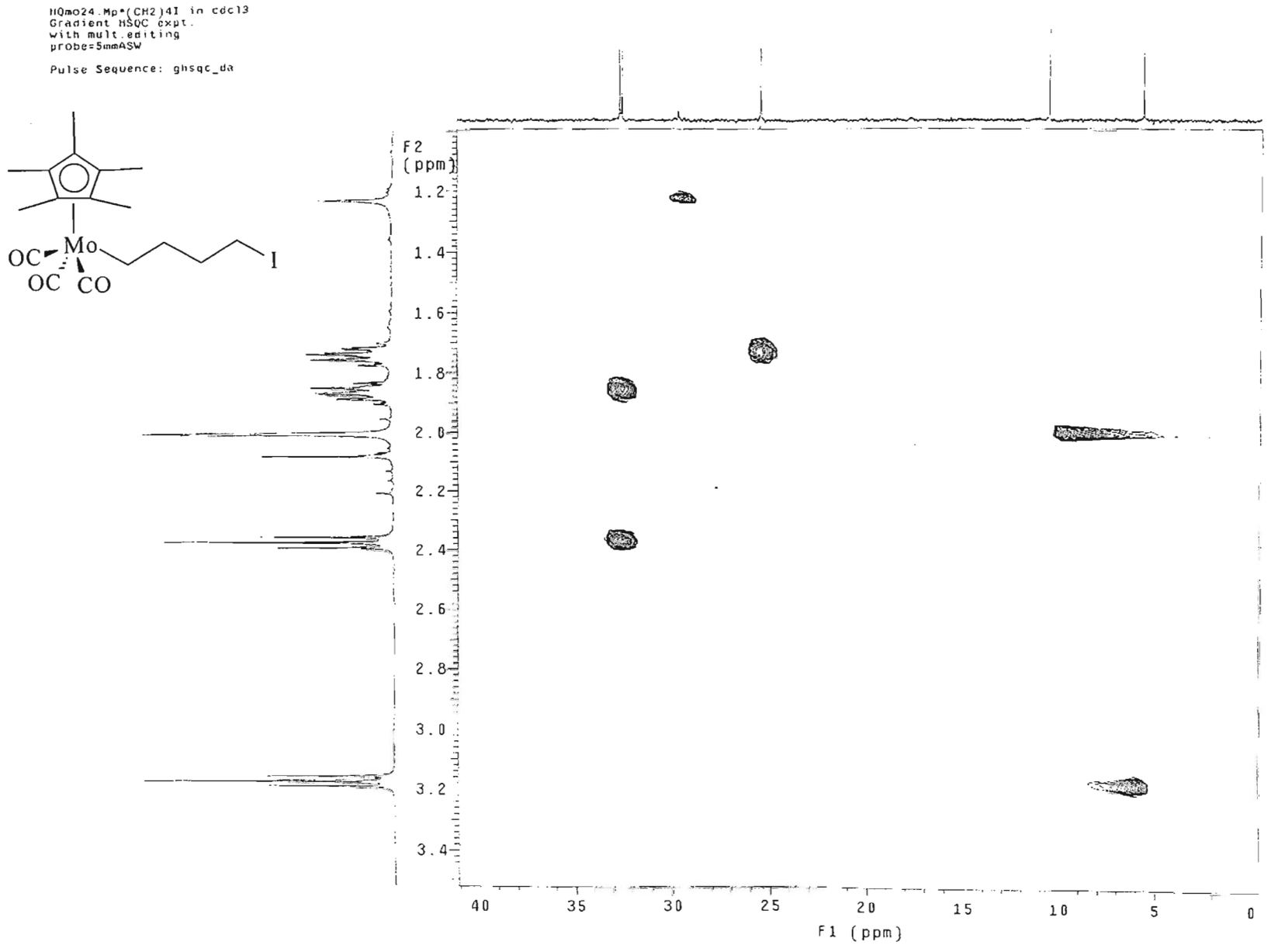

Figure 3.8: HETCOR of $[Cp^*(CO)_3Mo\{(CH_2)_4I\}]$

3.3 Crystal Structure of the Compound $[Cp(CO)_2(PPh_3)Mo\{(CH_2)_3I\}]$, 1b.

Compound **1b** forms crystals in the monoclinic space group $P2_1/n$. Selected bond distances and angles for **1b** are given in Tables 3.4 and 3.5; non-hydrogen atomic coordinates, anisotropic temperature factors, H atom coordinates, and crystal data are given in Appendix 2 and in the attached compact disc, while the complete crystallographic details are given in the supplementary material which have been deposited with the Cambridge Crystallographic Data Centre [17]. The structure of the molecule **1b** and its packing in the crystal are shown in Figures 3.9 and 3.10 respectively. Similar packing as was seen for $[Cp(CO)_3W\{(CH_2)_3Br\}]$ (Figure 2.4) in Chapter 2, is also observed in this case. The halogenoalkyl ligand is *trans* to PPh_3. Superficially the compound could be viewed as trigonal bipyramidal, however, the P–Mo–C(1) dihedral angle is obtuse (138.2°), significantly 42° away from the180° angle required for a trigonal bipyramidal structure and only 48° from 90°. This view is therefore invalid. Alternatively, the compound may appear as a distorted square pyramid (Cp at the apex) but when the Mo atom is viewed through the centre of the square plane, the axis which should pass through the centre of the cyclopentadienyl ring is found to be only 0.34 Å from C(9), (the distance should be about 1.1 Å).

Table 3.4: Selected bond distances for $[Cp(CO)_2(PPh_3)Mo\{(CH_2)_3I\}]$ [a]

Bond	Distance (Å)	Bond	Distance (Å)
Mo–C(4)	1.946(7)	Mo–C(5)	1.982(7)
Mo–C(6)	2.318(7)	Mo–C(10)	2.331(7)
Mo–C(7)	2.341(7)	Mo–C(9)	2.342(7)
Mo–C(8)	2.376(7)	Mo–C(1)	2.402(7)
Mo–P	2.4541(17)	I–C(3)	2.134(9)
P–C(17)	1.834(6)	P–C(23)	1.834(6)
P–C(11)	1.840(6)	O(1)–C(4)	1.132(8)
O(2)–C(5)	1.127(8)	C(1)–C(2)	1.264(10)
C(2)–C(3)	1.627(10)	C(6)–C(10)	1.374(11)
C(6)–C(7)	1.380(11)	C(7)–C(8)	1.357(13)
C(8)–C(9)	1.376(13)	C(9)–C(10)	1.402(13)

[a] The esd's of the least significant digits are given in parentheses.

Also when the diagonals are drawn between opposite atoms making up the square plane, the point of intersection should divide the distances from this intersection to the atoms into half, but here the distances are unequal, C(4) – intersection is 1.32 Å and C(5) – intersection is 1.75 Å. Also, the angle between the carbonyl carbon C(4) and the alkyl chain (C(1)) through the centre of the plane is 79.2° (not 90°) and C(1) is above this plane by 0.72 Å. The four sides of the square base have different lengths; P–C(4) 2.868 Å, C(4)–C(1) 2.661 Å, C(1)–C(5) 2.634 Å, C(5)–P 2.890 Å, which is a further confirmation of a rather distorted square plane. As such, at best, the structure represents a very distorted square pyramid. The molybdenum to carbon bond in the alkyl chain was found to be 2.40 Å, which is within the range reported for Mo–C (alkyl) bonds (2.27 – 2.41 Å) [15,18]. Very few structures of molybdenum-alkyl compounds have been reported and to our knowledge none with the $Cp(CO)_2(PR_3)$ ligand pattern. The Mo–C (alkyl) bond lengths of the two $Cp(CO)_3MoR$ compounds previously reported are marginally shorter at 2.36 and 2.38 Å.

The Mo–C (carbonyl) bond is also marginally shorter for compound **1b** compared to the Mo–CO bond in the tricarbonyl compounds, indicating the expected greater degree of back-bonding in the PPh_3 substituted compound. No corresponding lengthening of the C–O bond is observed, however, the weakening of this bond is reflected in the comparative IR data. The bond lengths between the alkyl carbons in $[\{Cp(CO)_3Mo\}_2(\mu\text{-}CH_2)_4]$ are reported as being 1.53 Å [15]. The C(2)–C(3) bond in compound **1b** is rather longer at 1.63 Å, whilst the C(1)–C(2) bond is very short (1.26 Å). However, these values are unlikely to be real and it is likely that they are artifacts due to the large thermal motion of the haloalkyl ligand.

Table 3.5: Selected bond angles for $[Cp(CO)_2(PPh_3)Mo\{(CH_2)_3I\}]$ [a]

Bond angle	(°)	Bond angle	(°)
C(4)–Mo–C(5)	102.9(3)	C(4)–Mo–C(6)	101.4(3)
C(5)–Mo–C(6)	153.5(3)	C(4)–Mo–C(10)	98.8(3)
C(5)–Mo–C(10)	147.8(3)	C(6)–Mo–C(10)	34.4(3)
C(4)–Mo–C(7)	131.9(3)	C(5)–Mo–C(7)	119.0(3)
C(6)–Mo–C(7)	34.5(3)	C(10)–Mo–C(7)	57.1(3)
C(4)–Mo–C(9)	127.3(3)	C(5)–Mo–C(9)	113.7(3)
C(6)–Mo–C(9)	57.1(3)	C(10)–Mo–C(9)	34.9(3)
C(7)–Mo–C(9)	56.3(3)	C(4)–Mo–C(8)	155.4(3)
C(5)–Mo–C(8)	101.0(3)	C(6)–Mo–C(8)	56.6(3)
C(10)–Mo–C(8)	57.1(3)	C(7)–Mo–C(8)	33.4(3)
C(9)–Mo–C(8)	33.9(3)	C(4)–Mo–C(1)	74.7(3)
C(5)–Mo–C(1)	73.1(2)	C(6)–Mo–C(1)	124.2(3)
C(10)–Mo–C(1)	90.2(3)	C(7)–Mo–C(1)	137.2(3)
C(9)–Mo–C(1)	81.0(3)	C(8)–Mo–C(1)	107.3(3)
C(4)–Mo–P	80.5(2)	C(5)–Mo–P	80.54(17)
C(6)–Mo–P	93.1(2)	C(10)–Mo–P	126.8(2)
C(7)–Mo–P	84.1(2)	C(9)–Mo–P	140.2(2)
C(8)–Mo–P	109.2(3)	C(1)–Mo–P	138.20(18)
C(17)–P–C(23)	103.1(3)	C(17)–P–C(11)	104.0(3)
C(23)–P–C(11)	100.7(3)	C(17)–P–Mo	109.90(19)
C(23)–P–Mo	118.97(18)	C(11)–P–Mo	118.13(19)
C(2)–C(1)–Mo	115.8(5)	C(1)–C(2)–C(3)	113.2(6)
C(2)–C(3)–I	116.9(5)	O(1)–C(4)–Mo	174.9(6)
O(2)–C(5)–Mo	176.8(5)	C(10)–C(6)–C(7)	108.3(7)
C(10)–C(6)–Mo	73.3(4)	C(7)–C(6)–Mo	73.7(4)
C(8)–C(7)–C(6)	108.9(7)	C(8)–C(7)–Mo	74.7(4)
C(6)–C(7)–Mo	71.9(4)	C(7)–C(8)–C(9)	107.9(8)
C(7)–C(8)–Mo	71.8(4)	C(9)–C(8)–Mo	71.7(4)
C(8)–C(9)–C(10)	108.2(7)	C(8)–C(9)–Mo	74.4(4)
C(10)–C(9)–Mo	72.1(4)	C(6)–C(10)–C(9)	106.7(7)
C(6)–C(10)–Mo	72.3(4)	C(9)–C(10)–Mo	73.0(4)

[a] The esd's of the least significant digits are given in parentheses.

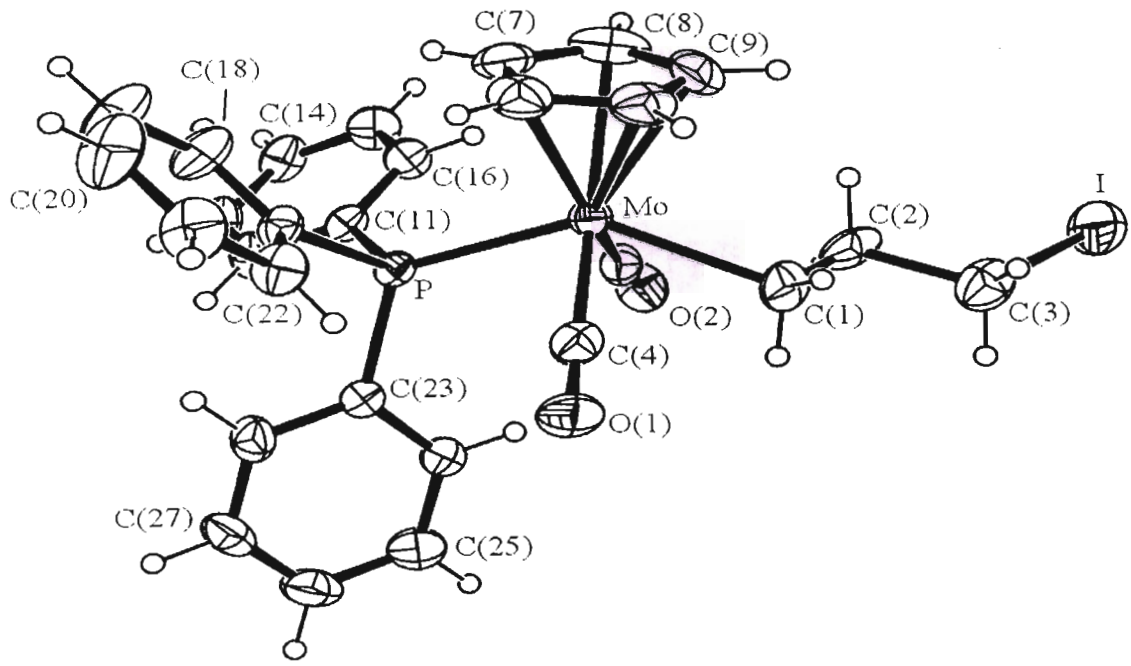

Figure 3.9: ORTEP diagram of the X-ray structure of $[Cp(CO)_2(PPh_3)Mo\{(CH_2)_3I\}]$ **1b**; selected atom labels are shown. Thermal ellipsoids are contoured at the 35% probability level; H atoms have an arbitrary radius of 0.1 Å.

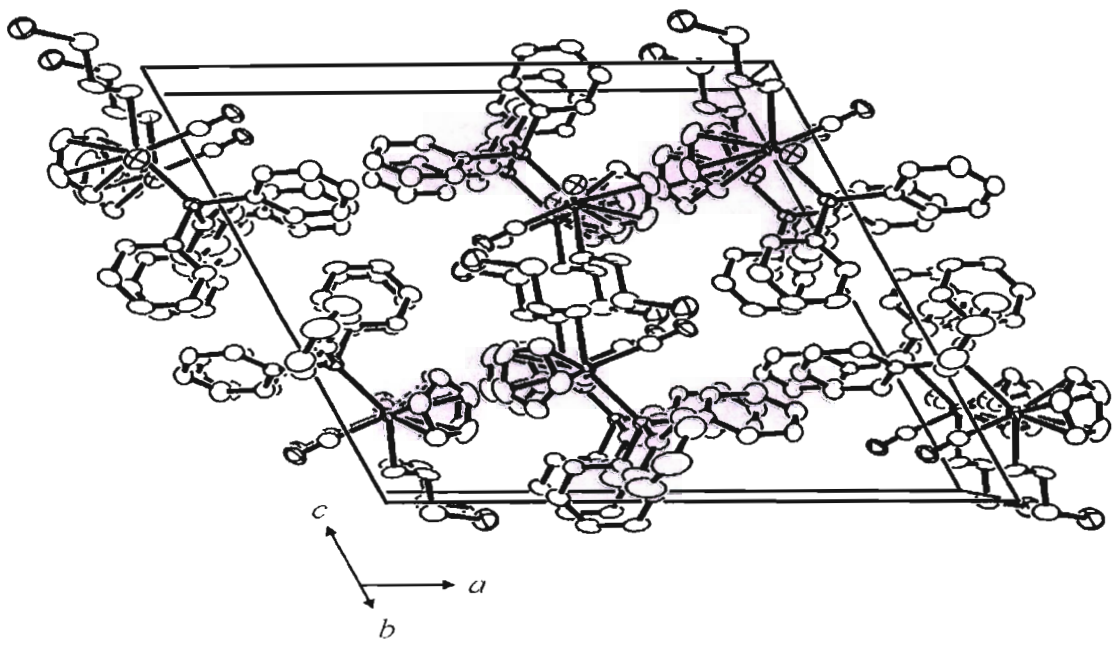

Figure 3.10: ORTEP diagram showing the unit cell packing of $[Cp(CO)_2(PPh_3)Mo\{(CH_2)_3I\}]$ **1b** viewed down the crystallographic *a*-axis. Thermal ellipsoids are contoured at the 35% probability level; H atoms have been omitted for clarity.

3.4 Reaction Studies on Some of the Molybdenum Halogenoalkyl Compounds.

The halogenoalkyl compounds react with iodide ion in tetrahydrofuran or 1,2-dimethoxymethane at reflux to form cyclic carbene complexes. A mechanism (Scheme 3.1) has been suggested in which an initial attack of the nucleophile takes place at the metal atom and the alkyl moiety ($-(CH_2)_3X$) migrates to an adjacent carbonyl group, followed by a ring closing step on the nucleophile acyl oxygen forming a carbene complex [3,19].

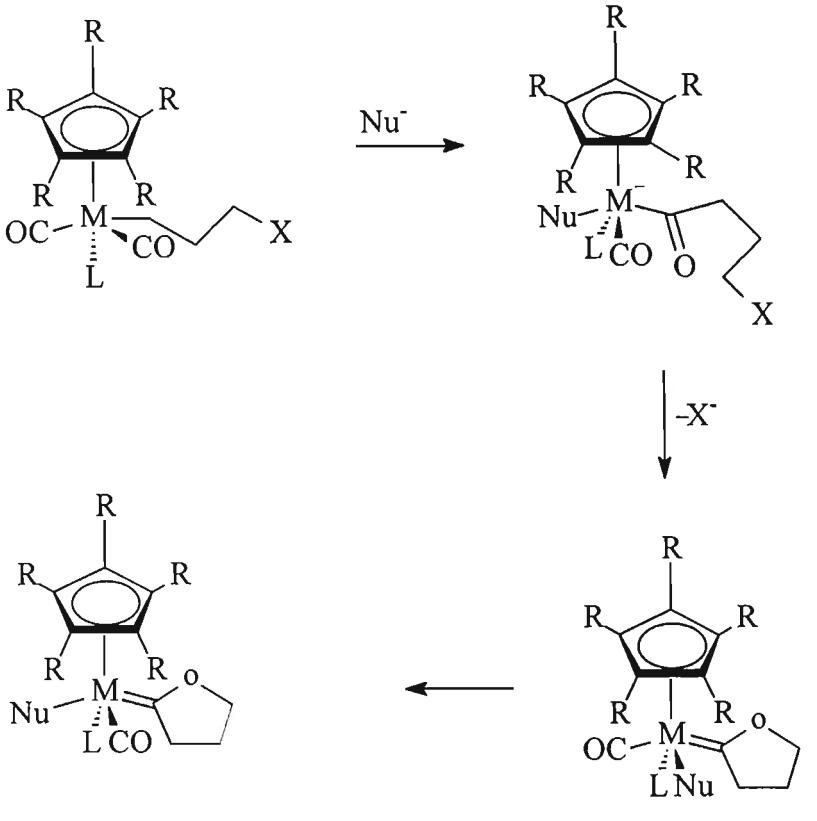

X = Br^-, I^- , Nu^- = I^-, CN^-, SPh^-; R = H, CH_3

Scheme 3.1: A general reaction where a halogenoalkyl compound react with a nucleophile to form a carbene complex [3,19]

Transition metal anions also have been reported to induce similar cyclisation reactions as observed in the Scheme 3.1 [8]. However, all the known reactions above were carried out in THF as the solvent and under reflux. Similar investigations have been reportedly carried out in acetonitrile at room temperature, and differing results were obtained [20]. This was because the compounds used in this study were unsubstituted chloromethyl and

methoxymethyl halogenoalkyl complexes of molybdenum, which are compounds of single carbon chains. We now report on investigations of the compound $[Cp(CO)_2(PhMe_2)Mo(CH_2)_3Br]$, reacting with different nucleophiles in acetonitrile at both low and room temperatures.

The compound of $[Cp(CO)_2(PPhMe_2)Mo\{(CH_2)_3Br\}]$ was reacted with silver nitrate in acetonitrile to form $[Cp(CO)_2(PPhMe_2)Mo\{(CH_2)_3ONO_2\}]$ according to Equation 11 below,

$$[Cp(CO)_2(PPhMe_2)Mo\{(CH_2)_3Br\}] + AgNO_3 \longrightarrow [Cp(CO)_2(PPhMe_2)Mo\{(CH_2)_3ONO_2\}] + AgBr \qquad (11)$$

In the ^1H NMR spectrum, the Cp peak shifted downfield from 4.70 pm (starting material) to 5.33 ppm (product), and the triplet at 3.34 ppm (*sm*)) shifted downfield to 4.33 ppm (*p*). These observations were confirmed in the ^{13}C NMR spectrum where the Cp signal of the product was observed downfield at 94.93 ppm instead of 91.83 ppm (*sm*), and the -CH_2Br moved from 37.69 ppm (*sm*) to 68.14 ppm (*p*). There was no carbene carbon peak observed further downfield. Winter *et al.* reported observing a carbene peak at 316 ppm [8]. These observations therefore strongly suggests that the compound, $[Cp(CO)_2(PPhMe_2)Mo\{(CH_2)_3ONO_2\}]$ was formed from the reaction.

The compound, $[Cp(CO)_2(PPhMe_2)Mo\{(CH_2)_3Br\}]$ and silver cyanide were reacted in acetonitrile. The reaction proceeded according to Equation 12, as shown

$$[Cp(CO)_2(PPhMe_2)Mo\{(CH_2)_3Br\}] + AgCN \longrightarrow [Cp(CO)(CN)(PPhMe_2)Mo\{(\overline{COCH_2)_2CH_2}\}] + AgBr \qquad (12)$$

The characterisation of the compound suggests that the nucleophile CN^- induced cyclisation, despite the fact that the less polar aprotic solvent acetonitrile was used at room temperature. Winter *et al.* had to do a reaction in refluxing polar aprotic tetrahydrofuran to obtain the carbene complex, but it can be seen from our results that those extreme conditions are not necessary [8].

The carbene carbons are known to show low chemical shift in the ^{13}C NMR spectrum, consistent with their formulation as electron-deficient sp^2 carbons, though other factors other than the electron deficiency, are also reported to contribute to the observed large low chemical shifts [21]. In comparison, other sp^2 carbons bound to a transition metal have also shown large downfield shifts, for example, $[CpFe(CO)_2C(O)Me]$ (254.4 ppm) and $[CpFe(CO)_2C(O)Ph]$ (255.5 ppm) [22]. This observation is attributed to the multiple bonding that take place between the *d*-orbitals of the transition metal and the sp^2 carbon atoms, and a second-order paramagnetic term found on the neighbouring metal atom which induces the paramagnetic currents on the carbene carbon atom [23].

The carbene carbon of the compound $[Cp(CO)(CN)(PPhMe_2)Mo\{(\overline{COCH_2)_2CH_2}\}]$ was observed at 366 ppm. This is at a slightly lower position than that observed for the akoxy-carbene complexes, 313 – 362 ppm [20]. This could be due to the molybdenum metal atom that is not known to be very electron rich, and hence reactive.

The reaction above was repeated by using the compound $[Cp(CO)_2(PPhMe_2)Mo\{(CH_2)_3Br\}]$ and sodium cyanide in ethanol ('super dry'). Similar results to the above were obtained. The compound was less stable and full characterisation was difficult. The low temperature NMR facility was not readily available to further investigate this observation. The proposed reaction pathway, though very much similar to Scheme 3.1, is shown in Scheme 3.2.

The reaction of the compound $[Cp(CO)_2(PPhMe_2)Mo\{(CH_2)_3Br\}]$ with sodium azide in acetonitrile at room temperature, gave a cyclic carbene as interpreted from the spectroscopic data obtained. The reaction reflects that shown in Scheme 3.1 above. The mechanism follows that shown in Scheme 3.2 below.

The above reaction was repeated at low temperatures (-40 °C – 8 °C), and gave similar products to those obtained at room temperature. This suggests that the azide is a reactive nucleophile capable of inducing cyclisation even at much lower temperatures.

The compound $[Cp(CO)_2(PPhMe_2)Mo\{(CH_2)_3Br\}]$ and silver sulphide were also reacted in acetonitrile at room temperature. A mixture of products, that were difficult to separate, was obtained. A close examination at the ^1H NMR and the ^{13}C NMR spectra indicated the

formation of two or an asymmetric product. Two Cp peaks were observed at 6.32 ppm and 5.31 ppm in the ^{1}H NMR spectrum. A further confirmation was obtained from the observation of the corresponding Cp peaks 96.44 ppm and 93.89 ppm respectively in the ^{13}C NMR spectrum. No further characterisations were attempted on this product. A repeat of this reaction using a 2:1 molar ratio of the compound $[Cp(CO)_2(PPhMe_2)Mo\{(CH_2)_3Br\}]$ and silver sulphide, gave a mixture of products. A summary of selected characterisation data are reported in Table 3.6 below.

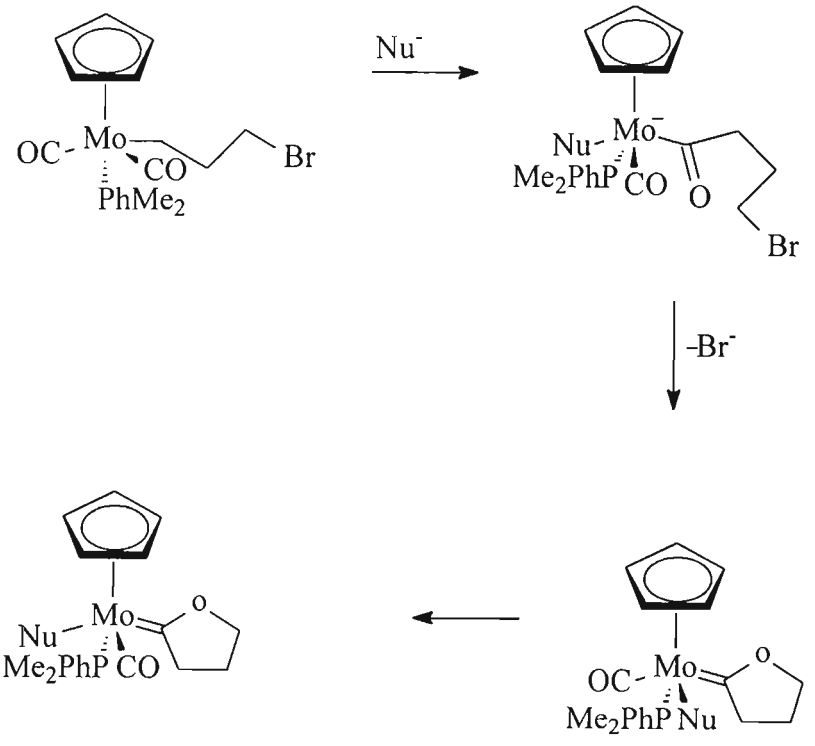

Nu = CN^-, N_3^-

Scheme 3.2: The reaction pathway of the compound, $[Cp(CO)_2(PPhMe_2)Mo\{(CH_2)_3Br\}]$ with CN^- and N_3^-.

Table 3.6: IR , Yields and ^{1}H NMR Data from Reaction Studies of Some of the Molybdenum Halogenoalkyl Compounds

Cpd	IR ν(CO)[a] cm^{-1}	Yield (%)	Cp	α-CH_2	CH_2Nu	CH_2CH_2Nu	P–Ph	P–CH_3
$[Cp(CO)_2(PPhMe_2)Mo\{(CH_2)_3ONO_2\}]$	1992smb, 1910sms	95	5.31s,5H	1.77s	4.33t,2H,6.7[b]	1.99s	7.42m, 5H	1.70d, 6H,10.7
$[Cp(CO)_2(PPhMe_2)Mo\{(CH_2)_3CN\}]$	1911sms, 1838smb	98	5.31s,5H	3.70t, 2H,6.0	2.39s	1.99s	7.44m, 5H	1.70d, 6H,13.1
$[Cp(CO)_2(PPhMe_2)Mo\{(CH_2)_3CN\}]$ (reaction in ethanol)	1970sms, 1838 smb	97	5.31s,5H	3.70t, 2H,6.0	2.39s	1.69s	7.44m, 5H	1.70d, 6H,12.5
$[Cp(CO)_2(PPhMe_2)Mo\{(CH_2)_3N_3\}]$	1967smb, 1911sms	90	5.30s,5H	3.70t, 2H,7.6	4.30s	1.86s	7.41m, 5H	1.74d, 6H,8.4
$[Cp(CO)_2(PPhMe_2)Mo\{(CH_2)_3Br\}] + Ag_2S$	1911sms, 1838smb	98	5.31s,5H	3.45s	2.13s	1.94s	7.44m, 5H	1.70d, 6H,10.1

[a] Measured in CH_2Cl_2; [b] measured in $CDCl_3$ relative to TMS (δ = 0.00 ppm), J values are given in Hz; α-CH_2 refers to the CH_2-group α- to molybdenum *etc.*

^{13}C NMR Data from Reaction Studies of Some of the Molybdenum Halogenoalkyl Compounds

Cpd	Mo-CO	Cp	α-CH_2	CH_2Nu	CH_2CH_2Nu	P–Ph	P–CH_3
$[Cp(CO)_2(PPhMe_2)Mo\{(CH_2)_3ONO_2\}]$	[b]	94.93s[a]	14.01s	68.14s	38.67s	128d, 9.7	18.43d, 32.8
$[Cp(CO)_2(PPhMe_2)Mo\{(CH_2)_3CN\}]$ (reaction in ethanol)	[b]	94.45s	14.08s	61.62s	31.27s	128d, 9.6	18.47d, 33.1
$[Cp(CO)_2(PPhMe_2)Mo\{(CH_2)_3N_3\}]$	238d, 24.0	94.48s	10.80	62.08s	32.91s	128d, 9.7	19.14d, 34.3

[a] measured in $CDCl_3$ relative to TMS (δ = 0.00 ppm), J values are given in Hz; α-CH_2 refers to the CH_2-group α- to molybdenum *etc.* [b]Not observed.

3.5 Conclusions

We have synthesized halogenoalkyl compounds of molybdenum containing various phosphine ligands, from triphenylphosphine to trimethylphosphine.

The crystal structure of $[Cp(CO)_2(PhMe_2)Mo\{(CH_2)_3I\}]$ confirming the synthesis of one of the compounds, and to our knowledge, the first halogenoakyl compound with phosphine as a ligand, has been reported.

Some simple reactions were carried out, and it has been shown that strong nucleophiles, for example N_3^-, will induce cyclisation in a halogenoalkyl compound where n = 3, to form a carbene complex, irrespective of the solvent and temperature used. We have also confirmed some of the reported results in the literature on similar types of investigations.

Whereas in the reactions involving the halogenoalkyl compounds of tungsten (Chapter 2) nucleophillic substitution products were obtained, suggesting a low reactivity of the tungsten centre towards the nucleophile, the molybdenum metal was attacked by the nucleophile, thus forming the carbene complexes. This suggests a greater reactivity of the molybdenum centre compared to tungsten.

We have also shown that the molybdenum centre is very reactive, despite having a phosphine ligand present. Phosphines have been known to stabilize both low and high oxidation state transition metal compounds because of the dπ-pπ overlap. Contrary to this observation, we did not observed a drastic reduction in the reactivity of the molybdenum centre despite the presence of phosphine as a ligand.

Again as stated in the conclusions of Chapter 2, these halogenoalkyl compounds are known to be precursors to heterodinuclear compounds and will be used for further reactions as can be seen in Chapter 4.

3.6 References

[1] R.B. King, Inorg. Chem., 2 (1963) 531.

[2] N.A. Bailey, D.A. Dunn, C.N. Foxcroft, G.R. Harris, M.J. Winter, S. Woodward, *J. Chem. Soc., Dalton Trans.*, (1988) 1449.

[3] N.A. Bailey, P.L. Chell, C.P. Manuel, A. Mukhopadhyay, D. Rodgers, H.E. Tabron, M.J. Winter, *J. Chem. Soc., Dalton Trans.*, (1983) 2397.

[4] M.L.H. Green, M. Ishaq, R.N. Whiteley, *J. Chem. Soc. A*, (1967) 1508.

[5] R.B. King, D.M. Braitsch, *J. Organomet. Chem.*, **54** (1973) 9.

[6] D.H. Gibson, S.K. Mandal, K. Owen, W.E. Sattich, J.O. Franco, *Organometallics*, **8** (1989) 1114.

[7] R.B. King, M.B. Bisnette, *J. Organomet. Chem.*, **7** (1967) 311.

[8] H. Adams, N.A. Bailey, M.J. Winter, *J. Chem. Soc., Dalton Trans.*, (1984) 273.

[9] C.P. Casey, L.J. Smith, *Organometallics*, **7** (1988) 2419.

[10] C. Nataro, R.J. Angelici, *Inorg. Chem.*, **37** (1998) 2975.

[11] A.R. Manning, P. Hackett, R. Birdwhistell, P. Soye, *Inorg. Synth.*, **28** (1990) 148.

[12] R.J. Klinger, W. Butler, M.D. Curtis, *J. Amer. Chem. Soc.*, **97** (1975) 3535.

[13] M. Fei, S.K. Sur, D.R. Tyler, *Organometallics.*, **10** (1991) 419.

[14] H.B. Friedrich, M.O. Onani, O.Q. Munro, *J. Organomet. Chem.*, **633** (2001) 39.

[15] R. Boese, H-C. Weiss, D. Bläser, *Angew. Chem., Int. Ed. Engl.*, **38** (1999) 988.

[16] A.P. Malanoski, P.A. Monson, *J. Chem. Phys.*, **110** (1999) 664.

[17] Cambridge Crystallographic Data Centre, CCDC no. 158287.

[18] M.R. Churchill, S.W.-Y. Chang, *Inorg. Chem.*, **14** (1975) 99.

[19] N.A. Bailey, P.L. Chell, A. Mukhopadhyay, H.E. Tabbron, M.J. Winter, *J. Chem. Soc., Chem. Commun.*, (1982) 215.

[20] S. Peiling, C. Botha, J.R. Moss, *J. Chem. Soc., Dalton Trans.*, (1983) 1495.

[21] B.E. Mann, *Adv. Organomet. Chem.*, **12** (1974) 135.

[22] L.F. Farnnell, E. Rosenberg, E.W. Randall, *J. Chem. Soc., Chem. Commun.*, (1971) 1078.

[23] J.A. Connor, M.E. Jones, E.W. Randall, E. Rosenberg, *J. Chem. Soc., Dalton Trans.*, (1972) 2419 and references therein.

CHAPTER 4

HETERODINUCLEAR TRANSITION METAL SUBSTITUTED PARAFFINS

4.1 Introduction

The transition metal substituted paraffins referred to above, are compounds in which the paraffin chains bridge two different transition metal centres. They have the general formula $[L_xM\{(CH_2)_n\}M'L_y]$; $M \neq M'$, $n \geq 1$, L_xM, $M'L_y$ = transition metal and its associated ligands. The nature of heterodinuclear complexes, that they are mixed metallic, containing two or more adjacent metal centers, could add some other chemical dimension over those containing a single metal; not only can the metals act independently but they can also act in a cooperative manner leading to chemistry that differs appreciably from that displayed by the single metal counterparts. The possibility of metals influencing one another at close proximity has been acknowledged because different metals posses different potentials [1]. Heterodinuclear compounds may also have their stability and electronic properties drastically improved when they have additional ligands with π-backbonding properties incorporated. The synthesis and reactivity of heterodinuclear transition metal complexes, continues to attract considerable interest because of their envisaged catalytic superiority over their homometallic analogues. Such complexes, but with conjugated bridges, can act as molecular wires or switches [2,3]. The compounds also find application in the area of organic syntheses.

Metal substituted paraffin compounds could be good catalyst precursors or model compounds for catalytic intermediates or act as catalysts themselves. They have been proposed to be good models for Fischer-Tropsch processes [1]. These reasons have led to a considerable amount of work being carried out on these transition metal complexes [4,5]. Bimetallic compounds with direct metal–metal bonds are reported to be commonly synthesized by a metathesis of a halide ligand, like on a group 4 metal, with an organometallic anion, such as $[(Cp)(CO)_2M]^-$ (M = Fe, Ru) [6-10] or $[(CO)_4M]^-$ (M = Co, Rh) [6-7,11-15]. The same procedure has been used to prepare heterobimetallic lanthanide [11] and group 6 and 9 complexes [12,13]. The most successful route to heterodinuclear alkyl bridged compounds reported so far is via the use of halogenoalkyl compounds,

especially those with the iodoalkyl group. These compounds are also useful precursors to cyclic carbenes [2,16,17].

Whilst large numbers of homometallic complexes incorporating polymethylene bridges (also called alkanediyl bridges or bridging alkyl chains) are known [17,18] and most are well covered in a recent review [19], very few complexes of the type $[(\eta^5\text{-}C_5R_5)(CO)_3M(CH_2)_nM'(CO)_i(L)(\eta^5\text{-}C_5R_5)]$ ($M \neq M'$, $i > 1$ $n \geq 2$) have been reported and to our knowledge none with phosphine ligands. Only phosphine acyl complexes resulting from migratory insertion reactions have been reported [16,20]. Here follows a discussion of our contribution towards this dynamic field of research.

4.2 Preparation and Properties of the Heterodinuclear Transition Metal Substituted Paraffins

Originally, King and Bisnette attempted the synthesis of mixed metal dinuclear complexes containing saturated polymethylene bridges by the reaction of $Na[Cp(CO)_2Fe]$ with $[Cp(CO)_3Mo\{(CH_2)_3Br\}]$ as represented in Equation 1. The anion $Na[Cp(CO)_2Fe]$, replaced both the bromine atom and the $Cp(CO)_3Mo$- to give the known compounds $[(Cp(CO)_2Fe)_2(CH_2)_n]$ in 23 – 28% yields [21]. This was probably due to the strong nucleophilicity of iron [22,23].

$$Na[Cp(CO)_2Fe] + [Cp(CO)_3Mo\{(CH_2)_nBr\}] \searrow [(Cp(CO)_2Fe)_2(CH_2)_n] + [\{Cp(CO)_3Mo\}_2] + NaBr \quad n = 3 - 4 \qquad (1)$$

Moss prepared a propanediyl compound $[Cp(CO)_2Fe(CH_2)_3Mo(CO)_3Cp]$, from the reaction of $[Cp(CO)_2Fe\{(CH_2)_3Br\}]$ with $Na[Cp(CO)_3Mo]$, in 18% yield [24]. Knox and co-workers then demonstrated that the heterodinuclear complex $[Cp(CO)_2Fe(CH_2)_3Ru(CO)_2Cp]$ could be obtained in 87% yield by the reaction of the iodoalkyl compound, $[Cp(CO)_2Fe\{(CH_2)_3I\}]$ with $Na[Cp(CO)_2Ru]$ [16]. Several complexes of this type have since been reported [17, 18]. Friedrich and Moss, recently reported the syntheses of iron, rhenium, ruthenium, molybdenum and tungsten heterodinuclear complexes in good yields [5,17,25].

The new heterodinuclear complexes were synthesized by the direct displacement of the iodide of a metallo-iodoalkyl complex with an appropriate anion. In general, the complexes prepared can be categorised into two: Mo-W comprising of compounds **A** – **C** and Mo-Fe comprising the compounds **C** and **D** as shown below. Their synthetic pathway is shown in Scheme 4.1.

Mo-W category:

(A) Compounds where tungsten and molybdenum have unsubsitituted cyclopentadienyl ligands and three carbonyls each,

$$[Cp(CO)_3W\{(CH_2)_nI\}] + Na[Mo(CO)_3Cp] \longrightarrow [Cp(CO)_3W(CH_2)_nMo(CO)_3Cp],\ n = 3 - 6 \qquad (2)$$

(B) Tungsten with a cyclopentadienyl ligand and molybdenum with a pentamethylcyclopentadienyl ligand. Each has three carbonyls,

$$[Cp(CO)_3W\{(CH_2)_nI\}] + Na[Mo(CO)_3Cp^*] \longrightarrow [Cp(CO)_3W(CH_2)_nMo(CO)_3Cp^*],\ n = 3 - 4 \qquad (3)$$

Mo-Fe category:

(C) Tungsten with a cyclopentadienyl ligand and three carbonyls and Molybdenum with a cyclopentadienyl, a phosphine ligand and two carbonyls,

$$[Cp(CO)_3W\{(CH_2)_nI\}] + Na[Mo(CO)_2(PPh_iMe_{3-i})Cp] \searrow [Cp(CO)_3W(CH_2)_nMo(CO)_2(PPh_iMe_{3-i})Cp],\ n = 3 - 4,\ i = 0 - 3 \qquad (4)$$

(D) Iron with a cyclopentadienyl ligand and Molybdenum with a phosphine ligand; each metal also has two carbonyls,

$$[Cp(CO)_2Fe\{(CH_2)_nI\}] + Na[Mo(CO)_2(PPh_iMe_{3-i})Cp] \searrow [Cp(CO)_2Fe(CH_2)_nMo(CO)_2(PPh_iMe_{3-i})Cp],\ n = 3 - 4,\ i = 0 - 3 \qquad (5)$$

(E) Iron with a cyclopentadienyl ligand and two carbonyls and molybdenum with a pentamethylcyclopentadienyl and three carbonyls,

$$[Cp(CO)_2Fe\{(CH_2)_nI\}] + Na[Mo(CO)_3Cp^*] \rightarrow [Cp(CO)_2Fe(CH_2)_nMo(CO)_3Cp^*],\ n = 3 - 4 \qquad (6)$$

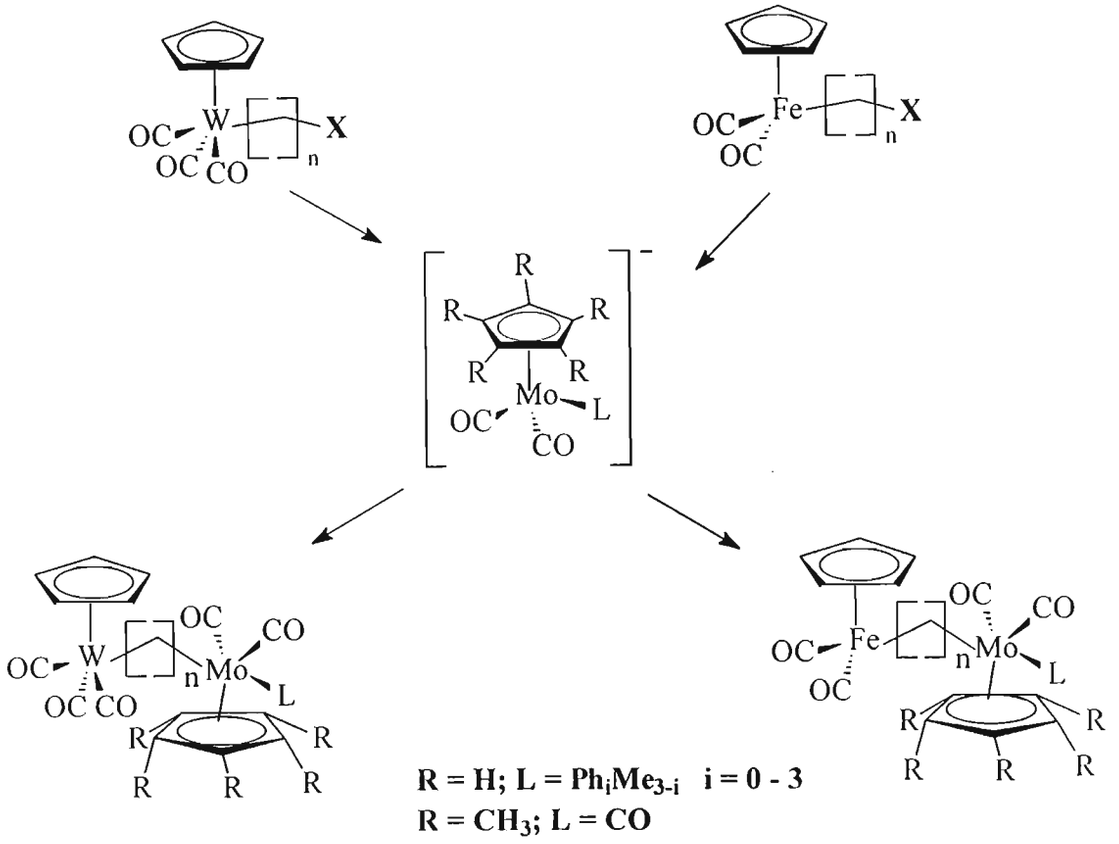

Scheme 4.1: The general synthetic pathway to the heterobimetallic complexes

The alkanediyl complexes were obtained in medium to high yields (Table 4.1). The complexes were synthesized in the order in which they are presented. During the initial preparations of the compounds of type **A** $[Cp(CO)_3W(CH_2)_nMo(CO)_3Cp]$, (**1a** – **1d**, several reaction parameters were investigated to establish the most suitable conditions which were then used as a guide for the preparation of the other compounds. These included changes in reaction temperature, media and times. The best yields of **A** were obtained when the temperature of the reactions were maintained at –78 °C for the total reaction times, which ranged from 64 – 105 hours depending on the compound prepared. Compounds **B** were prepared in an analogous manner to **A**, and were obtained in good yields. The reactions were found to take a shorter time when carried out at room temperature. However, the yields were low. This was attributed to a high decomposition

rate of the reactants. The reactions using the phosphine substituted anions to yield class **C** and **D** compounds were slow but gave good yields at room temperature, after four to five days of reaction. The alternative recrystallization procedure (see Chapter 2), also proved better than the chromatography route earlier reported [17] and gave good yields. The reaction times generally increased with an increase in chain length. This could be attributed to a decrease of influence of one metal on the halogen within the same molecule, resulting in a decrease in the bond polarity as the chain lengthens [26]. The complexes **1a - 2d** and **11a** and **11b** were soluble in hexane with their solubility increasing with increasing length of the alkyl chain. The rest of the complexes were, however, as expected insoluble in hexane due to the presence of the phosphine ligand. They were soluble in dichloromethane. High yields were obtained for complexes **C** and **E**, their insolubility in hexane made the recrystalisation process very efficient. They were precipitated from dichloromethane by adding hexane.

All the complexes were obtained as yellow crystalline solids, which were stable in air but unstable in solution. This is because of the presence of free electron providers like oxygen and water in solution, which easily donate their lone pairs into the low lying empty metallic orbitals making the compounds highly labile [27].

The melting points were generally sharp and decreased with increase in alkyl chain length. The notable exceptions are compounds **4a, 4b, 10a** and **10b**. The yields, spectral data and melting points are given in Table 4.1. Some of the compounds had their elemental analysis determined and this data is reported in the Experimental Section **5.4**.

In the IR spectra, the ν(CO) wave numbers of the complexes are in the expected range for terminal carbonyl groups. This observation agrees closely with similar data reported in the literature [17]. The compounds **2a** and **2b**, as expected, show a decrease in the position of their ν(CO) bands due to the high electron density contributed by the Cp* ligand to the molybdenum atom which results in the increase in the π-backbonding properties.

The phosphine ligands used in this study, in order of decreasing cone angles are: PPh_3 (145°), PPh_2Me (136°), $PPhMe_2$ (122°) and PMe_3 (118°) [28]. Phosphine ligands are well known as isosteric compounds. They are thus popular for the study of steric properties in coordination chemistry. Steric effects are difficult to separate from electronic factors and

hence are closely interrelated. Increasing the angles between the substituents on the phosphorus atom has been found to decrease the percentage of s character of the lone pair leading to a decrease in bonding ability [29]. Changes in bonding are used as an indicator of electron density at the metal center whenever a CO is coordinated together with a phosphine. Increasing the size of a molecule affects the vibrational spectra to a considerable extent. The lower the value of the ν(CO), the greater the backbonding to the metal and thus the higher the electron density at the metal centre [30]. We observe this trend in the complexes **3a – 6b** in which a CO ligand of the $CpMo(CO)_3$ moiety is substituted by PPh_iMe_{3-i} i = 0 – 3. These compounds have their ν(CO) bands lower by *ca.* 90 – 100 cm^{-1} in their infrared spectra. The PMe_3 is the most basic phosphine within the group with the lowest π-acceptor properties. Its complexes thus have the strongest M–C bonds and hence the lowest observed infrared bands in the ν(CO) region. The phenomenon is clearly shown in the data in Table 4.1. A decreasing trend is seen in the carbonyl stretching frequencies as we sequentially substitute the phenyl group by a methyl group in the phosphine ligands used.

Table 4.1: Data for the compounds $[Cp(CO)_2(L)Mo(CH_2)_nM(CO)_x(Cp]$;n = 3, 4; M = Fe (x = 2), W (x = 3); L = CO; PPh_iMe_{3-i} i = 0 – 3; n = 5,6;M = W (x = 3); L = CO; **1a - 11b**

Type	Compound		Yield (%)	M.P.(°C)	IR ν(CO) (cm^{-1})			
A	$[Cp(CO)_3W(CH_2)_3Mo(CO)_3Cp]$	**1a**	78	171-175(>,dec)	2013 [a] vs	1963s	1932vs	1918vs
	$[Cp(CO)_3W(CH_2)_4Mo(CO)_3Cp]$	**1b**	96	>145(dec)	2016s	1976s	1963vs	1920vs
	$[Cp(CO)_3W(CH_2)_5Mo(CO)_3Cp]$	**1c**	46	>95(dec)	2017vs	1976s	1927vs	1916s
	$[Cp(CO)_3W(CH_2)_6Mo(CO)_3Cp]$	**1d**	89	>89(dec)	2016vs	2005sh	1976s	1926vs
B	$[Cp(CO)_3W(CH_2)_3Mo(CO)_3Cp^*]$	**2a**	51	147-150	2007s	1996s	1910sb	
	$[Cp(CO)_3W(CH_2)_4Mo(CO)_3Cp^*]$	**2b**	61	119-124	2008s	1998sb	1911sb	
C	$[Cp(CO)_3W(CH_2)_3Mo(CO)_2(PPh_3)Cp]$	**3a**	45	95-99	2006 [b] s	1911vsb	1843s	
	$[Cp(CO)_3W(CH_2)_4Mo(CO)_2(PPh_3)Cp]$	**3b**	53	88-94	2008s	1912sb	1846s	
	$[Cp(CO)_3W(CH_2)_3Mo(CO)_2(PPh_2Me)Cp]$	**4a**	94	68-70	2008s	1912vsb	1845s	
	$[Cp(CO)_3W(CH_2)_4Mo(CO)_2(PPh_2Me)Cp]$	**4b**	96	112-115	2008s	1913vsb	1837s	
	$[Cp(CO)_3W(CH_2)_3Mo(CO)_2(PPhMe_2)Cp]$	**5a**	88	116-118	2005s	1916vsb	1833s	
	$[Cp(CO)_3W(CH_2)_4Mo(CO)_2(PPhMe_2)Cp]$	**5b**	91	109-110	2007s	1916vsb	1833s	
	$[Cp(CO)_3W(CH_2)_3Mo(CO)_2(PMe_3)Cp]$	**6a**	66	>120(dec)	2011s	1912vsb	1843s	
	$[Cp(CO)_3W(CH_2)_4Mo(CO)_2(PMe_3)Cp]$	**6b**	73	114-115	2007s	1916vsb	1831s	
D	$[Cp(CO)_2Fe(CH_2)_3Mo(CO)_2(PPh_3)Cp]$	**7a**	49	97-99	1998s	1938sb	1843s	
	$[Cp(CO)_2Fe(CH_2)_4Mo(CO)_2(PPh_3)Cp]$	**7b**	74	71-78	2000s	1939vsb	1844s	
	$[Cp(CO)_2Fe(CH_2)_3Mo(CO)_2(PPh_2Me)Cp]$	**8a**	69	>124(dec)	1997s	1962sh	1937vs	1838vs
	$[Cp(CO)_2Fe(CH_2)_4Mo(CO)_2(PPh_2Me)Cp]$	**8b**	73	69-72	2006s	1969s	1919s	1848vs
	$[Cp(CO)_2Fe(CH_2)_3Mo(CO)_2(PPhMe_2)Cp]$	**9a**	41	>138(dec)	1997s	1936sh	1917s	1845vs
	$[Cp(CO)_2Fe(CH_2)_4Mo(CO)_2(PPhMe_2)Cp]$	**9b**	69	97-98	2001s	1938sb	1915sh	1845vs
	$[Cp(CO)_2Fe(CH_2)_3Mo(CO)_2(PMe_3)Cp]$	**10a**	56	90-96	1996s	1936vs	1918sh	1831vs
	$[Cp(CO)_2Fe(CH_2)_4Mo(CO)_2(PMe_3)Cp]$	**10b**	75	108-110	1999s	1938vs	1921sh	1832vs
E	$[Cp(CO)_2Fe(CH_2)_3Mo(CO)_3Cp^*]$	**11a**	49	65-68	2028s	1998s	1941sb	
	$[Cp(CO)_2Fe(CH_2)_4Mo(CO)_3Cp^*]$	**11b**	94	71-78	2000s	1939s	1907sb	

[a]In Hexane; [b]In dichlomethane; vs = very strong, s = strong, b = broad, sh = shoulder

4.2.1 ^{1}H NMR data

Organometallic compounds provide better spectra on lower field instruments where they undergo decomposition at a slower rate [31a]. Nevertheless, the appearance of the spectra is affected by among other factors: nuclear spin, isotopic abundance, molecular tumbling, scalar coupling, symmetry and the conformation and the stereochemistry of the compound [29]. The ^{1}H NMR data for the complexes **1a - 11b** are summarised in Table 4.2. All the compounds are new and their data newly reported with the exception of compound **11a**, which has been reported by some other group, though without any characterization data [31b]. Data from similar compounds [17], as well as correlated spectroscopy (COSY), were used for chemical shift assignments. Examples of ^{1}H NMR spectra for each of the five classes of compounds, and a COSY spectrum of **1a** are shown in Figures 4.1 – 4.6.

The Cp proton resonances for compounds **1a** – **1d** are deshielded, and appear downfield at *ca.* 5.25 ppm, whereas those of compounds **2a** and **2b**, containing Cp*, are shielded and appear upfield at 1.85 ppm. Further effect is seen on the MoCH_2 protons of compounds **8a**, **9a**, **10a** and **10b** that are equally shielded and appear upfield. Tungsten, being a highly electron rich transition metal, had the α-protons shielded and their peaks were observed further upfield. The metallic influence diminishes as the chain gets longer, and has no effect at all on the chemical shifts of either Cp or Cp*. Also, neither tungsten nor molybdenum is observed to couple with the protons adjacent to them. The observations here support our earlier finding that the metal only influences the protons α and β to it and not those γ or beyond [17]. Because of these observations, compounds with longer alkyl chain length (5 and above) were not synthesized, as their chemistry would not be of much interest. A significant effect was seen on the Cp resonances of the compounds containing a phosphine as a ligand. The Cp resonances appear at a much lower position, 4.7 ppm, than in the unsubstituted compounds, due to the presence of the phosphine that increases electron density on the molybdenum.

All the Cp proton resonances were observed to couple with the NMR active phosphorus of the phosphine ligands. The peaks for the Cp ligands were all observed as doublets. In the type of complexes synthesized here, it has been noted that the alkyl ligand always preferentially migrates away from the bulky phosphine ligands giving a *trans* geometry about the central metal [32].

Table 4.2: ^{1}H NMR : Data for the compounds $[Cp(CO)_2(L)Mo(CH_2)_nM(CO)_iCp]$[a]; n = 3 – 6; 3, 4; M = Fe, W; L = CO, PPh_iMe_{3-i}) i = 0 – 3; **1a - 11b**

Type	Compound		CpMo	Cp*Mo	Cp'	α-Mo	α-M'	β-Mo	β-M'	γ-Mo	γ-W	P-Ph	P-CH_3
A													
	$[Cp(CO)_3W(CH_2)_3Mo(CO)_3Cp]$	**1a**	5.27s		5.36s	1.58m	1.53m	1.83s					
	$[Cp(CO)_3W(CH_2)_4Mo(CO)_3Cp]$	**1b**	5.25s		5.35s	1.59s	0.86s	1.83s	1.55s				
	$[Cp(CO)_3W(CH_2)_5Mo(CO)_3Cp]$	**1c**	5.26s		5.35s	1.58s	1.32s	1.84s	1.57s	1.82s			
	$[Cp(CO)_3W(CH_2)_6Mo(CO)_3Cp]$	**1d**	5.25s		5.40s	1.51s	1.23s	1.83s	1.56s	1.81s	1.76s		
B													
	$[Cp(CO)_3W(CH_2)_3Mo(CO)_3Cp^*]$	**2a**		1.85s	5.36s	1.67m	0.99m	1.63m					
	$[Cp(CO)_3W(CH_2)_4Mo(CO)_3Cp^*]$	**2b**		1.85s	5.35s	1.65s	0.85s	1.58s	1.23s				
C													
	$[Cp(CO)_3W(CH_2)_3Mo(CO)_2(PPh_3)Cp]$	**3a**	4.73s		5.36s	1.68m	1.29m	1.62m				7.36s, 15H	
	$[Cp(CO)_3W(CH_2)_4Mo(CO)_2(PPh_3)Cp]$	**3b**	4.70s		5.35s	1.63s	0.83s	1.54s	1.23s			7.37s, 15H	
	$[Cp(CO)_3W(CH_2)_3Mo(CO)_2(PPh_2Me)Cp]$	**4a**	4.96s		5.39s	1.66s	1.24s	1.48s				7.36m, 10H	2.10d, 8.9[b],3H
	$[Cp(CO)_3W(CH_2)_4Mo(CO)_2(PPh_2Me)Cp]$	**4b**	4.69s		5.35s	1.62s	0.89s	1.49s	1.23s			7.36m, 10H	2.07d, 8.8,3H
	$[Cp(CO)_3W(CH_2)_3Mo(CO)_2(PPhMe_2)Cp]$	**5a**	4.72s		5.37s	1.65s	1.22s	1.45s				7.37m, 5H	1.82d, 8.2,6H
	$[Cp(CO)_3W(CH_2)_4Mo(CO)_2(PPhMe_2)Cp]$	**5b**	4.70s		5.35s	1.61s	0.89s	1.47s	1.24s			7.37m, 5H	1.82d, 8.2,6H
	$[Cp(CO)_3W(CH_2)_3Mo(CO)_2(PMe_3)Cp]$	**6a**	4.88s		5.38s	1.64s	1.23s	1.47s					1.49d, 8.8,9H
	$[Cp(CO)_3W(CH_2)_4Mo(CO)_2(PMe_3)Cp]$	**6b**	4.87s		5.34s	1.66s	0.83s	1.46s	1.23s				1.49d, 8.9,9H
D													
	$[Cp(CO)_2Fe(CH_2)_3Mo(CO)_2(PPh_3)Cp]$	**7a**	4.71s		4.72s	1.63m	1.23m	1.52m				7.36m, 15H	
	$[Cp(CO)_2Fe(CH_2)_4Mo(CO)_2(PPh_3)Cp]$	**7b**	4.70s		4.70s	1.66s	0.84s	1.53s	1.23s			7.36m, 15H	
	$[Cp(CO)_2Fe(CH_2)_3Mo(CO)_2(PPh_2Me)Cp]$	**8a**	4.71s		4.70s	1.24s	1.48s	1.76s				7.37m, 10H	2.07d, 8.9,3H
	$[Cp(CO)_2Fe(CH_2)_4Mo(CO)_2(PPh_2Me)Cp]$	**8b**	4.95s		4.70s	1.62s	0.85s	1.49s	1.23s			7.37m, 10H	2.15d, 8.9,3H
	$[Cp(CO)_2Fe(CH_2)_3Mo(CO)_2(PPhMe_2)Cp]$	**9a**	4.94s		4.71s	1.23s	1.48s	1.79s				7.39m, 5H	2.00d, 8.2,6H
	$[Cp(CO)_2Fe(CH_2)_4Mo(CO)_2(PPhMe_2)Cp]$	**9b**	4.94s		4.70s	1.62s	0.85s	1.42s	1.23s			7.40m, 5H	2.05d, 8.2,6H
	$[Cp(CO)_2Fe(CH_2)_3Mo(CO)_2(PMe_3)Cp]$	**10a**	4.88s		4.71s	1.35s	1.43s	1.69s					1.48d, 10.4,9H
	$[Cp(CO)_2Fe(CH_2)_4Mo(CO)_2(PMe_3)Cp]$'	**10b**	4.88s		4.69s	1.34s	1.42s	1.66s					1.48d, 8.9,9H
E													
	$[Cp(CO)_2Fe(CH_2)_3Mo(CO)_3Cp^*]$	**11a**		2.07s	4.70s	1.64m	1.23m	1.46m					
	$[Cp(CO)_2Fe(CH_2)_4Mo(CO)_3Cp^*]$	**11b**		1.84s	4.70s	1.61s	0.96s	1.58s	1.46s				

[a] in $CDCl_3$ relative to TMS (0.00 ppm). [b] J values are given in Hz. M' = Fe or W. Cp' = Cp on either Fe or W. β-Mo refers to the carbon atom of the alkyl chain β to Mo etc.

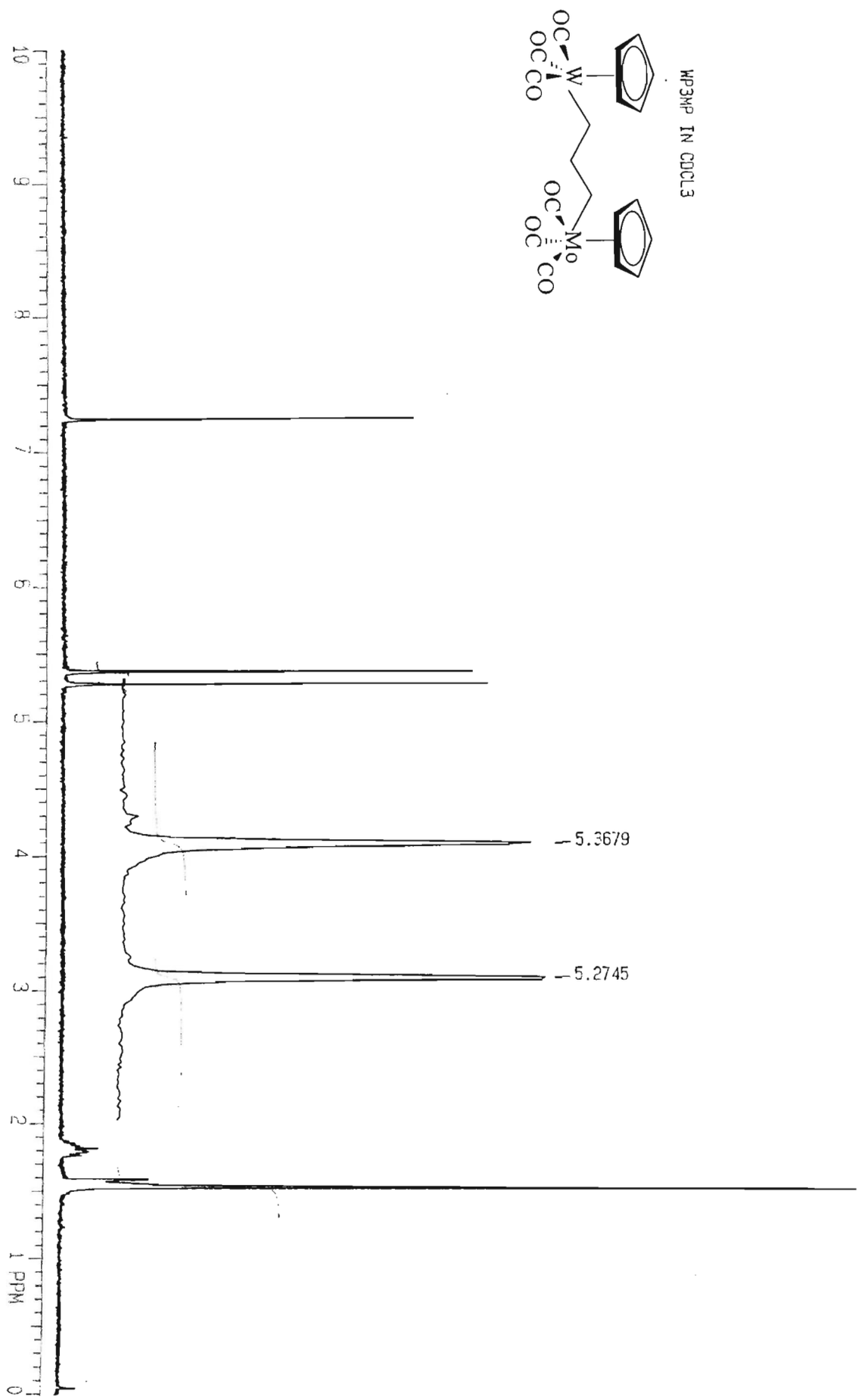

Figure 4.1: ^{1}H NMR spectrum of $[Cp(CO)_3W(CH_2)_3Mo(CO)_3Cp]$

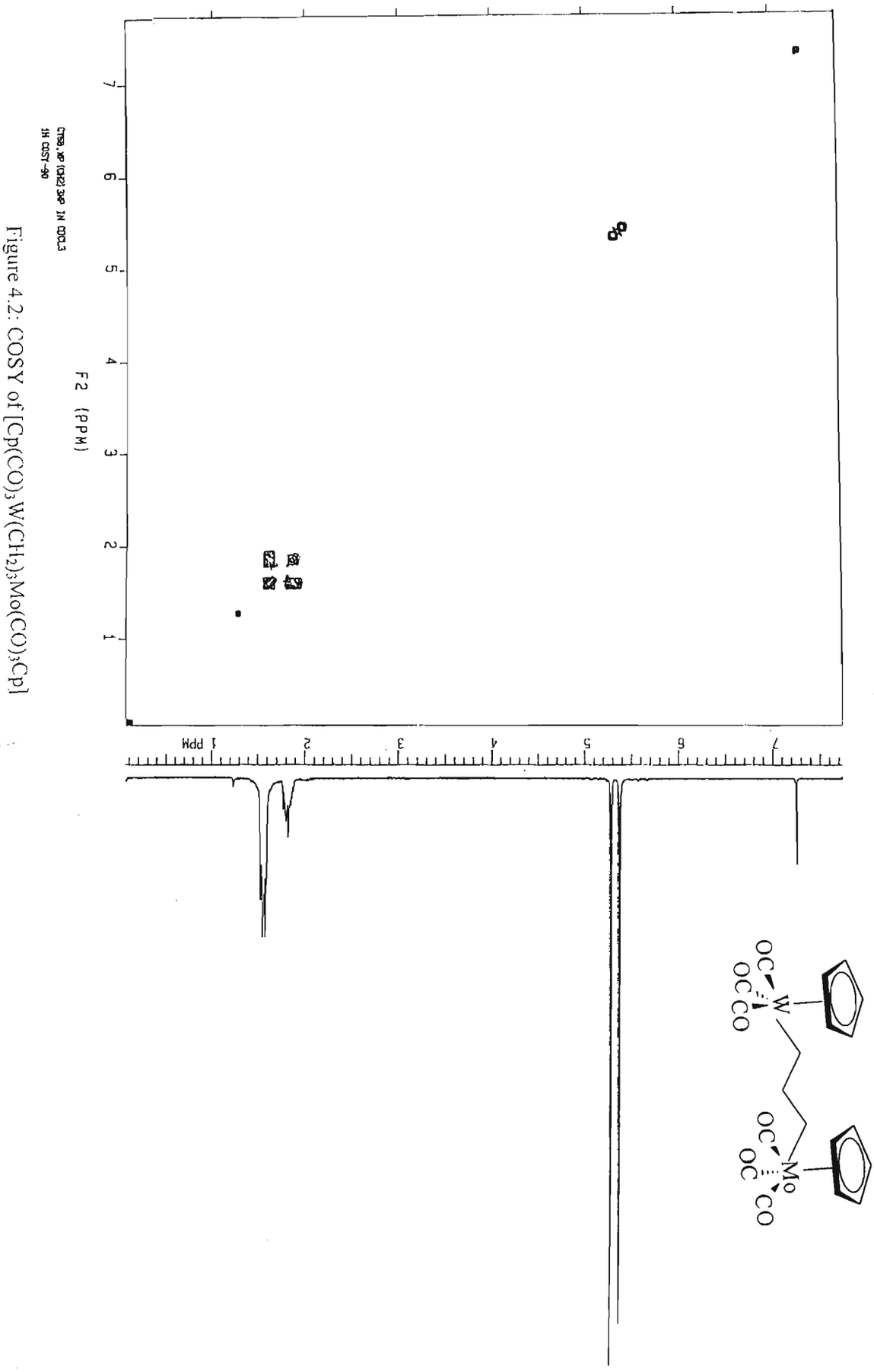

Figure 4.2: COSY of $[Cp(CO)_3W(CH_2)_3Mo(CO)_3Cp]$

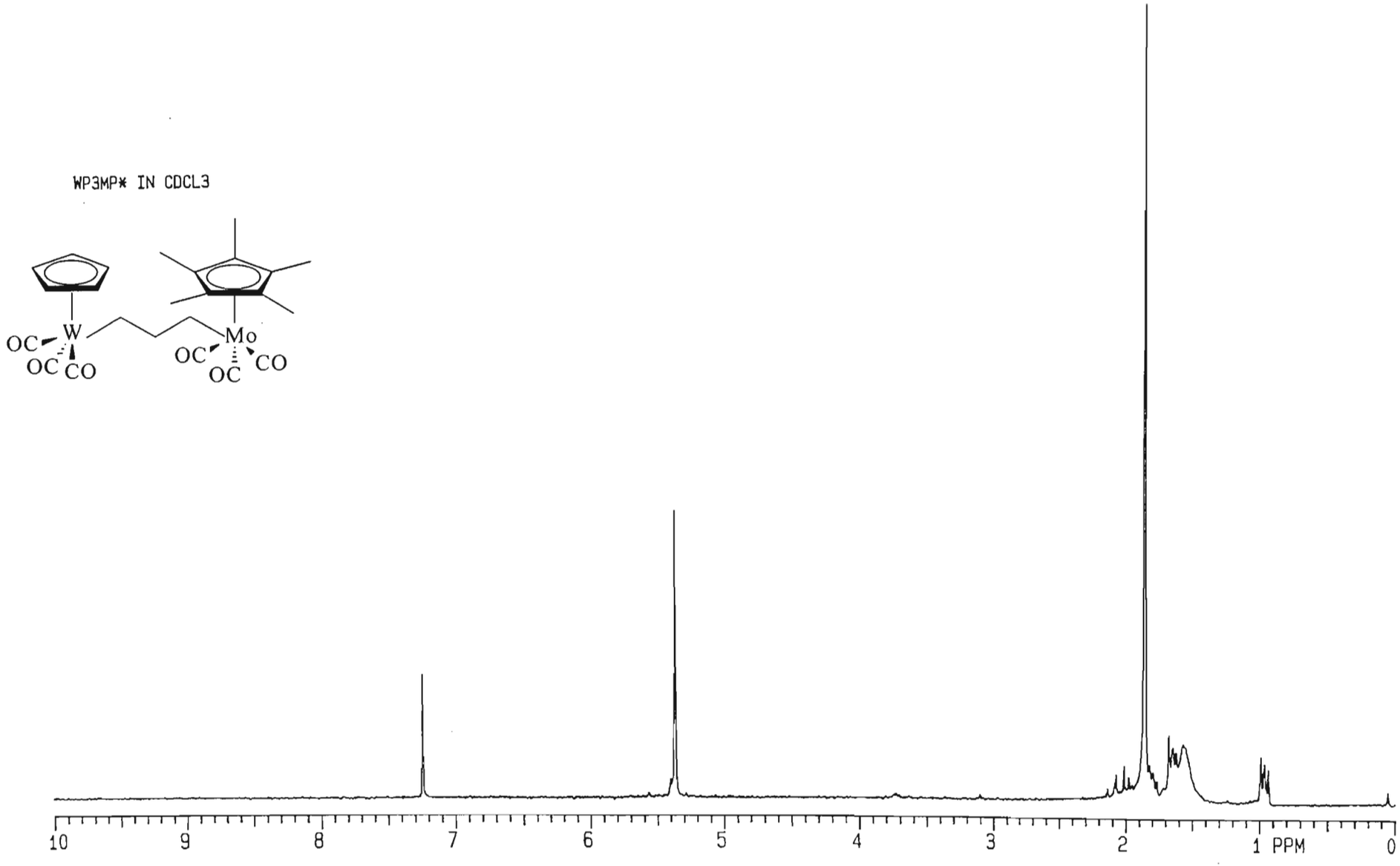

Figure 4.3: ^{1}H NMR spectrum of $[Cp(CO)_3W(CH_2)_3Mo(CO)_3Cp^*]$

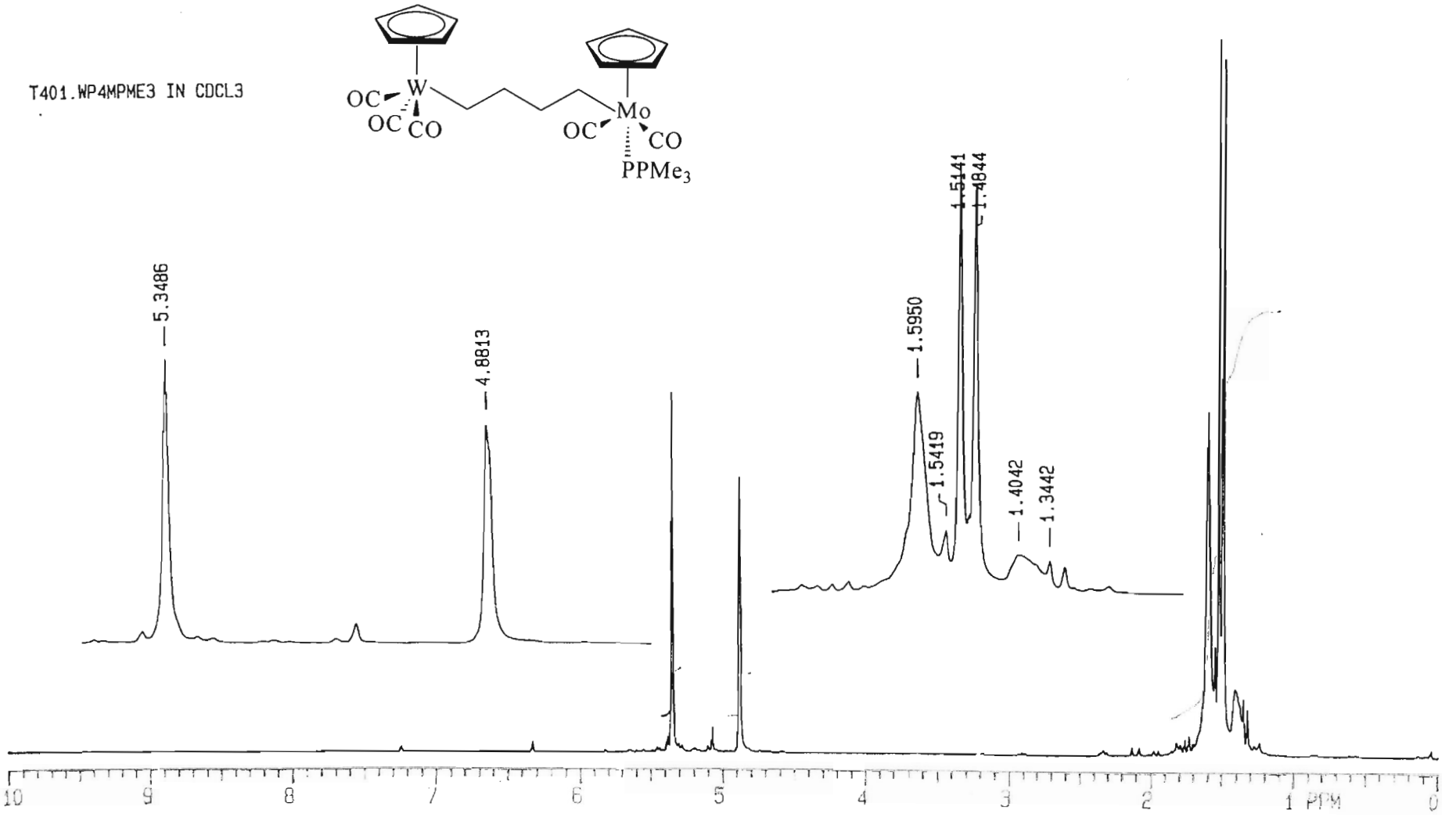

Figure 4.4: ^{1}H NMR spectrum of $[Cp(CO)_3W(CH_2)_4Mo(CO)_2(PMe_3)Cp]$

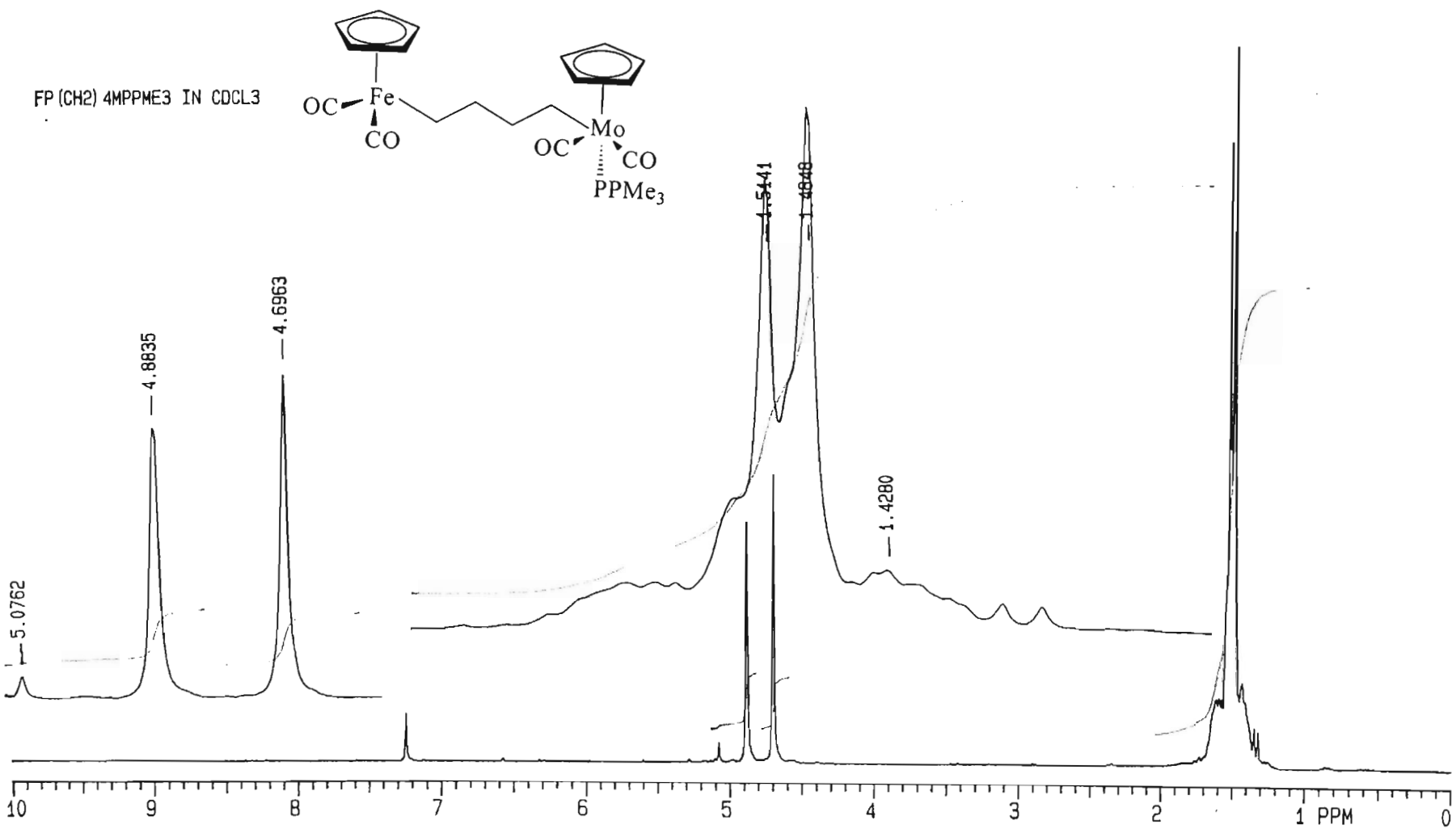

Figure 4.5: ^{1}H NMR spectrum of $[Cp(CO)_2Fe(CH_2)_4Mo(CO)_2(PMe_3)Cp]$

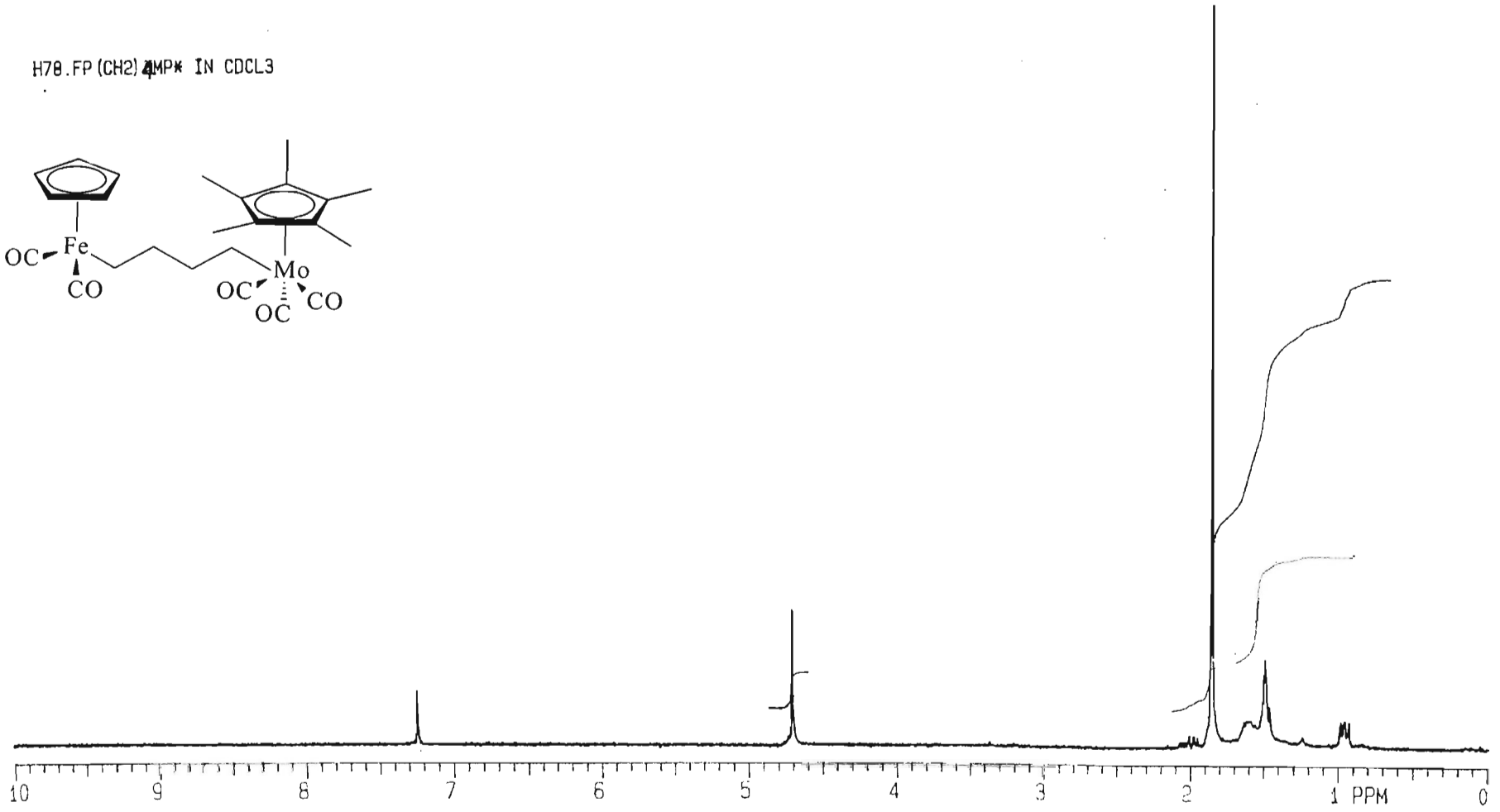

Figure 4.6: ^{1}H NMR spectrum of $[Cp(CO)_2Fe(CH_2)_4Mo(CO)_3Cp^*]$

We have also confirmed this observation from the crystal structures obtained for compounds **3a** and **7a** as can be seen in Figures 4.13 and 4.16. Generally, the $MoCH_2$ protons gave triplets around 1.6 ppm. The compounds that had PMe_3 as a ligand, had the peaks due to the protons α to the molybdenum appearing at a much lower positions, namely 1.35 ppm. This is expected, as there is greater shielding resulting from the high basicity of the trimethylphosphine ligand, contributing more electrons, both from the phosphorus atom and the three methyl groups onto the central metal. The phenyl protons of the phosphine ligand, being highly deshielded, were always observed at around 7.3 ppm. The methyl protons when present on the phosphine ligand appeared at around 2 ppm and were always observed as doublets due to coupling with the phosphorus atom. The $MoCH_2CH_2$ and $MoCH_2CH_2CH_2$ protons gave multiplets with overlapping peaks and thus their assignments are uncertain.

4.2.2 ^{13}C NMR data

The data for complexes **1a- 11b** are given in Table 4.3. Again, the peak assignments were made by using heteronuclear correlation (HETCOR) or heteronuclear single-quantum correlation (HSQC) experiments. In addition, to confirm our peak position assignments, comparisons were made to the ^{13}C NMR data reported for similar heterodinuclear complexes of Fe and Mo, W, Re and Ru [17]. Representative sample spectra for the compounds are presented in Figures 4.7 – 4.12, including a HETCOR of **1a**. The metals on the opposite end of the paraffin chain and the chain length were seen to have no effect on the chemical shifts of the carbonyl peaks. Similarly, the metals on the opposite end of the paraffin chain and chain length do not appear to affect the positions of Cp* and Cp peaks very much. These peaks for the complexes **4a – 10b** with phosphines as ligands, appear at slightly lower field, compared to unsubstituted compounds (**1a – 1d**). The higher the basicity of the phosphine ligand, the lower the field strength observed because of the known shielding effects.

The carbonyl ligands *cis* to the phosphine ligand were also observed as doublets because of coupling with the phosphorus atom. Again this interpretation was confirmed by the crystal structures of **3a** and **7a** (Figures 4.13 and 4.16).

Table 4.3: ^{13}C NMR : Data for the compounds $[Cp(CO)_2(L)Mo(CH_2)_nM(CO)_iCp]$[a]; n = 3 – 6; 3, 4; M = Fe, W; L = CO, PPh_iMe_{3-i}) i = 0 – 3; **1a - 11b**

Type/Cpd	MoCO	M'CO$_{(cis)}$[b]	M'CO$_{(trans)}$[b]	CpMo	Cp*(c)	Cp*(CH_3)	CpM'	α-Mo	α-M'	β-M'[c]	β-Mo[d]	γ-W	γ-Mo	Ph	P-Me
A															
1a	217s	227s	239	92.6s			91.4s	7.6s	-5.1s	44.3s					
1b	217s	227s	*f*	92.9s			91.7s	2.4s	-10.1s	43.2s	25.8s				
1c	218s	227s	*f*	93.7s			92.5s	3.8s	*f*	37.6s	26.6s	36.7s			
1d	217s	227s	240s	92.7s			91.4s	2.7s	-9.8s	36.8s[e]	14.1s	36.4s[e]	25.6s		
B															
2a	217s	231s	240s		104.02s	10.36s	91.33s	18.48s	-3.62s	43.71s					
2b	217s	231s	*f*		104.15s	10.32s	91.51s	20.80s	-9.99s	43.82s[e]	40.41s[e]				
C															
3a	*f*	229s	217s	92.50s			91.49s	1.02s	-3.69s	44.51s				128d, 10.0	
3b	*f*	229s	217s	92.67s			91.72s	3.72s	-9.47s	43.80s	42.45s			128d, 9.7	
4a	237d, 22.6	229s	217s	92.22s			91.41s	17.05s	-3.69s	44.67s				128d, 9.7	21.61d, 34.8
4b	237d, 22.6	229s	217s	91.76s			91.53s	2.55s	-9.39s	43.80s	43.14s			128d, 9.6	21.02d, 34.4
5a	237d, 22.7	228s	217s	91.62s			91.38s	8.61s	-3.61s	44.72s				128d, 9.6	21.00d, 32.9
5b	236d, 22.6	229s	217s	91.74s			91.49s	2.67s	-9.42s	43.78s	43.12s			128d, 9.7	21.00d, 32.9
6a	238d, 22.8	229s	217s	91.81s			91.37s	10.47s	-11.97s	44.57s					17.59d, 31.9
6b	238d, 22.6	229s	217s	91.51s			90.95s	1.92s	-9.35s	43.93s[e]	43.31s[e]				22.22d, 32.8
D															
7a	238d, 32.0	*f*	218s	92.51s			85.20s	43.03s	7.79s	47.38s				128d, 9.7	
7b	238d, 34.0	*f*	218s	92.87s			85.57s	41.66s	4.22s	45.41s	31.15s			128d, 9.7	
8a	236d, 34.1	*f*	217s	92.23s			85.18s	8.05s	9.45s	45.83s				127d, 9.6	21.15d, 34.3
8b	234d, 34.0	*f*	*f*	92.33s			85.58s	0.99s	14.09s	31.56s	22.63s			128d, 9.7	20.80d, 34.5
9a	234s	*f*	217s	91.66s			85.17s	7.57s	9.51s	45.95s				128d, 9.6	21.02d, 32.9
9b	237s	*f*	217s	91.96s			87.95s	3.32s	8.63s	41.75s	37.45s			128d, 9.6	18.50d, 32.4
10a	236s	*f*	217s	90.85s			85.16s	6.80s	9.60s	46.10s					21.84d, 29.8
10b	236s	*f*	217s	90.93s			85.31s	2.23s	4.05s	45.25s	42.35s				21.83d, 32.1
E															
11a	*f*	230s	218s		103.98s	11.8s	85.7s	1.5s	8.2s	47.4s					
11b	*f*	231s	217s		104.12s	10.4s	85.4s	3.6s	10.3s	45.4s	41.1s				

[a] measrured in $CDCl_3$ relative to TMS (δ = 0.00 ppm). [b] Relative the alkyl chain. [c] β-M' refers to the carbon atom of the alkyl chain β to M'. [d] β-Mo refers to the carbon atom of the alkyl chain β to Mo etc. [e] Assignments could be interchanges. *f* Not observed. Cp' = Cp on either Fe or W. M' refers to either W or Fe metal.

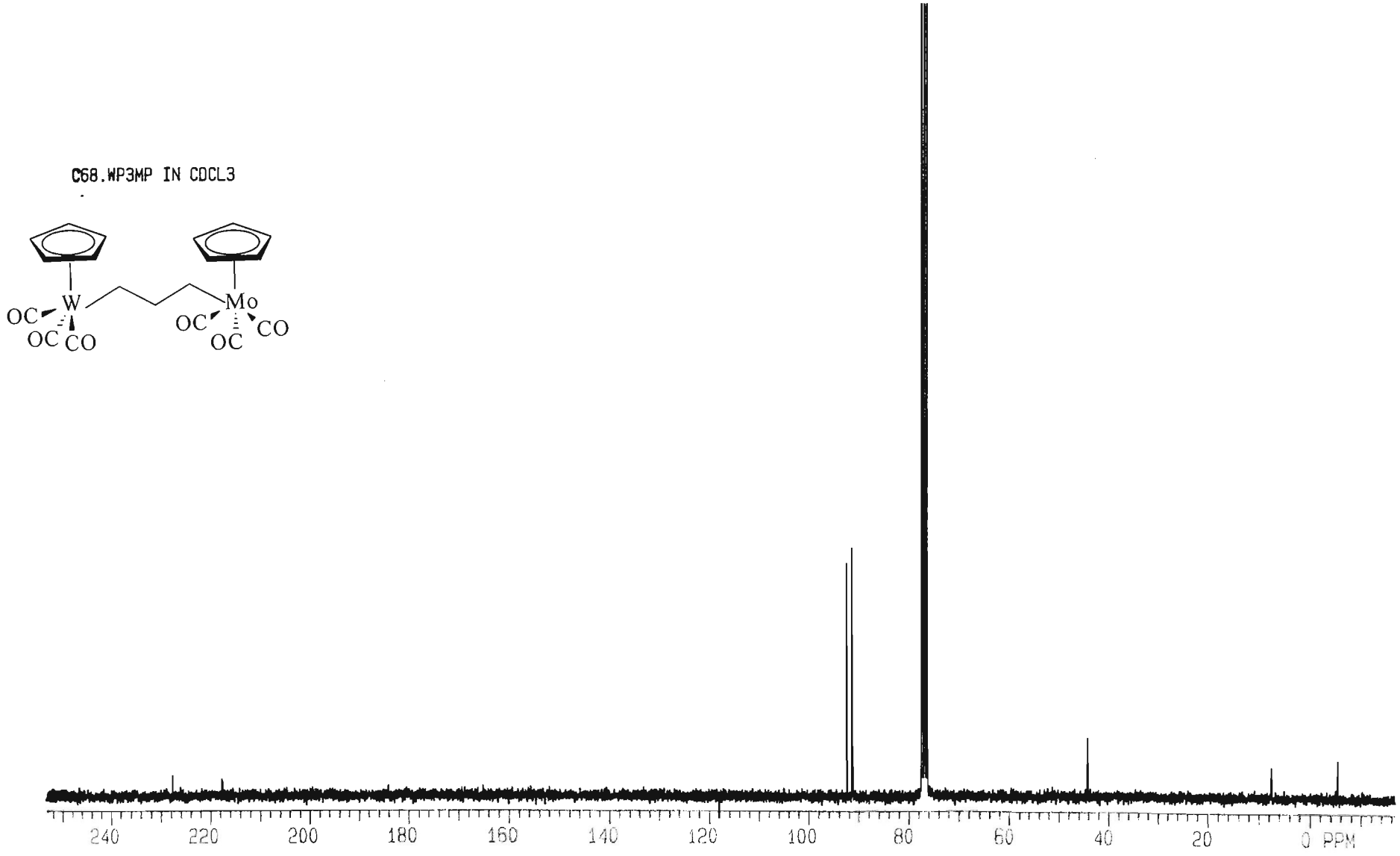

Figure 4.7: ^{13}C NMR spectrum of $[Cp(CO)_3W(CH_2)_3Mo(CO)_3Cp]$

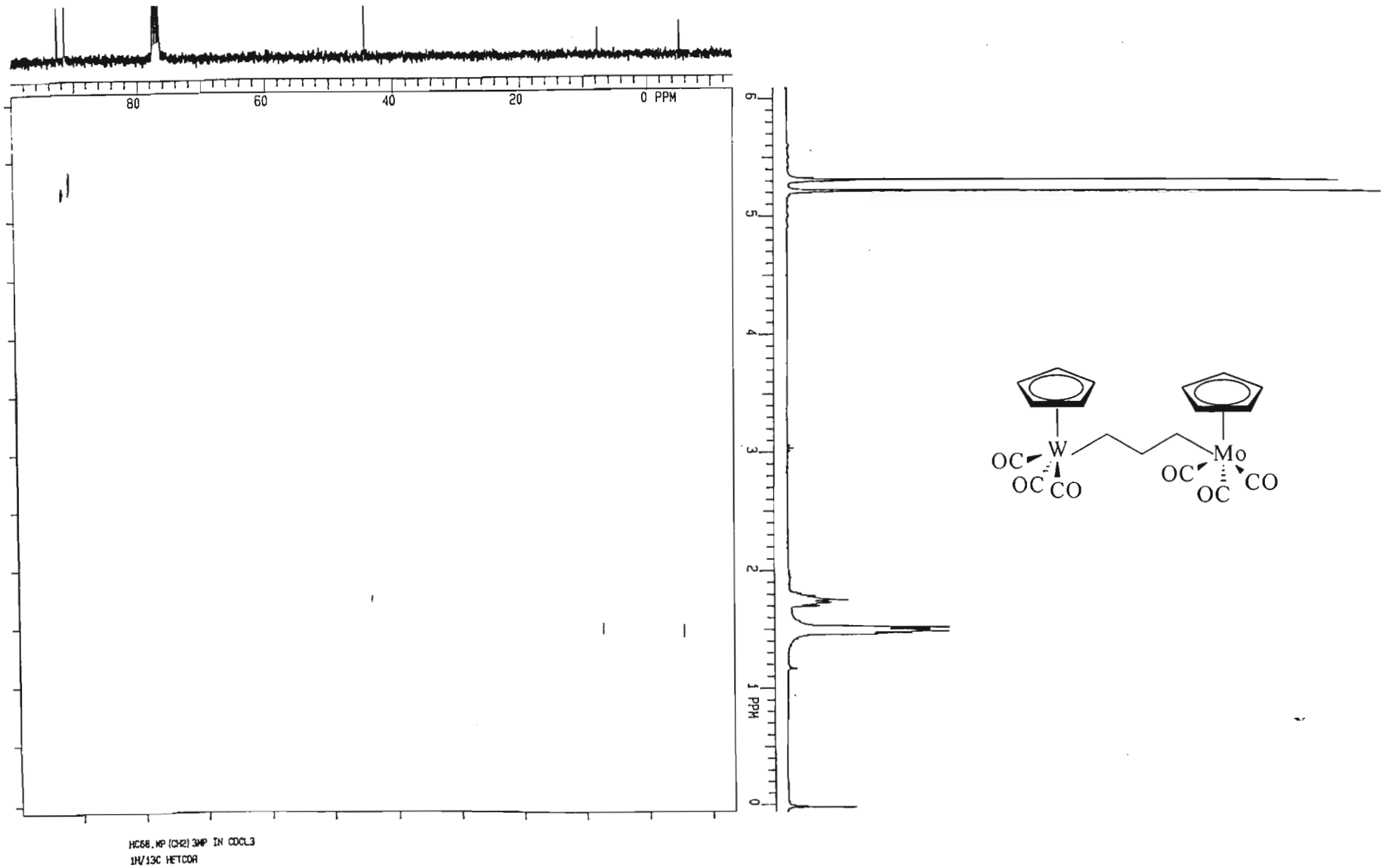

Figure 4.8: HETCOR of $[Cp(CO)_3W(CH_2)_3Mo(CO)_3Cp]$

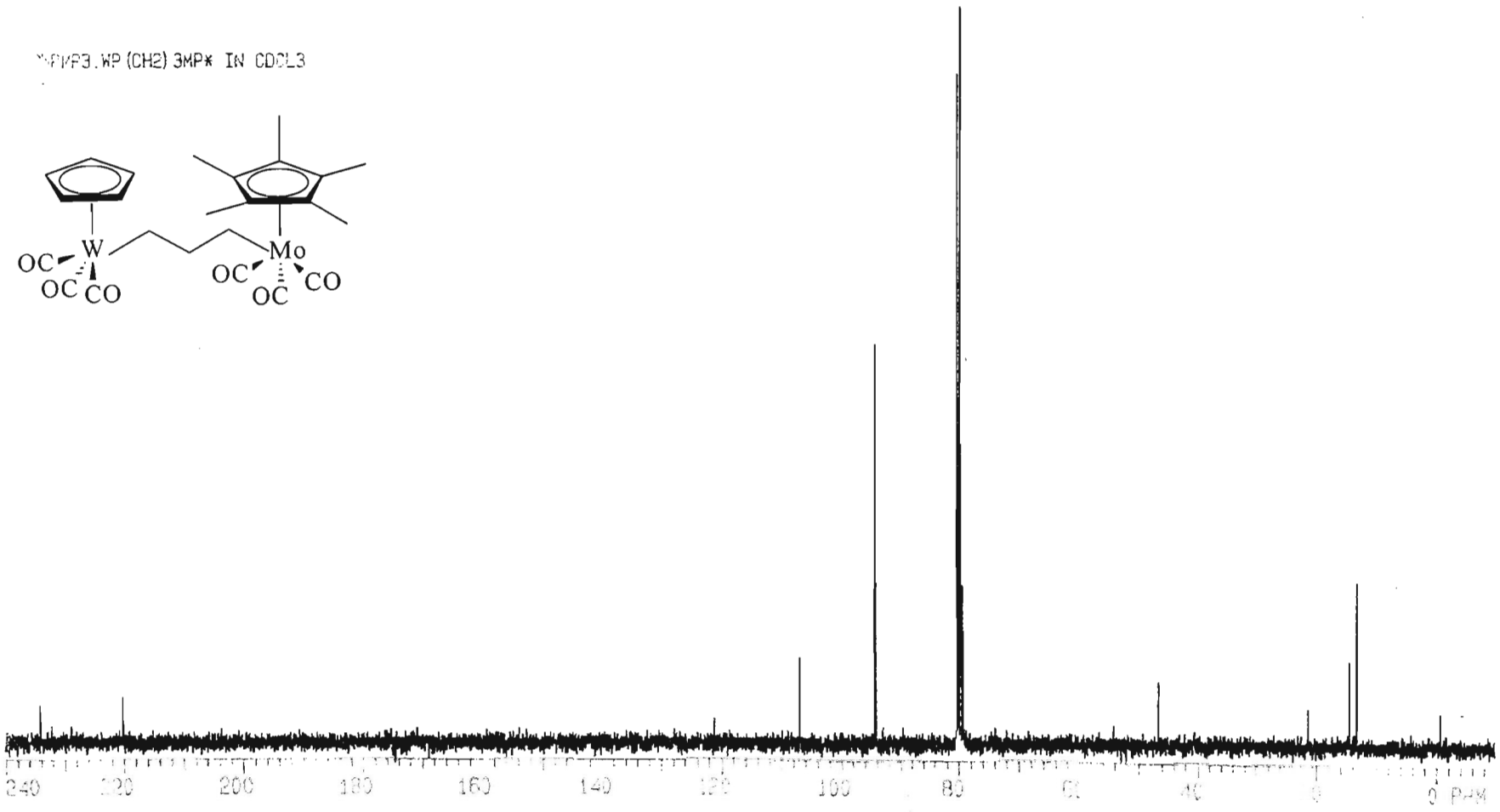

Figure 4.9: ^{13}C NMR spectrum of $[Cp(CO)_3W(CH_2)_3Mo(CO)_3Cp^*]$

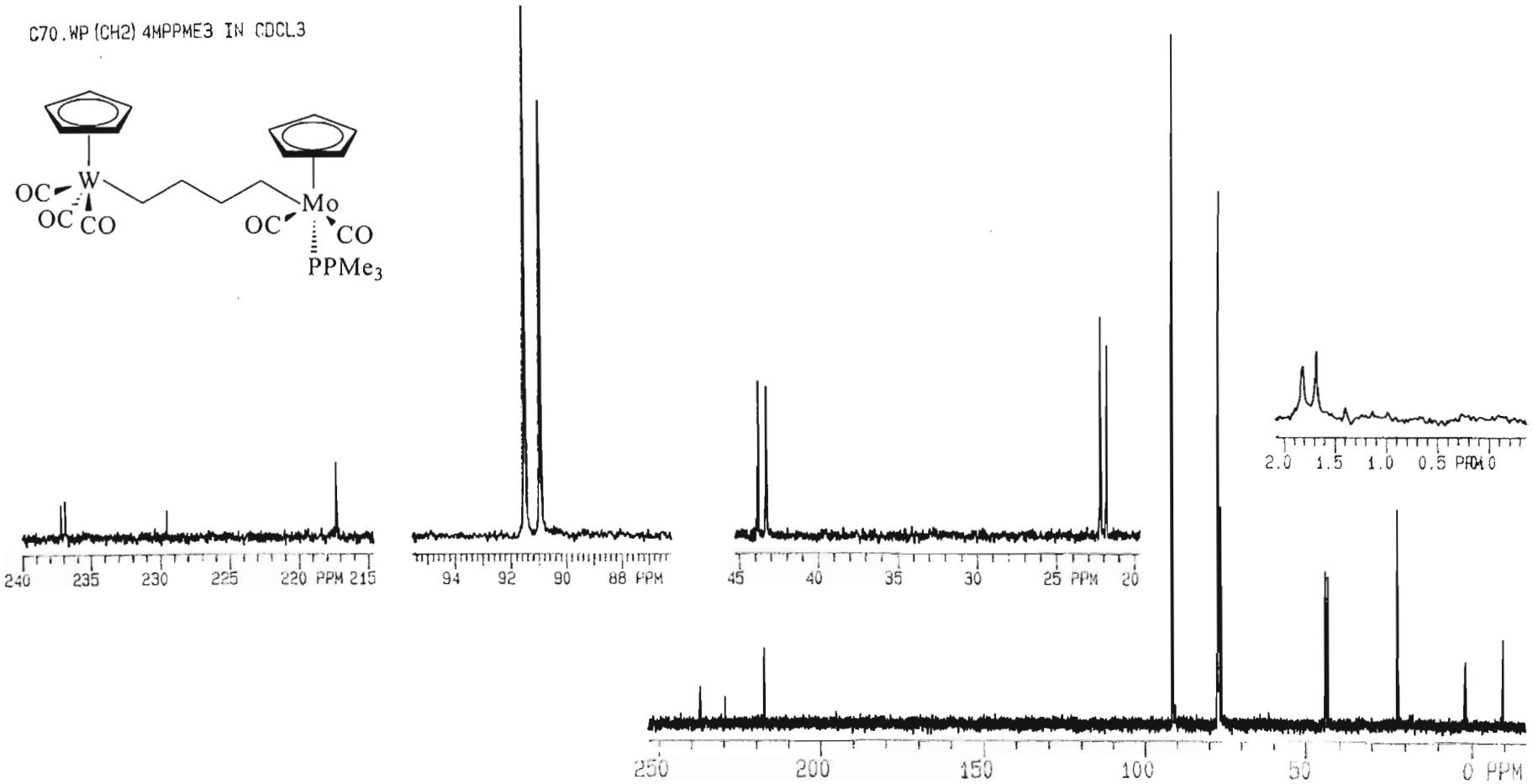

Figure 4.10: ^{13}C NMR spectrum of $[Cp(CO)_3W(CH_2)_4Mo(CO)_2(PMe_3)Cp]$

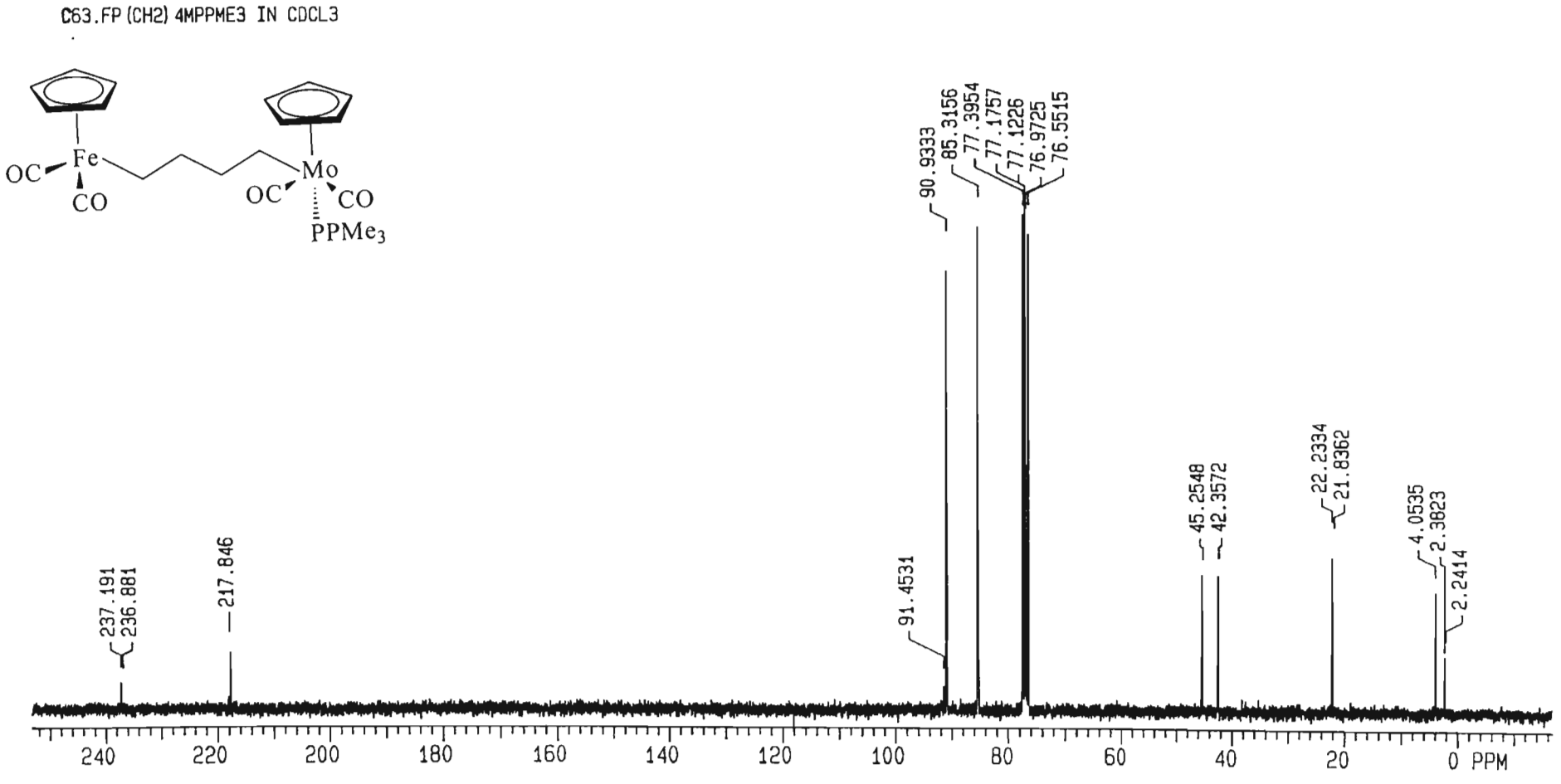

Figure 4.11: ^{13}C NMR spectrum of $[Cp(CO)_2Fe(CH_2)_4Mo(CO)_2(PMe_3)Cp]$

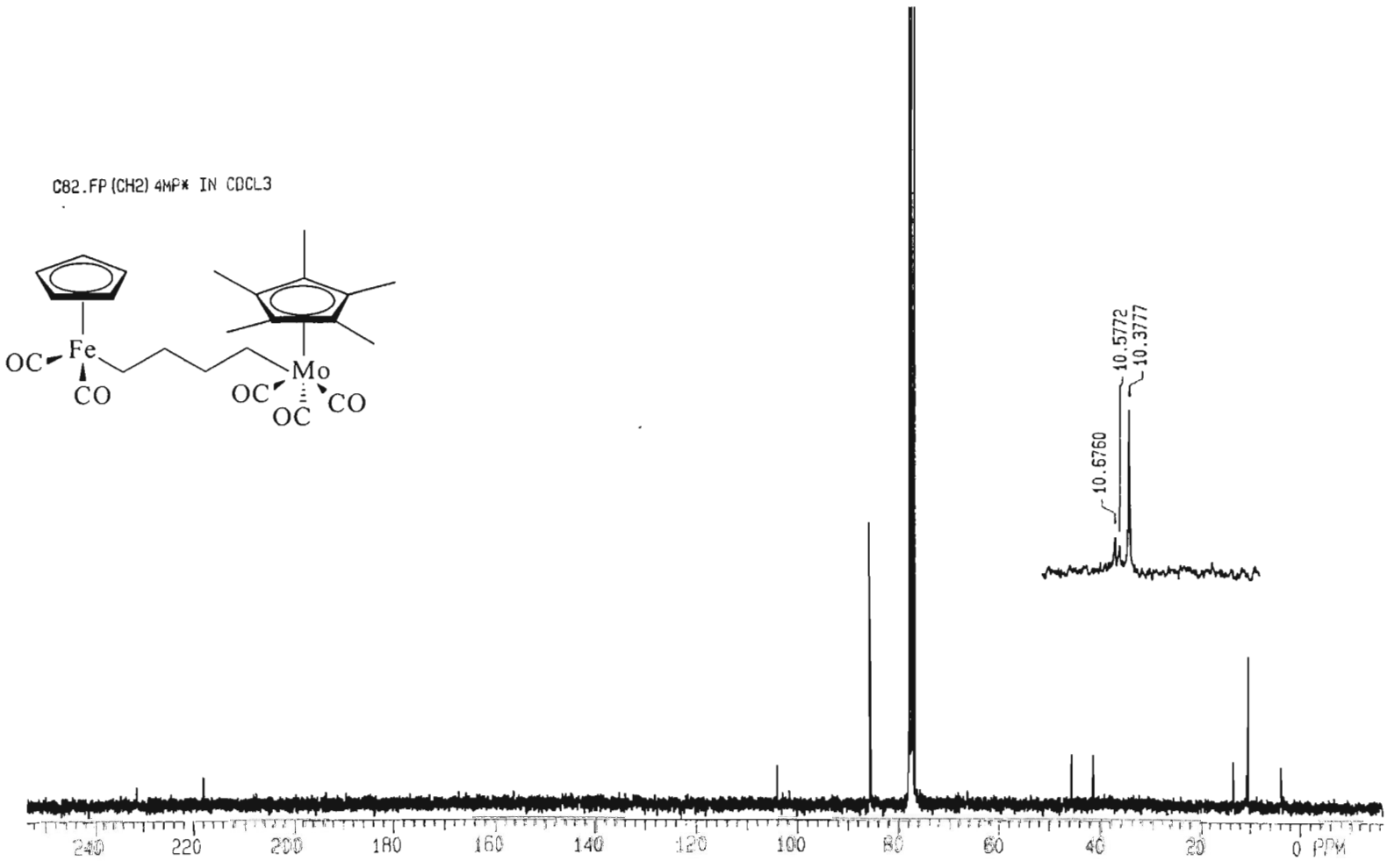

Figure 4.12: ^{13}C NMR spectrum of $[Cp(CO)_2Fe(CH_2)_4Mo(CO)_3Cp^*]$

The electronegative oxygen present in the molecule helps draw the electrons away from the carbonyl carbon, making them highly deshielded, such that their resonances appear downfield. As expected, the α -carbon to tungsten is highly shielded so that its resonance is found upfield.

From the ^{13}C NMR data in Table 4.3, it can be seen that the chemical shift of the carbon α to a metal, generally decreases with an increase in the bridging chain length. This suggests that an increase in the chain length of the heterodinuclear compound, results in a reduced influence that the metal on the one end of the chain has on the carbon that is α to the other metal. Probably, the electrons have to be redistributed over a longer chain, hence a weakened metallic influence. Compounds **2a** and **2b** seem to differ from this, again because of the electron pushing effect of the Cp*. We find that the MoCH_2 carbons in the Cp* compounds are significantly more deshielded than those of the Cp compounds and the deshielding effect is weaker on the MoCH_2CH_2 protons. The methyl and the phenyl subsitituents on the phosphorus atom show no change in their peak positions. The chemical shifts of the carbons of the phenyl substituents always occurred at around 128 ppm, while those of the methyl, when present, at about 20 ppm in the ^{13}C NMR spectrum.

4.3 Crystal Structures of $[Cp(CO)_2W(CH_2)_3Mo(CO)_2(PPh_3)Cp]$ 3a, and $[Cp(CO)_2Fe(CH_2)_3Mo(CO)_2(PPh_3)Cp]$ 7a

Crystals of the compounds **3a** and **7a** were obtained from slow cystallisation over several days in a dichloromethane/hexane mixture at –10 °C [33]. A suitable single crystal was selected and subjected to X-ray diffraction study. The structures of the compounds **3a** and **7a,** with the metals W and Mo, and Fe and Mo, respectively, linked by a polymethylene chain, where each of the transition metals was σ-bonded to a CH_2 group, was compatible with the NMR data presented in Tables 4.2 – 4.3.

Only homodinuclear structures of iron and molybdenum alkanediyl compounds are reported in the literature, and to our knowledge none with both metals present in the same molecule. The known homodinuclear structures have the ligand pattern $[Cp(CO)_iM(CH_2)_nM(CO)_iCp]$; for i = 2, M = Fe [34,35], Ru [36] and for i = 3, Mo [37]. Pope *et al.* reported that the Fe-CH_2 and –CH_2-CH_2-CH_2- protons were equivalent from a

^{1}H NMR study [34]. This was apparently found to be as a result of a fluxional process that causes the various methylene protons to rapidly exchange their sites. The understanding of this fluxional behaviour was further investigated by another group that helped shed some light upon the behaviour of a substrate on a metal surface in catalytic reactions [38]. Friedrich and Moss reported the structure of $[Cp(CO)_2Fe(CH_2)_6Ru(CO)_2Cp]$, which was disordered and hence only a gross conformation of the molecule was described. This structure, if fully solved, would have been the only structure of a heterobimetallic alkanediyl compound. It would also have contained the longest alkyl chain known [5]. The compounds $[Cp(CO)_3W(CH_2)_3Mo(CO)_2(PPh_3)Cp]$ **3a** and $[Cp(CO)_2Fe(CH_2)_3Mo(CO)_2(PPh_3)Cp]$ **7a**, discussed below, are therefore the first known crystal structures for heterodinuclear alkanediyl Group VIb compounds.

The structure of the complex **3a** was solved and refined in the monoclinic space group P 21/c and the molecule formed showed a glide on the c-plane. The structure is shown in Figure 4.13 (**3a**). Crystallographic details and fractional coordinates and temperature factors are listed in Appendix 3 and in the attached compact disc. Selected bond lengths and angles are given in Table 4.4.

Because there is no such similar structure to that of our compound in the literature, we have discussed the structures by looking at the tungsten and molybdenum moieties independently and comparing them with some reported structures from the literature, which are also discussed in Chapters 2 and 3 of this report. As expected the triphenylphosphine ligand on the molybdenum atom is *trans*, and the carbonyl groups and the cyclopentadienyl ligands are *cis*, to the alkyl chain. The ligands are disposed in a piano stool fashion similar to other reported complexes of this general type [39].

The angles between the contiguous legs on the tungsten unit range from 75.4 to 77.5°, typical values for this type of structure (Figures. 4.14 and 4.15 **3a**). The cyclopentadienyl ligand is bound in a pentahapto manner (Figure 4.13 **3a**), as inferred from the total value of the angles at the ring (540°) and metal – ring carbon distances which range from 2.31 (8) Å – 2.35 (9) Å. The carbonyl ligands have a linear arrangement, with W–C–O angles ranging from 176.1(8) to 179.0(7). The C–O bond lengths of between 1.146(10) to 1.16(11) Å, and the averaged W–C(CO) bond length of 1.97 Å (with bond lengths ranging from 1.97(10) – 1.99(10) Å) are normal for terminal carbonyl groups. The W–C(sp^3)

bond distance 2.32(9) Å is longer than that of the recently reported monometallic halogenoalkyl compound $[Cp(CO)_3W\{(CH_2)_5I\}]$ (2.08(3) Å [39]), but is in the general range of some of the reported W–C bonds (2.18–2.36 Å) [39-41], though most of these compounds have different ligands attached. This bond distance is known to be in the range of a methyl group bound to a d^4 –tungsten center, as seen for some relevant compounds, $[(\eta^5\text{-}C_5H_4)(CMe_2C_9H_7(CO)_3Me)W]$ (2.29(9) Å) [42], $[(\eta^5\text{-}C_5H_5)(CO)_3W(C_4H_9)]$ (2.34(9) Å) [43] and $[\{(CO_3)Me\}_2\{\eta\text{: }\eta^5\text{-}(C_9H_6CH_2)_2\}W]$ (2.29(9) Å) [44].

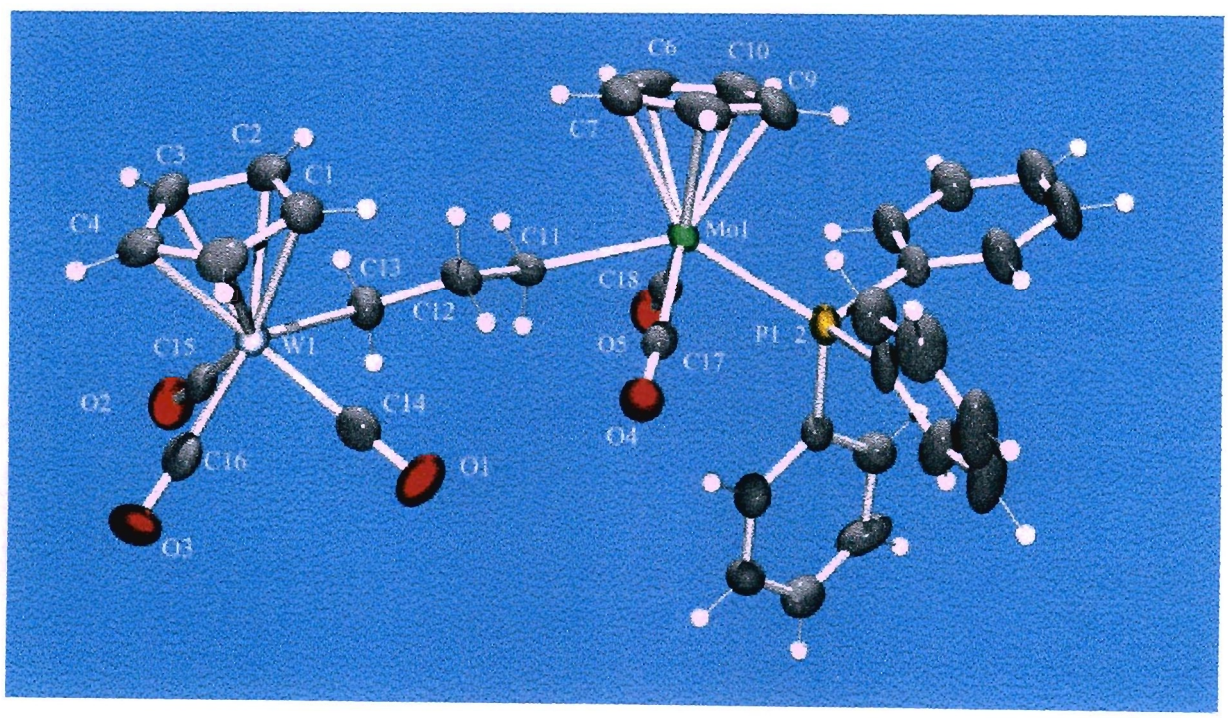

Figure 4.13: ORTEP diagram showing the X-ray structure of $[Cp(CO)_3W(CH_2)_3Mo(CO)_2(PPh_3)Cp]$ (**3a**).

Table 4.4: Selected bond lengths [Å] and Bond angles (°) of $[Cp(CO)_3W(CH_2)_3Mo(CO)_2(PPh_3)Cp]$, **3a.**

Bond Lengths (Å)		Bond Angles (°)	
W(1)-C(16)	1.984(8)	C(16)-W(1)-C(15)	77.8(3)
W(1)-C(15)	1.965(7)	C(16)-W(1)-C(14)	77.7(3)
W(1)-C(14)	1.988(8)	C(15)-W(1)-C(4)	112.7(3)
W(1)-C(4)	2.315(7)	C(16)-W(1)-C(4)	89.5(3)
W(1)-C(5)	2.316(6)	C(18)-Mo(1)-C(17)	103.8(3)
W(1)-C(13)	2.316(7)	C(18)-Mo(1)-C(11)	72.5(2)
W(1)-C(1)	2.317(7)	C(17)-Mo(1)-C(11)	74.5(2)
W(1)-C(3)	2.334(7)	C(18)-Mo(1)-P(1)	80.6(18)
W(1)-C(2)	2.349(7)	C(17)-Mo(1)-P(1)	78.0(18)
Mo(1)-P(1)	2.457(19)	C(11)-Mo(1)-P(1)	135.12(17)
O(1)-C(14)	1.149(8)	C(8)-Mo(1)-P(1)	110.4(2)
O(2)-C(15)	1.151(8)	C(1)-C(2)-C(3)	107.5(6)
O(3)-C(16)	1.147(9)	C(4)-C(3)-C(2)	107.6(6)
O(4)-C(17)	1.153(7)	C(3)-C(4)-C(5)	108.7(7)
O(5)-C(18)	1.151(7)	C(1)-C(5)-C(4)	107.2(8)
C(11)-C(12)	1.527(9)	C(10)-C(6)-C(7)	105.7(7)
C(12)-C(13)	1.519(9)	C(13)-C(12)-C(11)	110.1(6)
Mo(1)-C(18)	1.957(7)	C(12)-C(13)-W(1)	116.4(5)
Mo(1)C(17)	1.960(7)	O(1)-C(14)-W(1)	178.4(6)
Mo(1)C(11)	2.357(7)	O(2)-C(15)-W(1)	177.8(6)
C(31)-C(32)	1.381(9)	O(3)-C(16)-W(1)	177.2(6)
C(31)-C(36)	1.402(9)	O(4)-C(17)-Mo(1)	175.8(6)
C(32)-C(33)	1.396(10)	O(5)-C(18)-Mo(1)	175.2(5)
C(33)-C(34)	1.375(10)	C(31)-P(1)-C(25)	102.5(3)
C(34)-C(35)	1.367(10)	C(31)-P(1)-C(19)	103.1(3)
C(35)-C(36)	1.386(9)	C(25)-P(1)-C(19)	100.2(3)

The angles between the molybdenum and the ligands surrounding it, range from 72.3 to 80.6°. This is within the range of the related structures [39]. Very few molybdenum–alkyl structures are known and to date those with the $Cp(CO)_2(PR_3)$ ligand pattern have only recently been reported by us. The phenyl substituent of the structure of compound reported in Chapter 3, Figure 3.9 has a sum of its bond angles of averagely 719.8°, however, for compound **3a** the sum of the bond angles for the phenyl substituent adjacent to the Cp ring is 723.0°, *i.e.* 3° greater than the norm. The explanation for this observation could be that an electronic influence is experienced as a result of a ring current contributed by the cyclopentadienyl ring to the phenyl ring. The Mo–C (alkyl) bond length of 2.36(8) Å is similar to that seen for $[Cp(CO)_3Mo\{(CH_2)_3I\}]$ 2.40(7) Å and the Mo–C(CO), Mo–P and C–O bond distances also agree with those of the previously reported closely related compound reported in Chapter 3. The space-filling projections and stereo views of the molecule are given in Figures 4.14 – 4.15. The cyclopentadienyl ligands are *trans* to the carbonyl ligands, and *cis* to the alkyl chain.

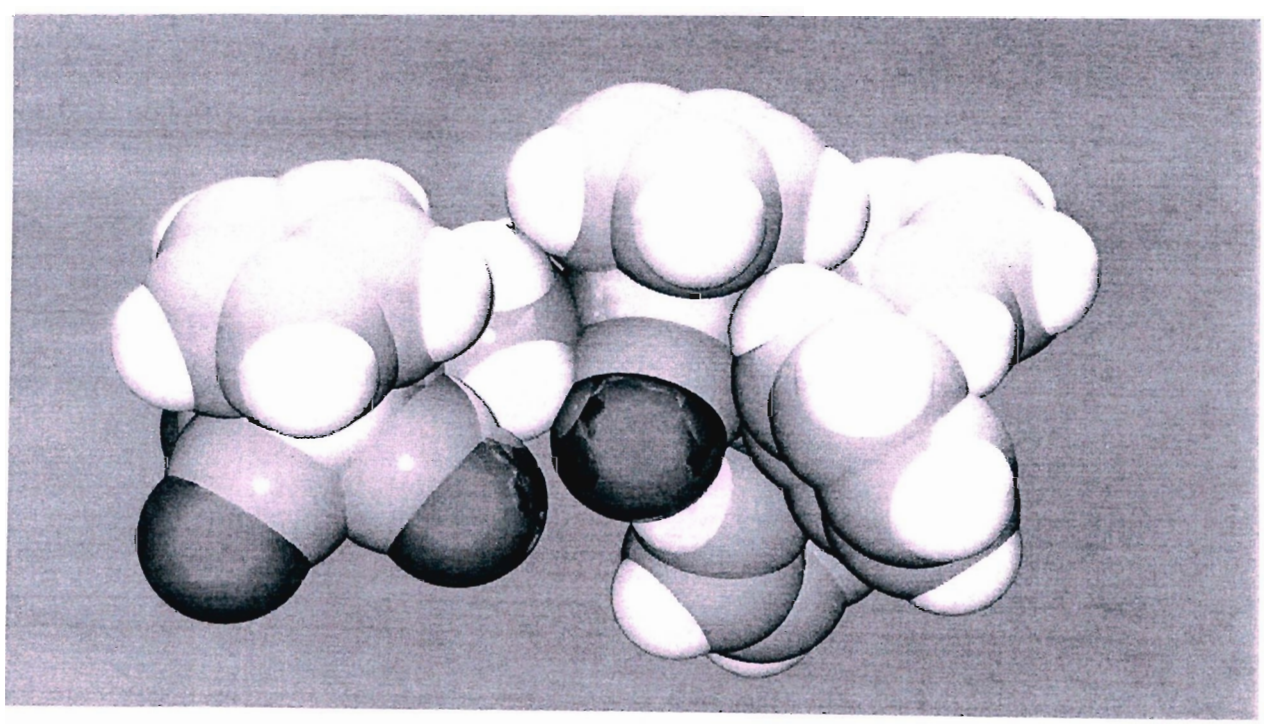

Figure 4.14: Space-filling model of $[Cp(CO)_3W(CH_2)_3Mo(CO)_2(PPh_3)Cp]$ (**3a**) showing conformations of the ligands. Colour codings; Blue colour = Tungsten. Green = Molybdenum. Red = Oxygen. Brown = Carbon. White = Hydrogen.

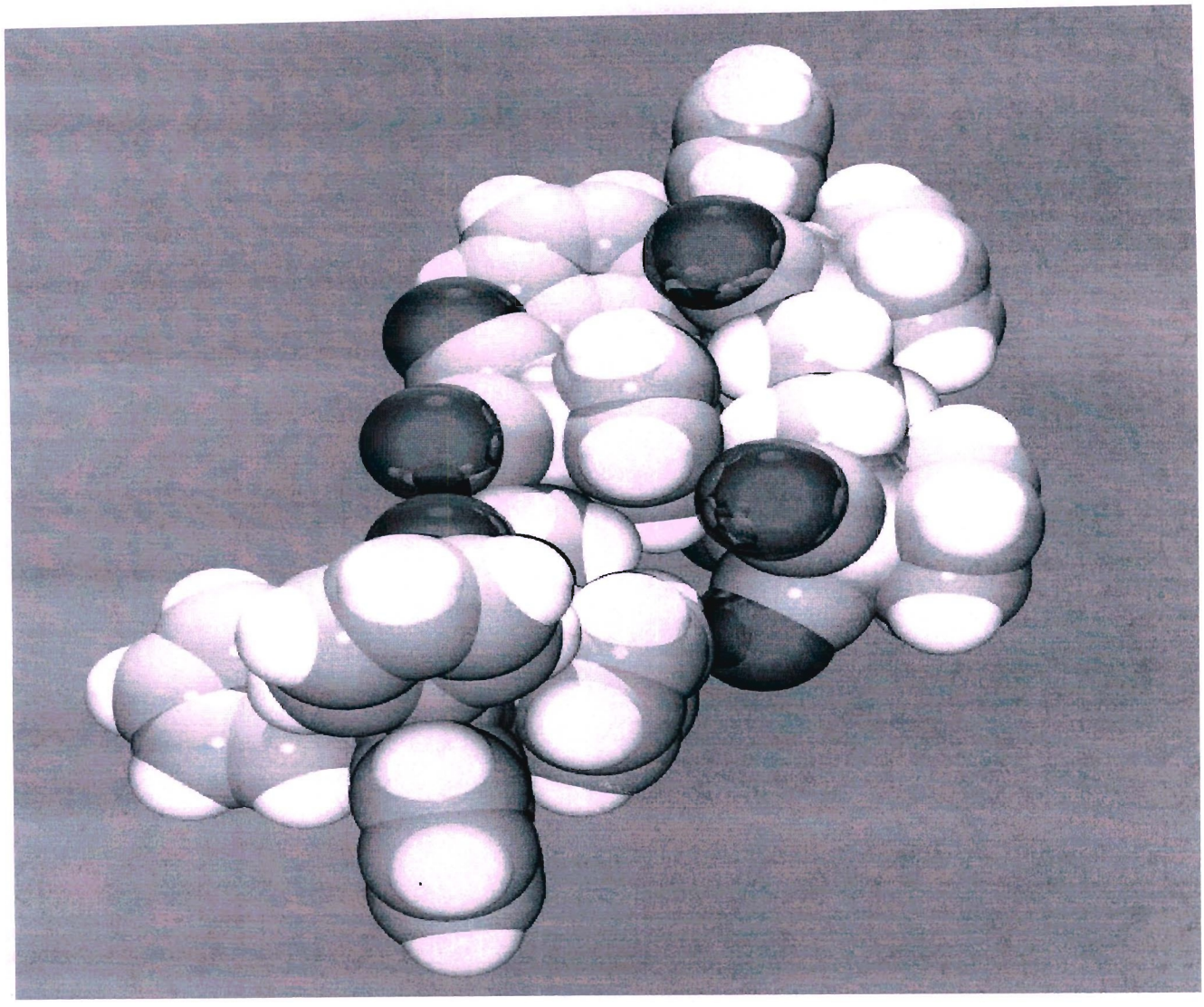

Figure 4.15: Space-filling model of the asymmetric unit of $[Cp(CO)_3W(CH_2)_3Mo(CO)_2(PPh_3)Cp]$ **3a** viewed down the crystallographic *a*-axis (100 projection). Colour codings; Blue colour = Tungsten. Green = Molybdenum. Red = Oxygen. Brown = Carbon. White = Hydrogen.

The compound, **7a**, crystallized in the monoclinic space group P 21/c. Again, the molecule showed a clear glide on the c-plane in the unit cell. The structure of the molecule is shown in Figure 4.16. Some relevant bond lengths and angles of the molecule are also listed in Table 4.5. The atomic coordinates, anisotropic temperature factors, H atom coordinates, and complete crystallographic details with standard deviations are listed in Appendix 3 and in the attached compact disc.

The molecule **7a**, contains molybdenum, bonded directly to two carbonyl group, an alkyl groups, a triphenylphosphine ligand, and a π-cyclopentadienyl ligand; and iron directly

bonded to two carbonyl groups, an alkyl and a π-cyclopentadienyl ligand respectively. As also seen from the structures of other alkanediyl complexes, compound **7a** has the two metals connected by a zigzag alkyl chain. The Cp on the Molybdenum center is, as expected, is *cis* to the alkyl chain. The Cp group on the iron centre appears equatorial to the alkyl chain, while that on the Mo centre is axial, and could thus be described as unusual. The observation suggests that this is the energetically favoured extended staggered conformation for this molecule, a phenomenon also observed for the compound $[Cp^*(CO)_2Fe(C_5H_{11})]$ [45]. The PPh_3 ligand is as expected, observed to be *trans* to the alkyl chain as necessitated by the symmetry of the compound. The structure of the molecule confirms the Cp and the CO ligands on the Molybdenum center as being on the same side to the PPh_3 ligand. This confirms the ^{13}C NMR interpretations that showed doublets for the two ligands as a result of coupling with the phosphorus atom. The Fe(1)-C(5) bond in the alkyl chain was found to be 2.08 Å. This bond length is in the general range of reported Fe-C bonds (2.05 Å - 2.08 Å) [32,34, 46- 48]. The compound follows the typical 'bump in hollow' packing, as is often observed in the packing of paraffins (Figures 4.17– 4.19) [40]. The C–C bond lengths are within the general range as observed in the similar compounds referred above (1.48 Å - 1.55 Å).

The Mo(1)–C(3) bond lengths was found to be 2.36 Å, again this is within the general range (2.26 Å - 2.38 Å) of the few reported molybdenum alkyl structures, though these compounds have different ligands bonded to the metal [34,49]. The Mo(1)–P(1) bond length (2.45 Å) was likewise found to be in the normal range (2.41 Å - 2.51 Å) [50-54].

The bond angles are also presented in Table 4.5. The parameters describing the plane of the molecule can be found in Appendix 3 and in the attached compact disc. The orientation of the cyclopentadienyl ring on the iron site appears unusual as discussed above. The projection of the similar compound, $[Cp(CO)_2Fe(CH_2)_3Fe(CO)_2Cp]$, though homobimetallic shows, in contrast to our molecule, the Van der Waals radii of the cyclopentadienyl ring near parallel to the alkyl chain [34]. The bond angles of the other species are generally in good agreement in comparison to similar angles found in other complexes [34,46,39] as listed;

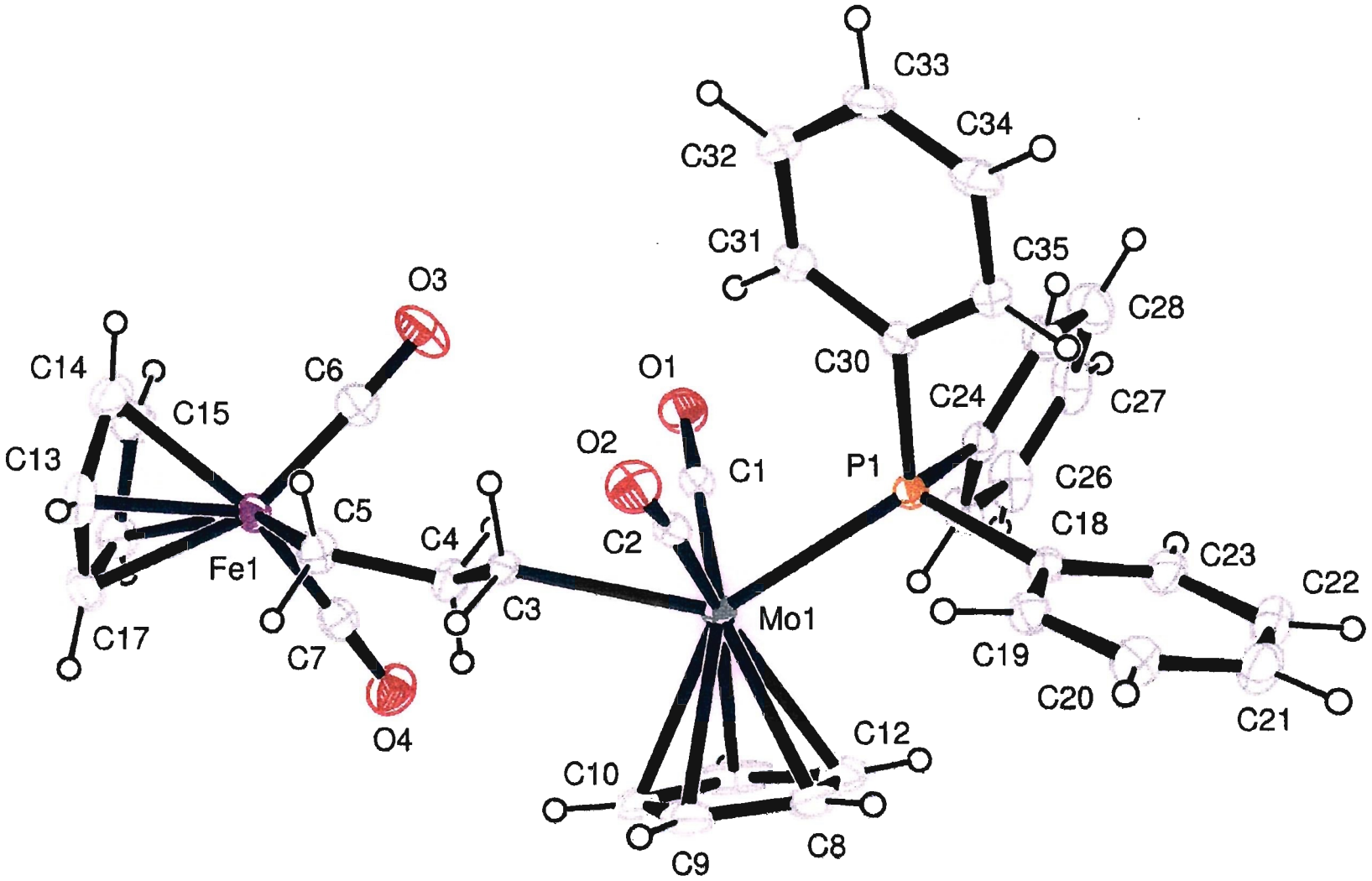

Figure 4.16: ORTEP diagrams showing the crystallographically molecule of the X-ray structure of $[Cp(CO)_2Fe(CH_2)_3Mo(CO)_2(PPh_3)Cp]$, **7a**; selected atom labels are indicated. Thermal ellipsoids are contoured at the 50% probability level; H atoms have an arbitrary radius of 0.1 Å

(i) In the carbonyl groups; O(3) ..C(6)..Fe(1) 176.0 (3) (179), O(4) ..C(7)..Fe(1) 178.1 (3) (180); O(1) ..C(1)..Mo(1) 178.0 (2) (177), O(2) ..C(2)..Mo(1) 174.2 (2) (175).

(ii) Around the iron atom; C(6)..Fe(1)..C(5) 84.65 (13) (87), C(7)..Fe(1)..C(6) 97.04 (13) (93), C(7)..Fe(1)..C(5) 89.02 (13) (87).

(iii) Around the Molybdenum atom; C(4)..Mo(1)..P 82.67 (8) (93), C(5)..Mo(1)..P 77.24(8) (84), C(1)..Mo(1)..P 135.85 (7) (138).

(iv) In the alkyl group; C(3)..C(4)..C(5) 112.8(2) (113), C(3)..C(4)..Fe(1) 117.0(2) (115), C(4)..C(3)..Mo(1) 118.70(18) (115)

The bond angles around the molybdenum atom and the alkyl group, appear anomalous though are scarcely different from that in other similar molecules.

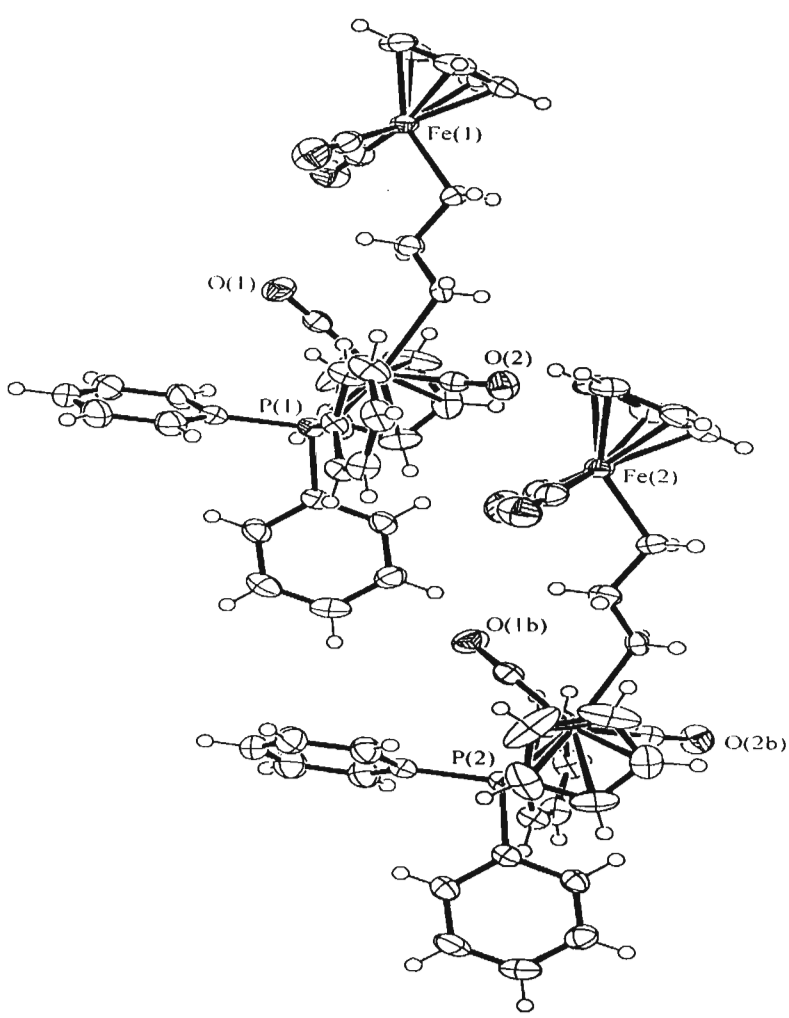

Figure 4.17: Asymmetric unit of $[Cp(CO)_2Fe(CH_2)_3Mo(CO)_2(PPh_3)Cp]$ **7a**, viewed down the crystallographic *a*-axis (100 projection).

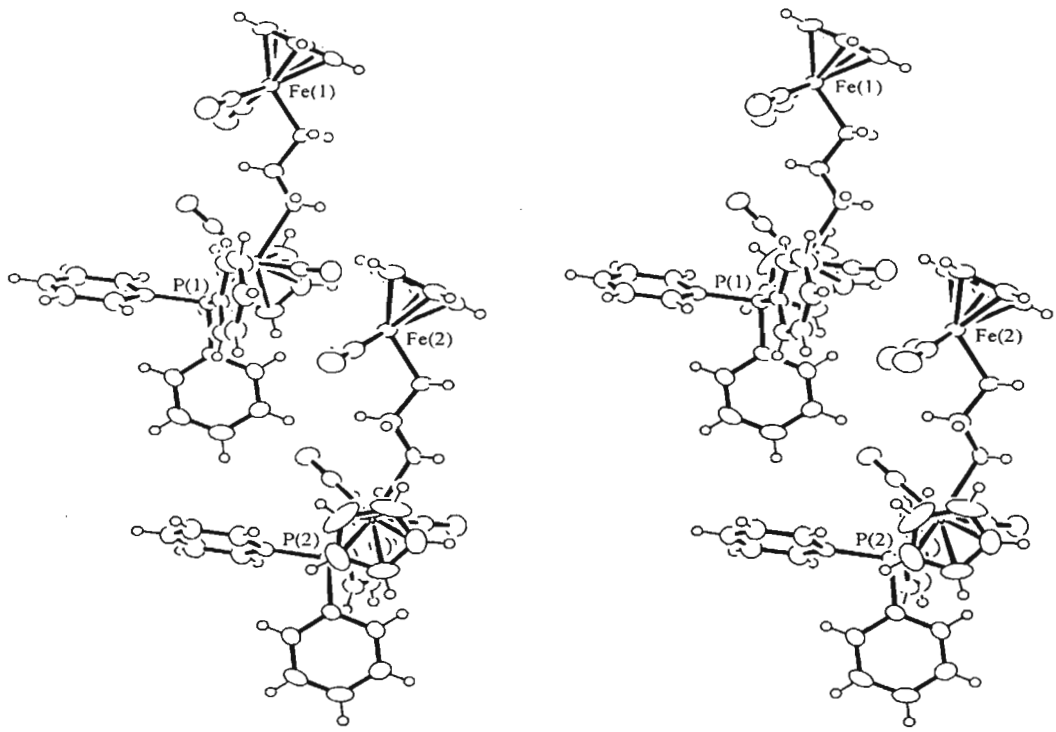

Figure 4.18: Stereo view (cross-eye) of asymmetric unit of $[Cp(CO)_2Fe(CH_2)_3Mo(CO)_2(PPh_3)Cp]$ **7a**,. Ellipsoids are contoured at the 50% probability level.

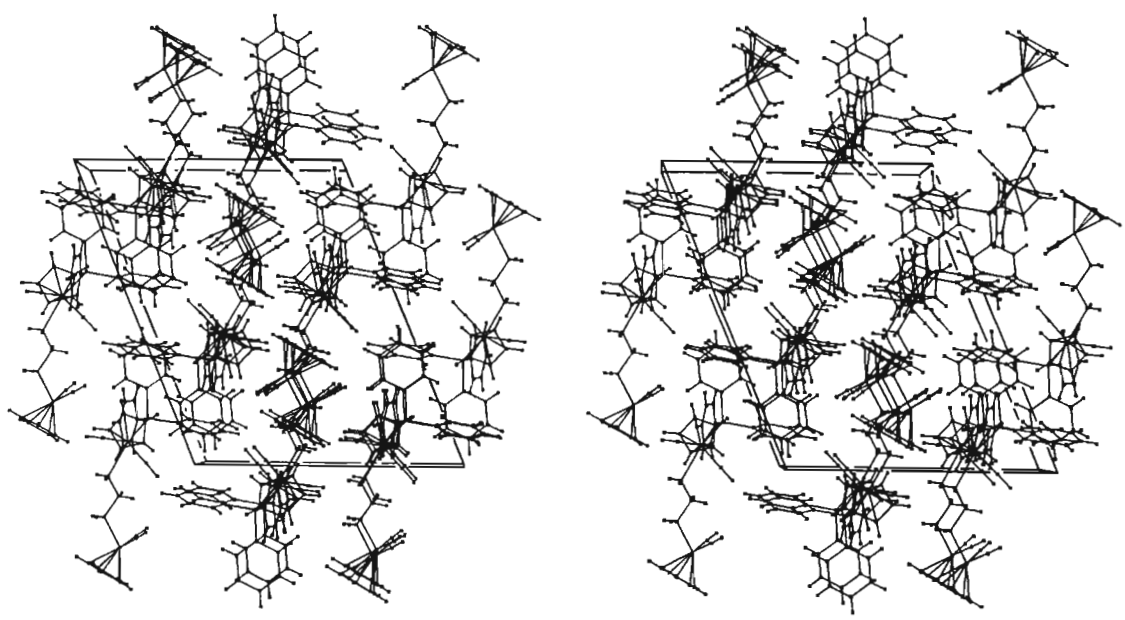

Figure 4.19: Stereo view (cross-eye) of the unit cell contents of $[Cp(CO)_2Fe(CH_2)_3Mo(CO)_2(PPh_3)Cp]$ **7a**, viewed down the crystallographic a-axis (100 projections)

Table 4.5: Selected bond lengths [Å] and Bond angles (°) of $[Cp(CO)_2Fe(CH_2)_3Mo(CO)_2(PPh_3)Cp]$, **7a**

Bond lengths [Å]		Bond angles [°]	
Mo(1)-C(2)	1.949(3)	C(2)-Mo(1)-C(1)	101.80(10)
Mo(1)-C(1)	1.954(3)	C(2)-Mo(1)-C(3)	73.64(9)
Mo(1)-C(3)	2.374(2)	C(1)-Mo(1)-C(3)	71.93(9)
Mo(1)-P(1)	2.455(10)	C(2)-Mo(1)-P(1)	82.68(8)
Fe(1)-C(7)	1.745(3)	C(1)-Mo(1)-P(1)	77.34(7)
Fe(1)-C(6)	1.748(3)	C(3)-Mo(1)-P(1)	135.83(6)
Fe(1)-C(5)	2.076(2)	C(7)-Fe(1)-C(6)	97.01(13)
O(1)-C(1)	1.154(3)	C(7)-Fe(1)-C(5)	89.27(11)
O(2)-C(2)	1.154(3)	C(6)-Fe(1)-C(5)	84.72(11)
O(3)-C(6)	1.145(3)	O(1)-C(1)-Mo(1)	178.1(2)
O(4)-C(7)	1.146(3)	O(2)-C(2)-Mo(1)	174.1(2)
C(3)-C(4)	1.488(3)	C(4)-C(3)-Mo(1)	118.20(5)
C(4)-C(5)	1.522(4)	C(3)-C(4)-C(5)	112.4(2)
C(10)-C(11)	1.403(5)	C(4)-C(5)-Fe(1)	116.93(17)
C(11)-C(11)	1.403(5)	O(3)-C(6)-Fe(1)	175.7(2)
C(10)-C(12)	1.386(5)	O(4)-C(7)-Fe(1)	178.4(2)
C(13)-C(14)	1.388(4)	C(12)-C(8)-C(9)	109.2(3)
C(14)-C(15)	1.420(4)	C(12)-C(8)-Mo(1)	73.22(16)
C(15)-C(16)	1.398(4)	C(9)-C(8)-Mo(1)	73.23(16)
C(16)-C(17)	1.491(4)	C(8)-C(9)-C(10)	108.4(3)
C(18)-C(23)	1.380(3)	C(8)-C(9)-Mo(1)	73.08(17)
C(18)-C(19)	1.393(3)	C(10)-C(9)-Mo(1)	73.08(17)
C(19)-C(20)	1.369(4)	C(9)-C(10)-C(11)	107.7(3)
C(20)-C(21)	1.378(4)	C(9)-C(10)-Mo(1)	72.82(16)
C(22)-C(23)	1.385(4)	C(11)-C(10)-Mo(1)	72.97(17)
C(24)-C(25)	1.381(4)	C(12)-C(11)-C(10)	106.5(3)
C(25)-C(26)	1.383(4)	C(12)-C(11)-Mo(1)	72.15(17)

4.4 Analysis of the Compounds $[Cp(CO)_3W(CH_2)_3Mo(CO)_3Cp^*]$ 2a, $[Cp(CO)_3W(CH_2)_4Mo(CO)_2(PPhMe_2)Cp]$ 5b and $[Cp(CO)_2Fe(CH_2)_3Mo(CO)_2(PMe_3)Cp]$ 10a by Liquid Chromatography Time - of - Flight Mass Spectrometry

The above samples were submitted to an American company for a demonstration of the suitability of LC-TOF-MS (Liquid Chromatography-Time-of-Flight Mass Spectrometer) for examining organometallic complexes of our type. These samples were analysed by direct infusion liquid chromatography coupled with the LECO Jaguar® (TOF-MS). Information available from the literature and the company databases indicate that the usefulness of liquid chromatography – mass spectrometry, using an electrospray interface and time-of-flight mass spectrometric detection, in analysing organometallic complexes had been successfully illustrated previously for ruthenium dendrimer [55], and Co(III) porphyrin complexes, with a conclusion that the technique has a capability of providing useful additional information in structural studies on organometallic molecules of our type. Other areas of research which have found use in this high precision instrument include: identification of new drugs, support of combinatorial chemistry activities, determination of metabolites and their breakdown products or pharmaceuticals, increase in product quality control, food analysis, pesticide analysis in foods, new product development and competitive product analysis.

Many elements exist in nature as a combination of a number of different isotopes. When analysed by mass spectrometry these elements, or compounds containing these elements, will show all the naturally occurring isotopes in the mass spectrum. While this results in more complex mass spectra, it also provides much additional information as to the elements present in a particular ion cluster, particularly as the theoretical appearance of these clusters can be calculated extremely accurately using the naturally occurring isotope abundances. Examples of such isotope patterns for the metallic elements Fe, Mo, W and combinations of FeMo and MoW present in samples **2a**, **5b** and **10a** are shown in Appendix 4. The remaining elements in these compounds (C, H, O and P) are either monoisotopic, or their isotope abundances are such that one isotope forms > 98.8% of the contribution. These simulations were generated by using the computer software called: (NIST) "Isoform". This programme was created by the American National Institute of Standards and Technology (NIST). Thus any ion cluster seen in a spectrum will

essentially have the pattern of the metal, or combination of metals contained in the ion. This is an extremely useful application in assigning elemental formulae to ion clusters as discussed below.

Positive ion mass spectra were acquired for the sample **2a** under the experimental conditions described in Chapter 5, Section **5.5**. The resultant mass spectrum is shown in Figure 4.20. The large ions present at m/z 922 and 622 arise from the solution used to calibrate the instrument for accurate mass measurements, and are not part of the spectrum of **2a**.

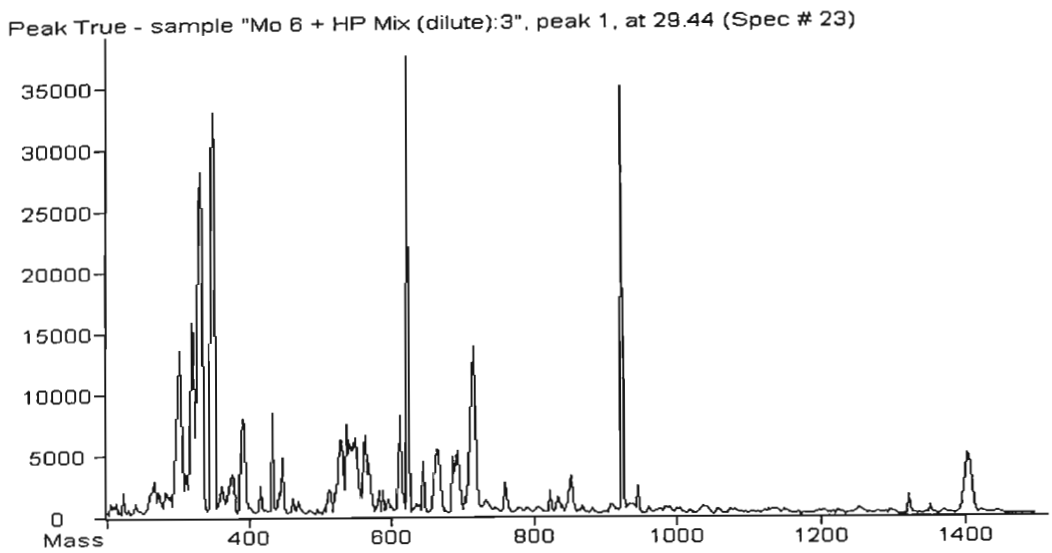

Figure 4.20: Electrospray Ionisation mass spectrum of **2a**.

The molecular formula for compound **2a** is $C_{24}H_{26}MoO_6W$. The predicted isotope distribution pattern and accurate mass for this formula is as shown in Appendix 4. The ion cluster shown in the spectrum centred around 1403 amu is dimeric in nature and may be attributed to the ion $[2M+Na]^+$. The mass spectra of compounds generated by electrospray ionisation (esi) very seldom show molecular ions $[M]^+$ at the value predicted by the molecular formula. Instead, under esi conditions, a "pseudo-molecular ion" is generated. Most commonly this takes the form $[M+ H]^+$, but $[M + Na]^+$ and $[M + K]^+$ are also often seen. The dimeric ion shows the addition of sodium. The isotope pattern obtained (Figure 4.21) is in good agreement with the pattern predicted from the molecular formula (Appendix 4), and the measured mass (1407.0387) compares well with the calculated value (1407.0484) (difference 6.9 ppm), confirming the assigned molecular formula.

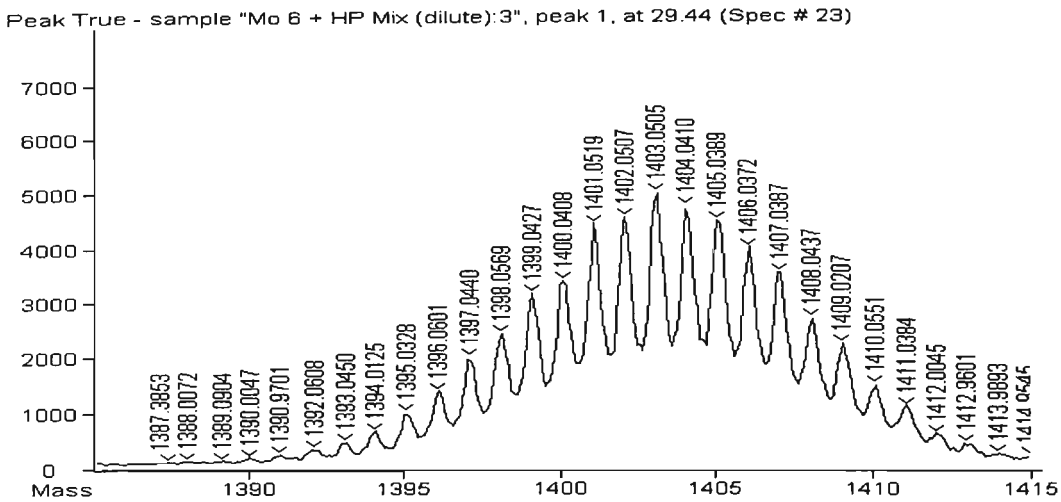

Figure 4.21: Measured dimeric isotope abundance pattern.

The mass range measured between 650 and 730 amu is shown below in Figure 4.22. Three distinct ion clusters are visible. The cluster at highest mass corresponds to the ion arising from $[M + Na]^+$, both the isotope abundance pattern and the accurate mass (measured 715.0150, calculated 715.0191, difference 5.7 ppm) confirming the structure of the compound.

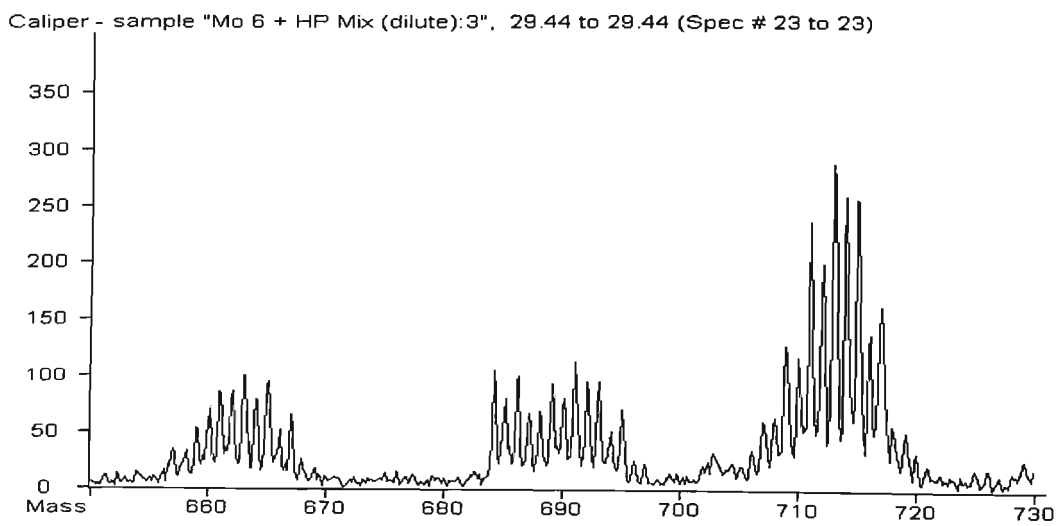

Figure 4.22: Expanded mass spectrum for **2a**.

The cluster centred around m/z 691 arises from the ion $[M + H]^+$, although the predicted abundance pattern is disturbed by interference at the low mass side of the cluster. Finally the cluster at the low mass end appears to arise from [M – CO + H]. The isotope ratio pattern showed that the ion cluster around 347 amu contains only tungsten, as does that around 388 amu.

The sample **5b** was also analysed for its positive ion mass spectra under the same conditions as used for compound **2a** above. The obtained spectrum is shown in Figure 4.23. Again the ions present at m/z 622 and 322 arise from the solution used to calibrate the instrument for accurate mass measurements, and are not part of the spectrum of **5b**. The predicted isotope distribution pattern and accurate mass for this formula are shown in Appendix 4. The mass range measured between 770 and 810 amu is shown in Figure 4.24. The isotope ratio pattern is in good agreement with the pattern predicted from the molecular formula in Appendix 4, but the cluster occurs at 42 mass units higher than expected. It appears that the "pseudo molecular ion" incorporates a molecule of the acetonitrile being used as solvent, and the formula for this ion is then $[M + CH_3CN + H]^+$. Both the isotope abundance pattern and the accurate mass (measured 788.0599, calculated 788.0660, difference 7.7 ppm) provide confirmation of the structure assigned. As mentioned above, addition of solvent molecules to compounds during the esi process is sometimes evident.

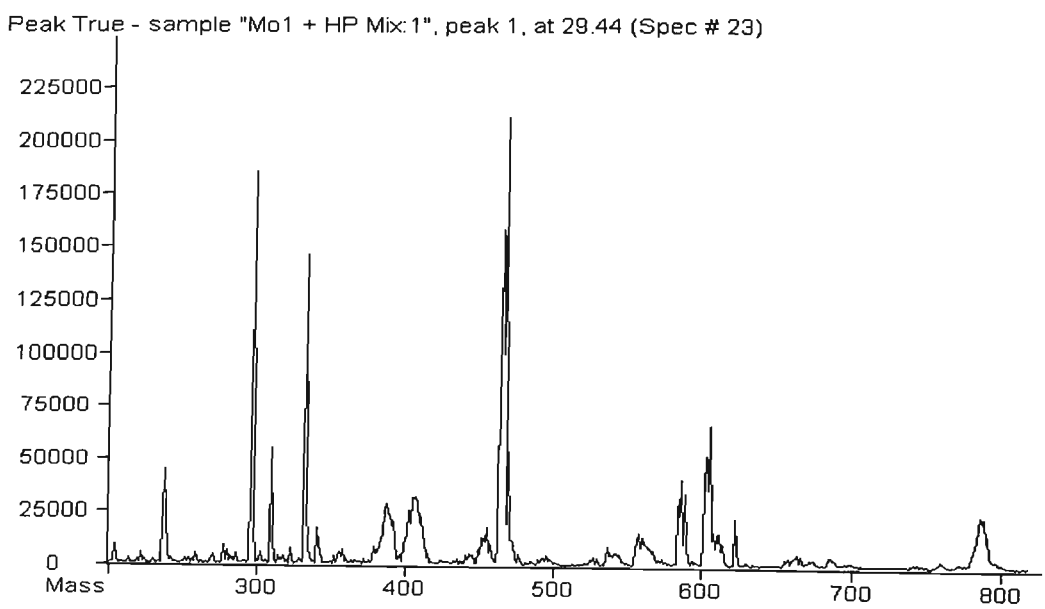

Figure 4.23: Electrospray Ionisation mass spectrum of **5b**

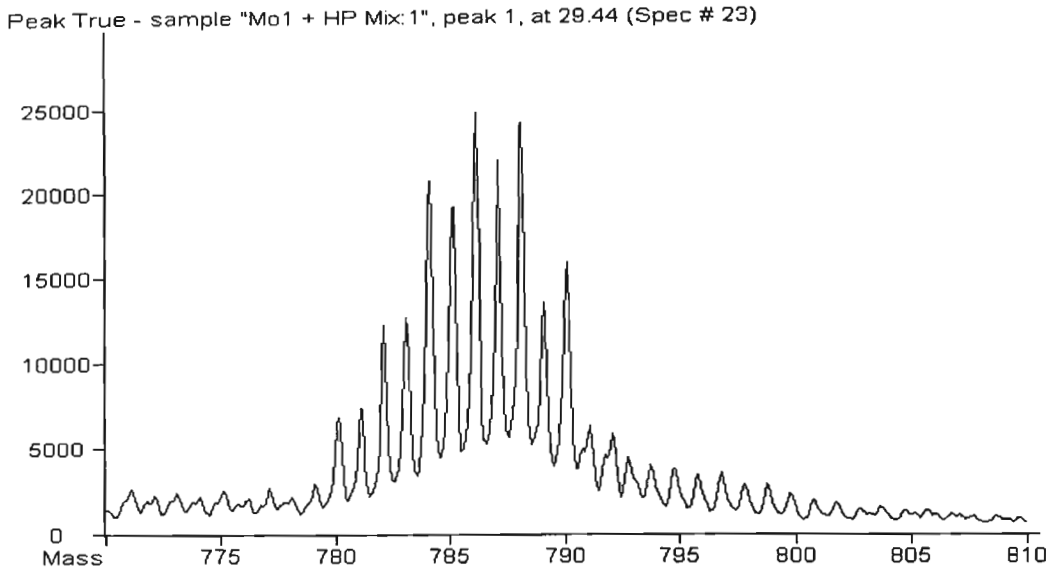

Figure 4.24: Expanded mass spectrum for **5b**.

From the developed isotope distribution pattern shown in Appendix 7, and the observed spectra (Figures 4.23 – 4.24), it can be concluded that the ion cluster around 586 amu contains tungsten, but no molybdenum.

For compound **10a**, the mass spectrum obtained is shown in Figure 4.25, and the ion present at m/z 322 arises from the solution used to calibrate the instrument for accurate mass measurements, and is therefore not part of the spectrum of **10a**.

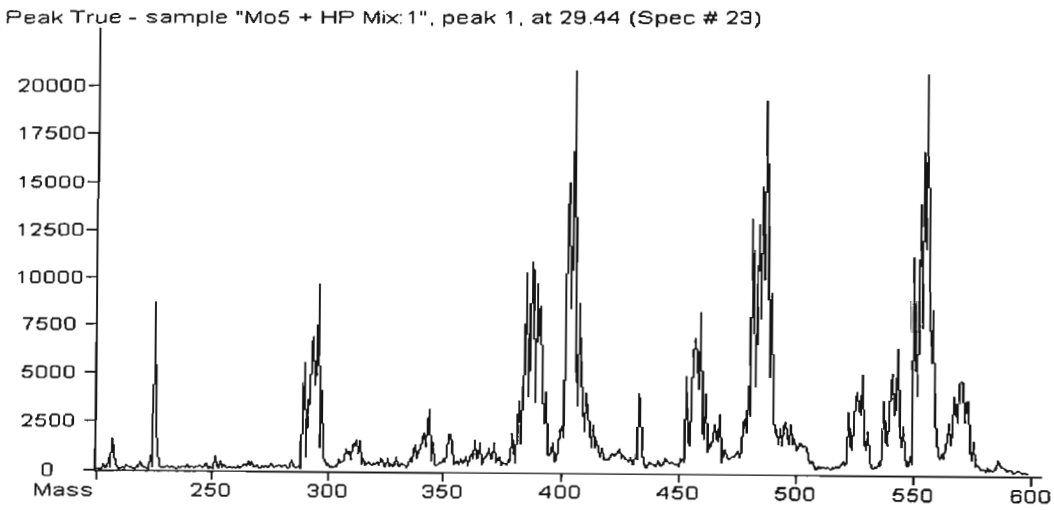

Figure 4.25: Electrospray Ionisation mass spectrum of **10a**.

The predicted isotope distribution pattern and accurate mass for this formula is shown in Appendix 4. The mass range measured between 510 and 580 amu is shown below in

Figure 4.26. The isotope ratio pattern of the most intense cluster around m/z 556 is in good agreement with the pattern predicted from the proposed molecular formula in Appendix 4, but also, as in the case of **5b** above, the cluster occurs at 42 mass units higher than expected. Again it appears possible that the "pseudo molecular ion" has incorporated a molecule of the acetonitrile being used as solvent, and the formula for this ion is then $[M + CH_3CN + H]^+$. However, there are two clusters at lower mass (m/z 543 and 528), having the same isotope ratio pattern, the origin of which is uncertain, although 528 may arise from $556 - 2(CH_2)$. Finally there is a cluster around 570 amu which has a totally different isotope ratio pattern, appearing closer to Mo_2 rather than MoFe.

An exhaustive study of the compounds **2a**, **5b** and **10a** were not carried out, because other characterization methods used earlier proved that the synthesis of the intended heterobimetallic compounds was a success.

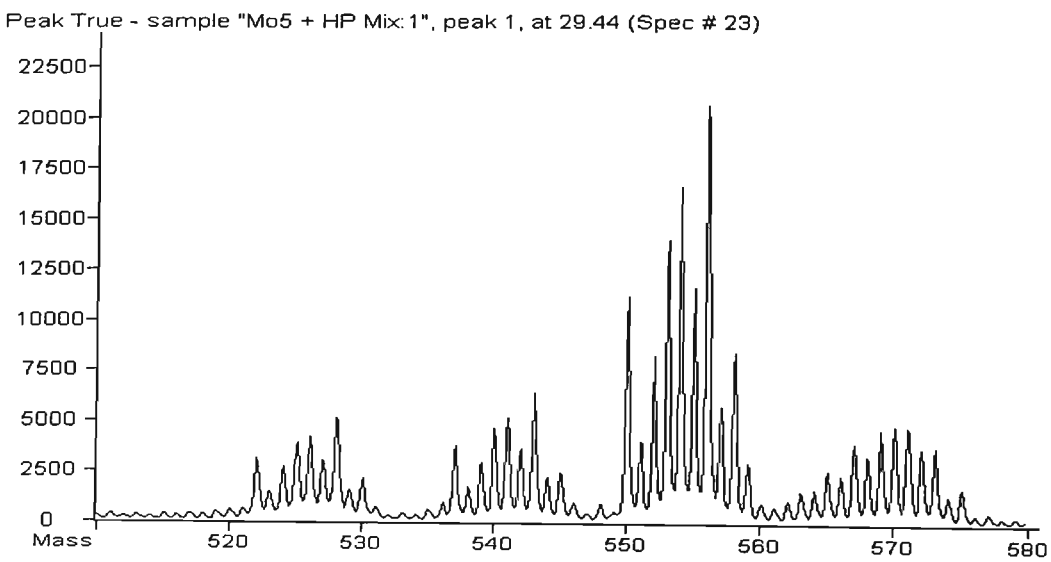

Figure 4.26: Expanded mass spectrum for **10a.**

4.5 Reactions Studies on Some of the Heterobimetallic Alkanediyl Complexes

Heterobimetallic compounds are proposed to posses' catalytic superiority, selectivity, and efficiency to their monometallic components [17,56]. The compounds should then make good catalysts, catalyst precursors or models for catalytic intermediates [57-61]. It is believed that their close study may lead to the ultimate understanding of well known processes such as Fischer-Tropsch, olefin polymerization, catalytic oxidation,

hydrogenation and hydroformylation reactions, as well as CO and CO_2 activation. The information on the nature of the chemical activities of these heterodinuclear metal functionalised paraffins is therefore of prime interest. Specifically we may be able to gain some information on how the adjacent metals present in a compound interact with substrate molecules during catalysis, and how the individual heterometals within a compound behave during a reaction or what influence one metal has on the other when both are present within the same molecule [1]. It is hoped that the findings obtained will help to relate the chemistry of mononuclear compounds to dinuclear compounds to metal clusters and to metal surfaces.

Few heterobimetallic alkanediyl complexes are known and therefore few reactivity studies have been carried out on them. It has been shown that due to the relief in steric crowding, the insertion of CO into $[CpRu(CO)_2CH_2Ru(CO)_2Cp]$ at room temperature is much more rapid than in the mononuclear complex $CpRu(CO)_2R$. In the same manner, the acylmolybdenum intermediates have been known to form more readily than their tungsten analogues on reaction with CO [62]. We now report on some of the reaction studies carried out on the synthesized compounds and discuss the results. In general, all the reaction studies reported here were monitored by either using infrared or NMR spectroscopy.

4.5.1 Reaction with a Neutral Molecule –Triphenylphosphine

Insertion reactions involve a ligand, usually unsaturated, undergoing formal insertion into another metal-ligand bond on the same complex as shown in Scheme 4.2.

U = CO, C_2H_4, C_2R_2, NO, CR_2, CNR, RCN, O_2, CO_2

X = H, alkyl, aryl, OR, NR_2

Scheme 4.2: A general scheme for an insertion reaction

A study has been carried out to ascertain the mechanism for this reaction, and the result showed that the alkyl group moves most of the time, thus the reference: migratory insertion reaction. For a generic insertion of CO into a metal alkyl bond, two mechanistic extremes are seen, one in which the alkyl group migrates to the carbonyl group and a second in which the carbonyl moves and inserts into the metal-alkyl bond. Either way, this generates an open coordination site denoted by the small box in Scheme 4.3 [63]. The incoming substituent can then occupy the available open coordination site.

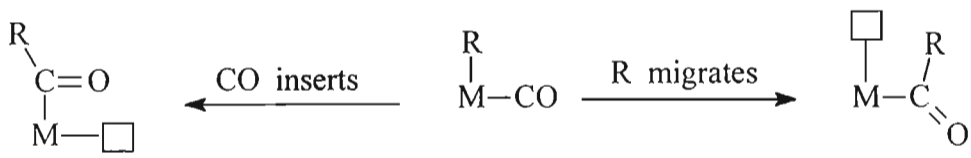

Scheme 4.3: A mechanism for insertion Insertion [63]

It is, however, known that not all the insertion reactions take place via this mechanism only. Flood has reported that sometimes solvents determine whether it is an alkyl or a CO group that migrates in such reactions [64]. An investigation of this fact used an optically active resolved transition metal complex to determine which group moved. The mechanism differs depending on the solvent used for the reaction as shown in Scheme 4.4. Solvents have been shown to directly attack the metal center, thereby inducing an insertion reaction [65,66]. The bulkiness of the migratory group also plays some role during this type of reaction. The lighter alkyl groups, as expected, move faster than the heavier groups during the process of migration [67].

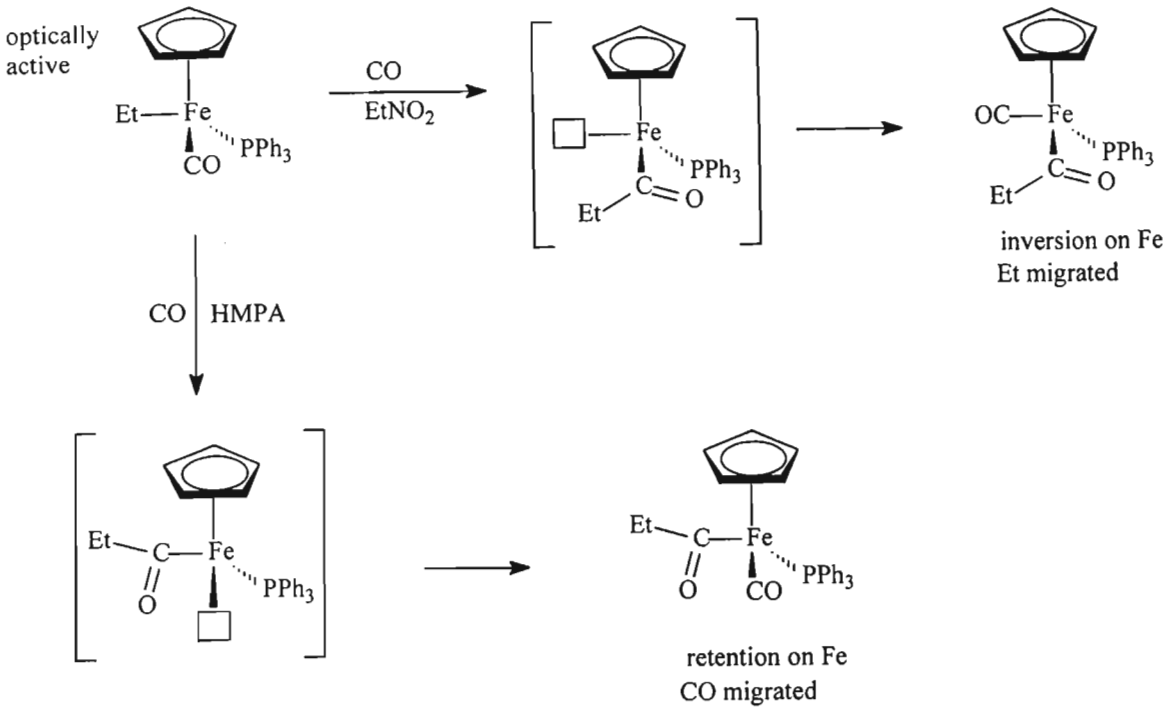

Scheme 4.4: The mechanism showing the solvent effect on insertion type of reaction [64].

The compound, $[Cp(CO)_3W(CH_2)_3Mo(CO)_3Cp]$ (**1a**) reacts with triphenylphosphine (PPh_3) via an alkyl migration at the molybdenum site, forming an orange compound, $[Cp(CO)_3W(CH_2)_3C(O)Mo(CO)_2(PPh_3)Cp]$ (**12**) as shown in Equation 7.

$$[Cp(CO)_3W(CH_2)_3Mo(CO)_3Cp] + PPh_3 \longrightarrow [Cp(CO)_3W(CH_2)_3C(O)Mo(CO)_2(PPh_3)Cp] \quad (7)$$

Monitoring this reaction by infrared spectroscopy showed the growth of an acyl peak at 1725 cm^{-1} and the concurrent disappearance of the band at 1963 cm^{-1}. A sharp triplet observed at 3.05 ppm in the ^1H NMR spectrum could be assigned to CH_2 next to an acyl group. Also, the CpMo peak moved upfield from 5.27 ppm to 4.97 ppm, a significant indication of a decrease in electron density around the molybdenum metal. This was further supported by the ^{13}C NMR spectrum where the CpMo peak moved downfield from 92.61 ppm to 96.49 ppm. The chemical shift of the WCH_2 peak changed from –5.14 pm to -9.92 ppm, and the $MoC(O)CH_2$ peak from 7.59 ppm to 71.11 ppm, while the $MoCH_2CH_2$ peak moved from 44.28 ppm to 33.15 ppm. The ^{13}C NMR chemical shift for the acyl group was observed downfield at 267 ppm. Similar compounds had acyl peaks around 261

ppm [34]. This formation of an acyl compound seems to create or enhance intermetallic interaction as shown by the observed changes in the chemical shifts [1].

Compound **1a**, when reacted with two equivalents of PPh_3 in the same solvent, did not yield any different products.

The compound $[Cp(CO)_3W(CH_2)_3Mo(CO)_3Cp]$ and PPh_3 were refluxed in tetrahydrofuran. An acyl band was observed in the IR spectrum after two days at 1710 cm^{-1}. No further changes were observed over 5 days. The ^1H and ^{13}C NMR spectra showed the presence of PPh_3 but not that of the acyl group, implying that a decarbonylation reaction occurred giving the compound $[Cp(CO)_3W(CH_2)_3Mo(CO)_2(PPh_3)]$.

The complex, $[Cp(CO)_3W(CH_2)_3Mo(CO)_3Cp^*]$ **2a** was refluxed with PPh_3 in THF. The compound underwent a migratory insertion reaction to yield an unstable complex, $[Cp(CO)_3W(CH_2)_3C(O)Mo(CO)_2(PPh_3)Cp^*]$ **14**, as shown in Equation 8.

$$[Cp(CO)_3W(CH_2)_3Mo(CO)_3Cp^*] + PPh_3 \longrightarrow [Cp(CO)_3W(CH_2)_3C(O)Mo(CO)_2(PPh_3)Cp^*] \quad (8)$$

A strong acyl band was observed at 1704 cm^{-1} in the IR spectrum. The compound showed a triplet downfield at 5.12 ppm due to $CH_2C(O)$ in the ^1H NMR spectrum. This is an expected observation because the Cp* enriches the molybdenum centre with electrons that are drawn by the electronegative oxygen of the acyl group thereby pushing the signal due to protons adjacent to the acyl, further downfield. The ^{13}C NMR spectrum only showed decomposition (because the compound was unstable) and as a result no useful information could be obtained from it.

The complex, $[Cp(CO)_3W(CH_2)_3Mo(CO)_3Cp^*]$ **2a** reacts with an equimolar quantity of PPh_3 in acetonitrile to give the acyl compound $Cp(CO)_3W(CH_2)_3C(O)Mo(CO)_2(PPh_3)Cp^*]$ **14**, in a similar manner as shown in Equation 8 above. Again a strong acyl band was observed at 1704 cm^{-1} in the IR spectrum and a triplet at 2.13 ppm due to $CH_2C(O)$ in the ^1H NMR spectrum. A repeat of this reaction using excess PPh_3 in acetonitrile also gave compound **14**, according to spectroscopic data.

The compound $[Cp(CO)_3W(CH_2)_3Mo(CO)_2(PMe_3)Cp]$, also reacts with an equimolar quantity or excess PPh_3 resulting in the formation of the acyl compound shown in Equation 9.

$$[Cp(CO)_3W(CH_2)_3Mo(CO)_2(PMe_3)Cp] + PPh_3 \longrightarrow [Cp(CO)_3W(CH_2)_3C(O)Mo(CO)(PPh_3)(PMe_3)Cp] \quad (9)$$

An acyl peak in the infrared spectrum at 1603 cm^{-1} and a triplet observed at *ca.* 2.9 ppm in the ^1H NMR spectrum due to $CH_2C(O)$ confirmed the insertion reaction taking place. Peaks due to both of the phosphine substituents were present in the NMR spectra. The chemical shift of the carbon α to molybdenum was shifted downfield, from 10.47 ppm (in the starting material) to 31.85 ppm (in the product) in the ^{13}C NMR spectrum, confirming the site of attack. Molybdenum being more reactive than tungsten, metalloselectively reacted with the bulky PPh_3, despite the already present highly basic trimethylphosphine substituent that should increase its electron density thereby lowering the reactivity. Trimethylphosphine also has a larger Tolman cone angle (118°) than the CO ligand (95°), but still provides little, if any, steric hindrance to further substitutions taking place on the molybdenum site. The wider the angle of the cone, the greater the steric influence of the ligand. A cone angle of 180° would indicate that the ligand effectively shields (or covers) one half of the coordination sphere of the metal complex.

An attempt to grow crystals of the compound $[Cp(CO)_3W(CH_2)_3C(O)Mo(CO)(PPh_3)(PMe_3)Cp]$ from slow diffusion of hexane in dichloromethane solution in the fridge gave yellow crystals after 5 days. An X-ray diffraction study on one of these crystals showed them to be an unexpected carboxylic acid derivative, as shown in Figure 4.27 below. The X-ray diffraction data was collected at room temperature (22 °C) anisotropically. The compound may degenerate into the carboxylic acid derivative by a OH group replacing the $Mo(CO)(PMe_3)(PPh_3)Cp$ moiety. We can propose two theories on how this reaction may occur. Firstly the method used for the X-ray data collection, which was thermally anisotropically at room temperature, might have been responsibility for this result [68]. If this is true, the fate of the displaced moiety ($Mo(CO)(PMe_3)(PPh_3)Cp$) is not clear. The second possibility, which we think is most

likely, is as follows. It is probable that the moisture and the activation thereof of the molybdenum in the vicinity of the acyl cause the conversion. The hydroxyl nucleophile, from water condensate most likely attacked the acyl carbonyl to give the carboxylic acid derivative product [69].

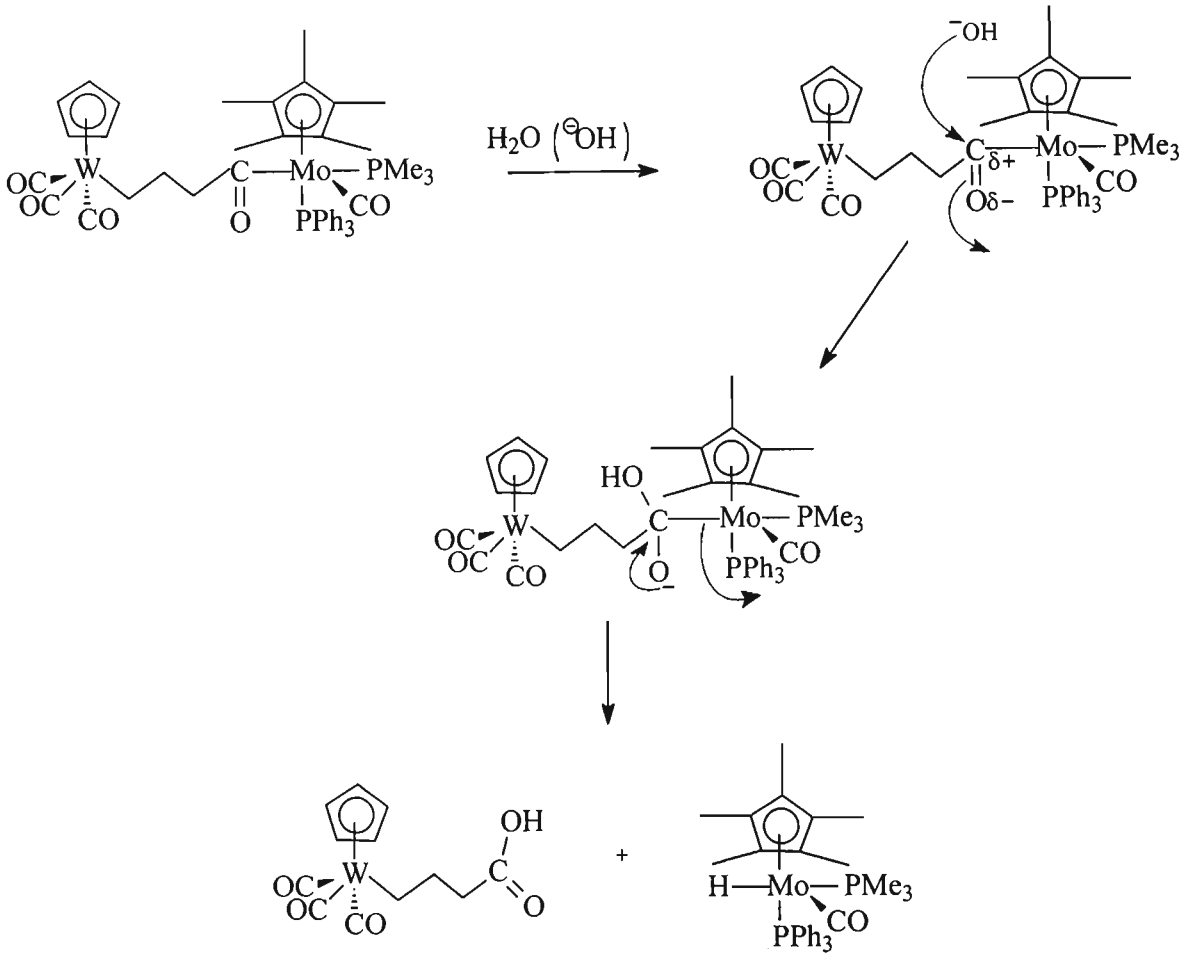

Scheme 4.5: Possible pathway to the compound $[Cp(CO)_3W\{(CH_2)_3COOH\}]$

The molecular stereochemistry and labeling of atoms of the compound $[Cp(CO)_3W\{(CH_2)_3COOH\}]$ is shown in Figure 4.27, with the crystal packing in Figure 4.28. Bond distances and angles around the metal centre are shown in Table 4.6. Listings of atomic coordinates, anisotropic temperature factors, H atom coordinates and complete crystallographic details are given in Appendix 5 and in the attached compact disc. The most striking feature of the molecule is the attached carboxylic acid at one end of an alkyl chain and tungsten metal at the other. The crystal is made up of a Cp ring, three CO groups and an alkyl chain with a terminal acid, all attached to the tungsten metal at the centre.

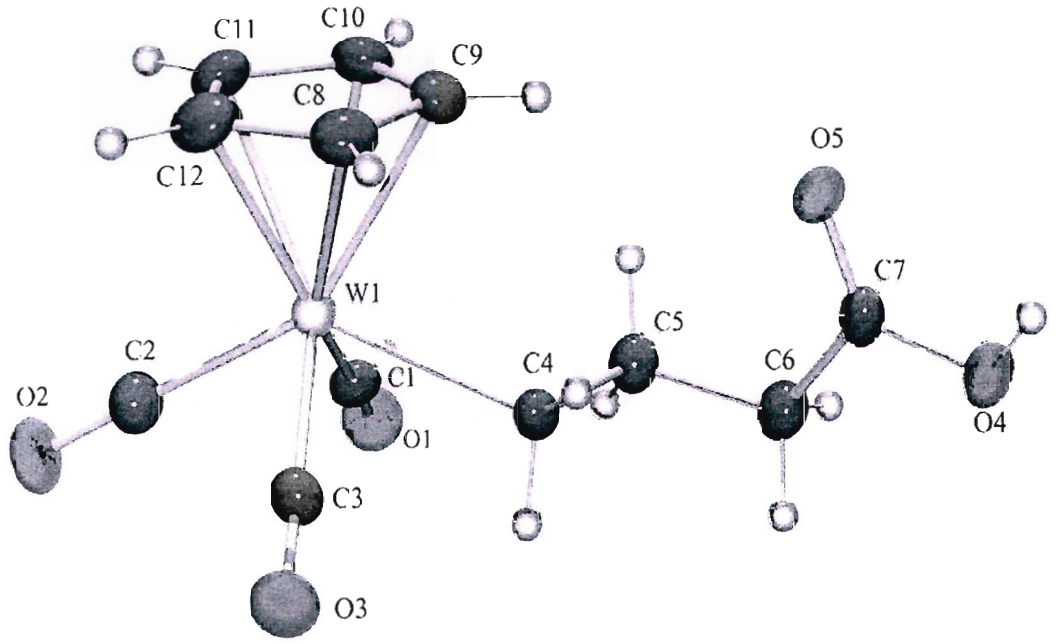

Figure 4.27: ORTEP diagram of the X-ray structure of $[Cp(CO)_3W\{(CH_2)_3COOH\}]$; selected atom labels are shown. Thermal ellipsoids are contoured at the 35% probability level; H atoms have an arbitrary radius of 0.1 Å.

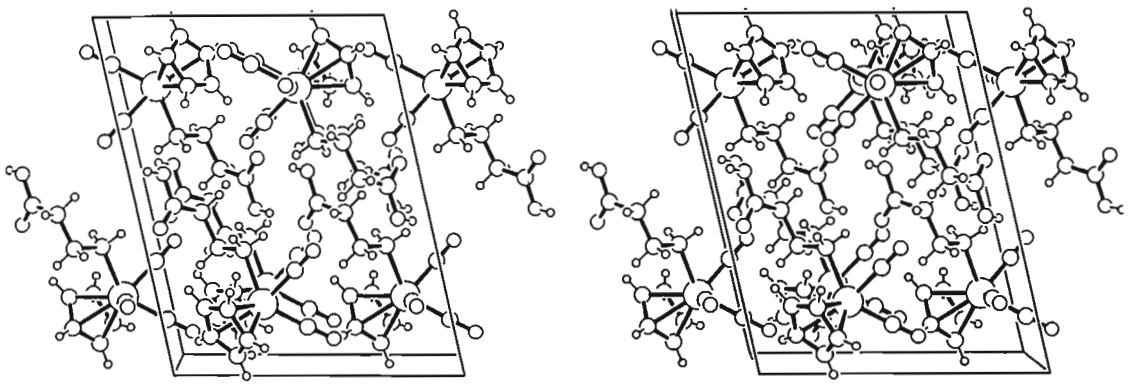

Figure 4.28: ORTEP diagram showing the unit cell packing of $[Cp(CO)_3W\{(CH_2)_3COOH\}]$ viewed down the crystallographic *a*-axis. Thermal ellipsoids are contoured at the 35% probability level; H atoms have been omitted for clarity

Table 4.6: Bond lengths [Å] and angles [°] for $[Cp(CO)_3W\{(CH_2)_3COOH\}]$.

C(1)–O(1)	1.148(8)	C(9)–C(10)–W(1)	73.3(4)
C(1)–W(1)	1.976(7)	C(10)–C(11)–W(1)	74.2(4)
C(2)–O(2)	1.144(9)	C(12)–C(11)–W(1)	72.2(4)
C(2)–W(1)	1.986(8)	C(8)–C(12)–W(1)	73.3(4)
C(3)–O(3)	1.141(9)	C(11)–C(12)–W(1)	72.4(4)
C(4)–C(5)	1.514(9)	C(3)–W(1)–C(2)	78.1(3)
C(4)–W(1)	2.326(6)	C(3)–W(1)–C(1)	107.0(3)
C(5)–C(6)	1.524(10)	C(2)–W(1)–C(1)	75.9(3)
C(6)–C(7)	1.506(10)	C(3)–W(1)–C(11)	136.5(3)
C(7)–O(5)	1.209(9)	C(2)–W(1)–C(11)	91.7(3)
C(7)–O(4)	1.303(8)	C(1)–W(1)–C(11)	111.2(3)
C(8)–C(9)	1.377(11)	C(3)–W(1)–C(12)	102.6(3)
C(8)–C(12)	1.419(12)	C(2)–W(1)–C(12)	94.3(3)
C(8)–W(1)	2.339(7)	C(1)–W(1)–C(12)	145.8(3)
C(9)–C(10)	1.400(12)	C(11)–W(1)–C(12)	35.4(3)
C(9)–W(1)	2.372(7)	C(3)–W(1)–C(4)	73.7(3)
C(10)–C(11)	1.407(12)	C(2)–W(1)–C(4)	130.9(3)
C(10)–W(1)	2.359(8)	C(1)–W(1)–C(4)	75.1(3)
C(11)–C(12)	1.406(12)	C(11)–W(1)–C(4)	135.8(3)
C(11)–W(1)	2.315(7)	C(12)–W(1)–C(4)	130.5(3)
O(1)–C(1)–W(1)	177.1(6)	C(3)–W(1)–C(8)	94.4(3)
O(2)–C(2)–W(1)	179.2(8)	C(2)–W(1)–C(8)	126.8(3)
O(3)–C(3)–W(1)	176.7(6)	C(1)–W(1)–C(8)	152.3(3)
C(5)–C(4)–W(1)	117.9(4)	C(11)–W(1)–C(8)	58.4(3)
C(4)–C(5)–C(6)	112.5(6)	C(12)–W(1)–C(8)	35.5(3)
C(5)–C(6)–C(7)	114.4(6)	C(4)–W(1)–C(8)	95.0(3)
O(5)–C(7)–O(4)	123.5(7)	C(3)–W(1)–C(10)	151.4(3)
O(5)–C(7)–C(6)	123.2(6)	C(2)–W(1)–C(10)	121.3(3)
O(4)–C(7)–C(6)	113.2(6)	C(1)–W(1)–C(10)	98.6(3)
C(9)–C(8)–C(12)	108.4(7)	C(11)–W(1)–C(10)	35.0(3)
C(9)–C(8)–W(1)	74.3(4)	C(12)–W(1)–C(10)	58.3(3)
C(12)–C(8)–W(1)	71.2(4)	C(4)–W(1)–C(10)	101.7(3)
C(8)–C(9)–C(10)	108.8(7)	C(3)–W(1)–C(9)	118.6(3)
C(8)–C(9)–W(1)	71.7(4)	C(2)–W(1)–C(9)	148.9(3)
C(10)–C(9)–W(1)	72.3(4)	C(1)–W(1)–C(9)	118.3(3)

The central tungsten atom may be regarded as in a formal oxidation state of +II; it has a d^4 outer electron configuration and achieves the expected "noble gas" configuration by the donation of six electrons from the π-cyclopentadienyl anion, two electrons from each of the three carbonyl ligands and two electrons from the alkyl ligand. The overall coordination geometry about the tungsten (II) atom is, perhaps, most graphically described as "resembling a four legged piano-stool" [53]. The W–C(Cp) bond distances range from 2.31 (7) to 2.37 (7) Å. The W–C(alkyl) bond length is 2.33 (6) Å and is in the range observed in other structures with similar geometry [70], the W–CO bonds are 1.97 (7), 1.98 (7) and 1.99 (8) Å in length. The bond lengths: C=O, 1.21 (9) Å and C–OH, 1.30 Å on the carboxylic acid group reflect those observed for the most similar organic structure , 7-oxo-7-(phenylamino)heptanoic acid ($C_6H_5NHCO(CH_2)_5CO_2H$) [71]. Also, the bond angles around the carboxylic acid group of our structure reflect those of the most similar structure. The difference observed for O4 – C7 – C6 (113.2 °) with its analogue moiety in the organic structure (114.3 °) is only 0.1°, which is negligible. The other molecule found in the literature that may be compared to this molecule is $[(\eta^5\text{-}C_5H_4COOH)(CO)_3W]_2$ [72]. The bond lengths of the carboxylic acid group resemble those of our molecule and that of the reported organic molecule mentioned above. Similarly, the bond angles around the tungsten metal in our structure virtually reflect those on this molecular unit. However, the bond angles around the carboxylic acid group of our structure differ with those of this compound $[(\eta^5\text{-}C_5H_4COOH)(CO)_3W]_2$, in the range of 0.8 – 3.2 °. This may probably be because the carboxylic acid group in our molecule is aliphatically attached in our compound, whereas in this reported compound it is on the cyclopentadienyl ring. The unit cell packing in $[Cp(CO)_3W\{(CH_2)_3COOH\}]$ is different from that of the paraffin ("bump in hollow") packing, which is also observed for similar compounds of the halogenoalkyl type [70, this thesis]. The dihedral angles C(2) –W–C(4) were always eclipsed to facilitate the favourable packing of the alkyl chains in a unit cell [70, this thesis]. In contrast the C(2) –W–C(4) angle observed in this molecule was rather staggered 130.9 (3) °.

4.5.2 Reaction with Carbon Monoxide

The bubbling of carbon monoxide gas through a solution of the complex $[Cp(CO)_3W(CH_2)_3Mo(CO)_3Cp]$ in acetonitrile yielded an unstable acyl complex, $[Cp(CO)_3W(CH_2)_3C(O)Mo(CO)_3)Cp]$ **13** as shown in Equation 10.

$$[Cp(CO)_3W(CH_2)_3Mo(CO)_3Cp] + CO \longrightarrow [Cp(CO)_3W(CH_2)_3C(O)Mo(CO)_3Cp] \quad (10)$$

The product was confirmed by an acyl peak observed in the infrared spectrum at 1604 cm^{-1}, and the triplet due to the protons next to the acyl group observed at around 3.72 ppm in the ^1H NMR spectrum. Again the reaction taking place here is on the molybdenum center because we observe the chemical shift of the CpMo at 5.36 ppm (p) compared to the starting material which was at 4.88 ppm (sm). The CpFe peak only slightly shifted from 4.71 ppm (sm) to 4.97 ppm (p).

The compound was too unstable for a ^{13}C NMR spectrum to be recorded. Nevertheless, the "carbonyl insertion" into the molybdenum-alkyl bond was confirmed.

The complex, $[Cp(CO)_2Fe(CH_2)_3Mo(CO)_2(PMe_3)Cp]$ reacted with carbon monoxide gas in acetonitrile to yield the complex, $[Cp(CO)_2Fe(CH_2)_3C(O)Mo(CO)_2(PMe_3)Cp]$ **14** (Equation 11).

$$[Cp(CO)_2Fe(CH_2)_3Mo(CO)_2(PMe_3)Cp] + CO \longrightarrow [Cp(CO)_2Fe(CH_2)_3C(O)Mo(CO)_2(PMe_3)Cp] \quad (11)$$

The high basicity of the substituent PMe_3 seems to stabilize the CO-inserted product by increasing the electron density on the metal. Consequently a ^{13}C NMR spectrum could be obtained. Strong spectroscopic evidence supporting this formulation was obtained. A strong acyl peak at 1603 cm^{-1} was observed in the carbonyl region of the infrared spectrum. The ^1H NMR spectrum showed a triplet at 2.90 ppm corresponding to the CH_2 protons adjacent to a carbonyl group. The following was observed in the ^{13}C NMR spectrum, the acyl, C=O (δ 151), a shift of *ca.* 5 ppm observed for the CpMo (from 90.85 ppm to 95.06 ppm), $MoC(O)CH_2$ 70.86 ppm, $FeCH_2$ 3.87 ppm (this peak is at 9.60 ppm in the starting material) and the central carbon of the alkyl chain at 33.88 ppm compared to 46.10 ppm of the starting material. The CpFe peak had a very slight shift of only 0.16 ppm in the product relative to the starting material.

4.5.3 Reaction with Triphenylcarbeniumhexafluorophosphate

Several attempts were made to abstract a hydride from some of the prepared heterobimetallic compounds. The abstraction of a hydride from the alkyl chain connecting

the two metal centers is an important reaction because it could provide information about which side of the molecule the hydride abstracted from. Moss and Johnson reacted some longer chain alkanediyl complexes of the type $[(Cp(CO)_2Fe)_2\{\mu\text{-}(CH_2)_n\}]$ (n = 4 - 6) with trityl salt and obtained yellow crystalline compounds of the structure $[(Cp(CO)_2Fe)_2\{\mu\text{-}C_nH_{2n-1}\}]PF_6$ [73]. The spectroscopic results suggested that the link of the iron to the carbon chain is via π-bonding on one side and σ-bonding on the other as shown in Figure 4.29(a). Similar reaction has been reported by Friedrich and Moss [1] on heterodinuclear compounds $[Cp(CO)_2Fe(CH_2)_3Mo(CO)_3Cp]$, $[Cp(CO)_2Fe(CH_2)_3Ru(CO)_2Cp]$, $[Cp(CO)_2Fe(CH_2)_3W(CO)_3Cp]$, as shown in Figure 4.29(b). Similar bonding to that of the diiron alkanediyl was proposed.

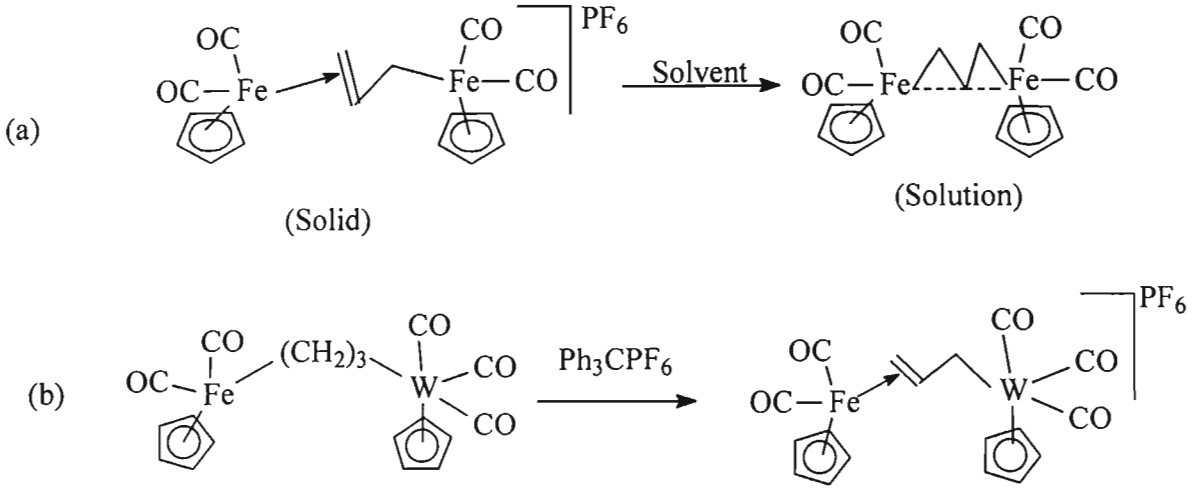

Figure 4.29: Proposed structure of (a) $[(Cp(CO)_2Fe)_2\{\mu\text{-}(C_3H_5)\}]PF_6$ in solid and (b) $[Cp(CO)_2Fe\{\mu\text{-}(C_3H_5)\}W(CO)_3Cp]PF_6$ in solution.

It could be of interest to learn what might result, in the event of a bimetallic compound losing a hydride; could this initiate intermetallic communication? We have seen earlier that developing a molecule connected by a conjugated system may lead to molecular wires or one-dimension molecular conductors. The hydride abstractor, Ph_3CPF_6, was used in these reactions with the following compounds, $[Cp(CO)_3W(CH_2)_3Mo(CO)_2(Ph_2Me)Cp]$, $[Cp(CO)_3W(CH_2)_4Mo(CO)_2(Ph_2Me)Cp]$, $[Cp(CO)_2Fe(CH_2)_4Mo(CO)_2(PMe_3)Cp]$, $[Cp(CO)_3W(CH_2)_3Mo(CO)_3Cp]$, $[Cp(CO)_3W(CH_2)_3Mo(CO)_3Cp^*]$, $[Cp(CO)_2Fe(CH_2)_3Mo(CO)_3Cp^*]$ and $[Cp(CO)_2Fe(CH_2)_4Mo(CO)_3Cp^*]$. Each time the experiments were attempted, an initial blue colour (elemental W) was obtained, a clear sign of decomposition of the compounds into their elemental atoms.

A modification to this experiment was tried, where the dichloromethane solvent to be used for the dissolution of the two reagents was saturated with nitrogen for 30 minutes then cooled down to –20 °C to precipitate any water that may be present. This was then used immediately to dissolve the reagents. The solution of $[Cp(CO)_2Fe(CH_2)_4Mo(CO)_3Cp^*]$ in dichloromethane was then brought down to –40 °C, as it was suspected that the reaction might as well have been exothermic and hence the generated heat was accelerating the observed decomposition. Then the trityl salt, Ph_3CPF_6 in dichloromethane was finally added down the side of the Schlenk tube while maintaining this low temperature. The mixture was allowed to slowly warm up to room temperature where it was left to stand for 6 days. A dark green precipitate formed which was filtered off. The product was finally washed with dry ether yielding a blue-green product, which was characterised; IR (nujol) 2126 cm^{-1} s, 2073 cm^{-1} bsh. The ^1H NMR (Aceton-d_6) had a very significant shift of the Cp peak downfield to 6.2 ppm relative to the starting material that had this peak at 4.9 ppm. The protons from the C*H*=C*H* moiety were also observed at 5.9 ppm. However, the product was so unstable in solution that ^{13}C NMR data could not be obtained. Low temperature ^{13}C NMR was not readily available. In comparison to similar experiments available in the literature [1], the trityl salt successfully abstracted a hydride from $[Cp(CO)_2Fe(CH_2)_4Mo(CO)_3Cp^*]$ (Equation 12). Investigations about the reaction medium polarity, revealed that the reactivity was slow in the more polar tetrahydrofuran solvent and fast in dichloromethane.

$$[Cp(CO)_2Fe(CH_2)_4Mo(CO)_3Cp^*] + Ph_3CPF_6 \longrightarrow [Cp(CO)_2Fe(C_4H_7)Mo(CO)_3)Cp^*]PF_6 \qquad (12)$$

4.5.4 Thermal Decomposition of Compounds 10a and 2a

The hydrocarbon products of the thermal and photochemical decomposition of organometallic compounds where two metal centres are linked by a polymethylene chain has been studied and evidence for the generation of metallacycle intermediates has been deduced [16]. The thermal decomposition of **10a** was effected by heating a Schlenk tube containing the compound in an oil bath, while connected to another Schlenk tube containing $CDCl_3$ immersed in liquid nitrogen, with the whole system under vacuum.

After the reaction was judged to be complete, the ^{1}H and ^{13}C NMR experiments were carried out. A mixture of products was obtained. A singlet due to cyclopropane was observed at 0.2 ppm along with other peaks.

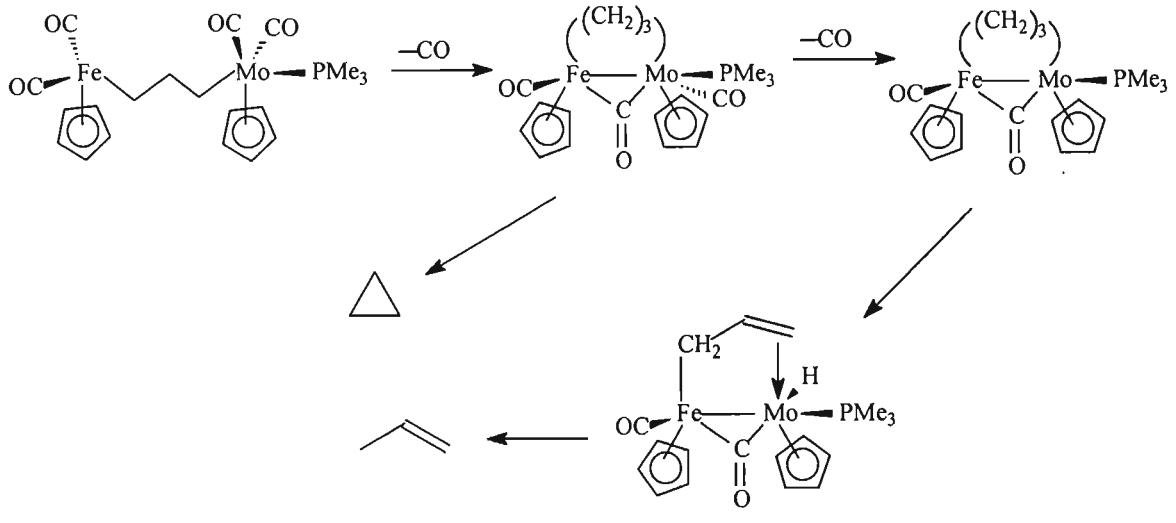

Scheme 4.6.: Proposed thermolysis pathway for compound **10a**

The other peaks appearing in the ^{1}H NMR spectrum at 5.6 ppm ($CH{=}CH_2$,) 3.7 ppm ($CH{=}CH_2$), 1.8 ppm (CH_3) were due to propene, an expected product from this type of reaction. The iron and molybdenum dimers were shown to be the main components of the dark red residue obtained. The mechanism for this type of reaction has also been reported to follow a β–elimination and reductive processes as shown in the proposed thermolysis for **10a** shown in Scheme 4.6. Knox and co-workers had reported on a thermolysis study of $[Cp(CO)_2Fe(CH_2)_3Ru(CO)_2Cp]$, that gave the products propene and cyclopropane in the ratio of 1:1.3 [16]. Our products could be estimated to be in the ratio of 4:1 respectively, reflecting the influence of the different metals. The thermolysis reaction was repeated using the compound $[Cp(CO)_3W(CH_2)_3Mo(CO)_3Cp^*]$ **2a**. Similar results as observed for the compound **10a** were obtained.

Some of the selected characterization data are given in Table 4.7 below. All the reaction studies carried out on the propanediyl heterobimetallic compounds are summarized in Scheme 4.7 below.

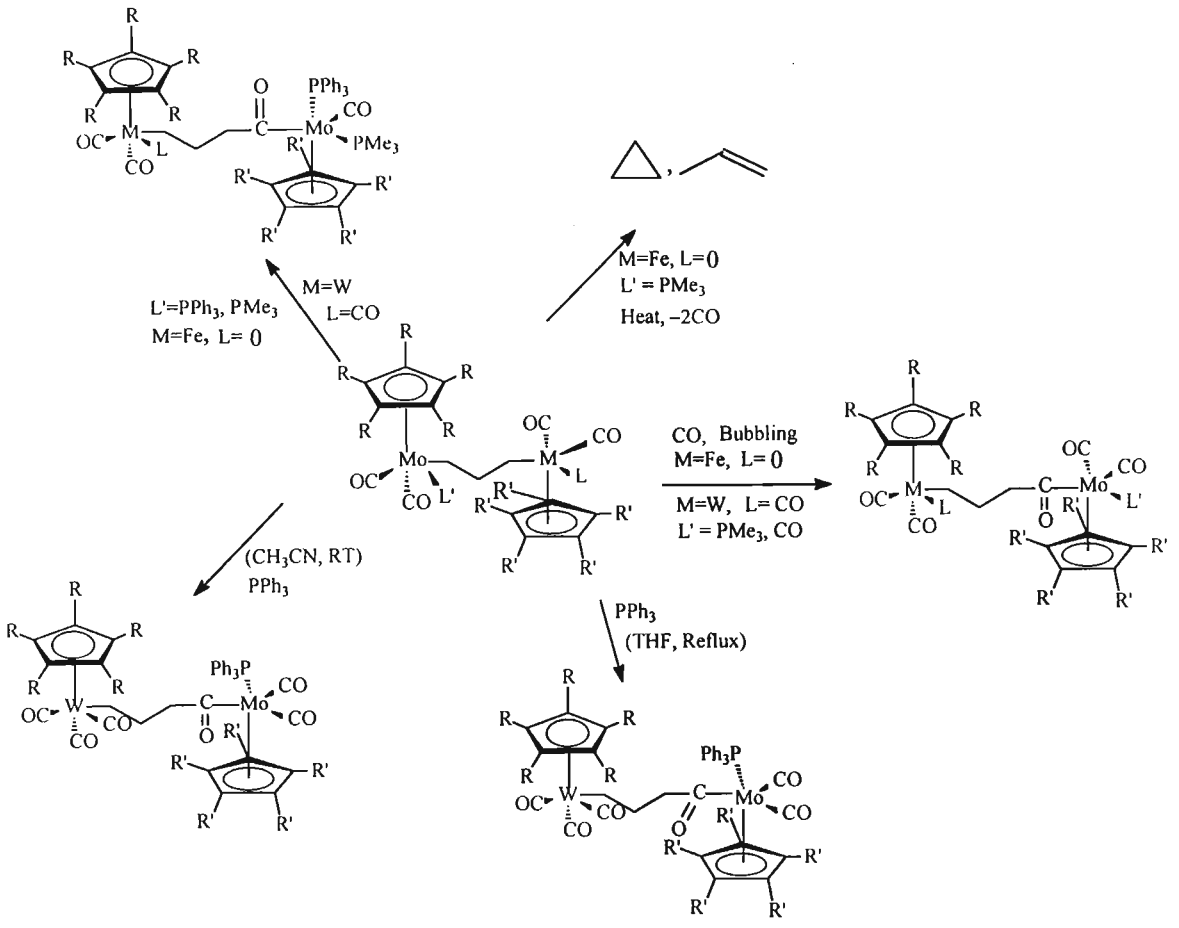

Scheme 4.7: Summary of some of the reactions on the heterobimetallic compounds where n = 3

Attempts to prepare the compounds $[Cp(CO)_2W(CH_2)_n]^+[SbF_6]^-$ (n = 3, 4), were not very successful. The products were very unstable and thus it could not be established whether they were prepared or not. Several attempts to investigate oxidative addition reactions, by the reactions of Vaska's complex, $[(Cl)(CO)(PPh_3)_2Ir]$ with $I(CH_2)_3I$ and $[Cp(CO)_3W\{(CH_2)_3I\}]$ failed.

Table 4.7: Yields, IR, ^{1}H NMR and ^{13}C NMR from Reaction Studies on Some of the Heterobimetallic Compounds.

Compound	Yield (%)	M.P. (°C)	IR ν(CO) (cm^{-1})			
$[Cp(CO)_3W(CH_2)_3C(O)Mo(CO)(PMe_3)(PPh_3)Cp]$	88	78 - 84	2010[a] s	1912sb	1843sh	1603w
$[Cp(CO)_3W(CH_2)_4C(O)Mo(CO)(PMe_3)_2Cp]$	92	dec.	2010s	1911sb	1838sh	1604w
$[Cp(CO)_2Fe(CH_2)_3C(O)Mo(CO)_2(PMe_3)Cp]$	90	118 - 124	2002s	1940sb	184310vsb	1793wb
$[Cp(CO)_3W(CH_2)_3C(O)Mo(CO)_3Cp]$	98	dec.	2010s	1979vsb	1911vsb	1604wb
$[Cp(CO)_2Fe(C_4H_7)^{+}Mo(CO)_3Cp^*]PF_6$	67	dec.	2126s	2073bsh		
$[Cp(CO)_3W(CH_2)_3C(O)Mo(CO)_2(PPh_3)Cp^*]$	93	82-86	2011ss	1912sb	1844sm	1704s
$[Cp(CO)_3W(CH_2)_3C(O)Mo(CO)_2(PPh_3)Cp]$	89	146 - 148	2009ss	1911sb	1850ss	1613wb
$[Cp(CO)_2Fe(CH_2)_3C(O)Mo(CO)_2(PMe_3)Cp]$	98	dec	1998s	1938vs	1921s	1713ss

[a] measured in dichloromethane

^{1}H NMR

Compound	CpMo[a]	Cp*Mo	CpW/Fe	α-Mo	α-W/Fe	β-Mo	γ-Mo	P-Ph	P-CH_3
$[Cp(CO)_3W(CH_2)_3C(O)Mo(CO)(PMe_3)(PPh_3)Cp]$	5.27s		5.39s	2.93t, 2H,7.5[b]	0.86s	2.35s		7.36d,2H 9.7	1.52d, 9H,9.3
$[Cp(CO)_3W(CH_2)_4C(O)Mo(CO)(PMe_3)_2Cp]$	5.10s		5.35s	2.93t, 2H,7.3	0.85s	2.33s	1.60m		1.54d, 18H,12.8
$[Cp(CO)_2Fe(C_4H_7)^{+}Mo(CO)_3Cp^*]PF_6$	5.90s		5.71s	1.15s	6.2d, 1H,8.6	3.43s	3.28d, 1H,13.3		2.07d, 5H,12.2
$[Cp(CO)_3W(CH_2)_3C(O)Mo(CO)_2(PPh_3)Cp^*]$		1.97s	5.39s	2.33t,2H,7.2	1.64s	2.13s	1.86s		2.00, 5H, 10.44
$[Cp(CO)_3W(CH_2)_3C(O)Mo(CO)_2(PPh_3)Cp]$	5.36s		4.97s	3.07t,2H,6.9	1.43s	1.65m		7.44d,2H,9.8	
$[Cp(CO)_2Fe(CH_2)_3C(O)Mo(CO)_2(PMe_3)Cp]$	5.10s		4.70s	2.95t,2H,7.4	1.34s	1.61s			1.57d,9H,9.6

^{13}C NMR

Compound	MoCO[a]	MoC=O	W/FeCO	CpMo	Cp*(C)	Cp*(CH_3)	CpW/Fe	α-Mo	α-W/Fe	β-Mo	γ-Mo	Ph	P-Me
$[Cp(CO)_3W(CH_2)_3C(O)Mo(CO)(PMe_3)(PPh_3)Cp]$	237d,24.4	176	217	95.01			91.52	39.27	-12.11	31.85		128	18.41
$[Cp(CO)_3W(CH_2)_4C(O)Mo(CO)(PMe_3)_2Cp]$	228d,24.1	176	[c]	94.03			91.46	36.39	-11.50	33.00	30.59		18.37
$[Cp(CO)_3W(CH_2)_3C(O)Mo(CO)_2(PPh_3)Cp^*]$	[c]	[c]	217	91.53	104	10.93	915.3	39.56	-11.96	31.93		128	
$[Cp(CO)_3W(CH_2)_3C(O)Mo(CO)_2(PPh_3)Cp]$	238d,22.6.	267	217	96.48			91.49	71.11	-9.92	33.15		128	
$[Cp(CO)_2Fe(CH_2)_3C(O)Mo(CO)_2(PMe_3)Cp]$	237d,24.1	[c]	217	95.06			85.32	70.86	3.84	33.87			21.03

[a] Measured in $CDCl_3$ relative to TMS (0.00 ppm), [b] J values are given in Hz. β-Mo refers to the carbon atom of the alkyl chain. β to Mo *etc.* All couplings not indicated are singlets. [c] Not observed.

4.6 Conclusions

A number of new compounds were prepared and fully characterized.

We are very pleased to report that several new methods for obtaining pure products were developed. For example, from within this Chapter and the previous Chapter, recrystallisation of the products from a dilute dichloromethane/hexane mixture at –78 °C rendered the use of chromatography unnecessary. Attempting research in organometallic chemistry is really an expensive venture, though interesting, thus it is exciting to develop a viable method to obtaining pure products quicker and in high yield and/or extending the life of the sensitive organometallic compound for better characterisation. Use of phosphine compounds is rather interesting, because they make the purification procedure much easier as they do not dissolve in hexane, they readily precipitate out of solution. Also their high basicity increases the stability of these low oxidation state transition metal compounds.

We have further confirmed that the most successful route to obtaining the polymethylene bridged heterodinuclear compounds is via the use of iodoalkyl compounds. These compounds were obtained by the reactions of $[Cp(CO)_3W\{(CH_2)_nI\}]$ (n = 3 – 6) and $[Cp(CO)_2Fe\{(CH_2)_nI\}]$ (n = 3, 4) with several transition metal carbonyl anions. The complexes were characterized by the usual methods. The ^1H and ^{13}C NMR data appear to support the fact that two different metal centres present within the same molecule could "communicate" to a degree. An independent characterisation of the compounds **2a**, **5b** and **10a** by the use of the electrospray ionisation mass spectrometry confirmed that the heterobimetallic compounds were successfully prepared.

The crystal structures of alkanediyl heterobimetallic compounds containing group VIB metals and iron, $[Cp(CO)_3W(CH_2)_3Mo(CO)_2(PPh_3)Cp]$ **3a** and $[Cp(CO)_2Fe(CH_2)_3Mo(CO)_2(PPh_3)Cp]$ **7a** are reported for the first time. The two crystals both resolve in triclinic space group. The structures were found to have a unique feature; compound **3a** had the two Cp rings in *cis* position, while those in **7a** were *trans*. These two structures further confirmed the preparation of the reported novel complexes. Very limited reactions involving these types of compounds are reported in the literature, we have further contributed to this area of research by performing some successful and

interesting reactions. However, we were disappointed in one area, the reaction studies involving the trityl salt gave unstable products that could not be fully characterized. We have established that some reactions are metalloselective. For example, when $[Cp(CO)_3W(CH_2)_3Mo(CO)_3Cp]$ reacted with the neutral molecule PPh_3 in THF and acetonitrile, the attack was always observed to take place on the molybdenum centre. Similar observations from the reactions of CO with $[Cp(CO)_3W(CH_2)_3Mo(CO)_3Cp]$ and $[Cp(CO)_3Fe(CH_2)_3Mo(CO)_2(PMe_3)Cp]$ in acetonitrile were made. The metal centre of a particular heterobimetallic compound that would be attacked by an incoming nucleophile was found to be predictable.

Some of the reaction products were unstable and therefore could not be fully characterized, for example, $[Cp(CO)_3W(CH_2)_3C(O)Mo(CO)_3Cp]$. An attempt to obtain crystals of some of these reaction products failed. A crystal which was thought to be $[Cp(CO)_3W(CH_2)_3C(O)MoC(O)(PMe_3)(PPh_3)Cp]$, ended up being an acid derivative $[Cp(CO)_3W\{(CH_2)_3COOH\}]$. The reason for this was attributed to the manner in which the crystal data was collected or the formation of a nitrile derivative which is then hydrolysed to the acid. Nevertheless, we are reporting for the first time, a crystal structure of an aliphatic acid derivative of the class of compounds studied.

The thermolysis studies that served to show the importance of these complexes as potential catalytic intermediates, as expected, gave cyclopropane and propene amongst other products.

4.7 References

[1] H.B. Friedrich, J.R. Moss, *J. Chem. Soc., Dalton Trans.*, (1993) 2863.

[2] J-M. Lehn *Angew. Chem. Int. Ed. Engl.*, **27** (1988) 89.

[3] P. Sautet, O. Eisenstien, K.M. Nicholas, *Organometallics*, **6** (1987) 1845.

[4] R. D. Adams *Polyhedron,* **7** (1988) 2251 and refs therein.

[5] S. J. Archer, K. P. Finch, H. B. Friedrich, J. R. Moss, *Inorg. Chim. Acta,* **182** (1991) 145 and references therein.

[6] B. Findeis, M. Schubart, C. Platzek, L.H. Gade, I. Scowen, M. McPartlin, *J. Chem. Soc., Chem. Commun.*, (1996) 219.

[7] S. Friedrich, H. Memmer, L.H. Gade, II.W.S. Li, I.J. Scowen, M. McPartlin, C.E. Housecroft, *Inorg. Chem.*, **35** (1996) 2433.

[8] D. Selent, M. Ram,, C. Janiak, *J. Organomet. Chem.*, **501** (1995) 235.

[9] J.Sundermeyer, D. Runge, J.S. Field, *Angew. Chem. Int. Ed. Engl.*, **33** (1994) 678.

[10] J. Sundermeyer, D. Runge, *Angew. Chem. Int. Ed. Engl.*, **33** (1994) 1255.

[11] I.P. Beletskaya, A.Z. Voskoboynikov, E.B. Chuklanova, N.I. Kirrilova, A.K. Shestakova, A.I. Parshina, A.I. Gusev, G.K-I. Magomedov, *J. Amer. Chem. Soc.*, **115** (1993) 3156.

[12] F.E. Hong, I-R. Lue, S-C. Lo, Y-C Yang, C-C. Lin, *Polyhedron,* **15** (1996) 2793.

[13] F.E. Hong, I-R. Lue, S-C. Lo, C-C. Lin, *Polyhedron,* **14** (1995) 1419.

[14] A.M. Martins, M.J. Carlhoda, C.C. Romao, C. Vokel, P. Kiprof, A.C. Filippou, *J. Organomet. Chem.,* **423** (1992) 367

[15] Y-Y. Liu, A. Mar, S.J. Rettig, A. Storr, J. Trotter, *Can. J. Chem.*, **66** (1988) 1997.

[16] M. Cooke, N. J. Forrow, S. A. R. Knox; *J. Chem. Soc., Dalton Trans.*, (1983) 2435.

[17] H.B. Friedrich, J.R. Moss B. K. Williamson; *J. Organomet. Chem.*, **394** (1990) 313-327.

[18] W. Beck, B. Niemer, M. Wieser; *Angew. Chem. Int. Ed. Engl.*, **32** (1993) 923-1110.

[19] N. Wheatley, P. Kalck, *Chem. Rev.,* 99 (1999) 3419.

[20] D. H. Gibson, J. O. Franco, M. T. Harris, T-S. Ong; *Organometallics*, **11** (1992) 1993.

[21] R.B. King, *Inorg. Chem.*, **2** (1963) 531.

[22] R.B. King, M.A. Bisnette, *J. Organomet. Chem.*, **7** (1967) 311.

[23] R.B. King , *Acc. Chem. Res.*, **3** (1970) 417.

[24] J.R. Moss, *J. Organomet. Chem.*, **231** (1982) 229.

[25] J.R. Moss, L.G. Scott, *J. Organomet. Chem.*, **363** (1989) 351.

[26] L.H. Gade, *Angew. Chem. Int. Ed.* Engl., **39** (2000) 2658.

[27] G.E. Coates, M.L.H. Green, P. Powell, K. Wade, "Principles of Organometallic Chemistry", Chapman, London, 1977 p10.

[28] C.A. Tolman, *Chem. Rev.*, **77** (177) 313.

[29] H.A. Bent, *Chem. Rev.*, **61** (1961) 275.

[30] J.T. Malito, R. Shakir, J. L. Atwood, *J. Chem. Soc., Dalton Trans.*, (1980) 1253.

[31] (a) S.E. Kegley, A.R. Pinhas, "Problems and Solutions in Organometallic Chemistry". Oxford University Press, New Yolk, 1985 p 20.
(b) N.A Bailey, D.A. Dunn, C. N. Foxcroft, G.R. Harrison, M.J. Winter, S. Woodward, *J. Chem. Soc., Dalton Trans.*, (1988) 1449.

[32] K.W. Barnet, T.G. Pollman, T.W.Solomon, *J. Organomet. Chem.*, **36** (1972) C23.

[33] P.G. Jones, *Chemistry in Britain*, **17** (1981) 222.

[34] L. Pope, P. Sommerville, M.J. Laing, K.J. Hindson, J.R. Moss, *J. Organomet. Chem.*, **112** (1976) 309.

[35] K. Raab, U. Nigel, W. Beck, *Z. Naturforsch.*, **38b** (1983) 1466.

[36] K.P. Finch, J.R. Moss, M.L. Niven, *Inorg. Chim. Acta*, **166** (1989) 181.

[37] H. Adams, N.A. Bailey, M.J. Winter, *J. Chem. Soc., Daltons Trans.*, (1984) 273.

[38] G.E. Jackson, J.R. Moss, L.G. Scott, *S. Afr. J. Chem.*, **36** (1983) 69.

[39] F. Amor, P. Royo, T.P. Spaniol, J. Okuda, *J. Organomet. Chem.*, **604** (2001) 126 and references therein.

[40] D.J. Darensbourg, R. Kudaroski, *J. Amer. Chem. Soc.*, **106** (1984) 3672.

[41] D.J. Debad, P. Legzdins, S.J. Rettig, J.E. Veltheer, *Organometallics*, 12 (1993) 2714.

[42] H.G. Alt, J.S. Han, R.D. Rogers, *J. Organomet. Chem.*, **445** (1993) 115.

[43] R. Poli, G. Wilkinson, M. Motevalli, M.B. Hursthouse, *J. Chem. Soc., Dalton Trans.*, (1985) 931.

[44] H.G. Alt, S.J. palackal, R.D. Rogers, *J. Organomet. Chem.*, **388** (1990) 105.

[45] R.O. Hill, C.F. Marais, J.R. Moss, K.J. Naidoo, *J. Organomet. Chem.*, **587** (1999) 28 and refs therein.

[46] O.E. Woisetchlager, K. Sunkel, W. Weigand, W. Beck, *J. Organomet. Chem.*, **584** (1999) 122.

[47] O.E. Woisetchlager, A. Geisbauer, K. Polborn, W. Beck, *J. Organomet. Chem.*, **599** (2000) 238.

[48] A.I. Kitaigorodskii, "Organic Chemical Crystallography", Consultants Bureau, New York, 1961, p65.

[49] M.R. Churchill, J.P. Fennesey, *Inorg. Chem.*, **18** (1979) 2454.

[50] R.C. Melvyn, *Inorg. Chem.*, **7** (1968) 953.

[51] R.C. Melvyn, W. –Y. Chang, *Inorg. Chem.*, **14** (1975) 98.

[52] T. Butters, *Acta Crystall. Sec. C Cryst. Struct. Commun.*, **C41** (19850 23.

[53] H. Adams, N.A. Bailey, P. Blenkiron, M.J. Morris, *J. Chem. Soc., Dalton Trans.*, (1997) 3589.

[54] G.A. Carmela, F. Faraone, M. Fochi, M. Lanfranchi, C. Mealli, R. Seeber, A. Tiripicchio, *J. Chem. Soc., Dalton Trans.*, (1992) 1847.

[55] S. Bodige, A. S. Torres, D. J. Maloney, D. Tate, G. R. Kinsel, A. K. Walker, F. M. MacDonnell, *J. Amer. Chem. Soc.*, **119** (1997) 10364.

[56] Z.T. Horrath, M. Garland, G. Bor, P. Pinto, *J. Organomet. Chem.*, **358** (1988) C17.

[57] J.R. Budge, J.P. Scott, B.C. Gates, *J. Chem Soc., Chem. Commun.*, (1983) 342.

[58] A. Fukuoka, T. kimura, M. Ichikawa, *J. Chem Soc., Chem. Commun.*, (1988) 428.

[59] E.N. Jacobsen, K.I. Goldberg, R.G. Bergman, *J. Amer. Chem. Soc.*, **110** (1988) 3706.

[60] F. Ozawa, J.W. Park, P.B. Mackenzie, W.P. Schaefer, L.M. Henling, R.H. Grubbs, *J. Amer. Chem. Soc.*, **111** (1988) 1319.

[61] I.J. Hart, J.C. Jeferry, R.M. Lowry, F.G.A. Stone, *Angew. Chem., Int. Ed. Engl.*, **27** (1988) 1703.

[62] C.P. Casey, J.D. Audett, *Chem. Rev.*, **86** (1986) 339.

[63] F. Calderazzo, *Angew. Chem. Int. Ed. Engl.*, **16** (1977) 299.

[64] T.C. Flood, K.D. Campbell, *Organometallics*, **2** (1983) 1590.

[65] I.S. Butler, F. Basolo, R.G. Pearson, *Inorg. Chem.*, **6** (1967) 2074.

[66] M.J. Wax, R.G. Bergman, *J. Amer. Chem. Soc.*, **103** (1981) 7028.

[67] K.A. Johnson, W.L. Gladfelter, *Organometallics*, **11** (1992) 2534.

[68] M.J. Laing, *private communication*, (2002).

[69] R. Justus, *Liebegs Ann. Chem.*, **582** (1953) 1.

[70] H.B. Friedrich, M.O. Onani, O.Q. Munro, *J. Organomet. Chem.*, **633** (2001) 39.

[71] N. Feeder, W. Jones, *Acta Crystall. Sec. C Cryst. Struct. Commun.,* **C50** (1994) 1732.

[72] A. Avey, C.S. Tenhaeff, T.J.R. Weakley, D.R. Tyler, *Organometallics*, **10** (1991) 3607.

[73] J.W. Johnson, J.R. Moss, *Polyhedron,* **4** (1985) 563.

CHAPTER 5

EXPERIMENTAL

5.1 General Details

All reactions were carried out under nitrogen using standard Schlenk tube techniques. The inert atmosphere suitable for our reactions was obtained by using the gases nitrogen (Afrox HP) or argon (Afrox HP). The tungsten hexacarbonyl (Aldrich 97%, Acros 99%, Fluka 90%), molybdenum hexacarbonyl (Aldrich 98%, Acros 98%) and pentane (Saarchem 99.5%) were obtained and used without further purifications. The dicyclopentadiene (Merck 97%, Fluka 90%) was always distilled prior to use. Also, the solvent tetrahydrofuran (Saarchem 99%) was distilled over sodium (Saarchem, H.W.O. Kleber) and benzophenone (Merck 99%), and stored over sodium wire. The molecular sieves 3Å (Acros Organics) and 4Å (Merck AR) were dried in a tube furnace at 250 °C for 10 hours priot to use. The acetone (Crest, technical grade) was double distilled in our School, but was further distilled from $CaCl_2$ (Saarchem 95%) and stored over molecular sieves 4Å or potassium carbonate (Saarchem 99.5%) under nitrogen. The solvent hexane (Unilab 96%, Crest Technical grade) was distilled over sodium, and stored over sodium wire prior to use. Acetonitrile (Merck 99%) was distilled over phosphorus pentoxide (Associated Chemical Enterprises 99%) and stored over molecular sieves 4Å under nitrogen. Methanol (Crest Technical grade) and ethanol (NCP 99.9%) were distilled over $CaCl_2$ or Mg/I_2 to obtain a 'super dry' solvent according to the reported literature method [1]. Dichloromethane (Shalom technical grade) and chloroform (Spectrochem 99.5%) were double distilled in our School and kept under molecular sieves 3Å under nitrogen, and were used without any further purification.

The ferric sulphate (Merck AR), glacial acetic acid (Kleber 99.5%), mercury (Associated Chemical Enterprises, triple distilled AR), 1,3-dibromopropane (Acros Organics 98%, Fluka 99%), 1,4-dibromobutane (Acros Organics 99%), 1,5-dibromopentane (Aldrich 97%), 1,6-dibromohexane (Aldrich 98%), 1,3-diiodopropane (Lancaster 98%) and 1,4-diiodobutane (Aldrich 99%) were used without further purification. Sodium iodide (Merck 99%, Riedel-de Hein 99.5%) was dried at 100 °C under vacuum for 6 – 8 hours and 2-methoxyethyl ether (Acros Organics 99%) was dried over sodium wire prior to use.

Alumina (Merck, aluminium oxide 90 acidic, active) was deactivated with deionised water and dried in the Oven kept at 110 °C before use. Melting points were recorded on a Kofler hot-stage microscope and are uncorrected. Elemental analyses were performed in the Chemistry Department of our Pietermaritzburg campus. Infrared spectra were recorded on a Nicolet Impact 400D 5DX FT-spectrophotometer (4000 cm^{-1} – 400 cm^{-1}) either in solution (liquid cell, NaCl windows (Aldrich 99.99%) liquid cell or KBr (Aldrich, 99.99%) discs. The NMR spectra were recorded on Varian Gemini 300 MHz and Varian Inova 400 spectrometers. The deuterated solvents used were $CDCl_3$, (Acros Organics 99.8%) and CD_3OCD_3, (Merck 99.8%), and were used as purchased. The solutions for the NMR studies were prepared under nitrogen, using nitrogen saturated solvents. The molar quantities of the reactants used in this thesis were at times increased by a 10 or 20% excess to be sure that the reactions went to completion.

5.2 Experimental Details Pertaining to Chapter 2

5.2.1 Preparation of [{Cp(CO)$_3$W}$_2$]

The compound [{$Cp(CO)_3W$}$_2$] was prepared by a modification of a reported literature method [2]. Dry sodium metal (0.2 g, 8.60 mmol) was reacted with freshly distilled dicyclopentadiene (2 ml, 11.5 mmol) in nitrogen-saturated diglyme (34 ml) for 3 hours. When all the metal had dissolved, hexacarbonyl tungsten (3.5 g, 9.94 mmol) was added and the reaction mixture refluxed under nitrogen (*ca.* 1¼ hours). The pink solution turned yellow at the end of the reaction. The product was allowed to cool to room temperature while under nitrogen flow (*ca.* 45 min.).

A solution of hydrated ferric sulphate was then prepared under nitrogen by dissolving hydrated ferric sulphate (3.5 g, 8.75 mmol) in nitrogen saturated distilled water (52.5 ml) and acetic acid (3.2 ml). The resulting light pink solution was used to precipitate the [{$Cp(CO)_3W$}$_2$] from the cooled solution above. The ferric sulphate solution was added slowly to the yellow solution over 30 minutes under nitrogen. The product was filtered off in air. The purple product was washed with cold distilled water (10 ml), methanol (10 ml) and pentane (10 ml) and dried in a dessicator overnight. The unreacted hexacarbonyl tungsten was sublimed off the product using a cold finger sublimation apparatus at 70 °C.

The product was obtained in about 60% yield, and had the properties stated in the literature [2].

5.2.2 Preparation of $Na[Cp(CO)_3W]$

Dried sodium (0.25 g, 10.8 mmol) was reacted with mercury (6 ml) under a nitrogen atmosphere in a Schlenk tube fitted with a tap at the bottom and the sodium amalgam left to cool to room temperature. Dry THF (10 ml) was added to the amalgam, followed by $[\{Cp(CO)_3W\}_2]$ (1.1 g, 1.65 mmol). Further THF (20 ml) was added making sure to wash down the tungsten dimer stuck on the sides of the dual-necked Schlenk tube. The dimer (red solution) was reduced to the anion (green solution), $Na[Cp(CO)_3W]$ (3.3 mmol), after 2 min of stirring. The mercury was drained off from the bottom of the Schlenk tube leaving the anion, which was used for the reaction described below.

5.2.3 Preparation of $[Cp(CO)_3W\{(CH_2)_nBr\}]$ n = 3 - 6

The $Na[Cp(CO)_3W]$ (3.3 mmol) in THF (30 ml) was added dropwise over 25 minutes, to a stirred solution of $Br(CH_2)_nBr$ (8.25 mmol) in THF (30 ml) while immersed at –25 to –30 °C. The solution was then allowed to attain room temperature (*ca.* 1 hr). The mixture was subsequently refluxed under nitrogen (using an oil bath set at 70 °C) for 14 hours. The product was allowed to cool to room temperature, filtered through a cannula under nitrogen, and the solvent removed under reduced pressure. The product was recrystallised from a dilute hexane/dichloromethane solvent mixture (10:1) at -78 °C. Analytically pure yellow solid was obtained. Yields and physical properties are listed in Table 2.1. Elemental Anal.: found. (calcd.): **1a** C 29.4 (29.0) H 2.8 (2.6); **2a** C 30.0 (30.7) H 2.7 (2.8); **3a** C 32.6 (32.9) 2.9 (2.1); **4a** C 34.2(33.8) H 3.1(3.4).

5.2.4 Preparation of $[Cp(CO)_3W\{(CH_2)_nI\}]$ n = 3 - 6

The dried sodium iodide and $[Cp(CO)_3W\{(CH_2)_nBr\}]$ n = 3 - 6, in a 2½:1 ratio, were dissolved in dry, nitrogen saturated acetone (10 ml). The solution was then stirred at room temperature for 18 hours, after which it was filtered via a cannula and the solvent removed under reduced pressure. The yellow solid was recrystallised twice from hexane (40 ml) at

–78 °C to give the analytically pure product. The yields and physical properties of the complexes are listed in Table 2.1. Elemental Anal.: found. (calcd.): **1b** C 26.1(26.3) H 3.1(3.2).

5.2.5 Some Reactions of the Tungsten Halogenoalkyl Compounds

5.2.5.1 $[Cp(CO)_3W\{(CH_2)_3CN\}]$

The compound $[Cp(CO)_3W\{(CH_2)_3I\}]$ (1.06 g, 2.11 mmol) was weighed into a small Schlenk tube. Sodium cyanide (0.124 g, 2.53 mmol) was added, followed by a mixture of nitrogen saturated double distilled de-ionised water (2 ml) and THF (2 ml). The mixture was stirred for 4 days. The solvent was removed under reduced pressure and the product recrystallised from a dichloromethane-hexane mixture and dried. The characterisation data are listed in Table 2.6.

5.2.5.2 $[Cp(CO)_3W\{(CH_2)_4ONO_2\}]$

A solution of $[Cp(CO)_3W\{(CH_2)_4Br\}]$ (0.1 g, 0.213 mmol) in acetonitrile (6 ml) was made and silver nitrate (0.036 g, 0.213 mmol) added. The reaction was monitored in the ν(CO) region of the infrared spectrum. The yellow solution turned green after 5 minutes. The solution was filtered via cannula under nitrogen into a pre-weighed Schlenk tube. Then the solvent was removed under reduced pressure leaving an orange precipitate. This was washed with hexane and the product dried under vacuum. This was characterised and data shown in Table 2.6.

5.2.5.3 $[Cp(CO)_3W\{(CH_2)_4N_3\}]$

The compound, $[Cp(CO)_3W\{(CH_2)_4Br\}]$ (0.1 g, 0.213 mmol) and sodium azide (0.014 g, 0.213 mmol) were weighed into an empty Schlenk tube. The Schlenk tube was evacuated and then filled with nitrogen and acetonitrile (7 ml) was subsequently added. There was a notable change in the ν(CO) region in the IR spectrum after 5 minutes. At the end of the reaction as determined by no further changes in the IR spectrum, the solution was filtered via cannula under nitrogen into a pre-weighed Schlenk tube. The solvent was removed

under reduced pressure leaving a yellow precipitate, which was washed with hexane and dried under vacuum (see Table 2.6).

5.2.5.4 [$Cp(CO)_3W\{(CH_2)_5N_3\}$]

A similar reaction to the above was carried out using [$Cp(CO)_3W\{(CH_2)_5I\}$] (0.054 g, 0.103 mmol). The compound [$Cp(CO)_3W\{(CH_2)_5N_3\}$] was obtained in 95% yield and the characterisation data was as shown in Table 2.6.

5.2.5.5 [$Cp(CO)_3W\{(CH_2)_4CN\}$]

The compound [$Cp(CO)_3W\{(CH_2)_4Br\}$] (0.1 g, 0.213 mmol) was weighed into a small Schlenk tube. An equimolar quantity of potassium cyanide (0.014 g, 0.215 mmol) was added into the tube and the air evacuated, after which the tube was filled with nitrogen. The mixture was dissolved in acetonitrile (5 ml), and stirred for 4 days while monitoring by ^1H NMR spectroscopy; after which the solution was filtered via a cannula and the solvent removed under reduced pressure. The yellow product obtained was recrystallised from dichloromethane/hexane, dried and characterised (Table 2.6).

5.2.5.6 [$Cp(CO)_3W\{(CH_2)_3CN\}$]

The compound [$Cp(CO)_3W\{(CH_2)_3I\}$] (0.1 g, 1.999 mmol) was weighed into a Schlenk tube. A 20% excess molar quantity of sodium cyanide (0.12 g, 0.239 mmol) was added followed by double distilled de-ionised nitrogen saturated water (5 ml). The mixture was stirred for 4 days. The solvents were removed under reduced pressure, and the sample recrystallised from dichloromethane/hexane and dried under vacuum to give a yellow product (see Table 2.6).

5.2.5.7 Reaction of [$Cp(CO)_3W\{(CH_2)_4Br\}$] with $Na_2S.2H_2O$

The compound, [$Cp(CO)_3W\{(CH_2)_4Br\}$] (0.1 g, 0.213 mmol) was weighed into an empty Schlenk tube. The crushed flakes of $Na_2S.2H_2O$ (0.028 g, 0.213 mmol) were added and the mixture dissolved in "super dry" Methanol (7 ml). A green solution was obtained after 4 hours of reaction. There was no significant change in the ν(CO) region of the IR spectrum.

The solution was filtered via cannula under nitrogen into a pre-weighed Schlenk tube. The solvent was removed under reduced pressure leaving behind a yellow precipitate. The residue was washed with hexane and dried under vacuum to give 81% yield of the product. IR(ν(CO) (CH_2Cl_2): 2011 cm^{-1} ss, 1912 cm^{-1} sb; m.p. 62 – 65 °C. No meaningful data were obtained from the ^1H NMR and ^{13}C NMR spectra.

The reaction was repeated in methanol. There were minimal changes in the NMR spectra and again the data could not be interpreted.

Also the bromoalkyl compounds **1a**, **2a**, **3a**, **4a**, were dissolved in water and left to stand overnight. They were then filtered and dried under reduced pressure the product analysed by using ^1H NMR. The spectra were identical to those of the original compounds.

5.2.6 Single-Crystal X-ray Diffraction Analyses of Compounds 1a and 3b

The X-ray diffraction data for the single crystals of [$Cp(CO)_3W\{(CH_2)_5I\}$], **3b** and [$Cp(CO)_3W\{(CH_2)_3Br\}$], **1a** presented in Figure 2.1 and 2.3 respectively, were collected on an Enraf-Nonius CAD4 diffractometer at 20(2) °C using Mo Kα wavelength radiation (0.70930 Å). The data were reduced with the program XCAD [3]. Semi-empirical absorption corrections were applied to the data for the iodo derivatives using a minimum of four reflections with χ-values > 75° (azimuthal ψ-scan method) with the program ABSCALC, as implemented in OSCAIL [4]. The data for the bromo derivative (**1a**) were corrected for absorption using the Fourier series method of DIFABS [5].

The structure of [$Cp(CO)_3W\{(CH_2)_5I\}$] was solved in the orthorhombic space group $P2_1nb$ with the direct methods program SHELXS-97 [6].

The structure of [$Cp(CO)_3W\{(CH_2)_3Br\}$] was solved in the triclinic space group $P\bar{1}$ with the direct methods program DIRDIF [7], as implemented by the crystallographic program WinGX [8].

In each case, the final model was plotted with Farrugia's 32-bit implementation of the program ORTEP [9]. Crystal data, lattice constants, and least-squares refinement details for the two compounds are listed in Appendix 1.

5.3 Experimental Details Pertaining to Chapter 3

Pentamethylcyclopentadiene (Aldrich 97%) was distilled prior to use. The compounds Ph_3P (Acros 98%), $MePh_2P$ (Acros 98%) and Me_2PhP Aldrich 97%) and Me_3P (Acros 97%, Silver iodide complex were used without further purification.

5.3.1 Preparation of the Dimers $[\{Cp(CO)_2(PPh_3)Mo\}_2]$, $[\{Cp(CO)_2(PPh_2Me)Mo\}_2]$, $[\{Cp(CO)_2(PPhMe_2)Mo\}_2]$, $[\{Cp(CO)_2(PMe_3)Mo\}_2]$ and $[\{Cp^*(CO)_3Mo\}_2]$

The molybdenum dimer $[\{Cp(CO)_3Mo\}_2]$ was synthesized according to a literature procedure [10]. The dimer was then used to prepare the compounds, $[\{Cp(CO)_2(PPh_3)Mo\}_2]$, $[\{Cp(CO)_2(PPh_2Me)Mo\}_2]$, $[\{Cp(CO)_2(PPhMe_2)Mo\}_2]$ according to the reported literature [11]. The dimer $[\{Cp^*(CO)_3Mo\}_2]$ was also prepared according to the literature procedure [12].

The molybdenum dimer, $[\{Cp(CO)_3Mo\}_2]$ (5.8 g, 11.8 mmol) was heated in diglyme (12 ml) and used to prepare $[\{Cp(CO)_2Mo\}_2]$ *in situ* (~9 mmol) according to literature procedure [10]. The mixture was allowed to cool to room temperature under nitrogen. The solvent dichloromethane (10 ml) was degassed using nitrogen gas and used to dissolve 2 equivalents of Ph_3P, $MePh_2P$ and Me_2PhP respectively. The solutions of the phosphines (18 mmol) were added into the prepared triple bonded dimer $[\{Cp(CO)_2Mo\}_2]$ (5.8 g, 913.4 mmol). The mixture was stirred at room temperature for a minimum of two and maximum of twenty-four hours. The formed precipitate was filtered at room temperature. The red to purple products of $[\{Cp(CO)_2(PPh_3)Mo\}_2]$, $[\{Cp(CO)_2(PPh_2Me)Mo\}_2]$ and $[\{Cp(CO)_2(PPhMe_2)Mo\}_2]$ were obtained in yields of 90 – 95%. The compounds had the respective spectroscopic data reported [11].

The compound $[\{Cp(CO)_2(PMe_3)Mo\}_2]$ was prepared in a similar manner, but with a further modification. The dimer $[\{Cp(CO)_2Mo\}_2]$ (11.8 mmol) was prepared by refluxing the compound $[\{Cp(CO)_3Mo\}_2]$ (5.8 g, 13.4 mmol) in 2-methoxyethyl ether (12 ml) under

a nitrogen sweep across the surface of the solution until the evolution of CO was judged to be complete [10]. The mixture was allowed to cool to room temperature under nitrogen. Degassed dichloromethane (10 ml) was added into the mixture. The solution was further degassed by using several freeze/thaw cycles under vacuum. The solution was connected to a U-tube connected to a flask containing the trimethylphosphine silver iodide complex (5.47 g, 18 mmol). The trimethylphosphine silver iodide complex was heated slowly and carefully to release a continuous flow of trimethylphosphine gas into the reaction vessel which was maintained in liquid nitrogen under vacuum. After all the trimethylphosphine gas had been driven into the reaction vessel, the mixture was allowed to attain room temperature while stirring. A bright red powdered dimer was obtained, filtered and kept in a dessicator. The yield of the product was 98% and the physical properties agreed with those in the literature [11].

5.3.2 Preparation of $[Cp(CO)_2(PPh_iMe_{3-i})Mo\{(CH_2)_nBr\}]$ i = 0 – 3, n = 3, 4

The solutions of the anions $Na[Cp(CO)_2(PPh_iMe_{3-i})Mo]$, i = 0 – 3, (0.477 mmol) in THF (25 ml) were prepared by reacting the dimers, $[\{Cp(CO)_2(PPh_iMe_{3-i})Mo\}_2]$ (i = 0 – 3) with Na/Hg amalgam { Na (0.3 g, 13.0 mmol)/Hg (8 ml)}. These anions were then added over 35 min to a stirred solution made by dissolving $Br(CH_2)_nBr$ (0.477 mmol) n = 3, 4, in THF (5 ml) and kept at –25 °C to –30 °C. The solutions were stirred for 15 min at this temperature and then allowed to attain room temperature (*ca.* 4 h). The reaction was followed by the spectroscopy, following the changes in the ν(CO) region. The reaction was stopped when the IR spectrum no longer showed the ν(CO) stretching frequencies due to the anions, $Na[Cp(CO)_2(PPh_iMe_{3-i})Mo]$. The solvent was removed under reduced pressure, leaving a yellow/black residue. This was extracted with dichloromethane (3 × 10 ml), and the solution filtered via a cannula under nitrogen and concentrated under reduced pressure to approximately a third of the total volume of the dichloromethane used. An excess of dry hexane was added to the concentrated solution until the product just started precipitating. The mixture, under a nitrogen atmosphere, was then immersed in a dry ice/acetone bath of temperature –78 °C (for *ca.* 2 h). The yellow product separated from the solution. The mother liquor was syringed off and the product dried under reduced pressure. Yields and physical properties are listed in Table 3.1. The residue after the dichloromethane extractions contained minor quantities of $[Cp(CO)_2(PPh_iMe_{3-i})(Br)Mo]$

and the respective dimers [{$Cp(CO)_2(PPh_iMe_{3-i})Mo\}_2$]. Elemental Anal.: found. (calcd.): **3a** C 51.52 (51.20), H 4.8 (4.49); **4a** C 52.07 (52.10), H 4.97 (4.74); **5a** C 44.52 (45.31) H 4.79 (4.65); **6a** C 46.37 (46.46), H 5.04 (4.92); **7a** C 37.98 (37.61), H 4.73 (4.86); **8a** C 38.71 (39.20), H 5.31 (5.17).

5.3.3 Preparation of $[Cp(CO)_2(PPh_iMe_{3-i})Mo\{(CH_2)_nI\}]$ i = 0 – 3, n = 3, 4

The bromoalkyl compounds were converted into their corresponding iodoalkyl compounds by the Finkelstein reaction [13]. NaI (0.45 g, 3.0 mmol) was added to a solution of $[Cp(CO)_2(PPh_iMe_{3-i})Mo\{(CH_2)_nBr\}]$ (0.15 mmol) in acetone (12 ml). The solutions were stirred at room temperature for 18–24 hours. This was stopped when a sample isolated from the reaction solution no longer showed the triplet due to the CH_2Br in the ^1H NMR spectrum. The solvent was removed under reduced pressure, leaving a yellow/orange residue. This was extracted with dichloromethane (3 × 10 ml), and the dichloromethane solution was filtered via a cannula under nitrogen. The filtrate was reduced to about a third of the total volume of the dichloromethane used. Hexane was then added to the concentrated solution until the product just started to precipitate. The mixture was cooled to –78 °C in a dry ice/acetone bath for several hours. A yellow product separated from the solution. The mother liquor was syringed off and the product dried under vacuum. Yields and physical properties are listed in Table 3.1. The syringed off mother liquor was concentrated and transferred to an alumina column. Elution with 10% dichloromethane/hexane gave an orange band which was identified as $[Cp(CO)_2(PPh_iMe_{3-i})(I)Mo]$ and a dark purple band which contained the respective dimers. Elemental Anal: found (calcd.): **3b** C 40.98 (41.24), H 4.09 (4.23); **4b** C 47.16 (48.02), H 4.63 (4.37).

5.3.4 Preparation of $[Cp(CO)_2(PPh_iMe_{3-i})Mo\{(CH_2)_nI\}]$ using $I(CH_2)_nI$ i = 0 – 3, n = 3, 4

A solution of $Na[Cp(CO)_2(PPh_iMe_{3-i})Mo]$ (0.25 mmol, 25 ml THF) was added dropwise into $I(CH_2)_nI$ (5 ml 0.25 mmol) n = 3, 4, immersed in a dry ice/acetone bath at –25 °C to –30 °C. After the complete transfer of the anion, the reaction solution was maintained at this temperature for 15 minutes while stirring, thereafter the mixture was stirred at room

temperature until the IR spectrum showed no ν(CO) bands due to the anion, $Na[Cp(CO)_2(PPh_iMe_{3-i})Mo]$. The solvent was removed under reduced pressure, leaving a yellow/orange residue. This was extracted with dichloromethane (3 × 10 ml), and the solution filtered via a cannula into a pre-weighed Schlenk tube. The filtrate was reduced to approximately a third of the total volume of dichloromethane used. Hexane was added drop by drop into the now concentrated filtrate until precipitation started. The mixture was immersed in an acetone/dry ice bath maintained at a temperature of –78 °C for several hours. The yellow product separated from the solution. The mother liquor was syringed off and the product dried under reduced pressure. Analytically pure products in very low yields (10 – 30%) were obtained. The physical properties matched with those reported for the compounds obtained in Section **5.3.3** above. Other minor products obtained were identified as $[Cp(CO)_2(PPh_iMe_{3-i})(I)Mo]$ and the respective dimers.

5.3.5 Preparation of $[\{Cp^*(CO)_3Mo\}_2]$

The dimer, $[\{Cp^*(CO)_3Mo\}_2]$, was prepared according to the literature [12], except that the Cp* was distilled prior to use and all reagents were degassed using nitrogen gas and thereafter the reactions carried out under nitrogen. The product had properties similar to those reported in the literature [12].

5.3.6 Preparation of $[Cp^*(CO)_3Mo\{(CH_2)_nBr\}]$, n = 3, 4

These were prepared using $[\{Cp^*(CO)_3Mo\}_2]$ in a similar manner to the above for the preparation of $[Cp(CO)_2(PPh_iMe_{3-i})Mo\{(CH_2)_nBr\}]$ in Section **5.3.2**. The characterization data are listed in Tables 3.1 – 3.3.

5.3.7 Preparation of $[Cp^*(CO)_3Mo\{(CH_2)_nI\}]$, n = 3, 4

These were prepared using the Finkelstein method, in the same manner as in the preparation of the $[Cp(CO)_2(PPh_iMe_{3-i})Mo\{(CH_2)_nI\}]$ compounds in Section **5.3.3** above. Again the characterization data are presented in Tables 3.1 – 3.3.

5.3.8 Single-Crystal X-ray Diffraction Analysis of Compound 1b

The X-ray data for the single crystal of $[Cp(CO)_2(PPh_3)Mo\{(CH_2)_3I\}]$ was collected on an Enraf-Nonius CAD4 diffractometer at 20(2) °C using Mo Kα wavelength radiation (0.70930 Å). The data were reduced with the program XCAD [2]. Semi-empirical absorption corrections were applied to the data using a minimum of four reflections with χ-values > 75° (azimuthal ψ-scan method) with the program ABSCALC, as implemented in OSCAIL [3]. The structure of $[Cp(CO)_2(PPh_3)Mo\{(CH_2)_3I\}]$ was solved in the monoclinic space groups $P2_1/n$; with the direct methods program DIRDIF [6], as implemented by the crystallographic program WinGX [7]. The final model was plotted with Farrugia's 32-bit implementation of the program ORTEP [8]. Crystal data, lattice constants, and least-squares refinement details are listed in Appendix 2.

5.3.9 Some Reactions of the Molybdenum Halogenoalkyl Compounds

5.3.9.1 $[Cp(CO)_2(PPhMe_2)Mo\{(CH_2)_3ONO_2\}]$

The compound $[Cp(CO)_2(PPhMe_2)Mo\{(CH_2)_3Br\}]$ (0.130 g, 0.257 mmol) and $AgNO_3$ (0.04 g, 0.257 mmol) were dissolved in acetonitrile (5 ml) and stirred for 24 hours. The resulting yellow solution was filtered by using a cannula under nitrogen into a pre-weighed Schlenk tube. The solution was removed under reduced pressure. The product was recrystallised from a dilute dichloromethane/hexane mixture. The orange precipitate was collected, dried and characterised as shown in Table 3.6.

5.3.9.2 $[Cp(CO)_2(PPhMe_2)Mo\{(CH_2)_3CN\}]$

(a) The compound, $[Cp(CO)_2(PPhMe_2)Mo\{(CH_2)_3Br\}]$ (0.102 g, 0.201 mmol) and AgCN (0.03 g, 0.201 mmol) were dissolved in acetonitrile (10 ml) and stirred for 18 hours. The resulting yellow-orange solution was filtered by using a cannula under nitrogen into a pre-weighed Schlenk tube. The solution was removed under vacuum. The product was recrystallised from a dilute dichloromethane/hexane mixture. The orange precipitate was collected and dried. The solution of the compound in $CDCl_3$ is unstable

and therefore no ^{13}C NMR spectrum was obtained. The compound was also observed to decompose immediately in air.

(b) The reaction above was repeated using sodium cyanide in ethanol ('super dry'). The compound, $[Cp(CO)_2(PPhMe_2)Mo\{(CH_2)_3Br\}]$ (0.124 g, 0.265 mmol) and NaCN (0.013 g, 0.265 mmol) were dissolved in dry ethanol (8 ml) and stirred for 8 days. The resulting yellow-orange solution was filtered by using a cannula under nitrogen into a pre-weighed Schlenk tube. The solvent was dried under vacuum. The product was recrystallised from a dilute dichloromethane/hexane mixture. An orange precipitate was obtained. The compound had no impurity and therefore was characterised and reported in Table 3.6.

5.3.9.3 $[Cp(CO)_2(PPhMe_2)Mo\{(CH_2)_3N_3\}]$

The compound, $[Cp(CO)_2(PPhMe_2)Mo\{(CH_2)_3Br\}]$ (0.08 g, 0.174 mmol) and NaN_3 (0.011 g, 0.175 mmol) were weighed into a Schlenk tube, dissolved in acetonitrile (8 ml) and stirred for 24 hours. The solution was then filtered via cannula under nitrogen and the solvent removed under reduced pressure. The residue was recrystallised from a dilute dichloromethane/hexane mixture. The orange precipitate was collected, dried and characterized as shown in Table 3.6.

5.3.9.4 Reaction of $[Cp(CO)_2(PPhMe_2)Mo\{(CH_2)_3Br\}]$ with Ag_2S

(a) The compound $[Cp(CO)_2(PPhMe_2)Mo\{(CH_2)_3Br\}]$ (0.042 g, 0.09 mmol) and Ag_2S (0.024 g, 0.096 mmol) were dissolved in acetonitrile (5 ml) and stirred for 18 hours. The solution was filtered via cannula under nitrogen and the solvent removed under reduced pressure. The product was recrystallised from a dilute dichloromethane/hexane mixture. The orange precipitate was collected and dried. The product was obtained in 38% yield. The compound was characterised and gave IR(ν(CO) (CH_2Cl_2): 2410 cm^{-1}s, 1967 cm^{-1}smb 1911 cm^{-1} sms; m.p. 71 – 78 °C; ^1H NMR ($CDCl_3$) Ph 7.4, 6.32 ppm, Cp 5.31 ppm, $-CH_2CH_2CH_2-$: 3.45, 2.13, 1.94, 0.042 ppm; ^{13}C NMR ($CDCl_3$) 128, 108, 96.44 ppm, Cp 94.62 ppm, Cp 93.89 ppm, $-CH_2CH_2CH_2-$: 61.67, 22.03, 18.48, 17.39 ppm.

(b) The reaction above was attempted in a similar manner with (2:1) $[Cp(CO)_2(PPhMe_2)Mo\{(CH_2)_3Br\}]$ (0.084 g, 0.18 mmol) and Ag_2S (0.024 g, 0.096 mmol) in acetonitrile (5 ml) and stirred for 18 hours. A mixture of products among them $[Cp(CO)_2(PPhMe_2)Mo\{(CH_2)_3SH\}]$, which was oily, in 42% yield was obtained. The compound was unstable that full characterisation was not possible.

5.4 Experimental Pertaining to Chapter 4

All the reagents used here were treated as previously described in Section **5.1** and **5.2**. Elemental analyses were performed by the LECO Company (USA) in addition to the SABS in Richards Bay. The carbon monoxide gas (Afrox HP) was used in the fumehood through a Parr 4842 Mini Bench Top Reactor, from where its flow was regulated.

5.4.1 Preparation of $[Cp(CO)_3W(CH_2)_3Mo(CO)_3Cp]$

The molybdenum dimer, $[\{Cp(CO)_3Mo\}_2]$ (0.88 g 1.65 mmol), was reduced to the anion by reacting with an amalgam made from the reaction of Na (0.25 g 10.8 mmol) and mercury (6 ml), and dissolved in tetrahydrofuran (25 ml). The resulting solution of the sodium anion, $Na[Cp(CO)_3Mo]$ (3.6 mmol), was added dropwise over 30 minutes to a stirred solution of $[Cp(CO)_3W\{(CH_2)_3I\}]$ (1.34 g, 2.67 mmol) dissolved in THF (6 ml) and maintained at -78 °C. The solution obtained was then stirred between -65 °C to -78 °C. The reaction was monitored for the changes within the ν(CO) region of the infrared spectrum. After 64 hours, no infrared bands due to the anion, $Na[Cp(CO)_3Mo]$ were observed. The mixture was, however, stirred for a further 12 hours to ensure complete reaction, after which it was filtered through a cannula under nitrogen. The solvent was removed under reduced pressure and the residue dissolved in a minimum amount of dichloromethane and transferred to a short chromatography column made up of alumina with hexane and maintained under nitrogen. Elution with hexane gave a light yellow band that was found only to contain the starting material. The second, intense, yellow band eluted was concentrated and cooled to -78 °C. The desired product separated from the solution. The mother liquor was syringed off and the product dried under reduced pressure.

It is also possible to avoid chromatography by four successive recrystallizations of the filtered product from a minimum of dichloromethane/hexane at –78 °C to give an analytically pure product. The yields, melting points and IR properties are found in Table 4.1. Elemental Anal.: found (calcd.): **1a** C 35.98 (36.69) H 2.77(2.59)

5.4.2 Preparation of $[Cp(CO)_3W(CH_2)_4Mo(CO)_3Cp]$

A Na/Hg amalgam (1%), was made by reacting Na (0.25 g, 10.8 mmol) and Hg (6 ml) under a nitrogen atmosphere. The amalgam was used to reduce the compound $[\{Cp(CO)_3Mo\}_2]$ (0.78 g, 1.59 mmol) in THF (30 ml) to the anion $Na[Cp(CO)_3Mo]$. A 30% excess of a solution of the sodium anion $Na[Cp(CO)_3Mo]$ (3.38 mmol), was added dropwise over 30 minutes into a stirred solution of $[Cp(CO)_3W\{(CH_2)_4I\}]$ (0.98 g, 1.89 mmol) in THF (6 ml) maintained at -78 °C. The reaction was maintained at this temperature for 84 hours while monitoring the ν(CO) changes within the infrared spectrum. Once the reaction was judged to be complete, the solution was filtered through a cannula under nitrogen and the solvent removed under reduced pressure. The residue was dissolved in a minimum of dichloromethane. An equal volume of hexane was added and the resulting mixture cooled to -78 °C. The product precipitated out, and the mother liquor was syringed off. The product was recrystallised out four times from dry hexane (80 ml in total) at -78 °C. The yield and physical properties are recorded in Table 4.1. Elemental Anal.: found (calcd.): **1b** C 36.84(37.77), H 2.87(2.85).

5.4.3 Preparation of $[Cp(CO)_3W(CH_2)_nMo(CO)_3Cp]$ n = 5, 6

The same reaction conditions and work-up procedures were done as in Section **5.4.2** above, except that the reactants, once mixed, were kept at -78 °C for 24 hours and then allowed to attain room temperature and stirred for a further 5 days. The physical data are listed in Table 4.1.

5.4.4 Preparation of $[Cp(CO)_3W(CH_2)_nMo(CO)_3Cp^*]$ n = 3, 4

The compound $[Cp^*Mo(CO)_3]_2$ (0.152 g, 0.242 mmol) was used to prepare the anion $Na[Cp^*Mo(CO)_3]$, by reducing it with Na (0.25 g, 10.8 mmol)/Hg (6 ml) in THF (25 ml). The anion $Na[Cp^*Mo(CO)_3]$ (0.484 mmol), was added dropwise over a period of 30 minutes to a stirred solution of $[Cp(CO)_3W\{(CH_2)_3I\}]$ (0.242 g, 0.484 mmol) dissolved in THF (5 ml) and maintained at -78 °C. The resulting mixture was kept at this temperature for a further 15 minutes. The solution was then allowed to attain room temperature and stirred for 64 hours until IR monitoring of the ν(CO) showed no signs of the anion present. The solution was then filtered through a cannula under nitrogen and the solvent removed under reduced pressure. The product was recrystallised from a dilute dichloromethane/hexane mixture immersed in an acetone/dry ice bath kept at -78 °C. The mother liquor was syringed off and the product dried under reduced pressure. The physical properties can be found in Table 4.1.

5.4.5 Preparation of $[Cp(CO)_2(PPh_iMe_{3-i})Mo(CH_2)_nW(CO)_3Cp]$ i = 0 - 3, n = 3 - 4

The anions $Na[Cp(CO)_2(PPh_iMe_{3-i})Mo]$ i = 0 - 3 (0.484 mmol) in THF (25 ml), were prepared by reducing the respective dimers, $[\{Cp(CO)_2(PPh_iMe_{3-i})Mo\}_2]$ (0.242 mmol) in a one percent solution of Na (0.25 g, 10.87 mmol)/Hg (6 ml). The solution of the anion was added dropwise over 30 minutes to a stirred solution of $[Cp(CO)_3W\{(CH_2)_nI\}]$ (0.484 mmol n = 3 – 4) in THF (5 ml) maintained at –78 °C in a dry ice/acetone bath. The resulting solution was stirred for a further 15 minutes at this temperature, and then allowed to attain room temperature before stirring for a further 3 days. The reaction was followed by IR spectrum, monitoring the ν(CO) stretching frequencies due to the anion, $Na[Cp(CO)_2(PPh_iMe_{3-i})Mo]$ i = 0 – 3 . When there were no more signs of the anion, the solvent was removed under reduced pressure, leaving a greenish/yellow residue. The residue was extracted with dichloromethane (3 x 10 ml), and the solution filtered via a cannula under nitrogen. The filtrate was reduced, under reduced pressure, to approximately a third of the total volume of the dichloromethane used. The yellow product was precipitated with hexane, and the mother liquor syringed off. The product was washed three times with hexane and dried under reduced pressure. The physical properties of the products are listed in Table 4.1. Elemental Anal.: found (calcd.): **6b** C 38.45(38.63) H 3.89(3.97).

5.4.6 Preparation of $[Cp(CO)_2(PPh_iMe_{3-i})Mo(CH_2)_nFe(CO)_2Cp]$ i = 0 - 3, n = 3, 4

By using Na (10.87 mmol)/Hg (6 ml), the dimers $[\{Cp(CO)_2Mo(PPh_iMe_{3-i})\}_2]$ i = 0 – 3 (0.28 mmol) were reduced to their respective anions, $Na[Cp(CO)_2Mo(PPh_iMe_{3-i})]$ i = 0 - 3 (0.56 mmol) in THF (25 ml). The solution of the anion was added drop by drop over 30 minutes to a stirred solution of $[Cp(CO)_2Fe\{(CH_2)_nI\}]$ n = 3, 4 (0.555 mmol) dissolved in THF (5 ml) at –78 °C. The solution was stirred for 15 minutes at this temperature, then allowed to attain room temperature and stirred for a further 5 days. This is when the infrared spectrum of a sample isolated from the reaction solution no longer showed the ν(CO) stretching frequencies due to the anion, $Na[Cp(CO)_2Mo(PPh_iMe_{3-i})]$. The solvent was removed under reduced pressure leaving a yellow/black residue. The residue was extracted with dichloromethane (3 x 10 ml), and the solution filtered via a cannula under nitrogen. The filtrate was concentrated under reduced pressure to approximately a third of the total volume of dichloromethane used originally. This solution was transferred to a short alumina column made up in hexane. The product was eluted with 90% dichloromethane/hexane, and the resulting solution concentrated and cooled to –78 °C under nitrogen for 30 minutes. The yellow product separated from the solution. The mother liquor was syringed off and the product dried under reduced pressure.

The chromatographical method used for the product purification was modified. Degassed alumina (~ 5g) was added to the filtrate after the extraction with dichloromethane. The solution was re-filtered through a cannula into another pre-weighed Schlenk tube. The solution was then reduced to a third of the total volume and the product precipitated out with hexane. This method gave better yield and cleaner products. Yields and physical properties are listed in Table 4.1. Elemental Anal.: found (calcd.): **7b** C 60.02(60.02), H 4.96(4.49); **9b** C 52.77(52.92), H 5.08(4.95); **10b** C 47.90(47.93), H 5.23(5.17).

5.4.7 Single-Crystal X-ray Diffraction Analyses of Compounds 3a and 7a

Slightly more than one equivalent volume hexane was added into a small concentrated solution of the compounds **3a** and **7a** in dichloromethane, in a vial. This mixture was left to stand in a refrigerator at –10 °C. The crystals grew by slow solvent diffusion after several days.

5.4.7.1 Crystal Structure of $[Cp(CO)_3W(CH_2)_3MoCO)_2(PPh_3)Cp]$

The X-ray data for the compound **3a** was collected as described below. Intensity measurements were made on a yellow crystal approximately 0.45 x 0.35 x 0.25 mm^3 in size on an Enraf-Nonius CAD4 diffractometer at 219(2) k. The unit cell was determined from 25 reflections (θ 2-12 deg.); the data were consistent with a triclinic lattice. Complete data collection (ω-2θ scan method, θ = 2-23 deg.) was effected with a scan angle of 1.10 deg. at a voltage of 55 kV and current of 35 mA(Mo K-α radiation). The data were reduced with the program XCAD (Oscail V8) [2], using Lorentz and polarization correction factors. The absorption correction was applied to the data using the program DIFABS (Oscail V8) [3].

The structure was solved in the monoclinic space group P 21/c with the direct methods program DIRDIF [5], as implemented by the crystallographic program WinGX [6]. The E-map led to the location of all non-hydrogen atoms; these were refined anisotropically with the program SHELXL-97 [7]. All hydrogens were included as idealized contributors in the least-squares process with standard SHELXL-97 idealization parameters. No evidence (difference Fourier map) for the inclusion of solvent in the lattice could be found. The final refinement converged to values of R1 = 0.0439 and wR2 = 0.1245 for 7363 unique observed reflections [I > 2.0 Σ (I)] and R1 = 0.0536 and wR2 = 0.1296 for all 8894 unique reflections. The maximum and minimum electron densities on the final difference Fourier map were 1.708 and -2.278 e/A^3, respectively. The final model was plotted using the program ORTEP [8].

5.4.7.2 Crystal Structure of $[Cp(CO)_2Fe(CH_2)_3Mo(CO)_2(PPh_3)Cp]$

The data Collection was carried out as described below. Intensity measurements were made on a yellow crystal approximately 0.45 x 0.4 x 0.3 mm^3 in size on an Enraf-Nonius CAD4 diffractometer at 228(2) K. The unit cell was determined from 25 reflections (θ 2-12 deg.); the data were consistent with a triclinic lattice. Complete data collection (ω-2θ scan method, θ = 2-23 deg.) was effected with a scan angle of 0.80 deg. at a voltage of 55 kV and current of 30 mA (Mo K-α radiation). Three reflections with the hkl indices 6 -2 3, 4 -6 -2, and 1 -8 -1 were used as intensity controls (14400 s intervals).

Two reflections (hkl indices 4 -6 -2 and 1 -8 -1) were used as orientation controls; these were checked automatically at intervals of 500 reflections. The data were reduced with the program XCAD (Oscail V8) [3] using Lorentz and polarization correction factors. A numerical absorption correction (DIFABS) [5] was applied to the data using the program Oscail [3].

The structure was solved in the monoclinic space group P 21/c with the direct methods program SHELXS-97 [3], as implemented by the crystallographic program Oscail [3]. The E-map led to the location of all non-hydrogen atoms; these were refined anisotropically with the program SHELXL-97 [7]. All hydrogens were included as idealized contributors in the least-squares process with standard SHELXL-97 idealization parameters. No evidence (difference Fourier map) for the inclusion of solvent in the lattice could be found. The final refinement converged to values of R1 = 0.0239 and wR2 = 0.0597 for 6786 unique observed reflections [$I > 2.0\ \Sigma(I)$] and 0.0366, wR2 = 0.0623 for all 8433 unique reflections. The maximum and minimum electron densities on the final difference Fourier map were 0.276 and -0.333 e/A^{-3}, respectively. The final model was plotted using the program ORTEP [8].

5.5 Analysis of Complexes 2a, 5b and 10a by Liquid Chromatography Time-of-Flight Mass Spectrometer

The three samples were analysed on the Jaguar LC-TOF-MS at the LECO Corporation Separation Science Laboratory in the United States.

The samples were analysed by direct infusion liquid chromatography (LC) coupled with the LECO Jaguar® Time-of-Flight Mass Spectrometer (TOF-MS). Approximately 1.7 mg of each complex was dissolved in 2 ml acetonitrile. Of the 2 ml solution, 1ml was diluted to 10 ml with acetonitrile and injected into the instrument with a flow rate of 1.5 µl/min. The instrument conditions used for the data acquisition in the analysis as reported to us are listed below.

Table 5.1: LC and TOF-MS conditions for the analysis of complexes **2a**, **5b** and **10a**

Detector:	LECO® Jaguar® Time-ofFlight Mass Spectrometer
Data Acquisition:	5 KHz Repitition, 800 summed spectra: positive ion mode
Stored Mass Range:	20 6000 amu
Direct Infusion:	Harvard microsyringe pump (Model PHD 2000)
Transfer Line:	PEEK
Infusion time:	2 min
Source	Microelectrospray (ESI) source
Ionisation conditions:	Nozzle voltage: 100 V; Skimmer voltage: 65 V

5.6 Some Reactions of the Heterobimetallic Compounds

5.6.1 $[Cp(CO)_3W(CH_2)_3C(O)Mo(CO)(PMe_3)(PPh_3)Cp]$

(a) A solution of the complex, $[Cp(CO)_3W(CH_2)_3Mo(CO)_2(PMe_3)Cp]$ **6a** (0.098 g, 0.173 mmol) was made up in acetonitrile (5 ml) and PPh_3 (0.038 g, 0.146 mmol) was added. The mixture was stirred at room temperature until no more changes were observed in the ν(CO) region in the IR spectrum (18 hours). An orange precipitate was obtained. The solvent was removed under reduced pressure. The light yellow residue was dissolved in minimum dichloromethane and the product precipitated with hexane. Light yellow precipitate was obtained in 88% yield and was characterised (see Table 4.7).

(b) The above reaction was repeated in a 1:2 molar reaction ratio of the compound **6a** and PPh_3 and results, similar to the above were obtained. The product yield was 72%. The compound was unstable and the ^{13}C NMR spectrum was not recorded.

5.6.2 $[Cp(CO)_3W(CH_2)_4C(O)Mo(CO)(PMe_3)_2Cp]$

A solution of $[Cp(CO)_3W(CH_2)_4Mo(CO)_2(PMe_3)Cp]$ (0.10 g, 0.172 mmol) and PMe_3 (0.013 g, 0.172 mmol) was made up in acetonitrile (5 ml). The mixture was stirred at room temperature for 3 days while monitoring the reaction progress using ^1H NMR spectroscopy, until the reaction was judged to be complete by monitoring the appearance

of an expected triplet. A dirty orange solution was obtained. The solvent was removed under reduced pressure. The light yellow residue obtained was dissolved in minimum dichloromethane, filtered and the product precipitated with hexane. A light brown precipitate was obtained and characterised to give the data as listed in Table 4.7.

5.6.3 $[Cp(CO)_2Fe(CH_2)_3C(O)Mo(CO)_2(PMe_3)Cp]$

The complex $[Cp(CO)_2Fe(CH_2)_3Mo(CO)_2(PMe_3)Cp]$ (0.15 g, 0.31 mmol) was dissolved in acetonitrile (5 ml) in a Schlenk tube and sealed with a rubber suba seal. Using a slender, flexible Teflon tube, carbon monoxide gas was bubbled into the solution from a Parr reactor maintained at a flow rate of 0.7 PSI per hour. The reaction was followed by observing changes in the ν(CO) region in the infrared spectrum, by using a liquid cell made up of a sodium chloride window. A sharp strong acyl band was observed in the carbonyl region of the IR spectrum. The bubbling was stopped after 30 hrs. The product was dried under vacuum and recrystallised from dichloromethane/hexane. The final product was characterised and gave the data as shown in Table 4.7.

5.6.4 $[Cp(CO)_3W(CH_2)_3C(O)Mo(CO)_3Cp]$

The above reaction in Section **5.6.3** was repeated using the complex $[Cp(CO)_3W(CH_2)_3Mo(CO)_3Cp]$ (0.115 g, 0.186 mmol) dissolved in acetonitrile (5 ml). The experimental observations were similar except that the acyl peak was observed intermittently; however, the final product contained the acyl group. The product in 98% yield, was unstable that the only partially characterised as indicated in Table 4.7.

5.6.5 $[Cp(CO)_2Fe(C_4H_7)^+Mo(CO)_3Cp^*]\ PF_6$

The compounds $[Cp(CO)_3W(CH_2)_3Mo(CO)_2(Ph_2Me)Cp]$ (0.128 g, 0.168 mmol), $[Cp(CO)_3W(CH_2)_4Mo(CO)_2(Ph_2Me)Cp]$ (0.078 g, 0.1 mmol), $[Cp(CO)_2Fe(CH_2)_4Mo(CO)_2(PMe_3)Cp]$ (0.10 g, 0.235 mmol), $[Cp(CO)_3W(CH_2)_3Mo(CO)_3Cp^*]$ (0.16 g, 0.232 mmol), $[Cp(CO)_2Fe(CH_2)_3Mo(CO)_3Cp^*]$ (0.168 g, 0.334 mmol) and, $[Cp(CO)_3W(CH_2)_3Mo(CO)_3Cp]$ (0.17 g, 0.275 mmol) were separately dissolved in a dry dichloromethane (2 ml) and a slightly more than one equivalent triphenylcarbeniumhexafluorophosphate in dichloromethane (4 ml) was added.

The mixtures were left to stand at room temperature and any significant changes monitored through observing the ν(CO) region in the infrared spectrum. A bluish solution was always obtained, which was an indication of the decomposition of the compounds to their respective metals. A modification to this experiment was done. The dichloromethane solvent used for the dissolution of the two reagents was saturated with nitrogen for 30 minutes then cooled down to –20 °C to precipitate any formed water that was suspected to cause the decomposition. This was then used immediately to dissolve the reagents. The solution of $[Cp(CO)_2Fe(CH_2)_4Mo(CO)_3Cp^*]$ (0.107 g, 0.207 mmol) in dichloromethane (2 ml) was then cooled down to –40 °C, as it was suspected that the reaction also might have been exothermic, and thus generated heat could contribute to the decomposition. The trityl salt, Ph_3CPF_6, (0.095 g, 0.244 mmol) in dichloromethane (4 ml) was added down the side of the Schlenk tube maintained at –40 °C. The reaction mixture was allowed to warm up to room temperature and left to stand for 6 days. The dark green precipitate that formed was filtered off and dried under vacuum. The product was recrystallised from a dry acetone/hexane. A purple solution was observed on the addition of acetone and a whitish precipitate observed on addition of the hexane. The precipitated mixture was stood in the fridge at 4 °C for 1 hour. The mother liquor was drained off and the residue dried under vacuum. The residue was finally washed with dry ether yielding a blue-green product that was characterised only by IR and ^{1}H NMR spectroscopy (see Table 4.7) since the product was unstable in the acetone solution to give a ^{13}C NMR spectrum. However, low temperature NMR that could have been used was not readily available.

5.6.6 $[Cp(CO)_3W(CH_2)_3C(O)Mo(CO)_2(PPh_3)Cp^*]$

(a) The compound $[Cp(CO)_3W(CH_2)_3Mo(CO)_3Cp^*]$ (0.20 g, 0.29 mmol) and PPh_3 (0.076 g, 0.29 mmol) in a 1:1 molar ratio, were weighed into a Schlenk tube and the mixture dissolved in acetonitrile (4 ml). The solution was stirred at room temperature for 3 days, after which the solvent was removed under reduced pressure. The yellow product was dissolved in a minimum of dry dichloromethane. Dry hexane was added until the product just started to precipitate. The mixture was then immersed in a cold dry-ice- acetone bath (-60 °C) for two minutes. The mother liquor was drained off and the residue dried under vacuum. A yellow powder was obtained and characterised (see Table 4.7).

(b) The above reaction **(a)** was repeated in a 1:2 reaction ratio. The compound $[Cp(CO)_3W(CH_2)_3Mo(CO)_3Cp^*]$ (0.20 g, 0.29 mmol) was reacted with PPh_3 (0.152 g, 0.58 mmol) in acetonitrile (4 ml) at room temperature for 4 days. The solvent was removed under reduced pressure. Again, as above, the product was recrystallised from dichloromethane/hexane and the product (yield 93%) dried under vacuum. Similar spectroscopic data were obtained as shown in Table 4.7.

5.6.7 $[Cp(CO)_3W(CH_2)_3C(O)Mo(CO)_2(PPh_3)Cp]$ (acetonitrile)

(a) A mixture of the complex $[Cp(CO)_3W(CH_2)_3Mo(CO)_3Cp]$ (0.11 g, 0.178 mmol) and PPh_3 (0.047 g, 0.179 mmol) were weighed into a Schlenk tube and dissolved in acetonitrile (4 ml). The resulting solution was stirred at room temperature. The solvent was removed under reduced pressure, after 3 days. During the second day of the reaction, a strong peak was observed at 1712 cm^{-1} in the spectrum. This peak was not observed on the third day of the reaction, but was again observed in the final product. The product, a yellow precipitate, was filtered off and recrystallised from a minimum of dry dichloromethane and hexane. The mixture was immersed in a cold dry-ice-acetone bath (-60 °C) for a minute. The mother liquor was decanted and the residue dried under reduced pressure. A yellow powder was obtained and characterised (Table 4.7).

(b) The reaction above was repeated with 1:2 molar ratio of the compounds, $[Cp(CO)_3W(CH_2)_3Mo(CO)_3Cp]$ (0.11 g, 0.178 mmol) and PPh_3 (0.094 g, 0.358 mmol) in acetonitrile (4 ml). The solution was stirred at room temperature for 3 days. The solvent was then removed under reduced pressure and the product recrystallised from a dilute dichloromethane/hexane mixture. The yellow precipitate was filtered off and dried to give the product $[Cp(CO)_3W(CH_2)_3C(O)Mo(CO)_2(PPh_3)Cp]$ as confirmed from the spectroscopic data (Table 4.7).

5.6.8 $[Cp(CO)_3W(CH_2)_3C(O)Mo(CO)_2(PPh_3)Cp]$ (THF)

(a) A mixture of the complex $[Cp(CO)_3W(CH_2)_3Mo(CO)_3Cp]$ (0.105 g, 0.17 mmol) and PPh_3 (0.044 g, 0.17 mmol) were weighed into a Schlenk tube and dissolved in a

minimum volume of THF (8 ml). The resulting solution was refluxed at room temperature, while monitoring the changes in the carbonyl region of the infrared spectrum twice a day. No further changes were observed on days 8 and 9. The reaction was allowed to cool to room temperature under nitrogen. The solvent was then removed under reduced pressure. A reddish residue was obtained and dissolved in a minimum of dichloromethane, precipitated using hexane and the product filtered off. An orange/yellow precipitate was obtained, which was dried under reduced pressure to give the product, which was partially characterised and gave similar data that suggested it to be similar to the compound in Section **5.6.7** above. The compound was unstable in the NMR solutions and thus the ^{1}H NMR and ^{13}C NMR gave "messy" spectra that were not meaningful.

(b) The above reaction was repeated for a 2:1 ratio of PPh_3 (0.084 g, 0.320 mmol) and $[Cp(CO)_3W(CH_2)_3Mo(CO)_3Cp]$ (0.10 g, 0.161 mmol) in THF (8 ml). Again the changes were monitored using IR in the carbonyl region of the IR spectrum, and the reaction was judged to be complete after 11 days. Work-up of the product was repeated as above and a yellow product was obtained which was dried and partially characterised, again it was similar to the compound in Section **5.6.7** above. The yield obtained was 84%. The IR(ν(CO) (CH_2Cl_2): 2010 cm^{-1} ss, 1913 cm^{-1} sm, 1870 ss cm^{-1}, 1848 cm^{-1} sh; m.p. 182 – 185 °C; ^{1}H NMR($CDCl_3$) Ph 7.4 ppm, Cp 5.45, 5.13 ppm, –$CH_2CH_2CH_2$–: 1.65, 1.23, 0.85 ppm; ^{13}C NMR($CDCl_3$) Ph 128 ppm, Cp 91.95, 91.74 ppm, (-CH_2-) 29.68 ppm.

5.6.9 $[Cp(CO)_3W(CH_2)_3C(O)Mo(CO)_2(PBu_3)Cp]$

A solution of the complex $[Cp(CO)_3W(CH_2)_3Mo(CO)_3Cp]$ (0.15 g, 0.242 mmol) and PBu_3 (0.048 g, 0.242 mmol) was made up in acetonitrile (5 ml). The mixture was stirred overnight at room temperature. An orange/red precipitate formed. The solvent was removed under reduced pressure. The light orange residue was dissolved in a minimum of dichloromethane and the product, precipitated with hexane and filtered off. A light orange/yellow precipitate was obtained and dried under reduced pressure to give $[Cp(CO)_3W(CH_2)_3C(O)Mo(CO)_2(PBu_3)Cp]$ in 92% yield. The characterisation data obtained are given below; IR(ν(CO) (CH_2Cl_2): 2009 cm^{-1} s, 1910 cm^{-1} sb, 1839 cm^{-1}, 1604

cm^{-1} w; ^1H NMR($CDCl_3$) 6.32 ppm, Cp 5.35, 5.10, 3.11 ppm, $-CH_2CH_2CH_2CH_2-$:2.52, 2.46, 1.54, 0.98, 0.85 ppm; ^{13}C NMR($CDCl_3$) (CO) 249, 228, 217, 177 ppm, Cp 95.01, 91.47 ppm, (P-Butyl), 31.57, 30.62, 24.00, 23.79, 22.62, 21.06, 19.80, 19.19, 18.36, 17.43 ppm, $-CH_2CH_2CH_2CH_2-$: 36.16, 33.16, 14.10, -13.42 ppm.

5.6.10 Thermal Decomposition of $[Cp(CO)_2Fe(CH_2)_3Mo(CO)_2(PMe_3)Cp]$, $[Cp(CO)_3W(CH_2)_3Mo(CO)_3Cp^*]$ and $[Cp(CO)_3W(CH_2)_3Mo(CO)_2(PMe_3)Cp]$

(a) The compound $[Cp(CO)_2Fe(CH_2)_3Mo(CO)_2(PMe_3)Cp]$ (0.1 g, 0.208 mmol) was weighed into a Schlenk tube, which was connected to another Schlenk tube containing $CDCl_3$ immersed in liquid nitrogen. The two Schlenk tubes were attached to a vacuum system. The Schlenk tube containing the compound was heated to decomposition. The gaseous products were trapped by the Schlenk tube immersed in the liquid nitrogen. The residue after the heating was reddish in colour. The collected gaseous product condensed and dissolved into the $CDCl_3$. The solution was allowed to attain room temperature and a ^1H NMR experiment was performed. The data obtained were as follows; (propene) 3.73 ppm and (Cyclopropane) 0.223 ppm, 1.83 ppm.

(b) The above experiment was repeated for $[Cp(CO)_3W(CH_2)_3Mo(CO)_3Cp^*]$ (0.1 g, 0.161 mmol) and $[Cp(CO)_3W(CH_2)_3Mo(CO)_2(PMe_3)Cp]$ (0.1 g, 0.15 mmol). Similar results were obtained that gave the following peaks in the ^1H NMR($CDCl_3$) spectrum: (Propene) 3.73, 2.96, 1.83 ppm and (Cyclopropane) 0.224, 0.85 ppm.

5.6.11 Crystal Structure of $[Cp(CO)_3W\{(CH_2)_3COOH\}]$

Crystals of $[W(Cp)(CO)_3\{(CH_2)_3COOH\}]$ were yellow rhombus with the approximate dimensions 0.40 × 0.30 × 0.30 mm. X-ray diffraction data were collected on an Enraf-Nonius CAD4 diffractometer at 295(2) K with graphite-monochromated Mo Kα radiation (λ = 0.71703 Å, 2.4 kW). The data were reduced with the program XCAD4 [14], as implemented in WinGX [15] and were corrected for absorption using the program DIFABS [16]. A total of 4483 unique reflections [$3926 > 2\sigma(I)$] were collected. The E-statistics were consistent with a centrosymmetric data set. The structure of $[Cp(CO)_3W\{(CH_2)_3COOH\}]$ was solved in the triclinic space group $P\bar{1}$ by direct methods,

using SHELX-97 [17]. The asymmetric unit comprised two full independent molecules at general positions. All non-hydrogen atoms were cleanly located in the difference Fourier map. Hydrogen atoms were included as idealized contributors in the least-squares process with standard SHELXL-97 idealization parameters. The final refinement converged to the discrepancy indices given in Table 1 of Appendix 5. The maximum (and minimum) electron densities on the final difference Fourier map were 1.470 and –1.595 e $Å^{-3}$, respectively. The final model was plotted with ORTEP3 for Windows [18].

Complete crystallographic details, fractional atomic coordinates, anisotropic thermal parameters, fixed hydrogen atom coordinates, bond lengths, bond angles, and dihedral angles for $[Cp(CO)_3W\{(CH_2)_3COOH\}]$ are given in the Supporting Information listed in Appendix 5.

5.6.12 Attempted Synthesis of $[Cp(CO)_2W(CH_2)_n]^+[SbF_6]^-$ n = 3, 4

(a) An empty Schlenk tube was evacuated and filled with nitrogen. The Schlenk tube (nitrogen filled) and a bottle of silverhexafluoroantimonate (I) ($AgSbF_6$, Riedel-de Haen 98%) were inserted into a glove bag (Instruments for Research and Industry, X-27 –27). The glove bag was then flushed and filled with nitrogen. Some weight of $AgSbF_6$ was transferred from the container of the $AgSbF_6$ into the empty Schlenk tube. The Schlenk tube now with the compound $AgSbF_6$, was stoppered, removed from the inside of the glove bag and weighed. A corresponding molar quantity of the halogenoalkyl compound $[Cp(CO)_2W(CH_2)_3I]$ to that of the $AgSbF_6$ was then added. The Schlenk tube containing the mixture of the reagents was re-evacuated again and filled with nitrogen. The two reactants were then dissolved in a minimum of THF and stirred at room temperature for 8 hours. The resulting mixture was dried under reduced pressure and extracted with 3x10 ml dry dichloromethane. The filtrate was reduced, under reduced pressure, to a third of the original volume and the product precipitated with dry hexane. The mother liquor was syringed off and the product dried under vacuum. Yield of 66% was obtained. The product was unstable in NMR solutions and thus could not be fully characterised.

(b) The above experiment was repeated in a similar manner by using the compound $[Cp(CO)_2W(CH_2)_4I]$. The product that was again, unstable and therefore not characterised, was obtained in 73% yield.

Several attempts to investigate the oxidative addition reactions, by the use of Vaska's complex, $[(Cl)(CO)(PPh_3)_2Ir]$ with $I(CH_2)_3I$ and $[Cp(CO)_3W\{(CH_2)_3I\}]$ failed.

5.7 References:

[1] B.S. Furniss, A.J. Hannaford, P.W.G. Smith, A.R. Tatchell, "Vogel's Textbook of Practical Organic Chemistry", 5th Ed.; Longman, New York, 1978 p 401.

[2] R. Birdwhistell, P Hacket, A.R. Manning, *J. Organomet. Chem.*, **157** (1978) 239.

[3] OSCAIL Version 8: P. McArdle, Crystallography Center, Chemistry Department, NUI Galway, Ireland. P. McArdle, *J.Appl.Cryst.*, **28** (1995) 65.

[4] OSCAIL Version 8: P. McArdle, Crystallography Center, Chemistry Department, NUI Galway, Ireland. P. McArdle, *J.Appl.Cryst.*, **28** (1995) 65.

[5] DIFABS: N. Walker, D. Stuart, *Acta Crystallogr., Sect. A*, **A39** (1983) 158.

[6] (a) SHELXL-97: G.M. Sheldrick, University of Gottingen.
(b) G.M. Sheldrick, *Acta Cryst.*, **A46** (1990) 467.
(c) G.M. Sheldrick, *Acta Cryst.*, **D49** (1993) 18.
(d) G.M. Sheldrick, T.R. Schneider, *Methods in Enzymology*, **277** (1997) 319.

[7] DIRDIF96: P.T. Beurskens, G. Beurskens, W.P. Bosman, R. de Gelder, S. Garcia-Granda, R.O. Gould, R. Israel, J.M.M. Smits, Crystallography Laboratory, University of Nijmegen, The Netherlands. 1996.

[8] WinGX: A Windows Program for Crystal Structure Analysis. L.J. Farrugia, University of Glasgow, Glasgow, 1998.

[9] (a) ORTEP3 for Windows V1.01 beta: L.J. Farrugia, Department of Chemistry, University of Glasgow, Glasgow G12 8QQ, Scotland, 1998.
(b) ORTEP III: M.N. Burnett, C.K. Johnson, Oak Ridge National Laboratory report ORNL-6895, 1996.

[10] M.D. Curtis, M.S. Hay, *Inorg. Synth.*, **28** (1990) 150.

[11] N. Chip, J.A. Robert, *Inorg. Chem.*, **37** (1998) 2975–2983.

[12] M. Fei, S.K. Sur, D.R. Tyler, *Organometallics*, **10** (1991) 419–423.

[13] J. March, "Advanced Organic Chemistry: Reactions, Mechanisms and Structure", 4th ed.; Wiley-Interscience: New Yolk, 1992; p 430.

[14] XCAD4 - CAD4 Data Reduction. K. Harms, S. Wocadlo, University of Marburg, Marburg, Germany, 1995.

[15] ORTEP3 for Windows - L. J. Farrugia, *J. Appl. Crystallogr.*, **30** (1997) 565.

[16] N. Walker, D. Stuart, *Acta Cryst.* **A39**, (1983)158.

[17] SHELX-97 - Programs for Crystal Structure Analysis (Release 97-2). G. M. Sheldrick, Institüt für Anorganische Chemie der Universität, Tammanstrasse 4, D-3400 Göttingen, Germany, 1998.

[18] WinGX - L. J. Farrugia, *J. Appl. Crystallogr.*, **32**,(1999) 837.

APPENDICES

APPENDIX 1

X-ray Crystal Data Pertaining to Chapter 2

Table 1: Crystal data and structure refinement for $[(\eta^5\text{-}C_5H_5)(CO)_3W\{(CH_2)_5I\}]$. [a]

Empirical formula	$C_{13}H_{15}IO_3W$
Formula weight	530.00
Temperature	293(2) K
Wavelength	0.70930 Å
Crystal system	Orthorhombic
Space group	$P2_1nb$
Unit cell dimensions	a = 8.3227(9) Å
	b = 14.0192(16) Å
	c = 12.5856(13) Å
Volume	1468.5(3) Å^3
Z	4
Density (calculated)	2.397 g cm^{-3}
Absorption coefficient	9.966 mm^{-1}
F(000)	976
Crystal size, colour	0.20 × 0.15 × 0.15 mm^3, yellow
Voltage, Current	55 kV, 30 mA
Scan angle	0.90°
Diffractometer	Enraf-Nonius CAD4
Theta range for data collection	2.17–22.97°
Index ranges	$-2 \le h \le 9$; $-5 \le k \le 15$; $-13 \le l \le 13$
Reflections collected	3181
Independent reflections	1409 [R_{int} = 0.0261]
Reflections observed (>2σ)	1219
Absorption correction	Semi-empirical
Max. and min. transmission	0.3164 and 0.2405
Refinement method	Full-matrix least-squares on F^2
Data / restraints / parameters	1409 / 37 / 140
Goodness-of-fit on F^2	1.036
Final R indices [$I > 2\sigma(I)$]	R_1 = 0.0234, wR_2 = 0.0615
R indices (all data)	R_1 = 0.0295, wR_2 = 0.0642
Absolute structure parameter	0.18(6)
Largest diff. peak and hole	0.547 and –0.893 e Å^{-3}

d's of the least significant digits are given in parentheses.

Table 2: Bond lengths for $[(\eta^5\text{-}C_5H_5)(CO)_3W\{(CH_2)_5I\}]$. [a]

Bond	Distance (Å)	Bond	Distance (Å)
W–C(3)	1.88(3)	W–C(2)	1.994(10)
W–C(1)	2.08(3)	W–CP1	2.347(12)
W–CP2	2.373(19)	W–CP5	2.307(14)
W–C(4)	2.348(10)	W–CP3	2.349(8)
W–CP4	2.308(19)	I–C(8) [b]	2.121(10)
O(2)–C(2)	1.140(12)	O(1)–C(1)	1.12(4)
O(3)–C(3)	1.14(3)	CP1–CP2	1.391(7)
CP1–CP5	1.391(7)	CP2–CP3	1.391(7)
CP3–CP4	1.391(7)	CP4–CP5	1.391(7)
C(4)–C(5)	1.532(16)	C(5)–C(6)	1.505(11)
C(6)–C(7)	1.507(12)	C(7)–C(8)	1.491(16)
C(8)–I [c]	2.121(10)		

[a] The esd's of the least significant digits are given in parentheses. [b] Symmetry transformation used to generate equivalent atoms: $x, y - 1/2, -z + 5/2$. [c] Symmetry transformation used to generate equivalent atoms: $x, y + 1/2, -z + 5/2$.

Table 3: Bond angles for $[(\eta^5\text{-}C_5H_5)(CO)_3W\{(CH_2)_5I\}]$. [a]

Bond angle	(°)	Bond angle	(°)
C(3)–W–C(2)	74.6(11)	C(3)–W–C(1)	106.7(3)
C(2)–W–C(1)	82.3(11)	C(3)–W–CP1	147.7(9)
C(2)–W–CP1	95.6(6)	C(1)–W–CP1	102.2(9)
C(3)–W–CP2	150.9(10)	C(2)–W–CP2	128.4(8)
C(1)–W–CP2	95.2(10)	CP1–W–CP2	34.3(3)
C(3)–W–CP5	113.2(9)	C(2)–W–CP5	88.6(5)
C(1)–W–CP5	134.9(10)	CP1–W–CP5	34.76(17)
CP2–W–CP5	57.5(3)	C(3)–W–C(4)	77.2(12)
C(2)–W–C(4)	133.2(3)	C(1)–W–C(4)	71.0(12)
CP1–W–C(4)	126.8(7)	CP2–W–C(4)	92.6(7)
CP5–W–C(4)	137.2(5)	C(3)–W–CP3	116.6(11)
C(2)–W–CP3	146.4(4)	C(1)–W–CP3	120.0(11)
CP1–W–CP3	57.3(3)	CP2–W–CP3	34.3(2)
CP5–W–CP3	57.8(3)	C(4)–W–CP3	80.1(3)
C(3)–W–CP4	98.3(10)	C(2)–W–CP4	115.9(9)
C(1)–W–CP4	152.5(11)	CP1–W–CP4	57.8(3)
CP2–W–CP4	57.5(3)	CP5–W–CP4	35.1(3)
C(4)–W–CP4	104.5(7)	CP3–W–CP4	34.74(19)
CP2–CP1–CP5	108.0	CP2–CP1–W	73.9(5)
CP5–CP1–W	71.0(9)	CP1–CP2–CP3	108.0
CP1–CP2–W	71.9(4)	CP3–CP2–W	71.9(6)
CP2–CP3–CP4	108.0	CP2–CP3–W	73.8(8)
CP4–CP3–W	71.0(8)	CP5–CP4–CP3	108.0
CP5–CP4–W	72.4(4)	CP3–CP4–W	74.2(7)
CP4–CP5–CP1	108.0	CP4–CP5–W	72.5(5)
CP1–CP5–W	74.2(9)	O(1)–C(1)–W	177(3)
O(2)–C(2)–W	170(4)	O(3)–C(3)–W	179(2)
C(5)–C(4)–W	121.0(8)	C(6)–C(5)–C(4)	112.7(10)
C(5)–C(6)–C(7)	113.9(7)	C(8)–C(7)–C(6)	114.3(9)
C(7)–C(8)–I [b]	113.0(9)		

[a] The esd's of the least significant digits are given in parentheses. [b] Symmetry transformation used to generate equivalent atoms: $x, y + 1/2, -z + 5/2$.

Table 4: Crystal data and structure refinement for $[Cp(CO)_3W\{(CH_2)_3Br\}]$.

	$[Cp(CO)_3W\{(CH_2)_3Br\}]$
Empirical formula	$C_{11}H_{11}BrO_3W$
Formula weight	454.96
Temperature	293(2) K
Wavelength	0.70930 Å
Crystal system	Triclinic
Space group	$P\bar{1}$
Unit cell dimensions	a = 6.8337(14) Å, α = 97.13(2)°
	b = 12.896(4)Å, β = 89.995(18)°
	c = 14.355(3)Å, γ = 90.08(3)°
Volume	1255.3(5) $Å^3$
Z	4
Density (calculated)	2.407 g cm^{-3}
Absorption coefficient	12.374 mm^{-1}
F(000)	840
Crystal size	0.35 × 0.25 × 0.15 mm^3
Voltage, Current	55 kV, 35 mA
Scan angle	1.45°
Diffractometer	Enraf-Nonius CAD4
Theta range for data collection	2.00 to 24.97°
Index ranges	$-8 \leq h \leq 8$; $-15 \leq k \leq 15$; $0 \leq l \leq 17$
Reflections collected	4397
Independent reflections	4397 [R_{int} = 0.0000]
Reflections observed (>2σ)	3025
Absorption correction	Fourier series
Max. and min. transmission	0.2583 and 0.0982
Refinement method	Full-matrix least-squares on F^2
Data / restraints / parameters	4397 / 0 / 289
Goodness-of-fit on F^2	1.052
Final R indices [$I > 2\sigma(I)$]	R_1 = 0.0493, wR_2 = 0.1236
R indices (all data)	R_1 = 0.0851, wR_2 = 0.1348
Largest diff. peak and hole	2.213 and −1.368 e $Å^{-3}$

[a] The esd's of the least significant digits are given in parentheses.

Table 5: Bond lengths for $[Cp(CO)_3W\{(CH_2)_3Br\}]$. [a]

Bond	Distance (Å)	Bond	Distance (Å)
W(1)–C(3)	1.949(17)	W(1)–C(1)	1.983(17)
W(1)–C(2)	2.03(2)	W(1)–C(10)	2.292(18)
W(1)–C(9)	2.304(17)	W(1)–C(11)	2.326(15)
W(1)–C(4)	2.347(15)	W(1)–C(7)	2.356(16)
W(1)–C(8)	2.362(16)	Br(1)–C(6)	1.946(17)
O(1)–C(1)	1.149(18)	O(2)–C(2)	1.06(2)
O(3)–C(3)	1.17(2)	C(4)–C(5)	1.48(2)
C(5)–C(6)	1.51(2)	C(7)–C(8)	1.39(3)
C(7)–C(11)	1.44(3)	C(8)–C(9)	1.37(3)
C(9)–C(10)	1.39(3)	C(10)–C(11)	1.39(3)
W(2)–C(1B)	1.964(17)	W(2)–C(3B)	2.013(18)
W(2)–C(2B)	2.03(2)	W(2)–C(11B)	2.285(16)
W(2)–C(10B)	2.308(17)	W(2)–C(9B)	2.324(17)
W(2)–C(4B)	2.336(14)	W(2)–C(8B)	2.361(16)
W(2)–C(7B)	2.364(18)	Br(2)–C(6B)	1.941(17)
O(1B)–C(1B)	1.15(2)	O(2B)–C(2B)	1.04(2)
O(3B)–C(3B)	1.118(19)	C(4B)–C(5B)	1.51(2)
C(5B)–C(6B)	1.53(2)	C(7B)–C(8B)	1.40(3)
C(7B)–C(11B)	1.40(3)	C(8B)–C(9B)	1.37(3)
C(9B)–C(10B)	1.40(3)	C(10B)–C(11B)	1.36(3)

[a] The esd's of the least significant digits are given in parentheses.

Table 6: Bond angles for $[Cp(CO)_3W\{(CH_2)_3Br\}]$. [a]

Bond angle	(°)	Bond angle	(°)
C(3)–W(1)–C(1)	106.7(7)	C(3)–W(1)–C(2)	78.9(7)
C(1)–W(1)–C(2)	78.2(6)	C(3)–W(1)–C(10)	144.7(7)
C(1)–W(1)–C(10)	104.1(7)	C(2)–W(1)–C(10)	90.9(7)
C(3)–W(1)–C(9)	152.8(8)	C(1)–W(1)–C(9)	94.9(6)
C(2)–W(1)–C(9)	122.6(8)	C(10)–W(1)–C(9)	35.1(7)
C(3)–W(1)–C(11)	110.5(7)	C(1)–W(1)–C(11)	137.7(7)
C(2)–W(1)–C(11)	89.5(7)	C(10)–W(1)–C(11)	35.0(7)
C(9)–W(1)–C(11)	58.3(7)	C(3)–W(1)–C(4)	72.4(6)
C(1)–W(1)–C(4)	74.6(6)	C(2)–W(1)–C(4)	132.2(6)
C(10)–W(1)–C(4)	133.4(7)	C(9)–W(1)–C(4)	98.4(7)
C(11)–W(1)–C(4)	136.1(7)	C(3)–W(1)–C(7)	98.4(7)
C(1)–W(1)–C(7)	151.3(7)	C(2)–W(1)–C(7)	121.1(7)
C(10)–W(1)–C(7)	58.3(7)	C(9)–W(1)–C(7)	57.3(7)
C(11)–W(1)–C(7)	35.8(7)	C(4)–W(1)–C(7)	100.6(7)
C(3)–W(1)–C(8)	118.8(8)	C(1)–W(1)–C(8)	118.1(7)
C(2)–W(1)–C(8)	146.5(7)	C(10)–W(1)–C(8)	57.8(7)
C(9)–W(1)–C(8)	34.1(7)	C(11)–W(1)–C(8)	58.4(7)
C(4)–W(1)–C(8)	81.3(6)	C(7)–W(1)–C(8)	34.3(7)
O(1)–C(1)–W(1)	176.6(14)	O(2)–C(2)–W(1)	176.4(18)
O(3)–C(3)–W(1)	177.3(17)	C(5)–C(4)–W(1)	116.2(10)
C(4)–C(5)–C(6)	109.0(13)	C(5)–C(6)–Br(1)	113.1(13)
C(8)–C(7)–C(11)	107.6(17)	C(8)–C(7)–W(1)	73.1(9)
C(11)–C(7)–W(1)	70.9(9)	C(9)–C(8)–C(7)	108.1(18)
C(9)–C(8)–W(1)	70.6(10)	C(7)–C(8)–W(1)	72.6(10)
C(8)–C(9)–C(10)	109.4(18)	C(8)–C(9)–W(1)	75.3(10)
C(10)–C(9)–W(1)	72.0(10)	C(9)–C(10)–C(11)	108.6(18)
C(9)–C(10)–W(1)	72.9(10)	C(11)–C(10)–W(1)	73.9(10)
C(10)–C(11)–C(7)	106.2(17)	C(10)–C(11)–W(1)	71.1(9)
C(7)–C(11)–W(1)	73.2(10)	C(1B)–W(2)–C(3B)	106.8(6)
C(1B)–W(2)–C(2B)	77.6(7)	C(3B)–W(2)–C(2B)	77.9(7)
C(1B)–W(2)–C(11B)	111.0(7)	C(3B)–W(2)–C(11B)	137.0(8)
C(2B)–W(2)–C(11B)	90.8(8)	C(1B)–W(2)–C(10B)	144.8(7)
C(3B)–W(2)–C(10B)	103.9(7)	C(2B)–W(2)–C(10B)	92.8(8)
C(11B)–W(2)–C(10B)	34.6(7)	C(1B)–W(2)–C(9B)	152.1(7)

(continued.....)

(.....continued)

C(3B)–W(2)–C(9B)	95.3(6)	C(2B)–W(2)–C(9B)	124.7(7)
C(11B)–W(2)–C(9B)	57.7(6)	C(10B)–W(2)–C(9B)	35.1(6)
C(1B)–W(2)–C(4B)	72.2(6)	C(3B)–W(2)–C(4B)	75.0(6)
C(2B)–W(2)–C(4B)	130.8(7)	C(11B)–W(2)–C(4B)	136.0(8)
C(10B)–W(2)–C(4B)	133.2(6)	C(9B)–W(2)–C(4B)	98.2(6)
C(1B)–W(2)–C(8B)	118.1(8)	C(3B)–W(2)–C(8B)	119.1(7)
C(2B)–W(2)–C(8B)	147.4(7)	C(11B)–W(2)–C(8B)	57.5(7)
C(10B)–W(2)–C(8B)	57.5(7)	C(9B)–W(2)–C(8B)	34.1(7)
C(4B)–W(2)–C(8B)	81.7(6)	C(1B)–W(2)–C(7B)	97.9(7)
C(3B)–W(2)–C(7B)	152.2(7)	C(2B)–W(2)–C(7B)	120.7(7)
C(11B)–W(2)–C(7B)	35.1(8)	C(10B)–W(2)–C(7B)	57.9(7)
C(9B)–W(2)–C(7B)	57.4(7)	C(4B)–W(2)–C(7B)	101.4(7)
C(8B)–W(2)–C(7B)	34.4(6)	O(1B)–C(1B)–W(2)	177.1(17)
O(2B)–C(2B)–W(2)	179.4(18)	O(3B)–C(3B)–W(2)	177.1(15)
C(5B)–C(4B)–W(2)	116.3(10)	C(4B)–C(5B)–C(6B)	109.2(15)
C(5B)–C(6B)–Br(2)	111.6(13)	C(8B)–C(7B)–C(11B)	105.8(18)
C(8B)–C(7B)–W(2)	72.7(10)	C(11B)–C(7B)–W(2)	69.4(10)
C(9B)–C(8B)–C(7B)	108.8(18)	C(9B)–C(8B)–W(2)	71.5(10)
C(7B)–C(8B)–W(2)	72.9(10)	C(8B)–C(9B)–C(10B)	108.4(17)
C(8B)–C(9B)–W(2)	74.5(10)	C(10B)–C(9B)–W(2)	71.9(10)
C(11B)–C(10B)–C(9B)	107(2)	C(11B)–C(10B)–W(2)	71.8(10)
C(9B)–C(10B)–W(2)	73.1(10)	C(10B)–C(11B)–C(7B)	109.7(18)
C(10B)–C(11B)–W(2)	73.6(10)	C(7B)–C(11B)–W(2)	75.5(11)

[a] The esd's of the least significant digits are given in parentheses.

APPENDIX 2

X-ray Crystal Data Pertaining to Chapter 3

Table 1: Crystal data and structure refinement for $[Cp(CO)_2(PPh_3)Mo\{(CH_2)_3I\}]$. [a]

	$[Cp(CO)_2(PPh_3)Mo\{(CH_2)_3I\}]$
Empirical formula	$C_{28}H_{26}IMoO_2P$
Formula weight	648.30
Temperature	293(2) K
Wavelength	0.70930 Å
Crystal system	Monoclinic
Space group	$P2_1/n$
Unit cell dimensions	a = 17.4796(12) Å
	b = 9.2587(13) Å
	c = 17.558(3) Å
Volume	2622.2(6) $Å^3$
Z	4
Density (calculated)	1.642 g cm^{-3}
Absorption coefficient	1.761 mm^{-1}
F(000)	1280
Crystal size	0.65 × 0.40 × 0.20 mm^3
Voltage, Current	55 kV, 25 mA
Scan angle	1.10°
Diffractometer	Enraf-Nonius CAD4
Theta range for data collection	2.10 to 22.97°
Index ranges	$-5 \le h \le 19$; $-4 \le k \le 10$; $-19 \le l \le 18$
Reflections collected	5606
Independent reflections	3629 [R_{int} = 0.0229]
Reflections observed (>2σ)	3180
Absorption correction	Semi-empirical
Max. and min. transmission	0.7196 and 0.3940
Refinement method	Full-matrix least-squares on F^2
Data / restraints / parameters	3629 / 0 / 298
Goodness-of-fit on F^2	1.106
Final R indices [$I > 2\sigma(I)$]	R_1 = 0.0464, wR_2 = 0.1411
R indices (all data)	R_1 = 0.0518, wR_2 = 0.1459
Largest diff. peak and hole	1.336 and −1.596 e $Å^{-3}$

[a] The esd's of the least significant digits are given in parentheses.

Table 2: Bond lengths for $[Cp(CO)_2(PPh_3)Mo\{(CH_2)_3I\}]$. [a]

Bond	Distance (Å)	Bond	Distance (Å)
Mo–C(4)	1.946(7)	Mo–C(5)	1.982(7)
Mo–C(6)	2.318(7)	Mo–C(10)	2.331(7)
Mo–C(7)	2.341(7)	Mo–C(9)	2.342(7)
Mo–C(8)	2.376(7)	Mo–C(1)	2.402(7)
Mo–P	2.4541(17)	I–C(3)	2.134(9)
P–C(17)	1.834(6)	P–C(23)	1.834(6)
P–C(11)	1.840(6)	O(1)–C(4)	1.132(8)
O(2)–C(5)	1.127(8)	C(1)–C(2)	1.264(10)
C(2)–C(3)	1.627(10)	C(6)–C(10)	1.374(11)
C(6)–C(7)	1.380(11)	C(7)–C(8)	1.357(13)
C(8)–C(9)	1.376(13)	C(9)–C(10)	1.402(13)
C(11)–C(16)	1.376(8)	C(11)–C(12)	1.380(8)
C(12)–C(13)	1.384(9)	C(13)–C(14)	1.369(10)
C(14)–C(15)	1.355(10)	C(15)–C(16)	1.388(9)
C(17)–C(18)	1.376(9)	C(17)–C(22)	1.400(9)
C(18)–C(19)	1.393(11)	C(19)–C(20)	1.363(13)
C(20)–C(21)	1.368(13)	C(21)–C(22)	1.396(10)
C(23)–C(24)	1.384(8)	C(23)–C(28)	1.388(8)
C(24)–C(25)	1.377(9)	C(25)–C(26)	1.363(11)
C(26)–C(27)	1.371(11)	C(27)–C(28)	1.383(10)

[a] The esd's of the least significant digits are given in parentheses.

Table 3: Bond angles for $[Cp(CO)_2(PPh_3)Mo\{(CH_2)_3I\}]$. [a]

Bond angle	(°)	Bond angle	(°)
C(4)–Mo–C(5)	102.9(3)	C(4)–Mo–C(6)	101.4(3)
C(5)–Mo–C(6)	153.5(3)	C(4)–Mo–C(10)	98.8(3)
C(5)–Mo–C(10)	147.8(3)	C(6)–Mo–C(10)	34.4(3)
C(4)–Mo–C(7)	131.9(3)	C(5)–Mo–C(7)	119.0(3)
C(6)–Mo–C(7)	34.5(3)	C(10)–Mo–C(7)	57.1(3)
C(4)–Mo–C(9)	127.3(3)	C(5)–Mo–C(9)	113.7(3)
C(6)–Mo–C(9)	57.1(3)	C(10)–Mo–C(9)	34.9(3)
C(7)–Mo–C(9)	56.3(3)	C(4)–Mo–C(8)	155.4(3)
C(5)–Mo–C(8)	101.0(3)	C(6)–Mo–C(8)	56.6(3)
C(10)–Mo–C(8)	57.1(3)	C(7)–Mo–C(8)	33.4(3)
C(9)–Mo–C(8)	33.9(3)	C(4)–Mo–C(1)	74.7(3)
C(5)–Mo–C(1)	73.1(2)	C(6)–Mo–C(1)	124.2(3)
C(10)–Mo–C(1)	90.2(3)	C(7)–Mo–C(1)	137.2(3)
C(9)–Mo–C(1)	81.0(3)	C(8)–Mo–C(1)	107.3(3)
C(4)–Mo–P	80.5(2)	C(5)–Mo–P	80.54(17)
C(6)–Mo–P	93.1(2)	C(10)–Mo–P	126.8(2)
C(7)–Mo–P	84.1(2)	C(9)–Mo–P	140.2(2)
C(8)–Mo–P	109.2(3)	C(1)–Mo–P	138.20(18)
C(17)–P–C(23)	103.1(3)	C(17)–P–C(11)	104.0(3)
C(23)–P–C(11)	100.7(3)	C(17)–P–Mo	109.90(19)
C(23)–P–Mo	118.97(18)	C(11)–P–Mo	118.13(19)
C(2)–C(1)–Mo	115.8(5)	C(1)–C(2)–C(3)	113.2(6)
C(2)–C(3)–I	116.9(5)	O(1)–C(4)–Mo	174.9(6)
O(2)–C(5)–Mo	176.8(5)	C(10)–C(6)–C(7)	108.3(7)
C(10)–C(6)–Mo	73.3(4)	C(7)–C(6)–Mo	73.7(4)
C(8)–C(7)–C(6)	108.9(7)	C(8)–C(7)–Mo	74.7(4)
C(6)–C(7)–Mo	71.9(4)	C(7)–C(8)–C(9)	107.9(8)
C(7)–C(8)–Mo	71.8(4)	C(9)–C(8)–Mo	71.7(4)
C(8)–C(9)–C(10)	108.2(7)	C(8)–C(9)–Mo	74.4(4)
C(10)–C(9)–Mo	72.1(4)	C(6)–C(10)–C(9)	106.7(7)
C(6)–C(10)–Mo	72.3(4)	C(9)–C(10)–Mo	73.0(4)
C(16)–C(11)–C(12)	117.7(5)	C(16)–C(11)–P	120.3(4)
C(12)–C(11)–P	122.0(4)	C(11)–C(12)–C(13)	120.8(6)
C(14)–C(13)–C(12)	120.5(6)	C(15)–C(14)–C(13)	119.4(6)

(continued……)

(.....continued)			
C(14)–C(15)–C(16)	120.3(6)	C(11)–C(16)–C(15)	121.2(6)
C(18)–C(17)–C(22)	119.4(6)	C(18)–C(17)–P	122.8(5)
C(22)–C(17)–P	117.5(4)	C(17)–C(18)–C(19)	119.9(7)
C(20)–C(19)–C(18)	120.6(8)	C(19)–C(20)–C(21)	120.4(7)
C(20)–C(21)–C(22)	120.1(7)	C(21)–C(22)–C(17)	119.6(7)
C(24)–C(23)–C(28)	118.5(5)	C(24)–C(23)–P	119.7(4)
C(28)–C(23)–P	121.6(4)	C(25)–C(24)–C(23)	120.6(6)
C(26)–C(25)–C(24)	120.2(7)	C(25)–C(26)–C(27)	120.3(6)
C(26)–C(27)–C(28)	120.0(6)	C(27)–C(28)–C(23)	120.3(6)

[a] The esd's of the least significant digits are given in parentheses.

APPENDIX 3

X-ray Crystal Data Pertaining to Chapter 4

Table 1:Crystal data and structure refinement for $[Cp(CO)_3W(CH_2)_3Mo(CO)_2(PPh_3)Cp]$.

Identification code	mowp
Empirical formula	C36 H31 Mo O5 P W
Formula weight	854.37
Temperature	219(2) K
Wavelength	0.71073 Å
Crystal system, space group	Monoclinic, P 21/c
Unit cell dimensions	a = 15.446(7)Å alpha = 90 deg. b = 12.204(6)Å beta = 113.27(4) deg. c = 18.483(9) Å gamma = 90 deg.
Volume	3201(3) $Å^3$
Z, Calculated density	4, 1.773 Mg/m^3
Absorption coefficient	4.075 mm^{-1}
F(000)	1672
Crystal size	0.45 x 0.35 x 0.25 mm
Theta range for data collection	2.06 to 23.01 deg.
Index ranges	-15<=h<=16, -13<=k<=13, -20<=l<=0
Reflections collected / unique	8643 / 4452 [R(int) = 0.0448]
Completeness to 2theta = 23.01	99.5%
Absorption correction	Empirical (SHELXA)
Max. and min. transmission	0.4290 and 0.2614
Refinement method	Full-matrix least-squares on F^2
Data / restraints / parameters	4452 / 0 / 397
Goodness-of-fit on F^2	1.038
Final R indices [I>2sigma(I)]	R1 = 0.0360, wR2 = 0.0989
R indices (all data)	R1 = 0.0421, wR2 = 0.1033
Largest diff. peak and hole	1.403 and -1.821 $e.A^{-3}$

Table 2:Bond lengths [Å] and angles [°] for $[Cp(CO)_3W(CH_2)_3Mo(CO)_2(PPh_3)Cp]$.

W(1)-C(15)	1.965(7)
W(1)-C(16)	1.984(8)
W(1)-C(14)	1.988(8)
W(1)-C(4)	2.315(7)
W(1)-C(5)	2.316(6)
W(1)-C(13)	2.316(7)
W(1)-C(1)	2.317(7)
W(1)-C(3)	2.334(7)
W(1)-C(2)	2.349(7)
Mo(1)-C(18)	1.957(7)
Mo(1)-C(17)	1.960(7)
Mo(1)-C(6)	2.322(7)
Mo(1)-C(7)	2.323(8)
Mo(1)-C(10)	2.330(7)
Mo(1)-C(9)	2.351(7)
Mo(1)-C(11)	2.357(7)
Mo(1)-C(8)	2.370(7)
Mo(1)-P(1)	2.4569(19)
O(1)-C(14)	1.149(8)
O(2)-C(15)	1.151(8)
O(3)-C(16)	1.147(9)
O(4)-C(17)	1.153(7)
O(5)-C(18)	1.151(7)
C(1)-C(5)	1.402(10)
C(1)-C(2)	1.404(10)
C(2)-C(3)	1.405(10)
C(3)-C(4)	1.408(10)
C(4)-C(5)	1.388(10)
C(6)-C(10)	1.382(12)
C(6)-C(7)	1.401(12)
C(7)-C(8)	1.368(11)
C(8)-C(9)	1.403(11)
C(9)-C(10)	1.365(11)
C(11)-C(12)	1.527(9)
C(12)-C(13)	1.519(9)
P(1)-C(31)	1.822(6)
P(1)-C(25)	1.840(7)
P(1)-C(19)	1.850(6)
C(19)-C(20)	1.370(10)
C(19)-C(24)	1.385(10)
C(20)-C(21)	1.392(11)
C(21)-C(22)	1.343(14)
C(22)-C(23)	1.372(14)
C(23)-C(24)	1.391(10)
C(25)-C(30)	1.376(10)
C(25)-C(26)	1.376(9)
C(26)-C(27)	1.396(11)
C(27)-C(28)	1.355(13)
C(28)-C(29)	1.360(12)

C(29)-C(30)	1.389(11)
C(31)-C(32)	1.381(9)
C(31)-C(36)	1.402(9)
C(32)-C(33)	1.396(10)
C(33)-C(34)	1.375(10)
C(34)-C(35)	1.367(10)
C(35)-C(36)	1.386(9)

C(15)-W(1)-C(16)	77.8(3)
C(15)-W(1)-C(14)	105.5(3)
C(16)-W(1)-C(14)	77.7(3)
C(15)-W(1)-C(4)	112.7(3)
C(16)-W(1)-C(4)	89.5(3)
C(14)-W(1)-C(4)	136.1(3)
C(15)-W(1)-C(5)	147.3(3)
C(16)-W(1)-C(5)	94.0(3)
C(14)-W(1)-C(5)	103.5(3)
C(4)-W(1)-C(5)	34.9(2)
C(15)-W(1)-C(13)	74.4(3)
C(16)-W(1)-C(13)	133.7(3)
C(14)-W(1)-C(13)	75.0(3)
C(4)-W(1)-C(13)	135.4(3)
C(5)-W(1)-C(13)	128.4(3)
C(15)-W(1)-C(1)	150.3(3)
C(16)-W(1)-C(1)	126.9(3)
C(14)-W(1)-C(1)	96.8(3)
C(4)-W(1)-C(1)	58.2(3)
C(5)-W(1)-C(1)	35.2(3)
C(13)-W(1)-C(1)	93.2(3)
C(15)-W(1)-C(3)	97.2(3)
C(16)-W(1)-C(3)	118.1(3)
C(14)-W(1)-C(3)	154.9(3)
C(4)-W(1)-C(3)	35.3(3)
C(5)-W(1)-C(3)	58.5(3)
C(13)-W(1)-C(3)	101.7(3)
C(1)-W(1)-C(3)	58.3(3)
C(15)-W(1)-C(2)	115.3(3)
C(16)-W(1)-C(2)	147.6(3)
C(14)-W(1)-C(2)	122.3(3)
C(4)-W(1)-C(2)	58.2(3)
C(5)-W(1)-C(2)	58.4(3)
C(13)-W(1)-C(2)	78.5(3)
C(1)-W(1)-C(2)	35.0(2)
C(3)-W(1)-C(2)	34.9(2)
C(18)-Mo(1)-C(17)	103.8(3)
C(18)-Mo(1)-C(6)	98.2(3)
C(17)-Mo(1)-C(6)	144.8(3)
C(18)-Mo(1)-C(7)	127.9(3)
C(17)-Mo(1)-C(7)	111.2(3)
C(6)-Mo(1)-C(7)	35.1(3)
C(18)-Mo(1)-C(10)	100.2(3)
C(17)-Mo(1)-C(10)	154.9(3)

C(6)-Mo(1)-C(10)	34.6(3)
C(7)-Mo(1)-C(10)	56.9(3)
C(18)-Mo(1)-C(9)	129.4(3)
C(17)-Mo(1)-C(9)	121.2(3)
C(6)-Mo(1)-C(9)	57.5(3)
C(7)-Mo(1)-C(9)	56.9(3)
C(10)-Mo(1)-C(9)	33.9(3)
C(18)-Mo(1)-C(11)	72.5(2)
C(17)-Mo(1)-C(11)	74.5(2)
C(6)-Mo(1)-C(11)	86.6(3)
C(7)-Mo(1)-C(11)	80.9(3)
C(10)-Mo(1)-C(11)	120.3(3)
C(9)-Mo(1)-C(11)	137.6(3)
C(18)-Mo(1)-C(8)	155.1(3)
C(17)-Mo(1)-C(8)	100.4(3)
C(6)-Mo(1)-C(8)	57.7(3)
C(7)-Mo(1)-C(8)	33.9(3)
C(10)-Mo(1)-C(8)	56.8(3)
C(9)-Mo(1)-C(8)	34.6(3)
C(11)-Mo(1)-C(8)	109.0(3)
C(18)-Mo(1)-P(1)	80.60(18)
C(17)-Mo(1)-P(1)	78.00(18)
C(6)-Mo(1)-P(1)	133.2(3)
C(7)-Mo(1)-P(1)	142.8(2)
C(10)-Mo(1)-P(1)	99.1(3)
C(9)-Mo(1)-P(1)	87.1(2)
C(11)-Mo(1)-P(1)	135.12(17)
C(8)-Mo(1)-P(1)	110.4(2)
C(5)-C(1)-C(2)	108.5(6)
C(5)-C(1)-W(1)	72.3(4)
C(2)-C(1)-W(1)	73.8(4)
C(1)-C(2)-C(3)	107.5(6)
C(1)-C(2)-W(1)	71.2(4)
C(3)-C(2)-W(1)	71.9(4)
C(2)-C(3)-C(4)	107.6(6)
C(2)-C(3)-W(1)	73.2(4)
C(4)-C(3)-W(1)	71.7(4)
C(5)-C(4)-C(3)	108.7(7)
C(5)-C(4)-W(1)	72.6(4)
C(3)-C(4)-W(1)	73.1(4)
C(4)-C(5)-C(1)	107.7(7)
C(4)-C(5)-W(1)	72.6(4)
C(1)-C(5)-W(1)	72.4(4)
C(10)-C(6)-C(7)	105.7(7)
C(10)-C(6)-Mo(1)	73.0(5)
C(7)-C(6)-Mo(1)	72.5(4)
C(8)-C(7)-C(6)	109.6(8)
C(8)-C(7)-Mo(1)	74.9(5)
C(6)-C(7)-Mo(1)	72.4(5)
C(7)-C(8)-C(9)	107.0(7)
C(7)-C(8)-Mo(1)	71.2(4)
C(9)-C(8)-Mo(1)	72.0(4)

C(10)-C(9)-C(8)	107.8(8)
C(10)-C(9)-Mo(1)	72.2(4)
C(8)-C(9)-Mo(1)	73.4(4)
C(9)-C(10)-C(6)	109.9(8)
C(9)-C(10)-Mo(1)	73.9(4)
C(6)-C(10)-Mo(1)	72.4(4)
C(12)-C(11)-Mo(1)	120.1(4)
C(13)-C(12)-C(11)	110.1(6)
C(12)-C(13)-W(1)	116.4(5)
O(1)-C(14)-W(1)	178.4(6)
O(2)-C(15)-W(1)	177.8(6)
O(3)-C(16)-W(1)	177.2(6)
O(4)-C(17)-Mo(1)	175.8(6)
O(5)-C(18)-Mo(1)	175.2(5)
C(31)-P(1)-C(25)	102.5(3)
C(31)-P(1)-C(19)	103.1(3)
C(25)-P(1)-C(19)	100.2(3)
C(31)-P(1)-Mo(1)	114.1(2)
C(25)-P(1)-Mo(1)	117.4(2)
C(19)-P(1)-Mo(1)	117.2(2)
C(20)-C(19)-C(24)	118.6(6)
C(20)-C(19)-P(1)	119.4(6)
C(24)-C(19)-P(1)	122.0(6)
C(19)-C(20)-C(21)	120.7(9)
C(22)-C(21)-C(20)	120.5(9)
C(21)-C(22)-C(23)	120.1(8)
C(22)-C(23)-C(24)	120.1(9)
C(19)-C(24)-C(23)	120.1(9)
C(30)-C(25)-C(26)	117.5(6)
C(30)-C(25)-P(1)	119.2(5)
C(26)-C(25)-P(1)	123.3(5)
C(25)-C(26)-C(27)	120.0(8)
C(28)-C(27)-C(26)	122.0(8)
C(27)-C(28)-C(29)	118.3(7)
C(28)-C(29)-C(30)	120.6(8)
C(25)-C(30)-C(29)	121.6(8)
C(32)-C(31)-C(36)	118.0(6)
C(32)-C(31)-P(1)	123.9(5)
C(36)-C(31)-P(1)	118.2(4)
C(31)-C(32)-C(33)	120.4(7)
C(34)-C(33)-C(32)	120.2(7)
C(35)-C(34)-C(33)	120.5(7)
C(34)-C(35)-C(36)	119.5(6)
C(35)-C(36)-C(31)	121.4(6)

Symmetry transformations used to generate equivalent atoms:
#1 -x,-y+1,-z #2 x,y+1,z #3 x,y-1,z

Table 3:Crystal data and structure refinement for $[Cp(CO)_2Fe(CH_2)_3Mo(CO)_2(PPh_3)Cp]$

Identification code	femo
Empirical formula	C35 H31 Fe Mo O4 P
Formula weight	698.36
Temperature	228(2) K
Wavelength	0.71073 Å
Crystal system, space group	Monoclinic, P 21/c
Unit cell dimensions	a = 15.414(7) Å alpha = 90 deg. b = 11.243(4) Å beta = 112.42(3)deg. c = 19.007(6) Å gamma = 90 deg.
Volume	3045(2) $Å^3$
Z, Calculated density	4, 1.523 Mg/m^3
Absorption coefficient	0.979 mm^{-1}
F(000)	1424
Crystal size	0.45 x 0.40 x 0.30 mm
Theta range for data collection	2.15 to 23.00 deg.
Index ranges	-15<=h<=16, -12<=k<=12, -20<=l<=0
Reflections collected / unique	8177 / 4230 [R(int) = 0.0187]
Completeness to 2theta = 23.00	99.6%
Absorption correction	Empirical (SHELXA)
Max. and min. transmission	0.7578 and 0.6671
Refinement method	Full-matrix least-squares on F^2
Data / restraints / parameters	4230 / 0 / 379
Goodness-of-fit on F^2	1.023
Final R indices [I>2sigma(I)]	R1 = 0.0214, wR2 = 0.0545
R indices (all data)	R1 = 0.0296, wR2 = 0.0570
Largest diff. peak and hole	0.327 and -0.297 $e.A^{-3}$

Table 4: Bond lengths [Å] and angles [°] for $[Cp(CO)_2Fe(CH_2)_3Mo(CO)_2(PPh_3)Cp]$.

Mo(1)-C(2)	1.949(3)
Mo(1)-C(1)	1.954(3)
Mo(1)-C(8)	2.323(3)
Mo(1)-C(12)	2.328(3)
Mo(1)-C(9)	2.328(3)
Mo(1)-C(10)	2.332(3)
Mo(1)-C(11)	2.343(3)
Mo(1)-C(3)	2.374(2)
Mo(1)-P(1)	2.4546(10)
Fe(1)-C(7)	1.745(3)
Fe(1)-C(6)	1.748(3)
Fe(1)-C(5)	2.076(2)
Fe(1)-C(14)	2.088(3)
Fe(1)-C(15)	2.094(3)
Fe(1)-C(13)	2.096(3)
Fe(1)-C(17)	2.096(3)
Fe(1)-C(16)	2.102(3)
P(1)-C(30)	1.835(2)
P(1)-C(18)	1.838(2)
P(1)-C(24)	1.838(3)
O(1)-C(1)	1.154(3)
O(2)-C(2)	1.154(3)
O(3)-C(6)	1.145(3)
O(4)-C(7)	1.146(3)
C(3)-C(4)	1.488(3)
C(4)-C(5)	1.522(4)
C(8)-C(12)	1.357(4)
C(8)-C(9)	1.357(4)
C(9)-C(10)	1.366(5)
C(10)-C(11)	1.403(5)
C(11)-C(12)	1.386(5)
C(13)-C(14)	1.388(4)
C(13)-C(17)	1.401(4)
C(14)-C(15)	1.420(4)
C(15)-C(16)	1.398(4)
C(16)-C(17)	1.419(4)
C(18)-C(23)	1.380(3)
C(18)-C(19)	1.393(3)
C(19)-C(20)	1.369(4)
C(20)-C(21)	1.378(4)
C(21)-C(22)	1.377(4)
C(22)-C(23)	1.385(4)
C(24)-C(25)	1.381(4)
C(24)-C(29)	1.384(4)
C(25)-C(26)	1.383(4)
C(26)-C(27)	1.362(5)
C(27)-C(28)	1.367(5)
C(28)-C(29)	1.392(4)

C(30)-C(35)	1.383(3)
C(30)-C(31)	1.389(4)
C(31)-C(32)	1.378(4)
C(32)-C(33)	1.376(4)
C(33)-C(34)	1.357(4)
C(34)-C(35)	1.383(4)

C(2)-Mo(1)-C(1)	101.80(10)
C(2)-Mo(1)-C(8)	104.70(11)
C(1)-Mo(1)-C(8)	150.86(11)
C(2)-Mo(1)-C(12)	136.88(12)
C(1)-Mo(1)-C(12)	117.16(12)
C(8)-Mo(1)-C(12)	33.93(11)
C(2)-Mo(1)-C(9)	96.25(10)
C(1)-Mo(1)-C(9)	152.22(11)
C(8)-Mo(1)-C(9)	33.93(10)
C(12)-Mo(1)-C(9)	56.73(11)
C(2)-Mo(1)-C(10)	119.76(13)
C(1)-Mo(1)-C(10)	118.22(12)
C(8)-Mo(1)-C(10)	56.67(10)
C(12)-Mo(1)-C(10)	57.32(12)
C(9)-Mo(1)-C(10)	34.10(12)
C(2)-Mo(1)-C(11)	153.01(12)
C(1)-Mo(1)-C(11)	101.47(11)
C(8)-Mo(1)-C(11)	56.88(11)
C(12)-Mo(1)-C(11)	34.52(13)
C(9)-Mo(1)-C(11)	57.20(11)
C(10)-Mo(1)-C(11)	34.93(13)
C(2)-Mo(1)-C(3)	73.64(9)
C(1)-Mo(1)-C(3)	71.93(9)
C(8)-Mo(1)-C(3)	127.42(10)
C(12)-Mo(1)-C(3)	133.96(11)
C(9)-Mo(1)-C(3)	93.50(10)
C(10)-Mo(1)-C(3)	78.20(9)
C(11)-Mo(1)-C(3)	101.05(14)
C(2)-Mo(1)-P(1)	82.68(8)
C(1)-Mo(1)-P(1)	77.34(7)
C(8)-Mo(1)-P(1)	94.15(8)
C(12)-Mo(1)-P(1)	88.27(9)
C(9)-Mo(1)-P(1)	126.26(9)
C(10)-Mo(1)-P(1)	145.51(8)
C(11)-Mo(1)-P(1)	115.77(14)
C(3)-Mo(1)-P(1)	135.83(6)
C(7)-Fe(1)-C(6)	97.01(13)
C(7)-Fe(1)-C(5)	89.27(11)
C(6)-Fe(1)-C(5)	84.72(11)
C(7)-Fe(1)-C(14)	160.61(12)
C(6)-Fe(1)-C(14)	94.12(13)
C(5)-Fe(1)-C(14)	107.57(11)
C(7)-Fe(1)-C(15)	123.03(12)
C(6)-Fe(1)-C(15)	95.39(12)
C(5)-Fe(1)-C(15)	147.25(12)

C(14)-Fe(1)-C(15)	39.69(11)
C(7)-Fe(1)-C(13)	136.25(13)
C(6)-Fe(1)-C(13)	126.12(13)
C(5)-Fe(1)-C(13)	87.93(11)
C(14)-Fe(1)-C(13)	38.75(12)
C(15)-Fe(1)-C(13)	65.58(12)
C(7)-Fe(1)-C(17)	101.04(13)
C(6)-Fe(1)-C(17)	159.06(12)
C(5)-Fe(1)-C(17)	105.93(11)
C(14)-Fe(1)-C(17)	65.67(12)
C(15)-Fe(1)-C(17)	65.81(12)
C(13)-Fe(1)-C(17)	39.04(12)
C(7)-Fe(1)-C(16)	94.81(12)
C(6)-Fe(1)-C(16)	128.62(11)
C(5)-Fe(1)-C(16)	145.32(11)
C(14)-Fe(1)-C(16)	65.89(11)
C(15)-Fe(1)-C(16)	38.93(11)
C(13)-Fe(1)-C(16)	65.63(12)
C(17)-Fe(1)-C(16)	39.51(11)
C(30)-P(1)-C(18)	101.20(11)
C(30)-P(1)-C(24)	102.18(11)
C(18)-P(1)-C(24)	102.76(11)
C(30)-P(1)-Mo(1)	116.29(8)
C(18)-P(1)-Mo(1)	115.76(8)
C(24)-P(1)-Mo(1)	116.38(8)
O(1)-C(1)-Mo(1)	178.1(2)
O(2)-C(2)-Mo(1)	174.1(2)
C(4)-C(3)-Mo(1)	118.20(15)
C(3)-C(4)-C(5)	112.4(2)
C(4)-C(5)-Fe(1)	116.93(17)
O(3)-C(6)-Fe(1)	175.7(2)
O(4)-C(7)-Fe(1)	178.4(2)
C(12)-C(8)-C(9)	109.2(3)
C(12)-C(8)-Mo(1)	73.22(16)
C(9)-C(8)-Mo(1)	73.23(16)
C(8)-C(9)-C(10)	108.4(3)
C(8)-C(9)-Mo(1)	72.83(16)
C(10)-C(9)-Mo(1)	73.08(17)
C(9)-C(10)-C(11)	107.7(3)
C(9)-C(10)-Mo(1)	72.82(16)
C(11)-C(10)-Mo(1)	72.97(17)
C(12)-C(11)-C(10)	106.5(3)
C(12)-C(11)-Mo(1)	72.15(17)
C(10)-C(11)-Mo(1)	72.10(17)
C(8)-C(12)-C(11)	108.2(3)
C(8)-C(12)-Mo(1)	72.86(16)
C(11)-C(12)-Mo(1)	73.33(18)
C(14)-C(13)-C(17)	108.9(3)
C(14)-C(13)-Fe(1)	70.33(16)
C(17)-C(13)-Fe(1)	70.50(16)
C(13)-C(14)-C(15)	107.8(3)
C(13)-C(14)-Fe(1)	70.92(17)

C(15)-C(14)-Fe(1)	70.36(16)
C(16)-C(15)-C(14)	107.9(3)
C(16)-C(15)-Fe(1)	70.83(15)
C(14)-C(15)-Fe(1)	69.95(15)
C(15)-C(16)-C(17)	107.8(3)
C(15)-C(16)-Fe(1)	70.24(15)
C(17)-C(16)-Fe(1)	70.05(15)
C(13)-C(17)-C(16)	107.6(3)
C(13)-C(17)-Fe(1)	70.46(16)
C(16)-C(17)-Fe(1)	70.44(15)
C(23)-C(18)-C(19)	118.5(2)
C(23)-C(18)-P(1)	123.28(19)
C(19)-C(18)-P(1)	117.98(17)
C(20)-C(19)-C(18)	120.9(2)
C(19)-C(20)-C(21)	120.3(3)
C(22)-C(21)-C(20)	119.5(3)
C(21)-C(22)-C(23)	120.3(3)
C(18)-C(23)-C(22)	120.4(2)
C(25)-C(24)-C(29)	118.4(2)
C(25)-C(24)-P(1)	119.68(19)
C(29)-C(24)-P(1)	121.9(2)
C(24)-C(25)-C(26)	121.1(3)
C(27)-C(26)-C(25)	119.8(3)
C(26)-C(27)-C(28)	120.5(3)
C(27)-C(28)-C(29)	119.8(3)
C(24)-C(29)-C(28)	120.4(3)
C(35)-C(30)-C(31)	118.1(2)
C(35)-C(30)-P(1)	122.35(18)
C(31)-C(30)-P(1)	119.50(19)
C(32)-C(31)-C(30)	120.6(3)
C(33)-C(32)-C(31)	120.3(3)
C(34)-C(33)-C(32)	119.7(2)
C(33)-C(34)-C(35)	120.5(3)
C(30)-C(35)-C(34)	120.7(2)

Symmetry transformations used to generate equivalent atoms

APPENDIX 4

Mass Spectra of:

(a) Individual and mixed metallic elements present in samples analysed

DISTRIBUTION OF ISOTOPES CALCULATED BY 'ISOFORM' PROGRAM FOR
Formula : Fe
Factor : 100 Nominal MW = 56 Exact MW = 55.93490 Average MW = 55.85

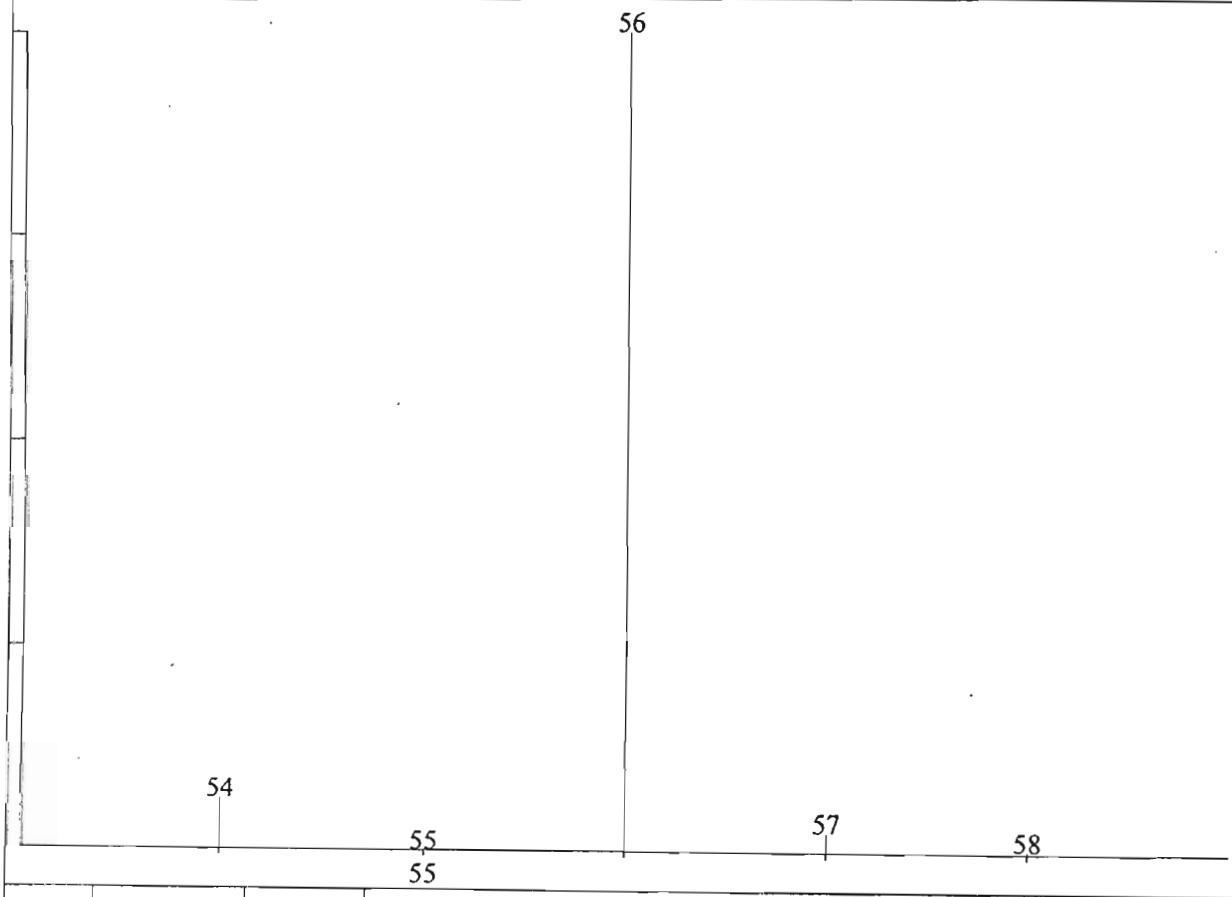

Mass	Abundance	*Factor
54	6.30000	6.30
55	0.00000	0.00
56	100.00000	100.00
57	2.39000	2.39
58	0.30400	0.30

DISTRIBUTION OF ISOTOPES CALCULATED BY 'ISOFORM' PROGRAM FOR
Formula : Mo
Factor : 100 Nominal MW = 98 Exact MW = 97.90540 Average MW = 95.93

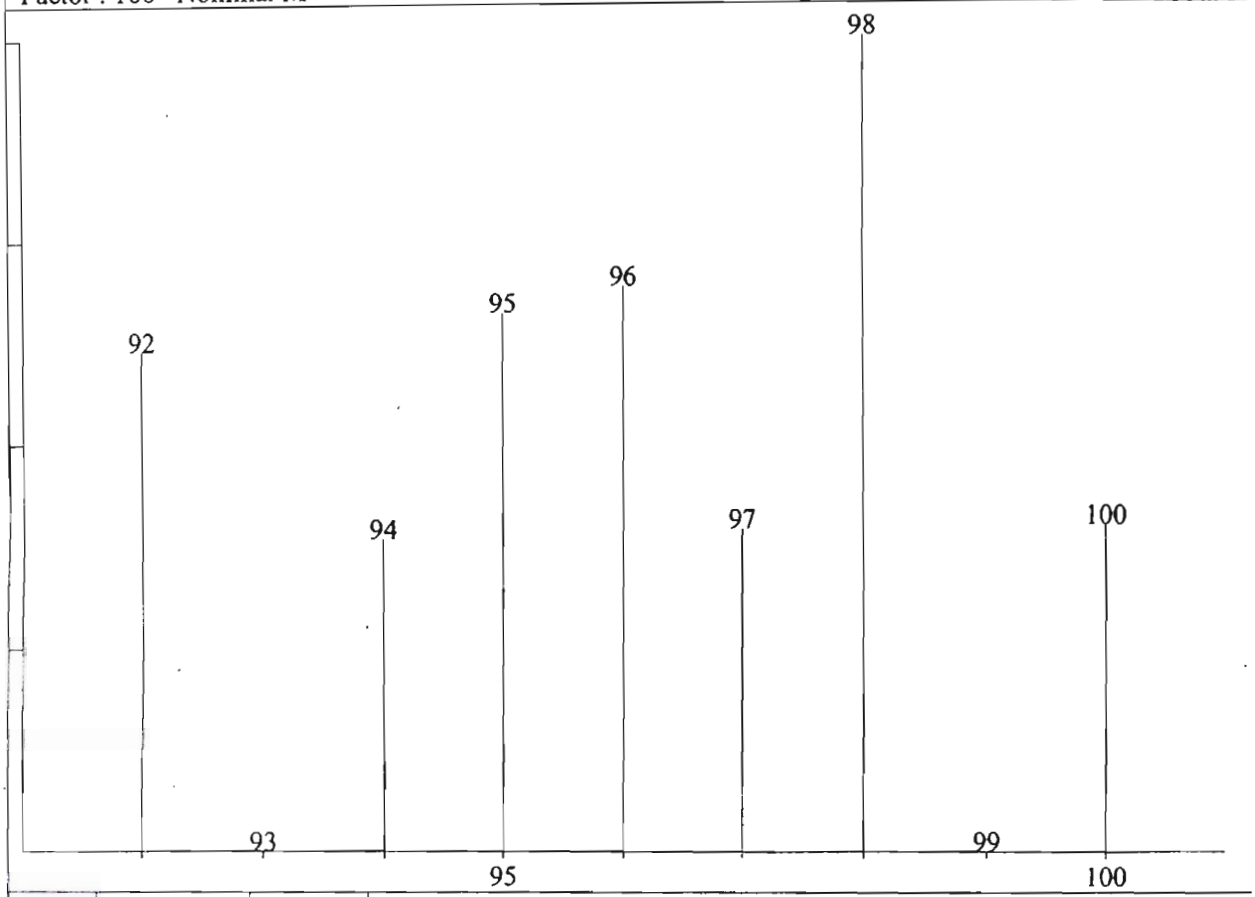

Mass	Abundance	*Factor
92	61.40000	61.40
93	0.00000	0.00
94	38.40000	38.40
95	66.00000	66.00
96	69.30000	69.30
97	39.60000	39.60
98	100.00000	100.00
99	0.00000	0.00
100	40.00000	40.00

DISTRIBUTION OF ISOTOPES CALCULATED BY 'ISOFORM' PROGRAM FOR
Formula : W
Factor : 100 Nominal MW = 184 Exact MW = 183.95100 Average MW = 183.84

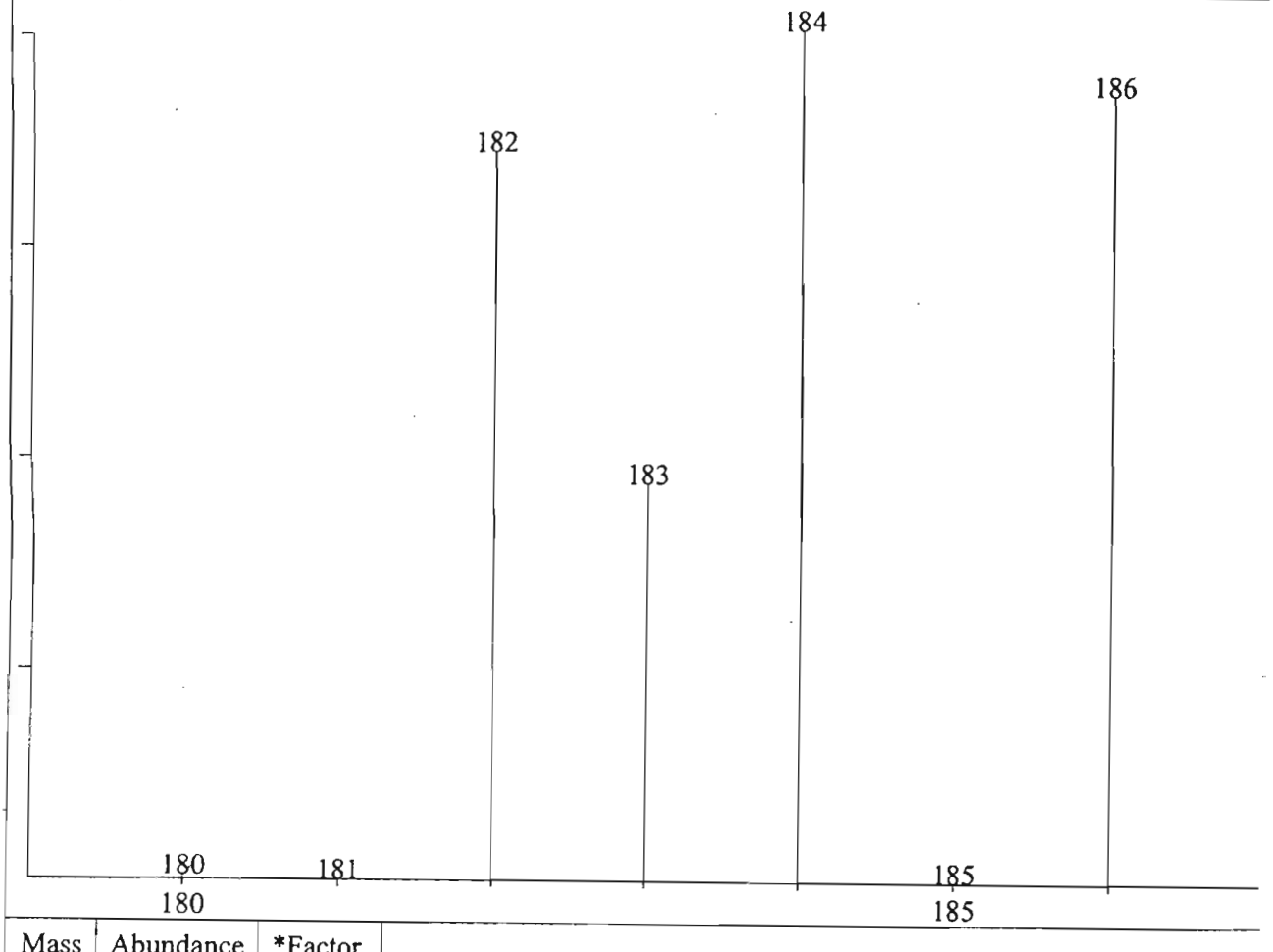

Mass	Abundance	*Factor
180	0.42387	0.42
181	0.00000	0.00
182	85.75155	85.75
183	46.62537	46.63
184	100.00000	100.00
185	0.00000	0.00
186	92.25073	92.25

DISTRIBUTION OF ISOTOPES CALCULATED BY 'ISOFORM' PROGRAM FOR
Formula : FeMo
Factor : 100 Nominal MW = 154 Exact MW = 153.84030 Average MW = 151.78

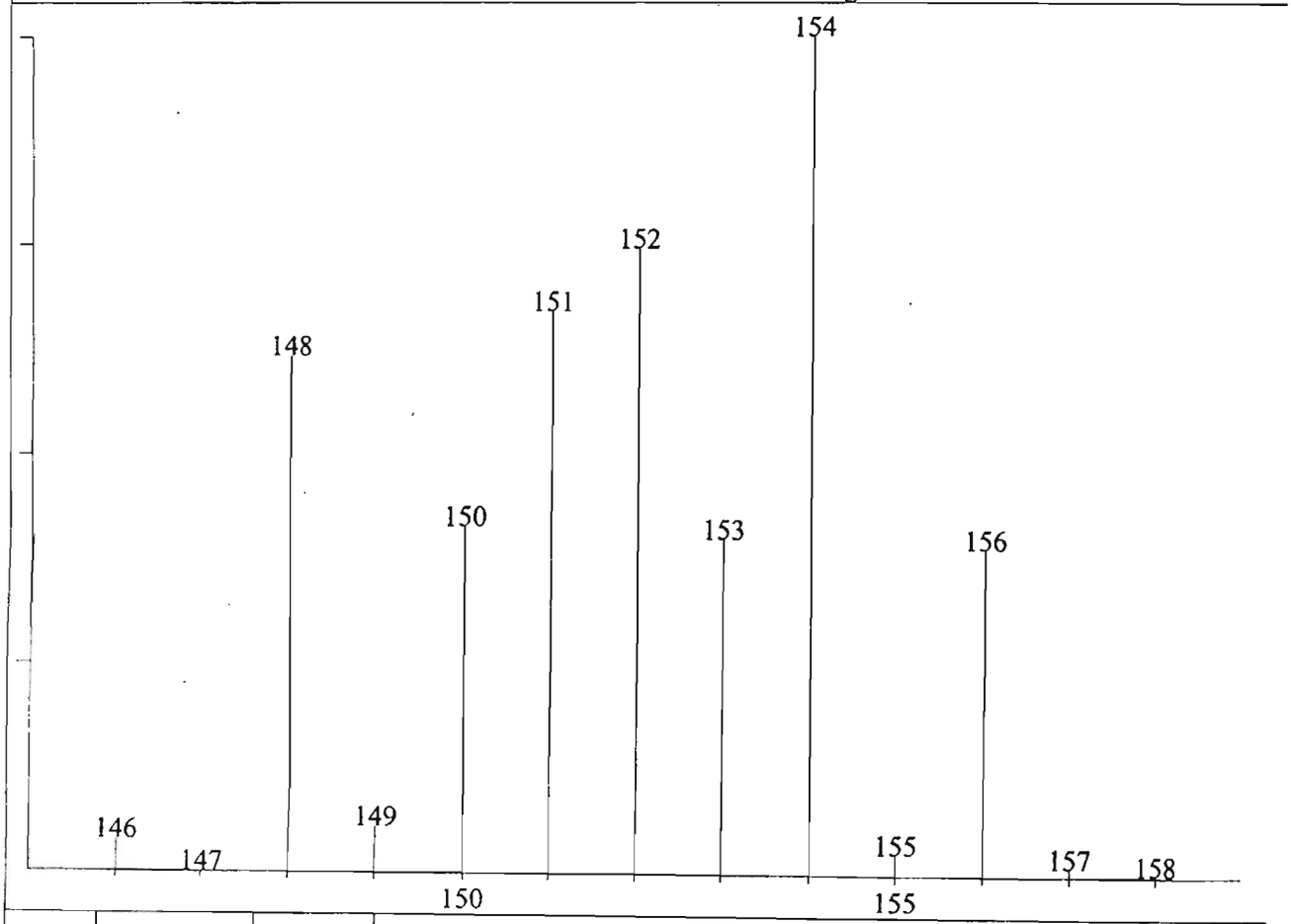

Mass	Abundance	*Factor
146	3.73101	3.73
147	0.00000	0.00
148	61.55573	61.56
149	5.42594	5.43
150	41.42916	41.43
151	66.95071	66.95
152	74.55275	74.55
153	39.98656	39.99
154	100.00000	100.00
155	2.42135	2.42
156	38.87454	38.87
157	0.92209	0.92
158	0.11729	0.12

DISTRIBUTION OF ISOTOPES CALCULATED BY 'ISOFORM' PROGRAM FOR
Formula : MoW
Factor : 100 Nominal MW = 282 Exact MW = 281.85641 Average MW = 279.77

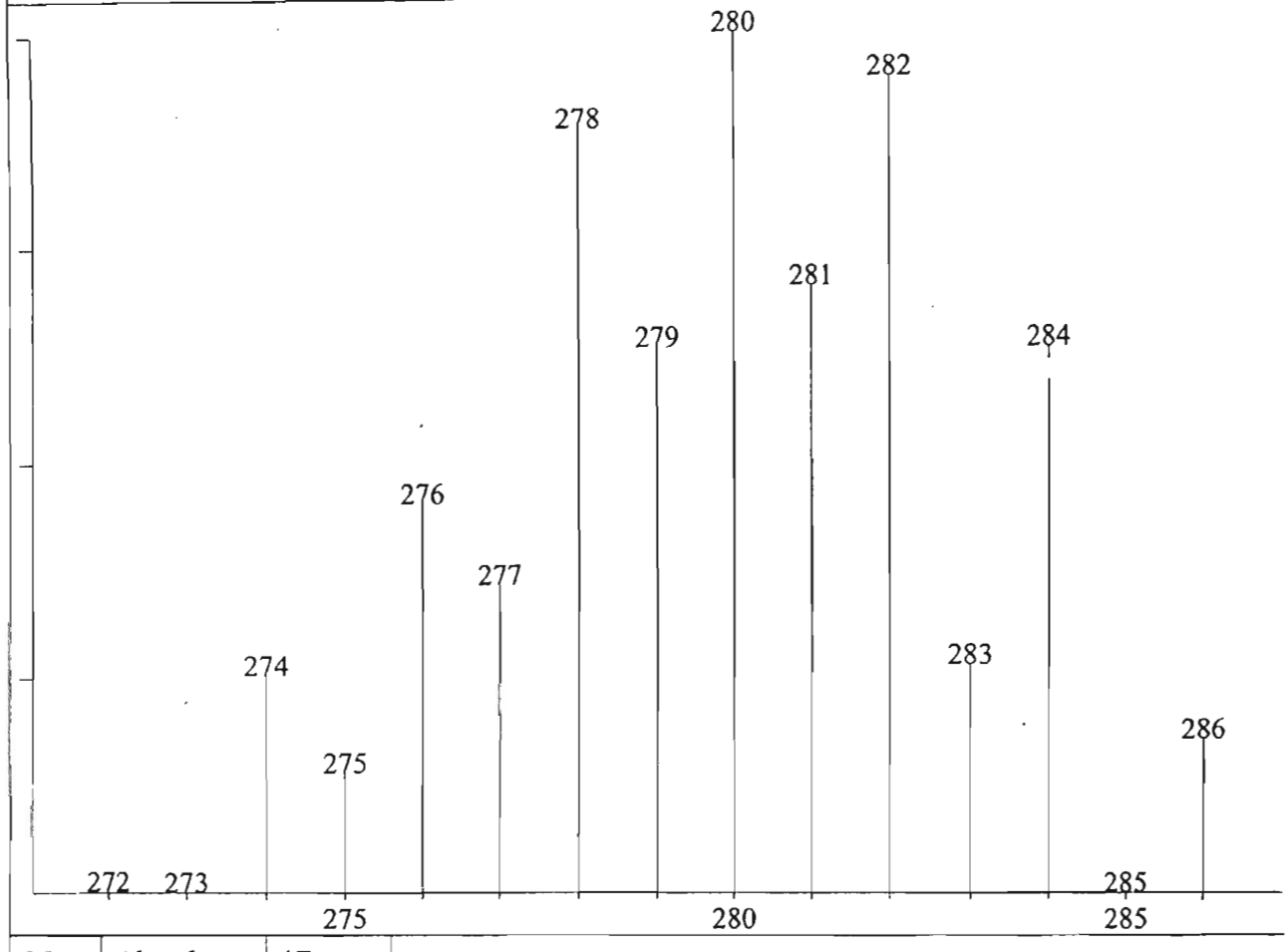

Mass	Abundance	*Factor
272	0.12446	0.12
273	0.00000	0.00
274	25.25679	25.26
275	13.82424	13.82
276	45.25024	45.25
277	35.70770	35.71
278	88.78832	88.79
279	63.25360	63.25
280	100.00000	100.00
281	70.35127	70.35
282	94.79762	94.80
283	26.38884	26.39
284	63.24487	63.24
285	0.00000	0.00
286	17.64644	17.65

(b) Mass Spectra related to the compound $[Cp(CO)_3W(CH_2)_3Mo(CO)_3Cp]$

DISTRIBUTION OF ISOTOPES CALCULATED BY 'ISOFORM' PROGRAM FOR
Formula : C27H29MoO5PW
Factor : 100 Nominal MW = 746 Exact MW = 746.03162 Average MW = 744.27

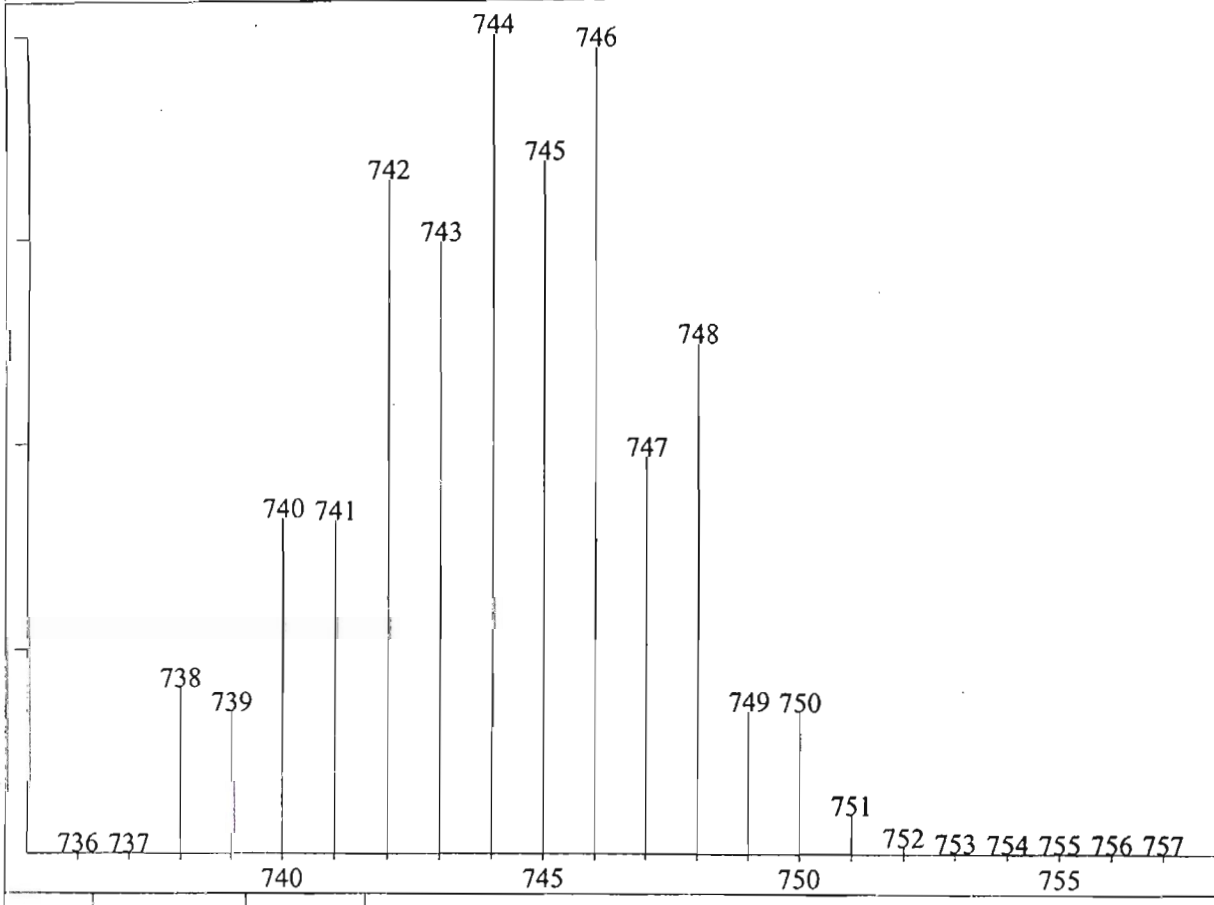

Mass	Abundance	*Factor
736	0.09992	0.10
737	0.03058	0.03
738	20.28330	20.28
739	17.30483	17.30
740	40.84517	40.85
741	40.54688	40.55
742	82.15976	82.16
743	74.45643	74.46
744	100.00000	100.00
745	84.40134	84.40
746	98.25476	98.25
747	48.22775	48.23
748	61.94163	61.94
749	17.31615	17.32
750	17.18922	17.19
751	4.73051	4.73
752	0.82351	0.82
753	0.10774	0.11
754	0.01140	0.01
755	0.00102	0.00
756	0.00008	0.00
757	0.00001	0.00

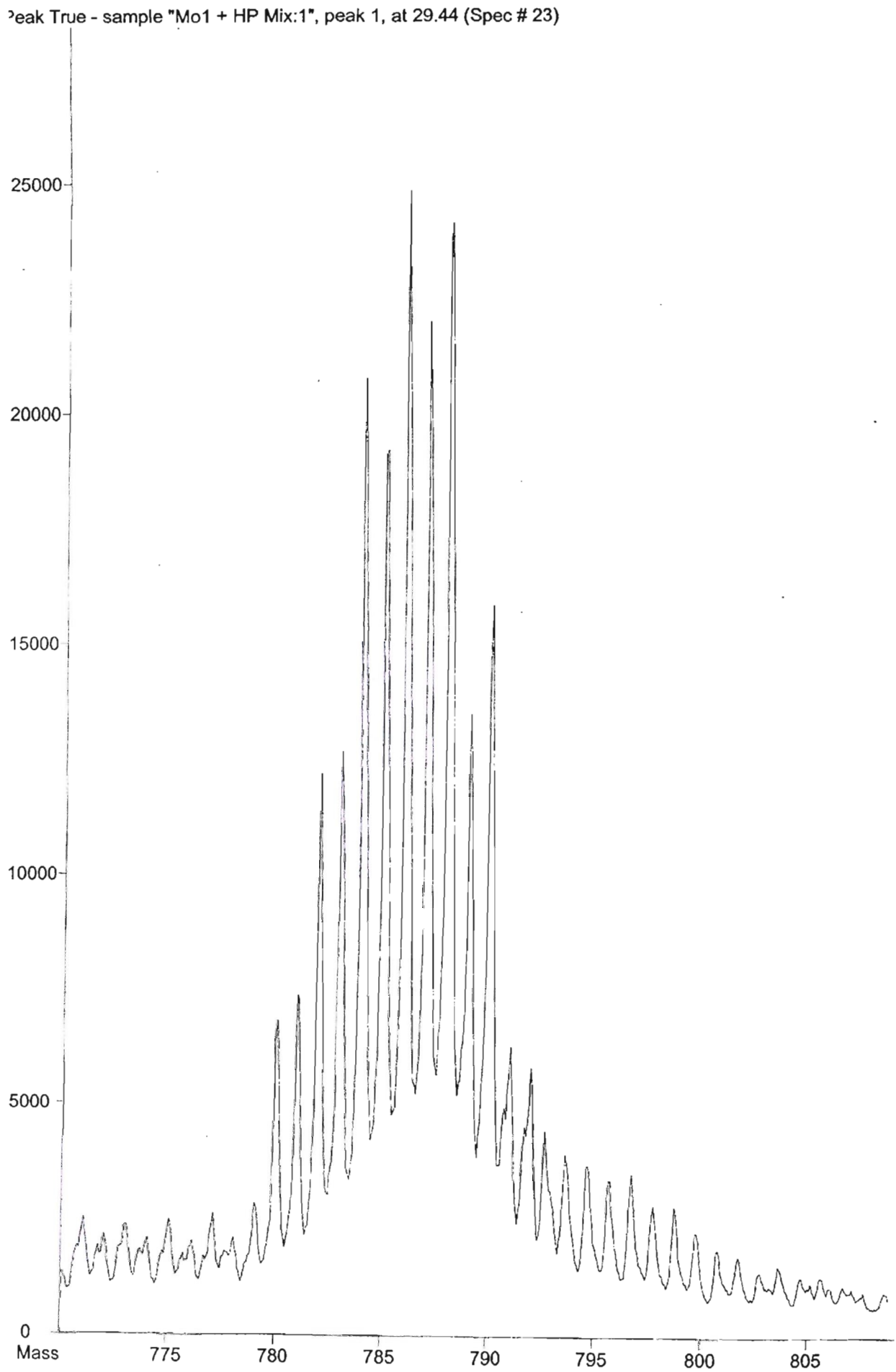
Peak True - sample "Mo1 + HP Mix:1", peak 1, at 29.44 (Spec # 23)
25000
20000
15000
10000
5000
0
Mass
775
780
785
790
795
800
805

(c) Mass Spectra related to the compound $[Cp(CO)_3W(CH_2)_4Mo(CO)_2(PPhMe_2)Cp]$

DISTRIBUTION OF ISOTOPES CALCULATED BY 'ISOFORM' PROGRAM FOR
Formula : C20H25FeMoO4P
Factor : 100 Nominal MW = 514 Exact MW = 513.98932 Average MW = 512.17

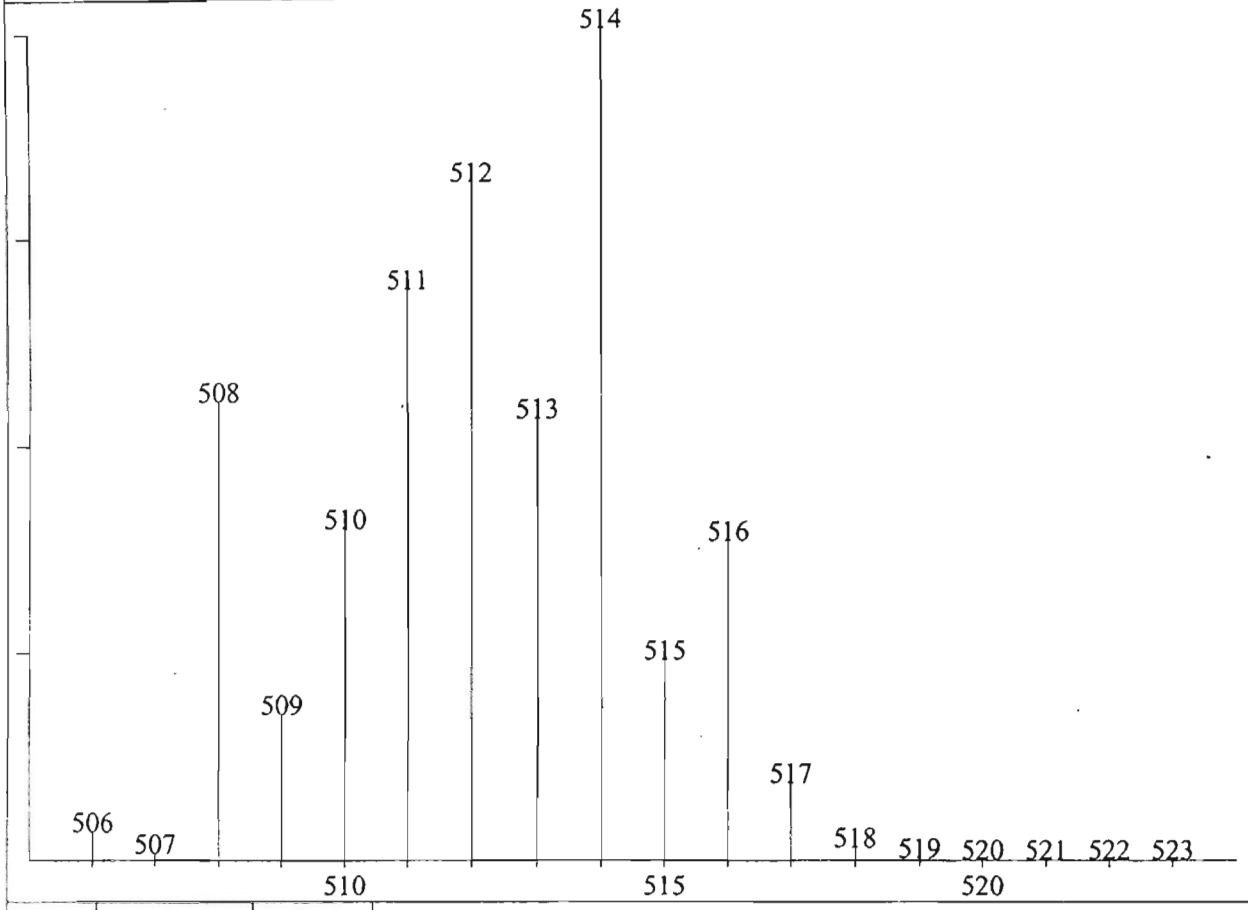

Mass	Abundance	*Factor
506	3.33814	3.34
507	0.75880	0.76
508	55.18292	55.18
509	17.38539	17.39
510	39.96792	39.97
511	68.67825	68.68
512	81.56169	81.56
513	53.02519	53.03
514	100.00000	100.00
515	23.92412	23.92
516	38.33930	38.34
517	9.12799	9.13
518	1.46268	1.46
519	0.17539	0.18
520	0.01702	0.02
521	0.00139	0.00
522	0.00010	0.00
523	0.00001	0.00

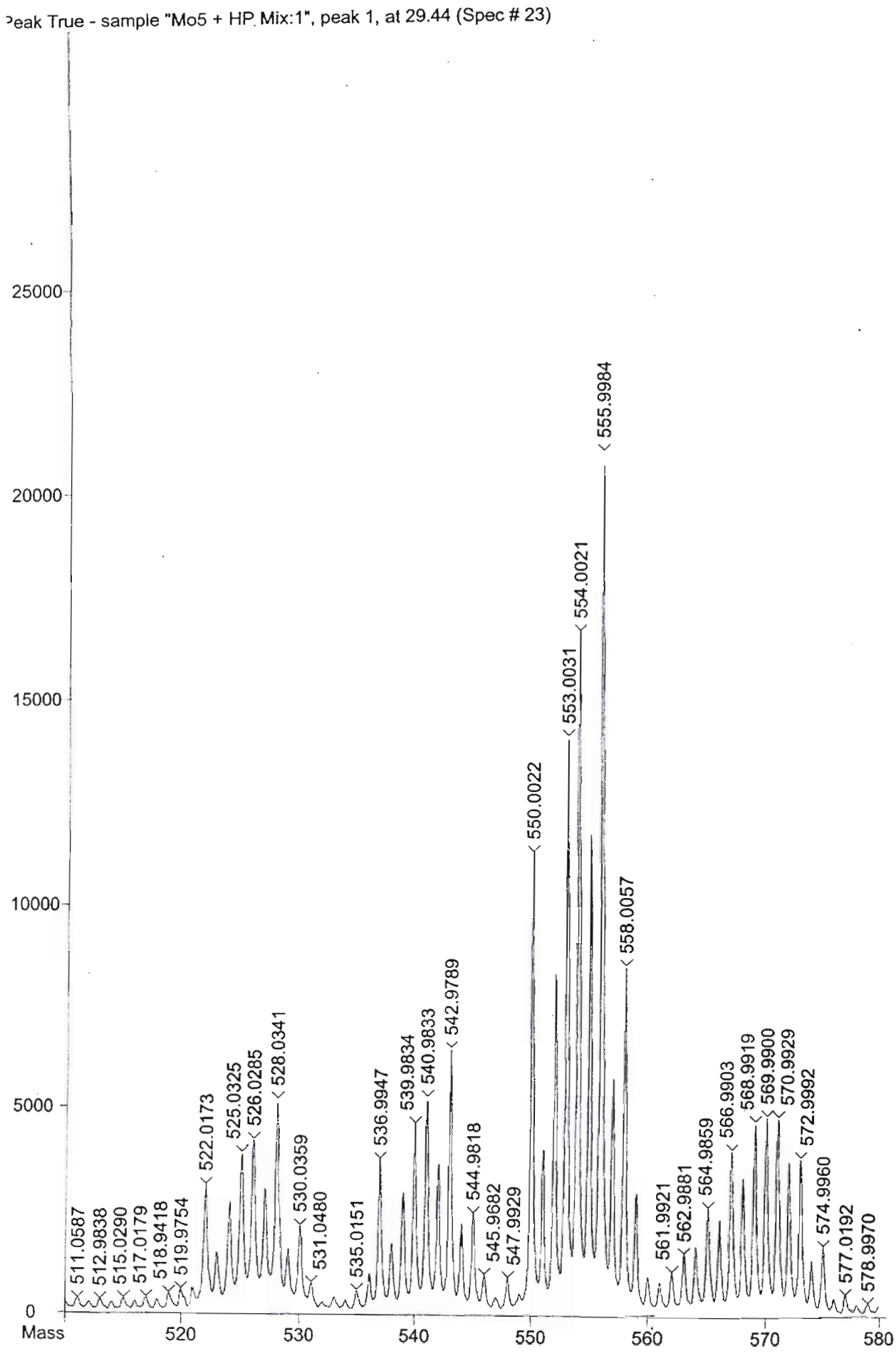
Peak True - sample "Mo5 + HP Mix:1", peak 1, at 29.44 (Spec # 23)
25000
20000
15000
10000
5000
0
Mass
520
530
540
550
560
570
580
511.0587
512.9838
515.0290
517.0179
518.9418
519.9754
522.0173
525.0325
526.0285
528.0341
530.0359
531.0480
535.0151
536.9947
539.9834
540.9833
542.9789
544.9818
545.9682
547.9929
550.0022
553.0031
554.0021
555.9984
558.0057
561.9921
562.9881
564.9859
566.9903
568.9919
569.9900
570.9929
572.9992
574.9960
577.0192
578.9970

(d) Mass Spectra related to the compound

$[Cp(CO)_2Fe(CH_2)_3Mo(CO)_2(PMe_3)Cp]$

DISTRIBUTION OF ISOTOPES CALCULATED BY 'ISOFORM' PROGRAM FOR
Formula : C24H26MoO6W
Factor : 100 Nominal MW = 692 Exact MW = 692.02936 Average MW = 690.24

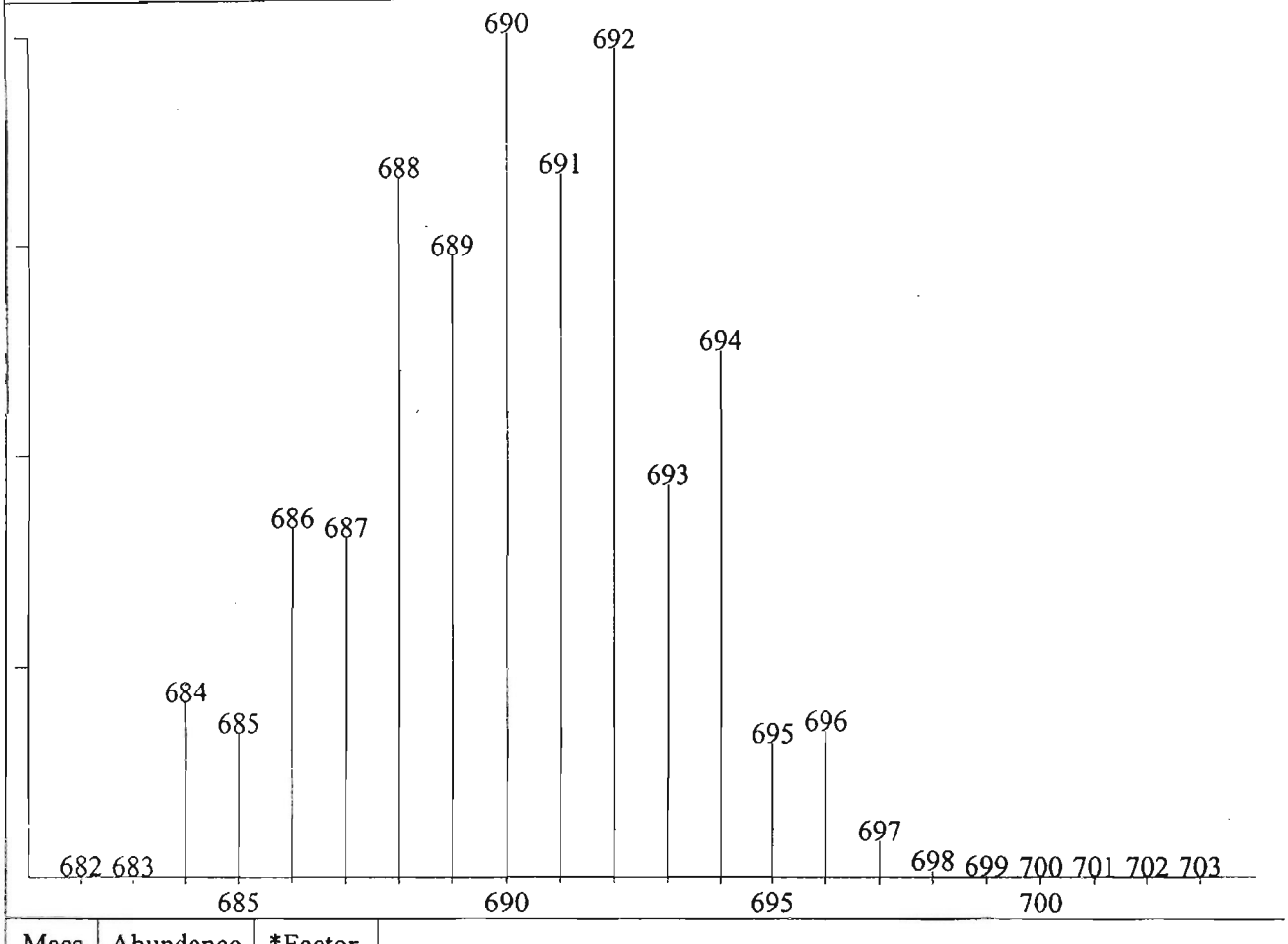

Mass	Abundance	*Factor
682	0.10224	0.10
683	0.02787	0.03
684	20.75184	20.75
685	17.01301	17.01
686	41.25658	41.26
687	40.13788	40.14
688	82.79017	82.79
689	73.48552	73.49
690	100.00000	100.00
691	83.14349	83.14
692	97.92232	97.92
693	46.21902	46.22
694	61.99794	62.00
695	15.73014	15.73
696	17.16610	17.17
697	4.29685	4.30
698	0.72807	0.73
699	0.09401	0.09
700	0.00993	0.01
701	0.00089	0.00
702	0.00007	0.00
703	0.00000	0.00

DISTRIBUTION OF ISOTOPES CALCULATED BY 'ISOFORM' PROGRAM FOR
Formula : C48H52Mo2O12W2Na
Factor : 100 Nominal MW = 1407 Exact MW = 1407.04846 Average MW = 1403.47

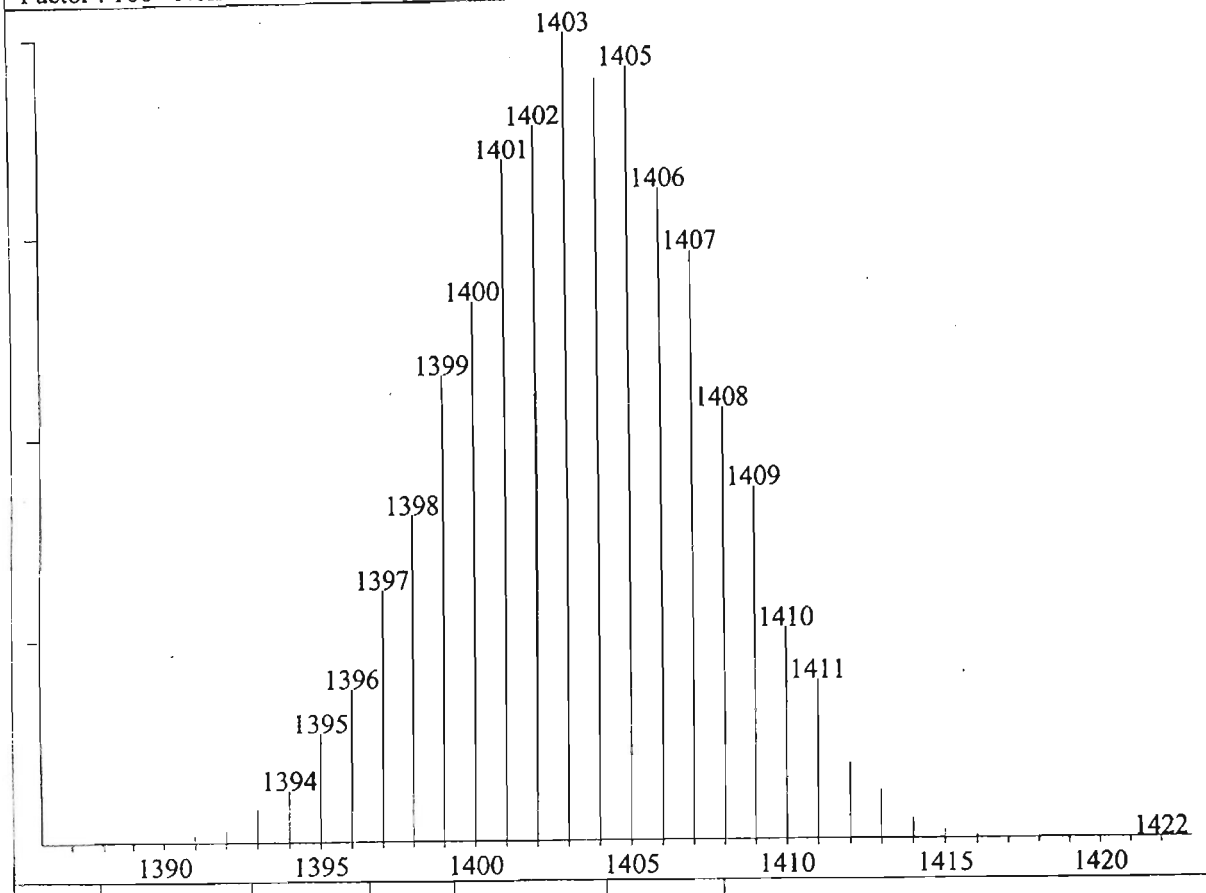

Mass	Abundance	*Factor	Mass	Abundance	*Factor
1387	0.00002	0.00	1412	9.31867	9.32
1388	0.00001	0.00	1413	6.04751	6.05
1389	0.00875	0.01	1414	2.39219	2.39
1390	0.00956	0.01	1415	1.09453	1.09
1391	0.90712	0.91	1416	0.37765	0.38
1392	1.47731	1.48	1417	0.09843	0.10
1393	4.16616	4.17	1418	0.02044	0.02
1394	6.36870	6.37	1419	0.00354	0.00
1395	13.45865	13.46	1420	0.00053	0.00
1396	18.96899	18.97	1421	0.00007	0.00
1397	31.16573	31.17	1422	0.00001	0.00
1398	40.36028	40.36			
1399	57.54359	57.54			
1400	66.61337	66.61			
1401	84.23947	84.24			
1402	88.44523	88.45			
1403	100.00000	100.00			
1404	94.23407	94.23			
1405	95.67846	95.68			
1406	80.40944	80.41			
1407	72.64179	72.64			
1408	53.20434	53.20			
1409	43.47262	43.47			
1410	26.07617	26.08			
1411	19.65742	19.66			

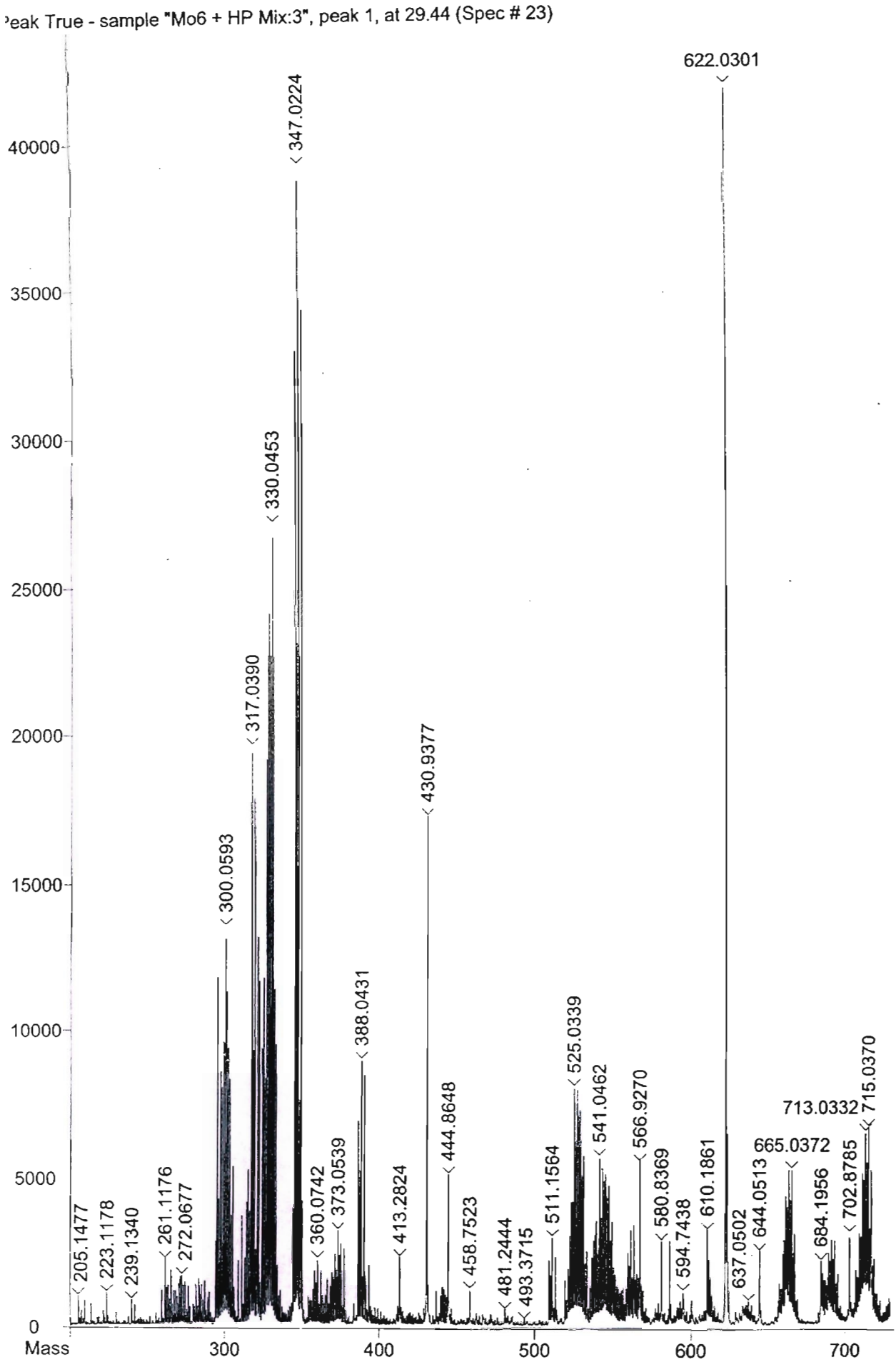
Peak True - sample "Mo6 + HP Mix:3", peak 1, at 29.44 (Spec # 23)
622.0301
347.0224
330.0453
317.0390
300.0593
430.9377
388.0431
444.8648
525.0339
541.0462
566.9270
580.8369
610.1861
665.0372
713.0332
715.0370
205.1477
223.1178
239.1340
261.1176
272.0677
360.0742
373.0539
413.2824
458.7523
481.2444
493.3715
511.1564
594.7438
637.0502
644.0513
684.1956
702.8785
40000
35000
30000
25000
20000
15000
10000
5000
0
Mass
300
400
500
600
700

APPENDIX 5

X-ray Crystal Data Pertaining to $[Cp(CO)_3W\{(CH_2)_3COOH\}]$

Table 1: Crystal data and structure refinement for $[Cp(CO)_3W\{(CH_2)_3COOH\}]$.

Identification code	$[Cp(CO)_3W\{(CH_2)_3COOH\}]$	
Empirical formula	$C_{12}H_{12}O_5W$	
Formula weight	420.07	
Temperature	295(2) K	
Wavelength	0.71073 Å	
Crystal system	Triclinic	
Space group	$P\bar{1}$	
Unit cell dimensions	a = 8.1540(11) Å	α = 102.800(15)°
	b = 11.229(2) Å	β = 89.981(11)°
	c = 14.265(2) Å	γ = 90.059(16)°
Volume	1273.7(4) $Å^3$	
Z	4	
Density (calculated)	2.191 Mg/m^3	
Absorption coefficient	9.079 mm^{-1}	
F(000)	792	
Crystal size	0.40 x 0.30 x 0.30 mm^3	
Theta range for data collection	2.10 to 24.97°.	
Index ranges	$-1 <= h <= 9, -13 <= k <= 13, -16 <= l <= 16$	
Reflections collected	5508	
Independent reflections	4483 [R(int) = 0.0314]	
Completeness to theta = 24.97°	100.0 %	
Absorption correction	Empirical (DIFABS)	
Max. and min. transmission	0.5460 and 0.0890	
Refinement method	Full-matrix least-squares on F^2	
Data / restraints / parameters	4483 / 0 / 325	
Goodness-of-fit on F^2	1.177	
Final R indices [$I > 2\sigma(I)$]	R_1 = 0.0305, wR_2 = 0.0887	
R indices (all data)	R_1 = 0.0353, wR_2 = 0.0920	
Largest diff. peak and hole	1.470 and –1.595 e.$Å^{-3}$	

Table 2: Bond lengths [Å] and angles [°] for $[Cp(CO)_3W\{(CH_2)_3COOH\}]$.

C(1)–O(1)	1.148(8)
C(1)–W(1)	1.976(7)
C(1')–O(1')	1.150(8)
C(1')–W(2)	1.971(7)
C(2')–O(2')	1.143(9)
C(2')–W(2)	1.989(8)
C(2)–O(2)	1.144(9)
C(2)–W(1)	1.986(8)
C(3')–O(3')	1.129(9)
C(3')–W(2)	1.979(8)
C(3)–O(3)	1.141(9)
C(3)–W(1)	1.969(7)
C(4')–C(5')	1.514(9)
C(4')–W(2)	2.313(7)
C(4)–C(5)	1.514(9)
C(4)–W(1)	2.326(6)
C(5)–C(6)	1.524(10)
C(5')–C(6')	1.537(10)
C(6')–C(7')	1.488(10)
C(6)–C(7)	1.506(10)
C(7)–O(5)	1.209(9)
C(7)–O(4)	1.303(8)
C(7')–O(5')	1.212(9)
C(7')–O(4')	1.309(8)
C(8)–C(9)	1.377(11)
C(8)–C(12)	1.419(12)
C(8)–W(1)	2.339(7)
C(8')–C(12')	1.381(11)
C(8')–C(9')	1.427(12)
C(8')–W(2)	2.312(7)
C(9)–C(10)	1.400(12)
C(9)–W(1)	2.372(7)
C(9')–C(10')	1.395(11)
C(9')–W(2)	2.335(7)
C(10')–C(11')	1.409(12)
C(10')–W(2)	2.377(7)

(continued...)

(…continued)

C(10)–C(11)	1.407(12)
C(10)–W(1)	2.359(8)
C(11')–C(12')	1.410(12)
C(11')–W(2)	2.361(8)
C(11)–C(12)	1.406(12)
C(11)–W(1)	2.315(7)
C(12')–W(2)	2.310(8)
C(12)–W(1)	2.312(7)

O(1)–C(1)–W(1)	177.1(6)
O(1')–C(1')–W(2)	177.1(6)
O(2')–C(2')–W(2)	178.1(7)
O(2)–C(2)–W(1)	179.2(8)
O(3')–C(3')–W(2)	177.2(7)
O(3)–C(3)–W(1)	176.7(6)
C(5')–C(4')–W(2)	118.3(5)
C(5)–C(4)–W(1)	117.9(4)
C(4)–C(5)–C(6)	112.5(6)
C(4')–C(5')–C(6')	112.7(6)
C(7')–C(6')–C(5')	114.5(6)
C(5)–C(6)–C(7)	114.4(6)
O(5)–C(7)–O(4)	123.5(7)
O(5)–C(7)–C(6)	123.2(6)
O(4)–C(7)–C(6)	113.2(6)
O(5')–C(7')–O(4')	122.9(7)
O(5')–C(7')–C(6')	123.8(6)
O(4')–C(7')–C(6')	113.3(6)
C(9)–C(8)–C(12)	108.4(7)
C(9)–C(8)–W(1)	74.3(4)
C(12)–C(8)–W(1)	71.2(4)
C(12')–C(8')–C(9')	108.2(7)
C(12')–C(8')–W(2)	72.6(4)
C(9')–C(8')–W(2)	73.0(4)
C(8)–C(9)–C(10)	108.8(7)
C(8)–C(9)–W(1)	71.7(4)
C(10)–C(9)–W(1)	72.3(4)
C(10')–C(9')–C(8')	107.4(7)

(continued…)

(…continued)

C(10')–C(9')–W(2)	74.4(4)
C(8')–C(9')–W(2)	71.2(4)
C(9')–C(10')–C(11')	108.2(8)
C(9')–C(10')–W(2)	71.1(4)
C(11')–C(10')–W(2)	72.1(4)
C(11)–C(10)–C(9)	107.7(7)
C(11)–C(10)–W(1)	70.8(4)
C(9)–C(10)–W(1)	73.3(4)
C(10')–C(11')–C(12')	107.8(8)
C(10')–C(11')–W(2)	73.3(5)
C(12')–C(11')–W(2)	70.5(5)
C(10)–C(11)–C(12)	108.0(8)
C(10)–C(11)–W(1)	74.2(4)
C(12)–C(11)–W(1)	72.2(4)
C(8')–C(12')–C(11')	108.3(8)
C(8')–C(12')–W(2)	72.7(4)
C(11')–C(12')–W(2)	74.4(5)
C(8)–C(12)–C(11)	107.1(7)
C(8)–C(12)–W(1)	73.3(4)
C(11)–C(12)–W(1)	72.4(4)
C(3)–W(1)–C(2)	78.1(3)
C(3)–W(1)–C(1)	107.0(3)
C(2)–W(1)–C(1)	75.9(3)
C(3)–W(1)–C(11)	136.5(3)
C(2)–W(1)–C(11)	91.7(3)
C(1)–W(1)–C(11)	111.2(3)
C(3)–W(1)–C(12)	102.6(3)
C(2)–W(1)–C(12)	94.3(3)
C(1)–W(1)–C(12)	145.8(3)
C(11)–W(1)–C(12)	35.4(3)
C(3)–W(1)–C(4)	73.7(3)
C(2)–W(1)–C(4)	130.9(3)
C(1)–W(1)–C(4)	75.1(3)
C(11)–W(1)–C(4)	135.8(3)
C(12)–W(1)–C(4)	130.5(3)
C(3)–W(1)–C(8)	94.4(3)

(continued…)

(...continued)

C(2)–W(1)–C(8)	126.8(3)
C(1)–W(1)–C(8)	152.3(3)
C(11)–W(1)–C(8)	58.4(3)
C(12)–W(1)–C(8)	35.5(3)
C(4)–W(1)–C(8)	95.0(3)
C(3)–W(1)–C(10)	151.4(3)
C(2)–W(1)–C(10)	121.3(3)
C(1)–W(1)–C(10)	98.6(3)
C(11)–W(1)–C(10)	35.0(3)
C(12)–W(1)–C(10)	58.3(3)
C(4)–W(1)–C(10)	101.7(3)
C(8)–W(1)–C(10)	57.4(3)
C(3)–W(1)–C(9)	118.6(3)
C(2)–W(1)–C(9)	148.9(3)
C(1)–W(1)–C(9)	118.3(3)
C(11)–W(1)–C(9)	57.8(3)
C(12)–W(1)–C(9)	57.9(3)
C(4)–W(1)–C(9)	80.2(3)
C(8)–W(1)–C(9)	34.0(3)
C(10)–W(1)–C(9)	34.4(3)
C(3')–W(2)–C(2')	78.4(3)
C(3')–W(2)–C(1')	106.6(3)
C(2')–W(2)–C(1')	75.2(3)
C(3')–W(2)–C(12')	136.7(3)
C(2')–W(2)–C(12')	91.2(3)
C(1')–W(2)–C(12')	111.1(3)
C(3')–W(2)–C(4')	73.8(3)
C(2')–W(2)–C(4')	131.0(3)
C(1')–W(2)–C(4')	75.3(2)
C(12')–W(2)–C(4')	136.0(3)
C(3')–W(2)–C(8')	103.4(3)
C(2')–W(2)–C(8')	93.8(3)
C(1')–W(2)–C(8')	144.9(3)
C(12')–W(2)–C(8')	34.8(3)
C(4')–W(2)–C(8')	131.3(3)
C(3')–W(2)–C(9')	94.2(3)

(continued...)

(…continued)

C(2')–W(2)–C(9')	126.3(3)
C(1')–W(2)–C(9')	153.4(3)
C(12')–W(2)–C(9')	58.6(3)
C(4')–W(2)–C(9')	95.5(3)
C(8')–W(2)–C(9')	35.8(3)
C(3')–W(2)–C(11')	151.6(3)
C(2')–W(2)–C(11')	120.9(3)
C(1')–W(2)–C(11')	99.0(3)
C(12')–W(2)–C(11')	35.1(3)
C(4')–W(2)–C(11')	101.7(3)
C(8')–W(2)–C(11')	57.9(3)
C(9')–W(2)–C(11')	57.8(3)
C(3')–W(2)–C(10')	118.6(3)
C(2')–W(2)–C(10')	148.8(3)
C(1')–W(2)–C(10')	119.0(3)
C(12')–W(2)–C(10')	58.1(3)
C(4')–W(2)–C(10')	80.3(3)
C(8')–W(2)–C(10')	58.0(3)
C(9')–W(2)–C(10')	34.4(3)
C(11')–W(2)–C(10')	34.6(3)

Symmetry transformations used to generate equivalent atoms:

APPENDIX 6

Compact Disk

Containing Other X-ray Crystal Data Pertaining to Chapters 2 to 4